

AD-A100 313

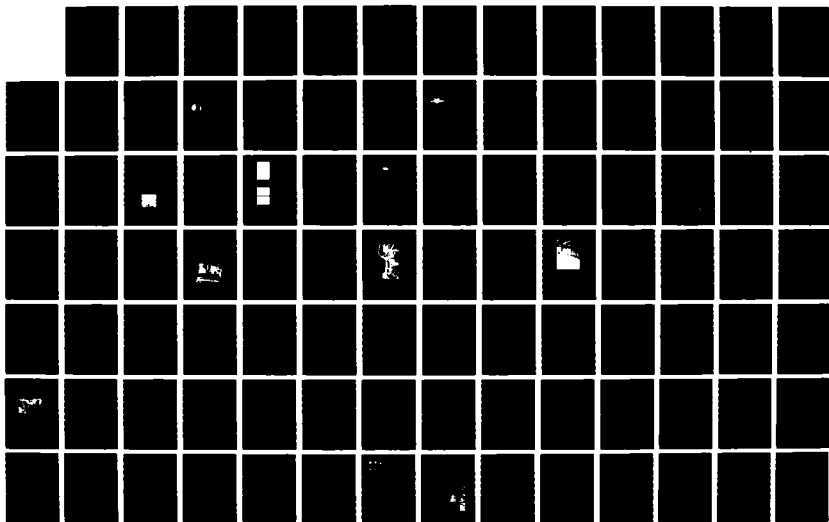
X-RAY LITHOGRAPHIC RESEARCH: A COLLECTION OF NRL
CONTRIBUTIONS(U) NAVAL RESEARCH LAB WASHINGTON DC
R R WHITLOCK 24 AUG 87 NRL-MR-5731

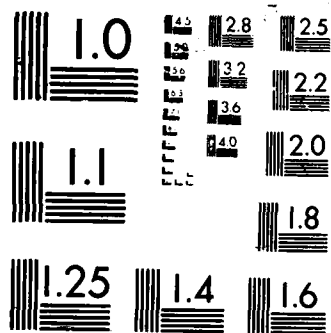
1/2

UNCLASSIFIED

F/G 13/0

NL





DTIC FILE COPY

Naval Research Laboratory

Washington, DC 20375-5000



NRL Memorandum Report 5731

X-Ray Lithography Research: A Collection of NRL Contributions

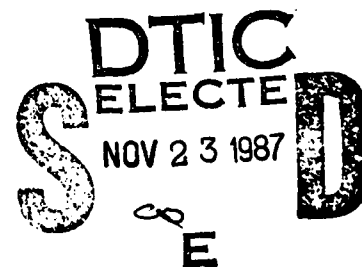
Edited by

ROBERT R. WHITLOCK

*Condensed Matter Physics Branch
Condensed Matter & Radiation Sciences Division*

AD-A188 313

August 24, 1987



87 11 5 009

Approved for public release; distribution unlimited.

REPORT DOCUMENTATION PAGE

1a. REPORT SECURITY CLASSIFICATION UNCLASSIFIED			1b. RESTRICTIVE MARKINGS		
2a. SECURITY CLASSIFICATION AUTHORITY			3. DISTRIBUTION/AVAILABILITY OF REPORT Approved for public release; distribution unlimited.		
2b. DECLASSIFICATION/DOWNGRADING SCHEDULE					
4. PERFORMING ORGANIZATION REPORT NUMBER(S) NRL Memorandum Report 5731			5. MONITORING ORGANIZATION REPORT NUMBER(S)		
6a. NAME OF PERFORMING ORGANIZATION Naval Research Laboratory		6b. OFFICE SYMBOL (If applicable) Code 4680		7a. NAME OF MONITORING ORGANIZATION	
6c. ADDRESS (City, State, and ZIP Code) Washington, DC 20375-5000			7b. ADDRESS (City, State, and ZIP Code)		
8a. NAME OF FUNDING/SPONSORING ORGANIZATION Office of Naval Research		8b. OFFICE SYMBOL (If applicable)		9. PROCUREMENT INSTRUMENT IDENTIFICATION NUMBER	
8c. ADDRESS (City, State, and ZIP Code) Arlington, VA 22217			10. SOURCE OF FUNDING NUMBERS		
			PROGRAM ELEMENT NO 63224C	PROJECT NO	TASK NO SBSG
11. TITLE (Include Security Classification) X-Ray Lithography Research: A Collection of NRL Contributions					
12. PERSONAL AUTHOR(S) Whitlock, Robert R., Editor					
13a. TYPE OF REPORT Final		13b. TIME COVERED FROM _____ TO _____		14. DATE OF REPORT (Year, Month, Day) 1987 August 24	
15. PAGE COUNT 181					
16. SUPPLEMENTARY NOTATION					
17. COSATI CODES			18. SUBJECT TERMS (Continue on reverse if necessary and identify by block number)		
FIELD	GROUP	SUB-GROUP			
			Laser-produced plasma		
			X-Ray lithography		
			Nanofabrication		
			Lithography		
			Microfabrication		
19. ABSTRACT (Continue on reverse if necessary and identify by block number)					
<p>We have examined x-ray and ultraviolet lithographic methods for the microfabrication of fine-line features, with particular emphasis on the use of high temperature plasmas as x-ray sources. Out of this work has come a series of scientific presentations and publications generated by a group of scientists at the Naval Research Laboratory, in collaboration with their coworkers at other institutions. These publications are collected under one cover in this Report.</p> <p>It is noteworthy that concepts first put forward in these publications have culminated in the commercial availability of a laser-plasma-based x-ray lithography system.</p> <p>Present efforts are aimed at the optimization of x-ray and UV sources suitable for the lithographic application.</p>					
20. DISTRIBUTION/AVAILABILITY OF ABSTRACT <input checked="" type="checkbox"/> UNCLASSIFIED/UNLIMITED <input type="checkbox"/> SAME AS RPT. <input type="checkbox"/> DTIC USERS			21. ABSTRACT SECURITY CLASSIFICATION UNCLASSIFIED		
22a. NAME OF RESPONSIBLE INDIVIDUAL Robert R. Whitlock			22b. TELEPHONE (Include Area Code) (202) 767-2154		22c. OFFICE SYMBOL Code 4680

CONTENTS

I. Background	v
II. Compendium	vii
III. Reprints	1.1

(Contents of Reprints Section are listed in the Compendium)

Selection For THIS COPY <input checked="" type="checkbox"/>	
THIS COPY <input type="checkbox"/>	
Unrecorded <input type="checkbox"/>	
Justification	
By	
Distribution/	
Availability Codes	
Dist	Avail and/or Special
A-1	



I. BACKGROUND

We have examined ^{are} x-ray and ultraviolet lithographic methods for the microfabrication of fine-line features, with particular emphasis on the use of high temperature plasmas as x-ray sources. Out of this work has come a series of scientific presentations and publications generated by a group of scientists at the Naval Research Laboratory, in collaboration with their coworkers at other institutions. These publications are collected under one cover in this report.

The individual papers are briefly synopsised in the Compendium, and reprinted in the Reprint section. The ordering of the papers is by date: for published proceedings of meetings, the meeting date takes precedence over the final publication or copyright date.

It is noteworthy that concepts first put forward in these publications have culminated in the commercial availability of a laser-plasma-based x-ray lithography system.

Present efforts are aimed at the optimization of x-ray and UV sources suitable for the lithographic application.

*... a list of ...
exposure (general); ...*

II. COMPENDIUM

1.1

"Pulsed X-ray Lithography"

D.J. Nagel, R. R. Whitlock, J. R. Greig, R. E. Pechacek, and M.C. Peckerar. Meeting held 9-11 April 1978, San Jose, CA, SPIE conference on Developments in Microlithography.

First Technical Demonstration

This is the first reported application of the laser-produced plasma x-ray source for x-ray lithography. Although our Technical Demonstration experiment was conducted under non-optimized exposure conditions, it successfully demonstrated the feasibility of the laser-plasma x-ray lithographic method, and pointed the way toward more practical prospects in the future.

2.1 - 2.8

"Laser-Plasma Source for Pulsed X-ray Lithography"

D.J. Nagel, R. R. Whitlock, J. R. Greig, R. E. Pechacek, and M.C. Peckerar. Meeting held 9-11 April 1978, San Jose, CA. Proceedings published as Developments in Semiconductor Microlithography III, SPIE Volume 135, R.L. Ruddell, et al., eds., Society of Photo-Optical Instrumentation Engineers, Bellingham, Washington, (September, 1978), pp. 46-53.

Experimental Details
Laser-Plasma X-Ray Source
Exposure Considerations
Laser Optimization Proposed

This Proceedings article of the April, 1978, meeting formally documents the basic findings of our Technical Demonstration (additional information in Electronics Letters article, below). Also important, the characteristics of the laser-heated plasma as an x-ray source are reviewed. Potential exposure system problems for this source (penumbral blurring, debris, excessive mask heating) are enumerated. The laser pulse energy required to achieve single shot resist exposure is estimated. The concept of a laser optimized for x-ray lithography is introduced.

3.1 - 3.12

"High Speed X-Ray Lithography with Radiation from Laser-Produced Plasmas"

M.C. Peckerar, J. R. Greig, D. J. Nagel, R. E. Pechacek and R. R. Whitlock. Meeting held 21-26 May 1978, Seattle, Washington. Published in Proceedings of the Symposium on Electron and Ion Beam Science and Tech., Eighth International Conference, Vol. 78-5, R. Bakish, ed. Electrochemical Society, Princeton, NJ (February, 1979), p. 432-443.

Potential Problems Examined

Target Debris

Mask Heating

CV Curves

Interface States

Resist Sensitivity

Methods for alleviating harmful effects of target debris and thermal cycling of masks during exposure are set forward in this review of potential problem areas associated with the laser plasma x-ray source. The premature laser-target interaction which was sometimes present in the Technical Demonstration, would not be a factor in a dedicated laser system designed for x-ray lithography. Capacitance-voltage curves for MOS capacitors exhibit a small shift in position after exposure to the laser-plasma x-ray source, implying only modest increases in the density of fast interface states at the oxide-silicon interface. The sensitivity of PBS for these short x-ray bursts was found to be essentially the same as for steady-state x-ray exposures. That is, the reciprocity loss experienced with visible light in photographic emulsions evidently does not operate here to any great degree.

4.1 - 4.4

"Lithography and High-Resolution Radiography with Pulsed X-Rays"

D.J. Nagel, J. M. McMahon, R. R. Whitlock, J. R. Greig, R. E. Pechacek and M. C. Peckerar. Meeting held 28 Aug. - 1 Sept. 1978, Sendai, Japan. Published in Proceedings of the International Conference on X-Ray and XUV Spectroscopy, Japanese J. Appl. Phys., Supplement 17-2, 17 (December, 1978), p. 472-475.

Exposure System

Biological Radiography

After briefly reciting the major findings of the laser-plasma Technical Demonstration experiment, we then discuss a concept for an integrated exposure system employing the laser-plasma x-ray source. Also, the feasibility of using the laser-plasma x-ray source to obtain 100 Å resolution (or better) of biological samples by contact exposure is predicted.

5.1 - 5.2

“Submicrosecond X-Ray Lithography”

D.J. Nagel, M. C. Peckerar, R. R. Whitlock, J. R. Greig and R. E. Pechacek. Electronics Letters (23 November 1978) 14/24, p. 781-782.

First Replication
Submicron Resolution
Details of Demonstration
Modest Interface State Density

The first lithographic replication by exposure to x-rays emitted from a laser-produced plasma is presented. Submicron resolution is substantiated. The conduct of the Technical Demonstration experiment is documented briefly but in detail. Electrical tests for damage induced by the lithographic x-rays in MOS capacitors indicate only modest increases in the density of fast traps at the oxide-silicon interface.

6.1 - 6.17

“Comparison of X-Ray Sources for Exposure of Photoresists ”

D.J. Nagel. Meeting held June 1979. Published in Annals of the New York Academy of Sciences, 342 (13 June 1980), pp. 235-251.

Concise Source Comparison
Spectrum and Resolution in
Resist
Tabulation of Source
Characteristics

The relationships between the spectral properties of x-ray sources and the relative sensitivity and ultimate resolution of photoresists are encapsulated. A concise and informative comparison of the major types of x-ray sources (electron beam impact, synchrotron, and plasma) is presented, with a *convenient tabulation of source characteristics* as they relate to x-ray lithographic exposures and microradiography. A transcript of the Discussion following the presentation is also included.

7.1 - 7.4

“Radiation effects in MOS devices caused by x-ray and e-beam lithography”

M. Peckerar, R. Fulton, P. Blaise, D. Brown and R. Whitlock. J. Vac. Sci. Tech., (November, 1979) 16/6, p. 1658-61.

Radiation Damage Tests
Electrical TBS Tests

MOS devices were irradiated by steady-state x-ray and electron sources at levels typical of lithographic exposures. The devices' electrical performance was observed to have a sizeable sensitivity to stressed conditions of increased temperature and bias (TBS tests); subsequent interpretation (Peckerar, et al., December, 1982, included herein) held that the high degradations were due to processing steps, and not to the lithographies directly. The direct deposition of exposure beam energy was calculated. (Later, more advanced calculations of the energy transport by photoelectrons were made by C.M. Dozier, D.B. Brown, et al., in works not included herein.)

8.1 - 8.3

"Radiation Hardness of LSI/VLSI Fabrication Processes"

H.L. Hughes. IEEE Transactions on Nuclear Sci., Vol. NS-26, No. 6 (December, 1979), 5053-5.

Inversion Voltage at a Constant
Irradiation-Bias Stress Test

During the Technical Demonstration, MOS capacitors were lithographically fabricated using positive PBS resist, exposed by a dose of kilovolt x-rays. Electrical tests were performed afterward on these MOS structures. The results imply that, for devices which are not subject to further ionizing radiation after fabrication is complete, no degradation in inversion voltage due to x-ray lithography is anticipated. However, significant changes in inversion levels were found in capacitors which were subsequently irradiated under bias by a Co^{60} source. Since important applications of high speed circuits (made by x-ray lithography) involve radiation environments, further investigation of these effects is in order.

9.1 - 9.13

"Ultraviolet and x-ray lithography"

D.J. Nagel. Meeting held 21-22 April 1981, Washington, D.C. Proceedings published as Ultraviolet and Vacuum Ultraviolet Systems, SPIE Vol. 279, W.R. Hunter, ed. Society of Photo-Optical Instrumentation Engineers, Bellingham, WA (December, 1982), pp. 98-110.

Review of X-UV Lithography
Size Scales
Basic Sources and Methods
Resolution and Absorption
UV and X-Ray Sources
X-Ray Masks and Resists

This well-organized paper on X-UV microlithography is an overall review containing numerous references to other related reviews offering further details. Included is a systematic classification of basic lithographic methods and their associated exposure sources. A didactic approach is taken to the influence of the absorption processes and the properties of materials on the attainability of high resolution replication in resists. A wide variety of UV and x-ray sources are portrayed. Works on x-ray masks, resists, alignment methods, and the development of x-ray exposure systems are discussed and referenced.

10.1 - 10.10

Capacitor Tests: TBS, IBS, CV,
GV
Transistor Tests: V_t , g_m &
slope, swing
Annealing of Effects
Subthreshold Leakage

"Radiation effects introduced by x-ray lithography in MOS devices"

M.C. Peckerar, C.M. Dozier, D.B. Brown, D. Patterson, D. McCarthy, and D. Ma. IEEE Trans. Nuc. Sci., NS-29 (December, 1982), pp. 1697-1701.

Soft x-rays from Al and Cu x-ray tubes were radiated onto MOS capacitors and transistors under a broad range of conditions to simulate x-ray lithographic exposures on the one hand, and the operation of finished devices in a field of ionizing radiation on the other. The MOS structures were tested for numerous effects, including threshold shifts, shifts under various combinations and levels of stressed conditions (temperature, irradiation, bias), subthreshold leakage, etc. Various annealing regimens were applied. Several measurements were also made with Co^{60} irradiations. It is concluded that the effects of soft x-ray lithography on MOS devices are at a sufficiently low damage level to accommodate integrated circuit technology, provided that proper design changes and modelling are introduced.

11.1 - 11.6

10 Hz X-Ray Source
Characteristics
Target Variations
Laser Parameters
Resist Exposure

"Repetitively-Pulsed-Plasma Soft X-Ray Source"

D.J. Nagel, C. M. Brown, M. C. Peckerar, M. L. Ginter, J. A. Robinson, T. J. McIlrath and P. K. Carroll. Applied Optics, 23/9 (May, 1984), pp. 1428-33.

A repetitively-pulsed Nd YAG laser (25 nsec pulses up to 0.8 Joule each), operating at up to 10 Hz, was focused onto a variety of targets. The behavior of the laser plasma as an X-UV source was charted over several dimensions of parameter variations, both laser-related and target-related. The exposure of a photoresist was performed in 20 minutes by 150-184 eV photons. Improved exposure times with excimer lasers is predicted.

12.1 - 12.34

General Review of the Field
Applications
Elements of Lithography
Engineering Requirements
X-Ray Sources Compared

"Plasma Sources for X-ray Lithography"

D.J. Nagel. Published in VLSI Electronics: Micro-structure Science, Vol. 8. N.G. Einspruch, ed., Academic Press (May, 1984), Ch. 6.

This general treatment and review of x-ray lithography begins with the applications of the manufacture of submicron structures, and moves onward through an orientation to lithographic principles. The powerful advantage which x-ray (compared to optical) lithography holds in spatial resolution of the replicated pattern is discussed in the context of the engineering specifications which lead to requirements for new sources, new masks, new mask aligners, and new resists — an entirely new lithographic system. X-ray sources are compared by type (electron impact, synchrotron, and high temperature plasma) in the light of the requirements of microcircuit production.

13.1 - 13.4

10 Hz Nd Laser Exposures
Advantages over Synchrotron
Demonstrated

"Soft X-ray Lithography Using Radiation from Laser- Produced Plasmas"

P. Gohil, H. Kapoor, D. Ma, M. C. Peckerar, T. J. McIlrath and M. L. Ginter, Appl. Opt. 24 (July, 1985), pp. 2024-7.

Exposures of COP photoresist were made to full depth in one hour, with x-rays emitted by metal targets placed at the focus of a Nd:YAG laser operating at 10 Hz and a mere 6 Watt average power. Exposure area coverage exceeded that of synchrotron exposures, as did exposure uniformity.

14.1 - 14.8

Laser-Plasma X-Ray Lithography
Status
Engineering of Exposure System

"Laser-Plasma Sources for X-Ray Lithography"

D.J. Nagel. Meeting held 23-25 September 1985, Rotterdam, The Netherlands. Published in Microelectronic Engineering 3 (Dec. 1985), and reprinted in Microcircuit Engineering 85, North Holland, Amsterdam, The Netherlands (1985), pp. 557- 564.

An up-to-date synopsis of the status of characterization and engineering of the laser-heated plasma source for x-ray lithography.

15.1 - 15.19

Demonstration Results Reviewed
Mask Thermalization
Perspective on Electrical Tests
Commercialization Status

"Laser Processing of High-Tech Materials at High Irradiance"

R.R. Whitlock. Meeting held 11-14 November 1985, San Francisco, CA. Published in Proceedings of the 1985 International Congress on Applications of Lasers and Electro-Optics (ICALEO 85), C.A. Albright, ed., Laser Institute of America, Toledo, Ohio (1 June 1985), pp. 187-200; and Naval Research Laboratory Memorandum Report 5915.

The potential importance of fine-line lithography to the continued growth of the microelectronics industry is reiterated. The results of our Technical Demonstration are reviewed. The possible role of thermal equilibration of the mask and its patterning layer, over times as short as the laser pulse, is pointed out for the first time. Comments regarding present perspectives on the meaning of electrical tests are presented. The status of commercialization of laser-plasma X-UV lithography is indicated.

16.1 - 16.14

Introduction to Lithographic
Methods
Visible, UV, X-Ray, e-Beam
Resolution
Depth of Focus
Positioning Accuracy

"Lithographic Techniques: An Overview"

M.C. Peckerar. Unpublished.

The basic methods employed in lithography for integrated circuitry are compared. Three basic criteria for the replication of fine lines are resolution, depth-of-focus, and positioning accuracy. The influence which these criteria exert is described with respect to the choice of exposure source (visible, UV, x-ray, or e-beam), the size of the instantaneous exposure field (focused pencil beam vs. areal beam), and the separation distance between the mask and the wafer (contact, proximity, or projection).

"Generation and Use of Spontaneous X-Ray Emission from Laser-Heated Plasmas"

D.J. Nagel. Meeting held 2-4 June 1986, Quebec City, Quebec, Canada. Original title "Incoherent x-rays from laser-heated plasmas," invited. Proceedings published as High Intensity Laser Processes, SPIE Vol. 664, Society of Photo-Optical Instrumentation Engineers, Bellingham, WA (21 Oct. 1986), pp. 142-150.

Repetitive Lasers
X-Ray Beam Line
Beam Line Applications

After a brief introduction to the various types of x-ray sources, both those in present use and those projected for the near future, attention is turned to repetitively pulsed lasers and their integration into laser-plasma XUV generation systems. The power levels of available repetitive lasers are graphed, and representative irradiances are tabulated. Recent x-ray emission studies are cited, with commentary on the need for further measurement. Advances are noted in the establishment of the first x-ray laser plasma beam line, which includes special collection optics. Areas of application for x-rays from such laser plasmas are cited.

"Pulsed X-ray Lithography"

D.J. Nagel, R. E. Pechacek, J. R. Greig,
R. R. Whitlock,
U. S. Naval Research Laboratory,
and M.C. Peckerar,
Westinghouse Electric Corporation

presented 10-11 April 1978, San Jose, CA
SPIE conference on
Developments in Microlithography

Flash x-ray sources, which can be used to expose photoresists, offer an alternative to the steady-state electron-impact and synchrotron radiation sources commonly used for x-ray lithography. Of the many pulsed x-ray devices*, laser-heated plasmas with temperatures in the 10^6 - 10^7 K range offer the best hope of providing practical (i.e., production line) exposures. We have demonstrated that x-rays with energies near 2 keV produced by focusing 30 joule, 40 nanosecond Nd laser pulses onto Al targets will expose an x-ray resist (PBS) on Si wafers placed behind 25 μ m Be foils. Capacitors consisting of 500 A of dry-grown SiO₂ covered with Al field-plates were exposed behind similar Be windows at the same time as the resist. They showed no change in the C-V characteristics, indicating the absence of radiation damage. Some Al evaporated and splattered from the target was observed on the Be foils which were placed 5 cm from the plasma.

This talk will describe the above experiments. Optimization of the x-ray intensity from laser-produced plasmas will be discussed in detail. Such information is available from on-going laser fusion research. Problems with the use of laser-plasmas as x-ray lithography sources will also be examined. Target debris and rapid heating of the mask are major concerns.

*D. J. Nagel and C. M. Dozier, SPIE Vol. 97, High Speed Photography
(Toronto 1976) p. 132-9.

LASER-PLASMA SOURCE FOR PULSED X-RAY LITHOGRAPHY

D. J. Nagel, R. R. Whitlock, J. R. Greig and R. E. Pechacek
Naval Research Laboratory, Washington, D. C. 20375
M. C. Peckerar
Westinghouse Electric Corporation, Baltimore, MD 21203

Abstract

The exposure of an x-ray resist by radiation from laser-heated plasmas was recently demonstrated. Single-shot submicrosecond exposures with a very favorable x-ray spectrum are possible. In order to reduce the cost of a laser-plasma x-ray lithography system, it is desirable to maximize the intensity in the soft (1 to about 3 keV) range. The x-ray output of laser-plasmas depends on laser pulse parameters (wavelength, pulse shape and energy), the focal conditions, and the target composition and geometry. Laser-plasma x-ray characteristics and their sensitivity to experimental parameters are reviewed in this paper. Presently available information indicates that a Nd:glass laser having pulse width in or near the 1-10 nsec range with at least 500 J of energy should be adequate for practical single-shot x-ray lithography.

1. Introduction

X-ray lithography will be used for routine replication of near-micron and submicron features in microelectronics and other devices. There are many sources which can be considered for x-ray lithography. However, only a few of them have an adequate combination of the characteristics required for x-ray lithography. An ideal x-ray source for lithography can be described as follows:

A. Size and Emission Direction: The source should be small (≤ 1 mm), or else collimated, in order to cast sharp shadows through a mask.

B. Intensity: The source should require an exposure time of no more than one minute and preferably much less.

C. Spectrum: The x-ray energy should exceed about 1 keV in order to penetrate the mask support but should not be much harder. This maximizes resist absorption and minimizes damage to radiation-sensitive structures.

D. Irradiated Area: The source should be able to uniformly illuminate several mask-substrate combinations simultaneously.

E. Repetition Rate: The turn-on time delay, if any, should be shorter than the time to align masks and substrates and place them in position for irradiation.

F. Cost: As low as possible.

Two x-ray sources have been used in lithographic research in the past five years:

(a) line and continuum radiation from electron impact on solids and (b) continuum radiation from electron radial acceleration, i.e., synchrotron radiation. Both of these sources have significant drawbacks. Electron-impact (x-ray tube) sources have their intensity limited by heat dissipation in the target. Exposure times are long, usually greater than five minutes. Also the spectra of electron-impact sources have a hard component which tends to produce radiation damage in silicon compounds. Synchrotron radiation sources are also slow. More importantly, they are very expensive and not readily available.

In the recent past, we addressed the question: Are there small, bright x-ray sources which are suitable for pulsed x-ray lithography? The spectral and temporal characteristics of flash x-ray sources, which are given in Figure 1,⁽¹⁾ provide part of the answer to the question. It is seen that several submicrosecond sources exist and some of them notably plasma sources, have desirable spectra (in the 1-5 keV range). Of these, laser-heated plasmas appear to be the most promising because they are small and very bright, with significant energy in the soft x-ray range. The repetition rate of high-power lasers, namely a few shots per hour, is acceptable, but their cost is a major question.

In order to demonstrate the technical feasibility of x-ray lithography with radiation from laser-heated plasmas, we performed a series of trial experiments.⁽²⁾ Wafers coated with polybutene-1-sulfone (PBS) were irradiated with x-rays from plasmas produced at the focus of a Nd laser. Multiple-shot exposure was required because the available laser was not optimum for x-ray production. Lines as fine as 7500 Å were replicated in the PBS. Quantitative x-ray measurements yielded a sensitivity value for PBS similar to that obtained with a steady state x-ray source. Hence, high-intensity reciprocity loss in PBS does not appear to be a problem. MOS capacitors were also exposed to x-rays from the laser-heated plasmas. Capacitance-voltage plots made before and after x-irradiation were almost identical. These indicate that the soft-x-ray laser-plasma source produces negligible substrate radiation damage. In brief, the work to date shows that single-shot exposure of resists with radiation from laser-heated plasmas is possible.

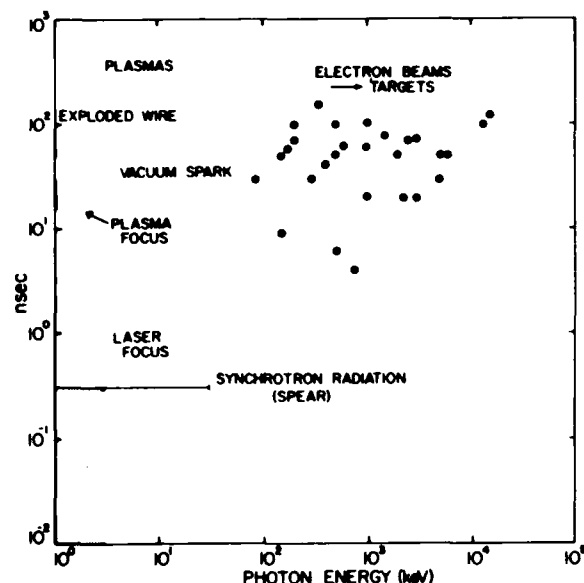


Fig. 1. Plot giving the pulse length and spectral energy of electron-impact, synchrotron-radiation and high-temperature-plasma flash x-ray sources.⁽¹⁾ The electron energy (maximum photon energy) is plotted for beam-target sources.

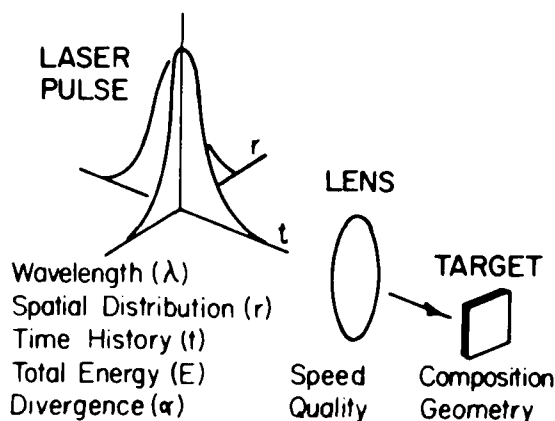


Fig. 2. Schematic indication of the pulse, focal and target characteristics which influence laser-plasma x-ray emission.

Problems with the laser-plasma source for x-ray lithography were observed during the demonstration experiments. The mask-substrate combinations were placed close (5 cm) to the plasma and the emission region is oblong (about 400 μm diameter parallel to the target surface and 600 μm along the target normal). As a result, penumbral effects were evident and they were different for lines in different directions. Also, material from the target was found on the mask support. Another potential problem, not measured to date, is rapid mask heating due to absorption of short, intense x-ray pulses. Work is in progress to clarify and alleviate these problems.⁽³⁾

It is clearly desirable to maximize the x-ray output of laser-plasmas in order to make resist exposures in a single shot and to increase the plasma to mask-wafer spacing. The x-ray emission from laser-heated plasmas depends on the characteristics of the laser pulse, how it is focused onto a target and the target characteristics. These parameters are indicated schematically in Figure 2. The laser wavelength is fundamentally important to x-ray generation. The temporal and spatial variations (shapes) of the pulse at focus determine the fractional absorption of the laser light, and hence the plasma and x-ray characteristics. The composition, geometry and orientation of the target are also important. This paper considers which combination of laser and target parameters yields the best intensity of x-rays in the soft x-ray region from laser-plasmas. Not all past laser-plasma x-ray research is surveyed. Our aim is to present enough data to make clear (a) which parameters are relevant and (b) their effects on x-ray yield. The next section (II) gives a general description of the characteristics of laser-heated x-ray sources. Dependence of the characteristics on laser and target parameters is considered in the following two sections (III and IV). The concluding section (V) summarizes the desirable and the undesirable qualities of the laser plasma source for x-ray lithography.

II. Laser-Plasma X-Ray Emission

The x-ray characteristics include the source size, pulse length, spectrum and intensity, and variations in these factors with view angle (emission direction). Many laser-plasma x-ray measurements have been made in recent years as part of fusion-energy research programs. Sample results will be given in this section in order to portray the general nature of the laser-plasma x-ray source. Attention will be given to x-ray emission above 1 keV which is useful for x-ray lithography. We will not review the instrumentation and techniques employed for plasma x-ray measurements. There is much information already available on those topics.⁽⁴⁾

The size of the x-ray emitting region in a laser-heated plasma is larger than the focal region due to thermal conduction and plasma blowoff. Focal diameters usually fall in the 30 to 300 μm range for high-temperature plasma production, while the intense x-ray emission comes from a region up to ten times larger parallel to the target surface. Actually, there is no well-defined limit to the emitting region. Images taken with small pinholes ($\sim 10 \mu\text{m}$) or high-resolution ($\sim 10 \mu\text{m}$) x-ray microscopes reveal structure finer than the focal half-energy diameter for some laser beams.⁽⁵⁾ Intense x-ray emission usually comes from a region about 1 mm in extent. However, use of high-efficiency (thermal) low-resolution x-ray imaging instruments shows that part of the emission occurs beyond 1 μm from the target surface in some cases.⁽⁶⁾ The low-intensity region is usually 2 to 10 times longer (along the target normal) than it is wide (parallel to planar target surfaces). Images taken with fine and coarse pinholes are shown in Figure 3.⁽⁷⁾ The extensive low-intensity region is striking, but the compact and intense core of the x-ray source is more important.

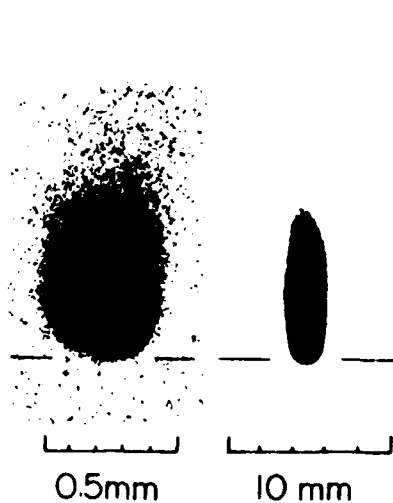


Fig. 3. X-ray pinhole-camera photographs of the Al plasma produced by 40 nsec, 40 J Nd laser pulses taken with 25 μm diameter (left) and 1.15 mm diameter (right) pinholes.⁽⁷⁾ The target surface is indicated.

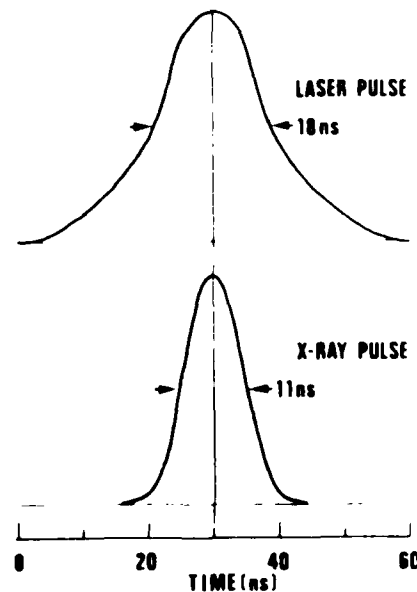


Fig. 4. Time history of a 10 J ruby laser pulse and the x-ray emission it produced when focused onto a Mo target.⁽⁸⁾

The time-variation of laser-plasma x-ray emission can be measured with a variety of fast detectors, some with response times approaching 1 psec.⁽⁸⁾ The x-ray pulse length is closely-related to the laser pulse length, that is, the FWHM of the two pulses tend to be the same within a factor of about three. X-ray emission from plasmas created by short laser pulses lasts somewhat longer than the laser pulse due to the plasma-cooling time. This is especially true for soft x-rays which can be emitted from relatively cool plasmas. X-ray pulses from laser-plasmas can be narrower than the laser pulse also. The x-ray intensity is very sensitive to the plasma temperature (which is largely determined by the irradiance in W/cm^2). For low laser irradiance, the plasma may not emit x-rays with enough intensity to be recorded except near the peak of the pulse. Then the useful x-ray emission occurs only near the laser-pulse maximum and the x-ray emission time is shorter than the laser pulse time. An example of such behavior is given in Figure 4.⁽⁸⁾

The space- and time-integrated x-ray spectrum of a laser-heated plasma is obtained forward to measure.⁽¹⁰⁾ There is usually intense soft x-ray emission in the region below 9.1 keV to about 3 keV. Many lines from various transition elements are observed. Ionization appear above continuum radiation, which is the most prominent feature of the spectrum. Such emission from plasma excitation of the K-shell of Al is shown in Figure 5a. There are usually no lines above a few keV in plasma spectra, but the continuum extends to high energies, sometimes in excess of 100 keV. However, the continuum intensity drops rapidly with photon energy so the total energy in photons above a few keV is small. Figure 5b.⁽¹²⁾

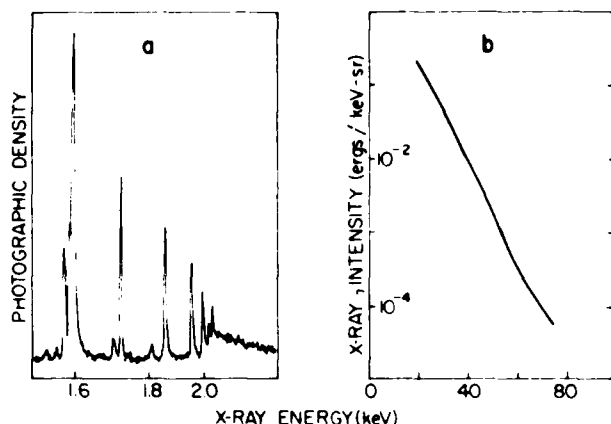


Fig. 5. X-ray spectra produced by 0.1 nsec, 15 J pulses incident on Al as measured with (a) crystal spectrograph⁽¹¹⁾ and (b) electronic detectors.⁽¹²⁾

in the integrated x-ray intensity with emission angle was reported also,⁽¹⁵⁾ although relatively little data are available. The dependence of total x-ray intensity on polar angle (measured with respect to the target normal) has been measured for plastic and aluminum targets.^(14,15) Maximum intensity is emitted along the target normal, with a decrease (due to self absorption of line radiation in the Al plasma) to a 30% lower value at 45° . There is one report⁽¹⁶⁾ of azimuthal anisotropy in x-ray emission (relative to the laser polarization direction) but such an effect was not found in other work.⁽¹⁵⁾

III. Laser Pulse and Focal Dependence

It would be desirable to know how each laser-plasma x-ray characteristic depends on the laser pulse parameters (wavelength, pulse shape and total energy) and focal parameters (lens speed and target position relative to best focus) for a wide range of target conditions (compositions and geometries). Although several measurements of x-ray sensitivity to laser pulse factors have been made, the overall picture is far from complete. We review much of the work that is available, with emphasis on x-rays in the soft x-ray region. There are a few measurements for most of the relevant parameters: the laser wavelength, pulse length and energy, and the lens-target spacing. Multiple pulse effects will also be discussed.

Laser wavelengths extend from the UV to the far IR regions. However, only high-power ruby ($\lambda = 0.69 \mu\text{m}$), Nd ($\lambda = 1.06 \mu\text{m}$) and CO_2 ($\lambda = 10.6 \mu\text{m}$) lasers have been used significantly for laser-plasma x-ray studies. Ruby lasers have not been used in x-ray work above about 10^{12} W/cm^2 , a relatively low power density. Hence, we compare only Nd and CO_2 laser wavelengths. Early work with irradiance values near or below 10^{13} W/cm^2 incident on low atomic number targets indicated that the conversion fraction for x-rays above 1 keV is at least one order of magnitude higher for the shorter-wavelength Nd lasers than for CO_2 lasers.⁽¹⁵⁾ Comparison of early Nd⁽¹⁰⁾ and recent CO_2 measurements^(17,18) across the periodic table at about 10^{14} W/cm^2 confirmed the inference. Nd lasers are more favorable than CO_2 lasers for x-ray production because of higher plasma electron density favors x-ray emission and Nd laser energy tends to be deposited in denser plasma regions compared to CO_2 laser energy.

X-ray production presently requires lasers with pulse duration less than about 100 psec, a time about 10^5 longer than the narrowest pulse laser now possible. The question of what pulse length in this wide range to use in order to maximize x-ray production will be addressed by referring to Figure 6.⁽¹⁹⁾ Plotted there is the conversion fraction for 1.5 keV Nd laser incident on Al targets. The curve was obtained by extrapolating data for pulse lengths of 50, 100, 250 and 500 psec and 4 nsec from Figure 5. An uncertainty of about 20% is associated with the curve due to the extrapolation, but the general shape is not in doubt. Knowledge of the laser pulse and focal parameters is essential to use this curve. The existence of a peak is reasonable, since the electron density in the plasma will be high in which ionization tends to be most efficient. However, the peak is at a pulse length of the high temperatures needed for x-ray production. The peak is at a pulse length of about 100 psec. Figure 6 is both uncertain and incomplete. The data are from a number of sources, and critical and experiments with longer pulse lengths are needed to complete the picture.

The total x-ray emission can be obtained by integration of spectra, or by use of broadband (spectrally-insensitive) detectors.⁽¹⁰⁾ Laser-plasma x-ray sources can have high efficiency for x-ray production. Over 10% of the incident laser energy can be emitted as x-rays.^(13,10) Such "up conversion" is remarkable in its extent (infrared or visible radiation is changed to x-rays) as well as its efficiency.

The emission from most x-ray sources is anisotropic for a variety of reasons. The same can be true of the laser-plasma source. Because the x-ray emitting region is not spherical, it appears to have a cross section which depends on the angle of view (the direction of emission). There is no data on variations of the x-ray time history with emission direction. However, relative intensities of time-integrated spectra have been found to depend significantly on the emission angle.⁽¹⁴⁾ Variation

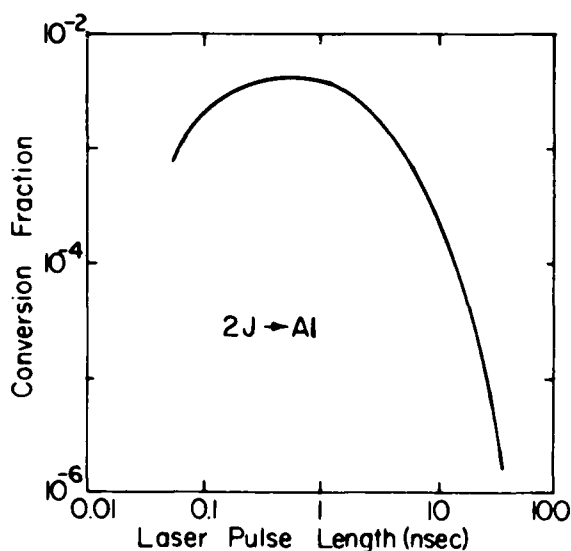


Fig. 6. X-ray conversion fraction (emission > 1 keV into 2π) for 2 J Nd-laser pulses incident on Al targets as obtained by extrapolation of data taken at several pulse lengths. (19)

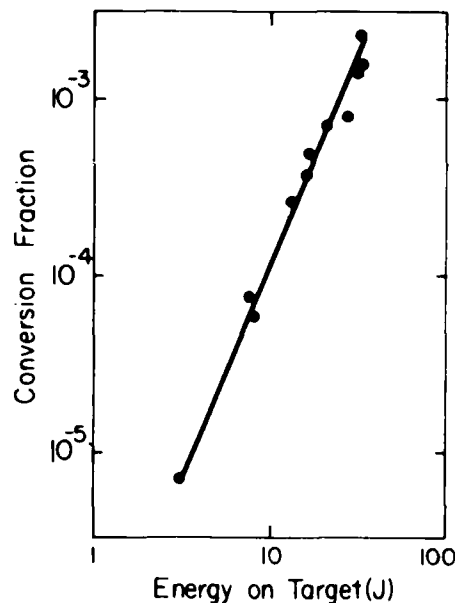


Fig. 7. X-ray conversion fraction (emission > 1 keV into 2π) for 40 nsec Nd-laser pulses incident on Al. (7)

If the peak in conversion efficiency vs pulse length is located at, say, 1 nsec, the most favorable pulse length will be several nsec because the energy which can be extracted from a laser increases with pulse length. That is, the total x-ray intensity (conversion fraction times laser energy) is what must be maximized.

The total energy in a laser pulse also significantly affects the x-ray conversion fraction. In general, increasing the laser energy on target increases the plasma temperature and improves the x-ray intensity. The x-ray intensity usually varies with laser energy as E^n where n is 2.5 to 3.0. An example is given in Figure 7. (7) However, there is a limit to this increase when the plasma is hot enough to strip all electrons from the atomic shell responsible for emission in the soft x-ray region. Then the x-ray output saturates, an effect which has been observed (10) and calculated. (20)

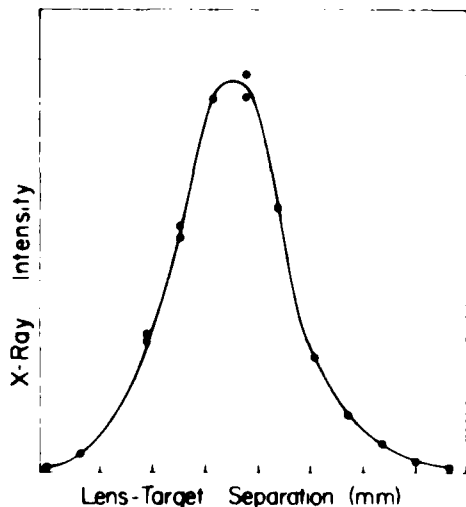


Fig. 8. Variation in x-ray intensity with changes in the lens-target spacing for the laser pulse shown in Figure 4. (9)

The variation in x-ray intensity with focus (lens-target spacing) has been measured in several experiments. Usually the intensity variation has a single peak as shown in Figure 8. (9) However, in some studies, the maximum x-ray intensity was not found at focus, but to either side of it. The cause of such variation is not clear, but it is an easy matter to experimentally determine the target position for maximum x-ray output for any laser.

The data presented in this section were taken with single laser pulses. Multiple pulse effects on x-ray production have been explored in only a few experiments. Some data have been taken with a single prepulse to create a plasma at the target prior to arrival of the larger main pulse. Although the data are sparse, it appears that a prepulse increases soft x-ray intensity for laser pulses of about 1 nsec or shorter. (10) However, use of a prepulse ahead of a 40 nsec

pulse decreased the x-ray output. (21) No general statements can be made now about what prepulse spacing and magnitude would be desirable for pulses near 10 nsec, which might be optimum for x-ray production. Possibly, a prepulse has little effect for such a pulse length.

IV. Target Dependence

The situation concerning dependence of laser-plasma x-ray intensity on target composition and geometry is similar to that for the laser pulse and focal characteristics. Again, a great deal of work remains to be done although some significant effects have already been discovered. The measured dependence of soft x-ray intensity on target composition will be given in this section. Target geometry effects will also be discussed.

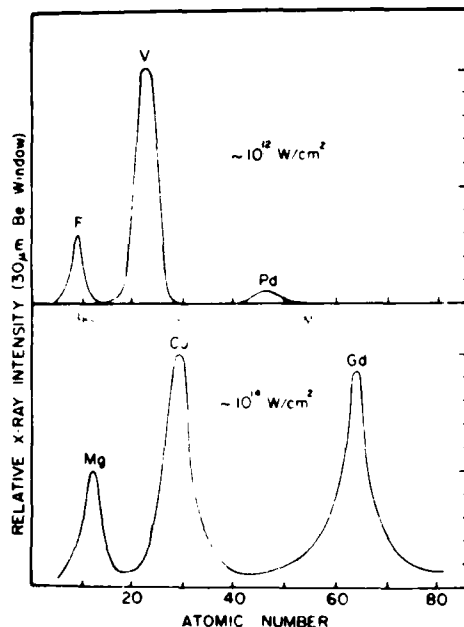


Fig. 9. Atomic-number dependence of x-ray intensity above 1 keV for 10^{12} W/cm² (top) and 10^{14} W/cm² (bottom). (22)

increase in x-ray intensity due to using a foil or multi-layer target. Many x-ray measurements have been made for mass-limited disc or spherical targets. Reduction of lateral energy transport should yield a hotter plasma and more x-ray emission.

There is little x-ray information on the effects of focusing the laser pulse into target indentations. The x-ray spectrum obtained by shooting into a crater from the previous shot was somewhat more intense than that from irradiation of the planar surface. (23) The use of targets with conical indentations yielded high density plasmas which should be intense x-ray emitters, but no comparison of x-ray intensity from conical and planar targets was reported in that work. (24) Nor is there information on the angular distribution of x-rays from indented targets.

V. Conclusion

The work summarized above shows that the laser-plasma x-ray source has most of the characteristics desirable for x-ray lithography, as listed in the introductory section. The most intensely-emitting region of the laser-heated planar target is at least as extended as is possible to obtain as such as about 0.1×10^{-2} cm of x-ray in the 1-keV range, as compared to planar targets, where it is the laser energy on target in a focused, circular spot. Exposure of polybutene-1-sulfone positive x-ray resist, which requires 14×10^{-2} cm of x-ray intensity, at a distance of 25×10^{-2} cm from the plasma, would require about 100 J of energy in a pulse with probably no more than the 1-keV intensity mentioned. With a 100 J laser-pulse separation, it should be possible to replicate a 1000-Å pattern at a 1000-Å pitch on the size of the maskwater alignment substrate. The intensity of the x-ray source is

Most work in which the target composition was varied was done for thick planar targets. In the first study, a Nd laser was used at 10^{14} W/cm². A strong atomic number (Z) dependence was found. Subsequent studies, done with ruby and CO₂ lasers, confirmed the oscillatory behavior of x-ray output with Z. Smooth curves drawn from the results of the Nd and ruby laser work are given in Figure 9. (22) The difference in laser wavelength (1.06 vs 0.69 μ m) is not as significant as the irradiance and temperature differences. In both cases, maxima occur when the binding energies of the atomic shells (K, L and M) are properly matched to the plasma electron energies (temperatures). The higher irradiance yields a higher temperature and the peaks are at higher Z values. More important, the maximum conversion fraction into 2π is about 10^{-1} for the higher temperature and 10^{-5} for the cooler plasmas. There is a clear need to choose the correct target as well as the best laser pulse and focal conditions in order to optimize x-ray output.

Most x-ray studies are done with the laser pulse normally incident on a planar target. Non-normal incidence is not expected to yield higher x-ray intensity, although no x-ray data as a function of incidence angle is available. There is some work with thin and layered planar targets, but none of it indicates an

500 μ m

We have concentrated on x-ray emission from laser-heated plasmas. However, other source characteristics are important to the use of laser-plasmas as sources for x-ray lithography. In particular, vapor and debris ejected from the focal region can coat masks, or alternatively, a thin x-ray-transmissive shield must be used between the plasma and the masks. The amount and angular distribution of material removed from the target is being measured and will be reported later.⁽³⁾ Here we merely present one picture showing the late-time development of a laser-target interaction. Figure 10 is a 5 psec exposure taken 171 nsec after a 5 nsec Nd pulse struck the edge of a clear plexiglass sheet.⁽²⁶⁾ Material ejected from the crater formed as the million-degree surface plasma dissipated is seen to have a conical distribution. A shock wave propagating into the material in response to the blowoff is also visible. Use of a thin target would not decrease the x-ray intensity, but it would substantially reduce the amount of molten material thrown out of the crater region. Furthermore, the debris from a thin target is primarily accelerated toward the back of the target.⁽²⁷⁾ Also, targets with high-vaporization energies (melting points) have smaller craters⁽²⁸⁾ hence, if two different materials yield the same x-ray intensity, the higher melting point material will be favored if its cost is not prohibitive.

The x-ray emission work which forms the basis of this paper was performed in several studies over the past five years (see references). Continued collaboration with L. J. Birks, R. D. Blech, P. G. Burkhalter and J. M. Dozier is a pleasure to acknowledge. We thank J. M. McMahon for providing information on laser system characteristics.

1. Nipel, D. J. and Dozier, G. M., in M. J. Whittlock, Editor, "High-Speed Photography," Int'l. Conf. on High-Speed Photography, SPIE Vol. 40, 1971, pp. 1-10.
2. Nipel, D. J., Becker, M. J., Whittlock, R. R., Young, J. C., and Mallezzi, R., submitted to Appl. Phys. Letters.
3. Becker, M. J., Young, J. C., Nipel, D. J., Whittlock, R. R., and Whittlock, R., Proc. of 1971 Meeting of the Applied Optics Society, Seattle, May 1971.
4. See periodical progress report, "High-Speed Photography," submitted to the Laboratory, Report UCR-69-21, 17 May 1969, Los Alamos Scientific Laboratory, UCRL-6519-ER (Nov. 1969) and Naval Research Laboratory, Memorandum Report 440, 1969.
5. Proc. of Symposium on X-Ray Imaging, 1970, Los Angeles, Calif.
6. Whittlock, R. R., Dozier, G. M., and Nipel, D. J., in M. J. Whittlock, Editor, "High-Speed Photography," SPIE Vol. 40, 1971, pp. 11-16.
7. Whittlock, R. R., Young, J. C., and Nipel, D. J., submitted to Appl. Phys. Letters.
8. Richards, M. D., in "High-Speed Photography," SPIE Vol. 40, 1971, pp. 17-20.
9. Lee, L. A. and Nipel, D. J., Appl. Opt., 10, 1971, pp. 21-23.
10. Nipel, D. J., et al., in M. J. Whittlock, Editor, "High-Speed Photography," SPIE Vol. 40, 1971, pp. 24-26.
11. Whittlock, R. R., et al., in Naval Research Laboratory, Report 440, 1969 (M. J. Whittlock, Editor, "High-Speed Photography," SPIE Vol. 40, 1971), pp. 165-172.
12. Young, J. C., et al., Appl. Opt., 10, 1971, pp. 27-29.
13. Mallezzi, R. J., et al., in M. J. Whittlock, Editor, "High-Speed Photography," SPIE Vol. 40, 1971, pp. 30-32.

Laser Physics, Wiley and Sons, New York, 1970, pp. 10-11.

14. Chase, L. F., et al., Appl. Phys. Letters, 30, 137 (1977).
15. Violet, C. E. and Petruzzzi, J., J. Appl. Phys., 48, 4984 (1977).
16. Krokhin, O. N., et al., JETP Letters, 20, 105 (1974).
17. Enright, G. D., Burnett, N. H. and Richardson, M. C., Appl. Phys. Letters, 31, 494 (1977).
18. Lee, P., et al., unpublished.
19. Whitlock, R. R., et al., Bull. Am. Phys. Soc. 22, 1119 (1977).
20. Whitney, K. G. and Davis, J., Appl. Phys. Letters, 24, 509 (1974).
21. Greig, J. R., Nagel, D. J. and Whitlock, R. R., unpublished.
22. Bleach, R. D. and Nagel, D. J., J. Appl. Phys., June 1978.
23. Nagel, D. J. and Whitlock, R. R., unpublished.
24. Boiko, V. A., et al., JETP Letters, 20, 50 (1974).
25. McMahon, J. M., private communication.
26. Ariqa, S. and Sigel, R., Max-Planck-Institut für Plasma Physik Report IV/81 (March 1975).
27. Greig, J. R. and Pechacek, R. E., J. Appl. Phys., 48, 596 (1977).
28. Bleach, R. D. and Nagel, D. J., unpublished.

HIGH SPEED X-RAY LITHOGRAPHY WITH RADIATION FROM LASER-PRODUCED PLASMAS

M. C. Peckerar, J. R. Greig, D. J. Nagel
R. E. Pechacek, R. R. Whitlock

Westinghouse Electric Corp. Baltimore, MD 21203
U. S. Naval Research Laboratory, Washington, D.C. 20375

I. INTRODUCTION

X-ray lithography offers the possibility of replication of micron-scale features without the diffraction and multiple reflection effects associated with UV radiation or the scattering effects present in electron-beam exposures.¹ Until recently, electron-impact and synchrotron-radiation sources were the only serious contenders for x-ray lithography exposures. However, a wide variety of pulsed x-ray sources are available.² It was shown recently that short pulses of x-rays from laser-heated, million-degree plasmas could expose an x-ray resist with negligible reciprocity loss and substrate radiation damage.³ That development required attention to both optimization of x-ray intensity from laser plasmas and problems associated with use of the laser plasma source for x-ray lithography. Maximization of x-ray intensity, which depends on laser pulse characteristics (wavelength, pulse-width and energy), focusing conditions, target composition and geometry, was reviewed in a recent paper.⁴ The purpose of this paper is to review the difficulties which may arise in routine use of laser-plasmas for replication and to present methods of overcoming these difficulties. Premature laser-target interaction, debris from the target, mask heating and resist sensitivity are treated in successive sections after the highlights of recent pulsed x-ray lithography measurements are reviewed.

II. SUMMARY OF EARLIER EXPERIMENTS

A Nd:glass laser with a 40ns pulse was used (see Figure 1). The total laser light output possible with the system employed is 100 Joules. However, laser target interaction (to be discussed below) limits the actual power which could be placed on target to 1/3 this value. The laser light incident on target heats the target material (in this case aluminum) to about three million degrees Kelvin. A plasma of free electrons and ions is produced. X-rays are emitted as a result of collisions between different charge species in this hot plasma. The x-ray spectrum contains both line and broad-band continuum. For the aluminum target case, about 90% of the x-ray energy is in an aluminum K-line at 1.6keV. The broad band continuum occurs mostly in the subkilovolt region and is easily filtered with a 25 μ m beryllium foil. The region of intense x-ray emission (as determined by pin-hole pictures) appears to be a circle of about 0.4mm when viewed face-on to the target. The emission region extends 0.6 mm in a direction normal to the surface. The plasma x-rays are emitted in a pulse with a FWHM of 15nsec.

With 30 Joules of laser light incident on target, we have been able to completely expose polybutene-1-sulfone (PBS) behind 25 μ m Be in 60 laser

shots. A relief image (recorded in PBS) of a gold pattern on 25 μ m beryllium is shown as Figure 2. The mask was 5 mils from the wafer and the mask-to-source distance was 5cm. Penumbra blurring due to the asymmetric source spot is evident and will be discussed in the next section. C-V dot radiation monitors run during a resist exposure show little radiation effect (see Figure 3). This is probably due to the absence of high energy continuum. The amount of x-ray energy incident on the mask was determined with a PIN detector placed in the target chamber. Five J/cm³ were needed to obtain exposure of PBS. This compares favorably with the fourteen J/cm³ published value⁵ and indicates no reciprocity loss.

With the present laser system, a fairly long time is required to produce 60 pulses. Five minute rod cooling times are needed between shots. But, by reducing the pulse length to the range between 5 and 10ns, conversion efficiencies of laser light to x-ray energy which are greater than 10% are possible (compared to the 0.3% efficiency of the present system). It should be possible to expose PBS with a single shot if the laser, focusing and target parameters are chosen properly.⁴

III. SOME PROBLEMS WITH LASER-PLASMA X-RAY LITHOGRAPHY

A. Laser-Target Interactions

High-power lasers generally consist of an oscillator in which a pulse is produced, commonly by Q-switching.⁶ The pulse is then sent through one or more amplifiers before being focused on to the target. In normal operation, the oscillator, amplifier(s) and target do not communicate with each other save for single pulse generation, amplification and use. The cause, effects and cures of unwanted interactions between laser components and the target are described in this section.

In the demonstration experiments described above, the target was an aluminum rectangular slab. The slab was tilted so that specular reflection could not send radiation back to the laser. But a "rough" aluminum surface can be a good diffuse reflector. Then as much as 5% of any radiation coming from the laser can be reflected back to it by the aluminum target. If this happens, the laser can be considered as consisting of three interacting cavities - Figure 4. The oscillator cavity contains the reflecting prism, the oscillator rod, a set of polarising plates, a Pockels cell (1) and the sapphire output mirror. What we call the external cavity contains the other side of the sapphire output mirror, a second Pockels cell (2), a set of polarising plates, the two amplifier rods, the focusing lens, and the aluminum target. The third cavity is the combination of these two cavities. While the laser rods are being pumped, the Pockels cells are stressed (electrically) so that they act as $\frac{1}{2}\lambda$ plates. Thus both cavities are prevented from lasing. However, as the population inversion rises, the small signal gain in the amplifier rods (length 82cm) becomes so large that even a few percent reflection from the target is sufficient to overcome the Pockels cell - polarizing stack combination (rejection ratio $\sim 10^3:1$) and produce net gain in the combined cavities. Such interaction can cause weak "normal mode" prelasing to occur as much as 50 μ sec before the desired giant pulse output. The subsequent giant pulse is very small and the x-ray yield negligible. With somewhat less reflection from the target ($\sim 1\%$) such pre-lasing does not occur. But once the

Pockels cells are opened (presently almost simultaneously) the three different cavities all begin to avalanche. Under normal operating conditions and with no reflections from the target, the oscillator cavity takes ~150ns to produce its output pulse. During this time, and because of the large gain in the amplifier rods, pulses also grow both in the external cavity and in the combined cavity. The growth is due to the fact that the single pulse transit time of the combined cavity is ~65ns (i.e., the distance from the retro-prism in the oscillator cavity to the target is ~65 feet). The resultant output pulse from the oscillator is a combination of two or even three pulses coming from the different cavities, which, although amplified non-linearly in the amplifiers (the first peak sees greatest gain), still results in a broadened output pulse with a slower rise and greatly reduced x-ray yield. In both cases the total energy in the laser output pulse remains about the same as in the normal Q-switched output but the power density achieved at the target and the x-ray yield are much lower.

Typical laser output pulses for a normal laser output pulse are shown in Figure 5A and those from a pulse showing small laser-target interaction are shown in Figure 5B. A reduction of about 50% in the laser output is seen to eliminate almost all of the x-ray output (as measured with a PIN diode).

Laser-Target interaction can be controlled by a combination of techniques

- i) If the laser is placed far enough from the target (~200 feet) small interactions cannot affect the laser output.
- ii) Simply delaying the opening of Pockels cell in the external cavity reduces the interaction of the cavities but is not very effective.
- iii) Using optically polished targets eliminates diffuse reflections.
- iv) Using anodized, sand-blasted, aluminum targets removes both specular and diffuse reflections.
- v) Insertion of a Faraday rotator and polarizing plates between the target and the laser (Figure 4) eliminates laser-target interaction by rotating the plane of polarization of the radiation returning through the Faraday rotator so that it is reflected at the polarizing plates.

In our case, not having a Faraday rotator, and before realizing the importance of target surface treatment, laser-target interaction was controlled by limiting the laser energy incident on the target to 1/3 the laser output energy. This was of course very wasteful but did allow us to demonstrate pulsed x-ray lithography. Now we have found that target surface treatment i.e., sand blasting and anodizing, maintains the characteristic aluminum x-ray emission but eliminates laser-target interaction. With higher powered lasers necessary for single pulse exposures, these surface treatments will probably have to be combined with a Faraday rotation system.

B. DEBRIS EJECTED FROM THE TARGET

Target debris can be a serious problem, damaging delicate x-ray

masks if care is not taken. Only a small amount (~a few %) of the material removed from the target is ablated, as vapor, during the laser pulse. The rest leaves the target as liquid material much later as the million-degree plasma dissipates. For thick targets the liquid ejecta is confined to a cone about the normal to the target surface. The setup used to measure the direction of ejected liquid is shown in Figure 6. The distribution obtained with Al target in 10 shots is given in Figure 7. A well-defined cone with a half angle of 55° was found. The obvious way of minimizing debris damage is by keeping the mask away from the main stream of ejected liquid material. The amount of ejected liquid is minimized by the use of high melting point targets. We have also found that by using thin aluminum targets ($\sim 500\mu\text{m}$) the x-ray yield is maintained but most of the liquid debris from the target is ejected through the target, i.e. away from the substrate-mask assembly. This situation is illustrated in Figure 8 using a polyethylene sheet target 0.5mm thick. The small amount of material ablated from the target during the laser pulse, which is inevitably emitted on the mask side of the target, can then be kept from the mask by using a thin film of beryllium or a light plastic sheet in front of the mask. This combination of techniques will, we believe, eliminate the problem of target debris.

C. THERMAL RESPONSE OF MASKS

The heating of masks by x-ray energy absorption is potentially undesirable for long exposures with conventional sources. Heating can cause small dimensional changes and deformation. Thermal cycling may lead to separation of the absorbing material (Au) in a mask from the substrates. Such mask degradation may be serious for pulsed sources in which energy is deposited in a time short compared to thermal-conduction times.

A schematic of an Au-on-Be x-ray mask is given in Figure 9. The maximum deposition and temperature will occur at the surface of each material. The absorbed energy (J) per unit area (A) in a thin surface layer (δ) can be written:

$$\frac{J}{A} = \frac{E}{A} \{1 - \text{Exp}(-\mu\delta)\} \approx \frac{E}{A} \mu\delta \quad (a)$$

where E is the incident energy. From the equation which relates J to specific heat (C) and Temperature rise ΔT , we have $J = MC\Delta T = \rho A\delta\Delta TC$ (b) where M is the absorber mass and ρ its density. Hence,

$$\Delta T = \frac{(E/A) (\mu/\rho)}{C} \quad (c)$$

where (μ/ρ) is the commonly-tabulated x-ray mass absorption coefficient.

To expose PBS, about $20\text{mJ}/\text{cm}^2$ of 1.5 keV radiation incident on the mask is required.⁵ Table I gives the numerical values of constants and results of using these values in equation (c). The Be temperature rise will be greater than the x-ray-induced value in Table I due to UV absorption, but this is not expected to be a problem.

Table I: Mask Heating by Pulsed Sources

	<u>Be</u>	<u>Cr</u>	<u>Au</u>
$\frac{\mu}{\rho}$ @ 1.5keV ($\frac{\text{cm}^2}{\text{gm}}$) (a)	181	2720	2300
Density	1.845	7.18	19.29
Transmission	0.43	0.96	0.05
E/A (mJ/cm^2)	20	8.6	8.3
C(J/gm deg) (b)	1.67	0.46	0.125
ΔT ($^{\circ}\text{C}$)	2.16	50.8	152.7
α (deg^{-1}) $\times 10^6$ (b)	12.3	6.8	14.3
$\Delta L/L = \alpha \Delta T$	2.66×10^{-5}	3.45×10^{-4}	2.18×10^{-3}

(a) W. J. Veigle in "Handbook of Spectroscopy," Vol. I, CRC Press
Cleveland, Ohio 1974

(b) CRC Handbook of Chemistry and Physics, CRC Press, Cleveland, Ohio
1977.

The preferential heating of the absorbant Au is clear from the tabulated figures. The resulting expansion, over 6 times that of the Cr layer, could lead to separation at the Au-Cr interface. These calculations indicate the need for experiments to determine the response of x-ray masks to rapid and repeated thermal cycling. However, the heating effect is not strong enough to seriously degrade resolutions of fine line structures. At most, a two micron Au line will swell 50Å when heated the 153 $^{\circ}\text{C}$ by the pulse.

D. SHORT PULSE EFFECTS IN THE RESIST

Finally, let us consider the response of the resist to pulsed x-rays. Two problems may arise in this area. First, we may see a change in sensitivity due to the rapid energy deposition (reciprocity failure). This was not true with pulses as short as 40ns. The development curve for the resist under pulsed conditions (see Figure 10) compares favorably with that obtained by steady state sources.⁵ For single shot exposures of PBS, however, 5ns-10ns pulses are required. Recipriocity must still be determined for these pulse lengths. Second, heating of the x-ray resist must be considered. From the above discussion, it was shown that heating is directly proportional to x-ray absorption coefficient (μ) in the film. A similar calculation to that performed above indicates (for PBS) a 5 $^{\circ}\text{C}$ temperature rise is possible for single-shot 5ns exposures. This is negligible.

V. CONCLUSION

To conclude, the following potential problems in laser-pulsed x-ray lithography were discussed:

- a) Laser-target interaction
- b) Debris damage
- c) Mask Heating
- d) Short-pulse resist effects

All of these appear to be controllable. Unwanted laser-target interaction can be reduced by a combination of surface treatments and optical isolation. Debris damage can be essentially eliminated by the use of thin targets, proper mask placement and a thin debris shield. Mask heating will not cause resolution degradation and we have observed no reciprocity failure for 40ns pulses.

BIBLIOGRAPHY

1. Spiller, E., Feder, R. "Topics in Applied Physics," H. J. Queisser, ed., Springer-Verlag Berlin, 35 (1977).
2. Nagel, D. J., Dozier, C. M., in Proceedings of the 12th International Conference on High Speed Photography, SPIE, 97, 132 (1977).
3. Nagel, D. J., Peckerar, M. C., Greig, J. R., Pechacek, R. E., Whitlock, R. R. submitted to Appl. Phys. Letters
4. Nagel, D. J., Peckerar, M. C., Greig, J. R., Pechacek, R. E., Whitlock, R. R. to be published, SPIE Proceedings, 135 (1978)
5. Thompson, L. F., Feit, E. D., Bowden, M.J., Lenzo, P.V., Spenser, E. G., J. Electrochem. Soc. 121, 1500 (1974).
6. Lengyel, B.A., "Lasers", Second ed., Wiley-Interscience, New York, (1971).

Figure	Caption
1	Experimental Set-Up of the Laser Plasma X-Ray Exposure System.
2	Relief Image in PBS Showing $1.5\mu\text{m}$ Lines and $0.75\mu\text{m}$ Spaces Exposed with X-Rays From Laser Heated Plasmas.
3	C-V Plots Taken Before and After Exposure to Laser-Plasma Generated X-Rays. Negligible Flatband Shift is Evident.
4	Schematic of Laser Illustrating Various Laser "Cavities". The 25% Sapphire Mirror is Common to Both Cavities.
5	Oscilloscope traces showing laser diagnostics (the fluorescence diode measured the fluorescence radiation from the oscillator rod. The fast diode recorded the laser pulse from the oscillator rod and the visible diode measured the output laser pulse at the target chamber and the x-ray pulse width within the chamber was recorded in the PIN diode). Figure 5a shows normal operation.
5b	Shows reduced laser output and almost no x-ray intensity due to premature laser-target interaction.
6	Schematic of Debris Distribution Experiment.
7	Debris Distribution on the Glass Slide from a Thick Al Target.
8	Shadowgram of Debris Emission From 0.5mm Polyethylene. For Thin Films, the Debris is Shot Out to the Rear, Away From the Wafer, Without Affecting X-Ray Output.
9	Schematic of Au on Be Mask.
10	The Development of Curve for PBS.T is the Post Development Thickness $^{\circ}$ (3500\AA). I_0 is 5 joules/cm^2 .

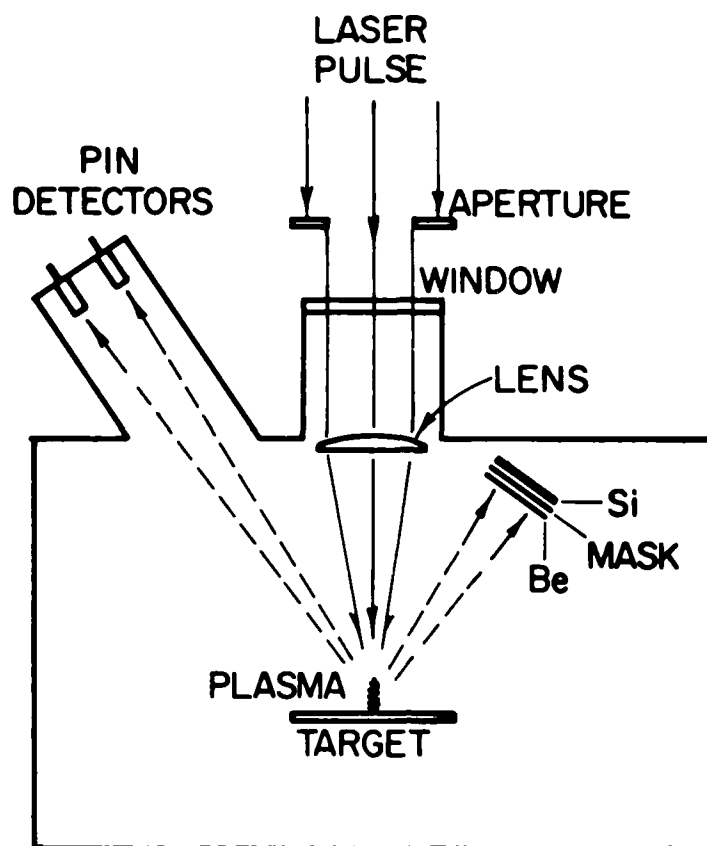


Figure 1

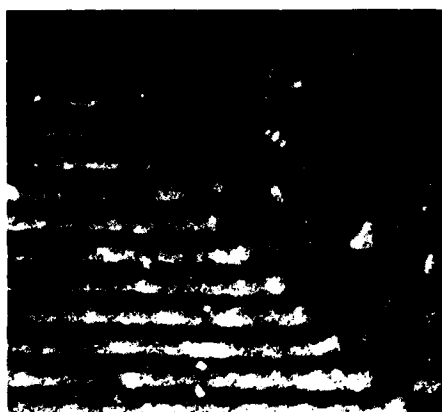


Figure 2

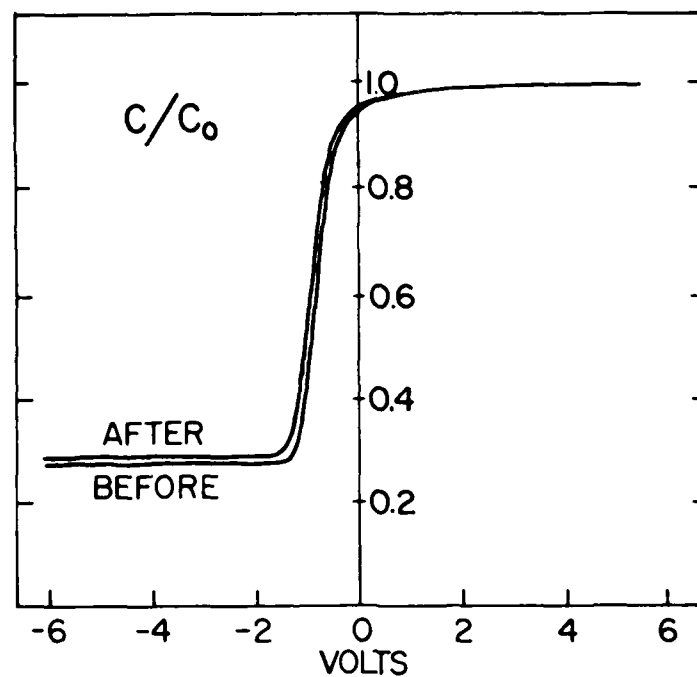
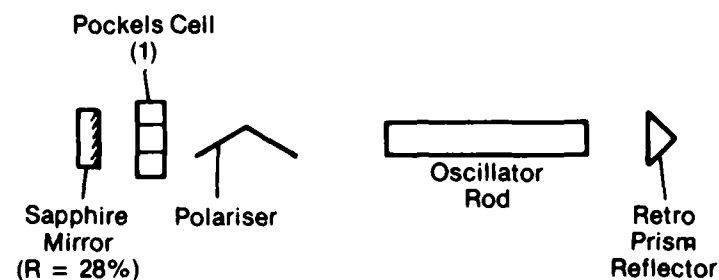


Figure 3

Oscillator Cavity



External Cavity

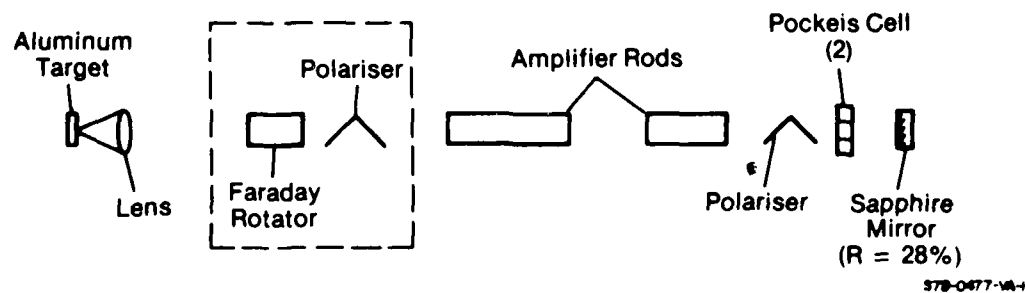
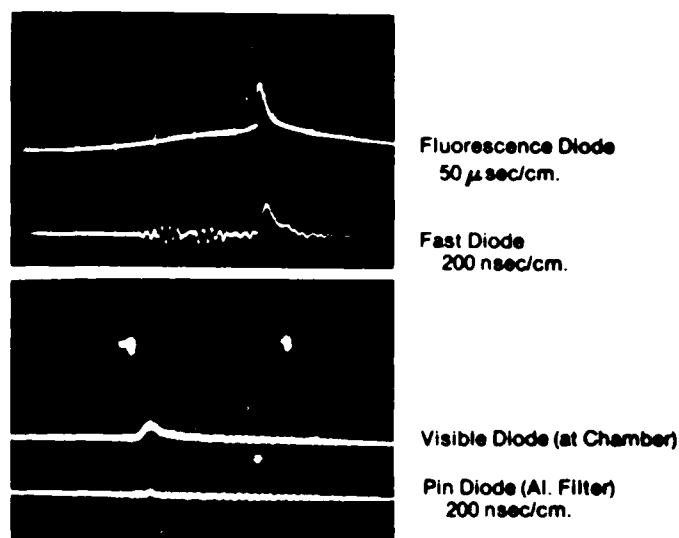
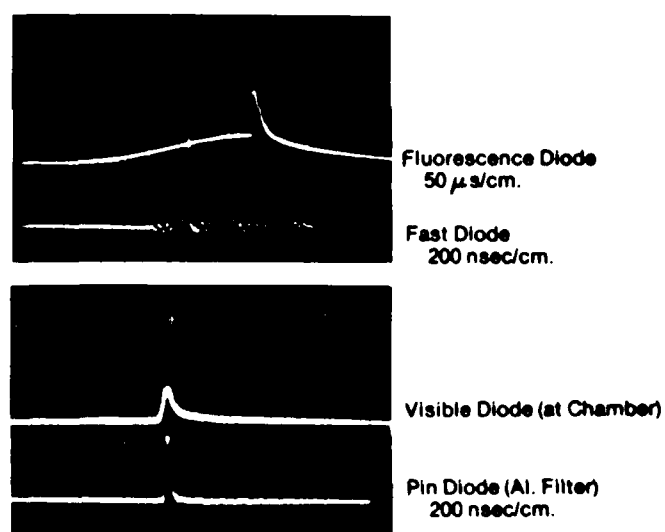


Figure 4



878-0477-PA-4

Figure 5a



878-0477-PA-5

Figure 5b

DEBRIS DISTRIBUTION

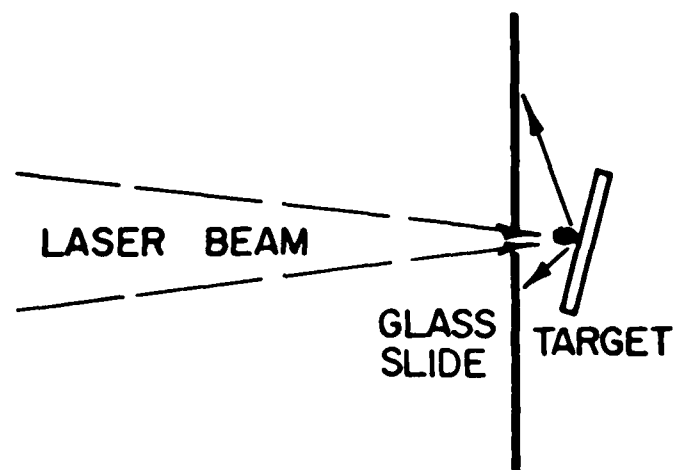


Figure 6



Figure 7

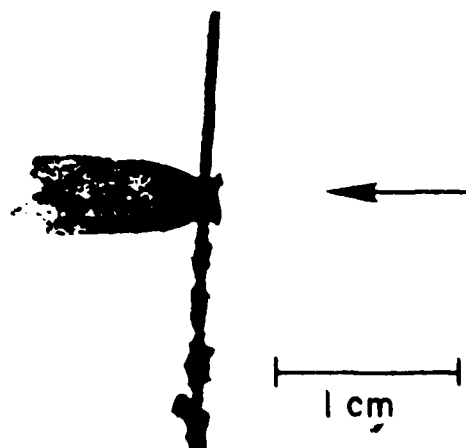
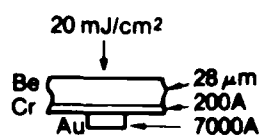


Figure 8



870-0477-M-1

Figure 9

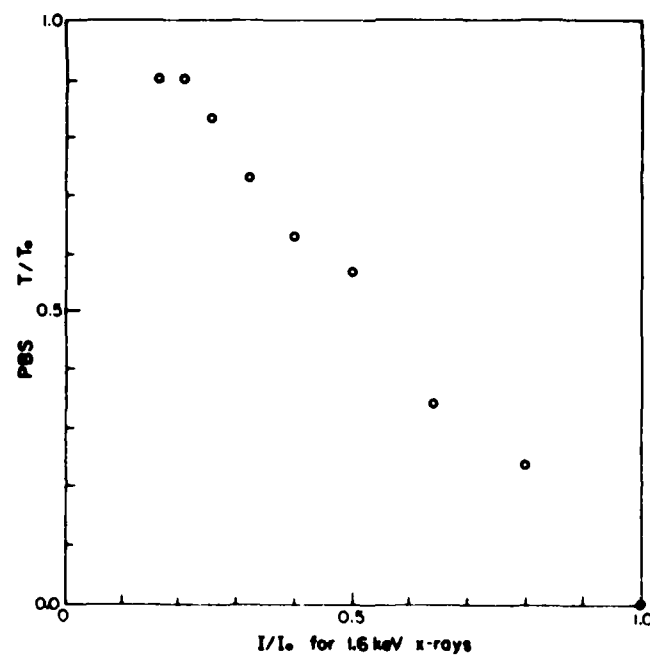


Figure 10

Lithography and High-Resolution Radiography with Pulsed X-Rays

D. J. NAGEL, J. M. MCMAHON, R. R. WHITLOCK,
J. R. GREIG, R. E. PECHACEK,
and M. C. PECKERAR*

Naval Research Laboratory, Washington, D. C. 20375 U.S.A.

**Westinghouse Advanced Technology Laboratories, Baltimore,
Maryland, 21203 U.S.A.*

X-rays from laser-heated plasmas can expose photoresists in less than a microsecond. Plasma emission above 1 keV is potentially applicable to routine replication of microelectronics and other masks by X-ray lithographic techniques. Intense subkilovolt radiation from laser-plasmas should also be useful for single-shot recording of high-resolution radiographs of biological materials.

§1. Introduction

Microelectronic circuits are produced by replication of a pattern (mask) through the use of thin, grainless, polymer films sensitive to ultraviolet radiation. Production of line widths below about $1\text{ }\mu\text{m}$ in microcircuits requires X-ray (or focused electron) exposures in order to avoid photon diffraction effects. X-ray lithography is an active field of research at present.¹⁾

X-ray radiographs are usually made with photographic emulsions, although xerographic and other techniques can be used. Recently, the polymer resists developed for lithography were used to record high-resolution (100 Å) radiographs.²⁾ Instead of the usual pattern of varying photographic densities, use of an X-ray resist to record radiographs leads to a surface with relief dependent on the X-ray absorption of the object which is placed on the resist. The profile is viewed in a scanning electron microscope. High-resolution radiography is often called X-ray microscopy.³⁾

Steady-state electron-impact (X-ray tube) and pulsed synchrotron-radiation (storage ring) sources have been used to expose X-ray resists. Of these, electron-impact sources are preferable for production-line device replication because synchrotron-radiation sources of X-rays are expensive and few in number. However, due to their collimated output, the synchrotron-radiation sources are preferable for high-resolution radiography. In the recent past, exposures of resists with intense pulses of

soft X-rays from laser-heated plasmas were reported.^{4,5)}

This paper first summarizes the available information on resist exposure with pulsed radiation from laser-heated plasmas. Then the design of a facility for routine production-line use of pulsed X-ray lithography is presented. Finally, the possibility of using laser-plasma radiation for high-resolution radiography is examined.

§2. Pulsed X-Ray Lithography

There are many bright, pulsed sources of X-rays.⁶⁾ Most of them involve the production of million-degree plasmas which emit strongly in the X-ray region near 1 keV. Of the plasma sources, those produced by focusing high-power lasers onto solids are among the brightest and are easy to use (relatively free of debris and reproducible).

Exposures of X-ray resists with radiation near 1 keV from laser-heated plasmas were reported recently.^{4,5)} In one study, a long-pulse (40 nsec) Nd laser was used to heat Al plasmas which emitted about 0.1% of the incident laser energy as X-rays.⁴⁾ Sixty shots with this relatively inefficient system are required to expose the resist, polybutene-1-sulfone (PBS), at a distance of 5 cm from the focus. Lines $0.75\text{ }\mu\text{m}$ wide were replicated in the resist. In a second study, a shorter pulse (1 nsec) Nd laser was employed.⁵⁾ It produces X-rays about 100 times more efficiently, and has three times as much energy compared to the 40 nsec laser. Hence, single-shot exposures

are possible with a copolymer resist at 10 cm from focus. Pattern replication from masks (of unspecified line width) was faithful to within the limits of optical microscopy. The use of single, submicrosecond X-ray pulses from laser-heated plasmas to replicate masks reduces resist exposure times by a factor near 10^9 compared to steady-state sources.

The use of laser-plasma X-rays for lithography is attended by potential problems which were examined recently.²¹ Masks may be degraded either by debris from the laser target or by thermal cycling. Molten target material ejected as the million-degree-temperature, megabar-pressure plasma cools and dissipates can coat and otherwise damage masks. But, the use of thin targets and thin plastic shields over the mask may negate the problem. The sharp temperature rise in the absorbing material (usually Au) of the mask relative to the mask membrane (Be or Si) could lead to delamination. This potential effect is not easily calculated and must be tested experimentally. Resist heating is negligible. Quantitative measurements have shown the response of PBS to be similar for steady-state and pulsed exposure.⁴¹ Also, capacitance-voltage measurements of substrate (SiO_2) radiation damage produced by laser-plasma X-rays showed a flat-band shift of only 0.25 V for full exposure of PBS. That is, the pulsed soft-X-ray source appears favorable from a radiation damage viewpoint. In short, the only significant potential problem known to be associated with pulsed X-ray lithography is mask failure due to thermal cycling.

Routine use of laser-plasmas to expose X-ray resists is possible. It is desirable to optimize the X-ray production efficiency, which depends on several parameters: laser pulse wavelength, shape and energy, focusing conditions, and target composition and geometry. It was projected that a Nd laser with pulse length near 10 nsec which can focus 500 J onto a Cu target is adequate for single-shot exposure of PBS at a distance of 25 cm.⁴¹ Because X-rays are emitted over a wide angle, it appears possible to expose ten 5 cm diameter replicas with one shot. Four shots per hour are feasible with a properly designed laser.

A schematic of a facility for production-line use of pulsed X-ray lithography is given

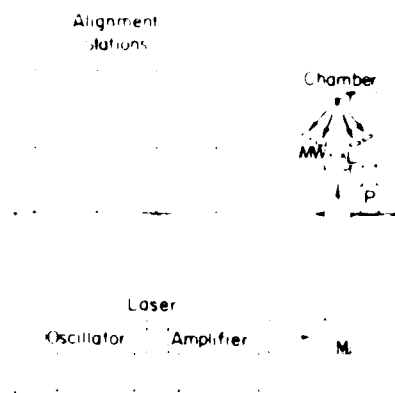


Fig. 1. Elevation-view schematic of a laser and exposure facility for single shot replication of multiple mask-wafer (MW) combinations aligned at nearby stations. The laser pulse, turned by mirror M, is focused by lens L onto target T in a chamber evacuated by pump P.

in Fig. 1. Mask-wafer combinations could be aligned, and held together in a magnetic device for movement to the exposure chamber. Multiple alignment stations would be needed to prepare enough workpieces for each pumpdown-laser-shot cycle. Alternative arrangements for pulsed X-ray lithography could be used but that sketched in Fig. 1 offers the greatest throughput and the simplest exposure chamber.

The single-shot exposure time with laser-plasma X-rays is much shorter than required. That is, the limiting factor is the interval between shots or the time needed to produce several aligned mask-wafer combinations. This raises the possibility of using a repetitively-pulsed laser, rather than a single-shot device. It may be possible to construct a Nd laser system which produces 1 J, 5 nsec pulses at 10 Hz. The X-ray conversion efficiency for such laser characteristics has not been measured, but an exposure time of about 10 minutes can be estimated for PBS.⁴¹ While such a time is acceptable, new target material must be positioned at focus for each shot. This requirement for target motion, and the amount of target debris produced by thousands of laser shots, make it unattractive to expose resists with X-rays from plasmas heated by a repetitively pulsed laser.

§3. Pulsed High-Resolution Radiography

Synchrotron radiation is favorable for pro-

duction of radiographs using an X-ray resist as a recording medium because of its natural collimation. With synchrotron radiation, a spatial resolution of 100 Å was demonstrated with polymethylmethacrylate (PMMA) as the resist.²¹ The likelihood that laser-heated plasmas will be useful for high-resolution radiography is discussed in this section.

In contrast to X-ray lithography, which requires photon energies in the range near 1 to 2 keV in order to penetrate the supporting membrane of the mask, there is no mask for high-resolution radiography. Hence, lower photon energies may be used. Energies from near 1 keV down to about 100 eV, where the wavelength of 120 Å is greater than the spatial resolution of PMMA, are best for radiography of biological materials. Laser-heated plasmas emit intense radiation in the 0.1–1 keV region. Proper choice of laser irradiance and target will maximize radiation useful for production of high-resolution radiographs. A power density of 10^{12} W cm⁻² will strip atoms in a carbon target to the K shell and produce intense radiation in the 300–400 eV range. Such photon energies are near and above the carbon K absorption edge. Hence, they will yield good contrast in a carbon-containing sample and will be efficiently absorbed by the resist.

Intensity available from laser-heated plasmas for pulsed high-resolution radiography can be estimated from existing data. The early pulsed-lithography experiments were done with 40 nsec, 40 J Nd laser pulses focused to 10^{13} W cm⁻² on Al.⁴¹ That combination of conditions was chosen to maximize available Al K radiation at 1.6 keV, which passed through a 25 µm Be foil to expose PBS. The subkilovolt radiation, the intensity of which was not optimized, was stopped by the Be. Some uncovered resist was exposed to all radiation from the plasma at the same time as the 1.6 keV exposures were being made. The subkilovolt radiation was so intense that the PBS "self-developed", that is, a clear substrate remained after exposure. Effects due to radiation with energy below and above 100 eV were not separated in the Al plasma exposures of PBS. Using measured laser-plasma radiation intensities above 1 keV,⁴² it is estimated that over 10% of the incident laser energy can be converted to radiation in the 0.1–1

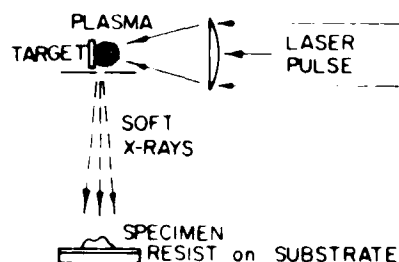


Fig. 2. Schematic arrangement for pulsed high-resolution contact radiography using an X-ray resist to record the non-uniform absorption of the specimen. An aperture is shown near the plasma to limit the source size and improve spatial resolution.

keV range. Single-shot subkilovolt exposure of PBS at 10 cm from the focus appears feasible with a 100 J laser.

The spatial resolution attainable in a pulsed high-resolution radiography can be estimated. The major limitation to the use of laser-heated plasmas might be the source size in relation to the source-to-resist spacing. The plasma volume which emits subkilovolt radiation can exceed 1 cm in diameter. If a 100 Å thick specimen were placed on 1000 Å thick layer of X-ray resist 10 cm from the source, a penumbral blurring of about 100 Å would result. Such a value is acceptable for some high-resolution radiography. If better definition is desired, an aperture can be used to limit the source size, as sketched in Fig. 2. This arrangement has been tested in experiments where a very small (100 µm diameter) aperture was employed.⁴³ Use of an aperture to improve resolution requires appropriate increase in the number of laser shots to compensate for the intensity loss due to using only part of the source volume.

§4. Conclusion

The routine use of pulsed X-rays (1–2 keV) for lithographic production of mask replicas appears practical, with one qualification. That is, the response of masks to thermal cycling is not known now and must be determined experimentally. The employment of laser-plasma radiation (0.1–1 keV) for high-resolution radiography of biological materials is also feasible. Single-shot radiographs with 100 Å resolution are expected on the basis of experiments to date.

References

- 1) E. Spiller and R. Feder: *X-Ray Lithography*, in *X-Ray Optics*, ed. H.-J. Quisser (Springer-Verlag, Berlin, 1977).
- 2) R. Feder, E. Spiller, J. Topalian, A. N. Broers, W. Gudat, R. J. Panessa and Z. A. Zadunaisky: *Science* **197** (1977) 259.
- 3) V. E. Cosslett and W. C. Nixon: *X-Ray Microscopy* (Cambridge University Press, 1960).
- 4) D. J. Nagel, M. C. Peckerar, R. R. Whitlock, J. R. Greig and R. E. Pechacek: Society of Photographic Instrumentation Engineers Meeting, San Jose, Calif., May 1978; *Electronics Letters* (to be published).
- 5) P. J. Mallozzi, H. M. Epstein and R. F. Schwerzel: Denver X-Ray Conference, Aug. 1978; *Adv. X-Ray Anal.* **22** (1979).
- 6) D. J. Nagel and C. M. Dozier: *Flash X-Ray Source Characteristics*, in *High-Speed Photography*, ed. M. C. Richardson (SPIE Vol. 97, Bellingham, 1977).
- 7) M. C. Peckerar, J. R. Greig, D. J. Nagel, R. E. Pechacek and R. R. Whitlock: *J. Vacuum Sci. Technol.* (1979) (to be published). *
- 8) D. J. Nagel, R. R. Whitlock, J. R. Greig, R. E. Pechacek and M. C. Peckerar: *Pulsed X-Ray Lithography*, in *Developments in Semiconductor Microlithography III*, ed. R. L. Ruddell (SPIE Vol. 135, Bellingham 1978).
- 9) D. J. Nagel: IEEE Plasma Physics Meeting, Monterey, Calif., May 1978.

*See M.C. Peckerar, J. R. Greig, D. J. Nagel, R. E. Pechacek and R. R. Whitlock, "High Speed X-Ray Lithography with Radiation from Laser-Produced Plasmas," in *Proceedings of the Symposium on Electron and Ion Beam Science and Tech., Eighth International Conference*, Vol. 78-5, R. Bakish, ed. Electrochemical Society, Princeton, NJ, (February, 1979), p. 432-443, reprinted herein.

SUBMICROSECOND X-RAY LITHOGRAPHY

Indexing terms Photolithography, X-ray applications

X-rays from laser-heated plasmas were used to replicate features as fine as 750 nm in the positive resist polybutene-1-sulfone (p.b.s.). The measured sensitivities of p.b.s. to pulsed and d.c. X-rays ($\approx 10^5$ ratio in exposure rate) are similar (no reciprocity loss). Laser-plasma X-rays produced only small (0.25 V) flat-band shifts in m.o.s. capacitors at irradiation levels sufficient to expose p.b.s.

The near-ultraviolet sources now commonly employed to replicate fine details are limited to line widths above about 1 μm because of diffraction effects. X-ray lithography will be employed to produce devices with submicrometre features.¹ Electron-beam lithography also yields submicrometre details, but only by programmed sequential replication of a pattern. X-rays, which can replicate an entire pattern simultaneously, are produced by electron impact on solids (line and continuum radiation) and by electron acceleration (synchrotron radiation). However, these sources have disadvantages for X-ray lithography. X-ray tubes and other solid-target sources do not efficiently convert electron energy to X-rays and, therefore, exposure times are long (usually in the 1-10 minute range). Furthermore, the continuum radiation from such sources is relatively hard. That is, it is not efficiently stopped in the mask or the resist and it deposits energy and produces damage in the silicon substrate and in superimposed oxides. Also, the photoelectrons released by hard X-rays in the substrate re-enter the resist and degrade resolution. Synchrotron radiation sources have softer, more appropriate spectra. But they are large, expensive and possibly unsuitable for routine manufacturing.

Many sources that produce submicrosecond pulses of X-rays are available.² Plasmas heated at the focus of high-power ($> 10^9$ W) lasers are intense X-ray sources.^{3,4} In fact, over 10% of the incident radiation from a high-power Nd glass laser can be converted to an X-ray pulse of a few nanoseconds ($> 10^9$ W). The X-ray emission usually has intense lines in the 1-3 keV range and a continuum that falls off rapidly at higher energies. The most intensely emitting region is generally smaller than about 500 μm in extent. X-ray emission above 1 keV from laser-heated plasmas is maximum along the target normal and decreases by 30% or less for emission angles within 45° of the target normal.⁵ Laser pulses can be fired every 15 min from a Nd laser capable of producing X-rays efficiently.

40 ns f.w.h.m. pulse.⁶ A 3 cm diameter aperture near the target chamber restricted the beam diameter to reduce laser-target interaction before the laser output pulse. An $f/1.9$, 125 mm focal-length lens focused the remaining laser energy (≈ 40 J) onto planar Al targets (tilted 15° about a horizontal axis) in the vacuum chamber (pressure < 50 mtorr). A target translator was used to expose fresh material for each shot. A silicon $p-i-n$ diode was a 25 μm Be window was used to measure quantitatively the X-ray intensity above about 1 keV.

The X-ray characteristics measured in an earlier study⁷ with the same arrangement include source size, emission time, spectrum and intensity. A pinhole camera, which viewed the source at almost 90° to the target normal, showed that the most intense source region was about 450 μm in diameter and 600 μm in a direction along the target normal. A $p-i-n$ detector yielded a f.w.h.m. X-ray pulse width of 15 ns. Bragg spectrograph measurements produced spectra that consist primarily of lines from He-like (L -electron) Al, which fall in the 1.5 to 2.3 keV region, with 90% of the energy in lines within a few eV of 1.6 keV. Only about 0.1% of the laser energy on target was converted to the 1.6 keV X-rays. Hence, the laser used in the present experiments is far from optimum for submicrosecond X-ray lithography.

The positive resist employed in this work was polybutene-1-sulfone (p.b.s.).⁸ Adhesion of this resist to SiO_2 was poor, and so a 20 nm Cr film was used between the p.b.s. and the 500 nm oxide layer. The 300 nm thick resist was prebaked at 100°C for 20 minutes, spray developed and spray rinsed each for 45 s and post-baked at 150°C for 20 min. A commercial electroformed Ni mesh that was 25 μm thick and had 200 μm diameter holes was placed close to the resist (< 125 μm estimated spacing) to form a coarse test pattern. The Ni mesh was covered with a 25 μm Be foil which passed no radiation below 800 eV. An electron-beam-produced, 500 nm thick Au mask supported on 25 μm Be was employed to form a fine pattern.⁹ It contained structures as narrow as 750 nm. This mask was placed within about 125 μm (estimated) of the resist. The Be support for the high-resolution Au mask, which was coated with a thin film of silicone remaining from ion milling of the fine-line structure, had reduced X-ray transmission.

The structures just described were positioned 5 cm from the laser focus at an angle of 40° to the beam direction. Ninety laser shots, each on a fresh Al target spot, were fired at 5 min intervals to ensure exposure. Not all of the shots yielded the normal X-ray output during this run. The total X-ray intensity was equal to that for 60 normal shots. The

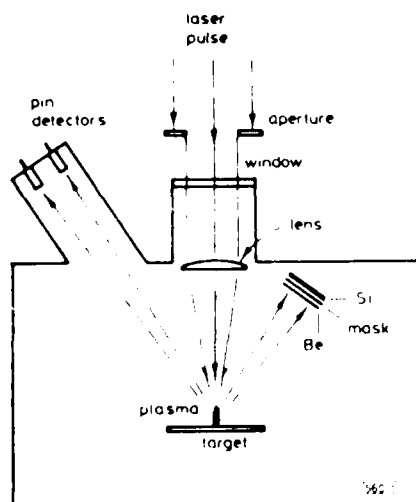


Fig. 1 Schema of the experiment

Fig. 1 is a schematic diagram of the experimental arrangement. The Nd laser system, which consists of a Q-switched oscillator and two amplifiers, produced about 100 J in a



Fig. 2 Optical micrograph of structure in p.b.s. consisting of 1.5 μm lines (light) and 0.75 μm spacings (dark), taken at normal incidence

p.b.s. behind the mesh developed fully, permitting etching of the Cr and SiO₂. The exposure of the resist behind the high-resolution mask was incomplete due to absorption in the silicone layer. Fig 2 is an optical micrograph of the partially developed p.b.s. from the higher-resolution test. The pattern is a faithful replica of the mask. However, the horizontal lines, which were nearly parallel to the longer axis of the plasma source, are somewhat sharper than those which were vertical and almost orthogonal to the maximum source dimension. Such penumbral blurring would not appear for smaller mask-water spacings and greater source-to-mask spacings, such as would be used in practice.

A 'step-wedge' experiment was performed simultaneously with the mask exposures to obtain the pulsed-exposure properties of p.b.s. Successively more numerous layers of 2.5 μ m Mylar were placed over an 18 μ m Be foil above a resist-coated prebaked wafer. After exposure, developing, rinsing and the postbake, the thickness of resist remaining under each absorber region was measured by stylus and interferometer techniques and by colour comparison. The incident and p.b.s.-absorbed X-ray exposures were computed from the *p-i-n* signals and tabulated absorption coefficients assuming a dominant X-ray energy of 1.6 keV. A value of approximately 5 J/cm² was found for full exposure of the 300 nm thick p.b.s., compared with a value of 14 J/cm² measured with a steady state X-ray source.^{8,10} These values may be the same within experimental uncertainty. Thus reciprocity loss does not appear to be a problem for short-pulse exposure of p.b.s. Heating of the resist is also negligible ($< 1^\circ\text{C}$).

Radiation effects were measured with *in-situ* capacitors placed behind an 18 μ m Be foil, 5 cm from the laser focus. Aluminum field plates, 100 nm thick, were evaporated onto dry oxide. The silicon substrate was (100) *n*-type 4-8 Ω cm material. Capacitance/voltage (*C/V*) curves were obtained before and after irradiation. An exposure sufficient to fully develop p.b.s. yielded a flat-band shift of only 0.25 V, with no evidence of changes in the *C/V* curve shape due to fast interface states.

Problems with the use of the laser plasmas for X-ray lithography are addressed elsewhere.¹¹ The most obvious, deposition of evaporated and melted target material on masks, can be defeated by the use of thin targets and X-ray transmissive plastic shields over the mask. Effects due to sudden heating of the absorbing material (Au) in the mask remain to be assessed.

Optimisation of laser-plasma X-ray output has been addressed.¹² Available data indicate that a single laser pulse, with width in or near the 1-10 ns range and energy of about 500 J, incident on a target element near Cu, would be useful for routine microreplication. Design studies, aimed at minimum cost systems, are in progress for single- and repetitively pulsed lasers.

Mallozzi *et al.* have recently reported the exposure of a negative X-ray resist (c.o.p.) with X-rays from laser-heated

plasma.¹³ They obtained single-shot exposures at a distance of 10 cm with 1 ns 100 J pulses from a Nd laser.

Acknowledgment We thank C. J. Taylor, P. D. Blais and J. M. McMahon for advice and assistance.

D. J. NAGEL

6th October 1978

U.S. Naval Research Laboratory
Washington DC 20375, USA

M. C. PECKERAR

Westinghouse Electric Corporation
Baltimore MD 21203, USA

R. R. WHITLOCK

J. R. GREIG

R. F. PECHACEK

U.S. Naval Research Laboratory
Washington DC 20375, USA

References

- 1 SPIELER, E., and EIDER, R., in QUÉSSIER, H. J. (Ed.), 'X-ray optics' (Springer-Verlag, Berlin, 1977), pp. 35-92.
- 2 NAGEL, D. J., and DOZIER, C. M., in RICHARDSON, M. C. (Ed.), 'Proceedings of the 12th international conference on high-speed photography, 1977, SPIE vol. 97', p. 132.
- 3 MALLOZZI, P. J., EPSTEIN, H. M., JUNG, R. G., APPELBAUM, D. C., FAIRAND, B. P., and GALLAGHER, W. J., in FEELD, M. S., JAVAN, A., and KURNIT, N. A. (Eds.), 'Fundamental and applied laser physics' (Wiley, New York, 1973), pp. 165-220.
- 4 NAGEL, D. J., BURKHALTER, P. G., DOZIER, C. M., HOLZRICHTER, J. L., KLEIN, B. M., MCMAHON, J. M., STAMPER, J. A., and WHITLOCK, R. R. *Phys. Rev. Lett.* 1974, 33, p. 743.
- 5 CHASE, L. E., JORDAN, W. C., PEREZ, J. D., and PRONKO, J. G. *Appl. Phys. Lett.* 1977, 30, p. 137.
- 6 GREIG, J. R., and PECHACEK, R. F. NRI Memorandum Report 3461, 1977 (unpublished).
- 7 WHITLOCK, R. R., GREIG, J. R., TOPSCHER, S. J., and NAGEL, D. J. (unpublished).
- 8 THOMPSON, L. E., FELL, E. D., BOWDEN, M. J., LENZO, P. V., and SPENSER, E. G. *J. Electrochem. Soc.* 1974, 121, p. 1500.
- 9 PECKERAR, M. C. Westinghouse Patent Disclosure AA 76-283.
- 10 BLAIS, P. D. Private communication.
- 11 PECKERAR, M. C., GREIG, J. R., NAGEL, D. J., PECHACEK, R. F., and WHITLOCK, R. R. *J. Vac. Sci. & Technol.* (to be published).
- 12 NAGEL, D. J., WHITLOCK, R. R., GREIG, J. R., PECHACEK, R. F., and PECKERAR, M. C., in RUDDLE, R. E. (Ed.), 'Semiconductor microlithography III' (Soc. Photo. Instr. Eng., Bellingham, 1978).
- 13 MALLOZZI, P. J., EPSTEIN, H. M., SCHWERTZ, R. F. 'Advances in X-ray analysis' (to be published).

0013-5194/78/240781-02\$1.50/0

COMPARISON OF X-RAY SOURCES FOR EXPOSURE OF PHOTORESISTS

D. J. Nagel

*Naval Research Laboratory
Washington, D.C. 20375*

INTRODUCTION

Thin films of materials may be damaged (exposed) by ionizing radiation from a wide variety of sources. Of the many types of radiation-sensitive materials,^{1,2} photoresists are receiving greatly increased attention. Although much less sensitive (10^{-4}) than AgBr photographic films, photoresists can offer substantially better spatial resolution (10^2) than small-grain films. Hence, photoresists are being used for replication of fine-scale patterns, most notably for microelectronics fabrication. Photon, electron, and ion sources are all being employed to expose resists. There are two reasons that x-ray sources have been used to expose resists for the past several years. First, x-rays permit replication of finer scale patterns than uv exposures because the shorter x-ray wavelengths yield smaller diffraction effects. Second, since x-rays can penetrate and yield images of the interior of objects, radiography can be pushed to higher (submicrometer) resolution by the use of resists as recording media in place of photographic film. Because fine-scale structures can be examined by such x-ray resist techniques (and because the images are usually small), high-resolution radiography is also called x-ray microscopy.³

Many physical mechanisms are available to produce x-rays.⁴ Natural (astrophysical), nuclear device, and laboratory sources produce x-rays that could conceivably be used to expose resists. From this rich array of sources, only three types of laboratory devices have been used to date for resist work: (a) electron-impact devices, such as x-ray tubes, (b) synchrotron-radiation sources, usually storage rings, and (c) multimillion degree plasmas heated with photons or electrons. The characteristics of those laboratory sources vary widely. However, they all produce useful intensities in the x-ray region near 0.1-1 keV, where resists have appreciable absorption.

The purpose of this paper is to review and compare the characteristics of those x-ray sources that have been used to expose photoresists. Emphasis will be given to the recently employed and less familiar plasma sources. A discussion of photon energy and intensity requirements for resist exposure is given in the next section. The following three sections will summarize work with electron impact, synchrotron radiation, and plasma sources. Photographs of relatively small and inexpensive sources of each type are included. Finally, a tabulation of source characteristics will be presented and discussed.

Recent comprehensive reviews of x-ray lithography and microscopy are available.⁵⁻⁷ These include discussions of x-ray resists, masks, and alignment techniques, in addition to x-ray sources. Specific recent material on resists,⁸ masks,⁹ and alignment methods¹⁰ is also noted. Detailed references to x-ray sources for resist exposure are given in the following sections.

X-RAY SOURCE REQUIREMENTS

The photon energy and intensity of various x-ray sources must be gauged against what is needed for high-resolution exposures of resists in acceptable times ($\leq 10^5$ s). The photon energy heavily influences the resist absorption, which, along with the available intensity, determines the exposure time for a given resist. Also, the photon energy influences the energy and range of electrons produced in the resist by and after photon absorption. These ranges determine the spatial resolution limit.

The computation of the exposure time for a particular source-resist combination is straightforward if the following three factors are known quantitatively: (a) the absolute source intensity (photons/eV-cm²-s) at the resist, as modified by any filters and the mask substrate, as a function of photon energy, (b) the resist absorption versus x-ray energy, and (c) the amount of energy (J/cm²) that must be absorbed in order to achieve the desired relief in the resist (full or partial exposure). The absolute intensities of x-ray sources can be measured or, in many cases, calculated. Such work is discussed in subsequent sections. The fractional absorption of x-rays in a resist film is readily computed. Whitlock has written a program that will produce absorption values at specified photon energies, densities, and thicknesses.¹¹ It employs tabulated absorption coefficients, which, although less reliable below 100 eV, are conveniently parameterized.¹² Results for polymethyl methacrylate (PMMA) films of various thicknesses are given in FIGURE 1. The photon energy range of interest (10 eV to 10 keV) is evident, as is the low absorption values for the higher x-ray energies. Values of the absorbed energy needed for full or partial exposures of several resists are available.^{5, 8} For example, PMMA requires an absorbed energy of 500 J/cm² for full exposure. X-ray resist sensitivities vary from this value to about 5 J/cm². Various x-ray resists have been exposed in times ranging from less than 10^{-6} to somewhat over 10^5 sec, depending on the source spectrum and strength and the source-resist separation.

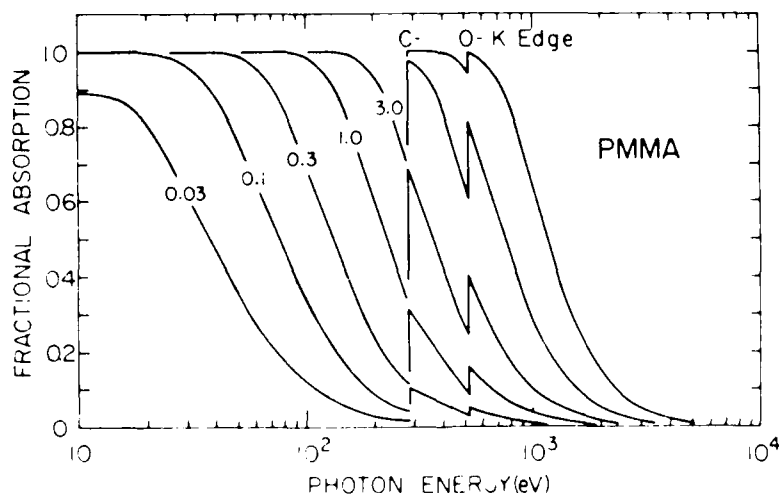


FIGURE 1. The fractional absorption of PMMA layers of the thicknesses (μm) indicated, as computed by Whitlock.¹¹ The carbon and oxygen absorption edges are labeled.

The ultimate sensitivity attainable with resists remains to be determined. Attention has already been given to (a) increasing the fractional x-ray absorption by including atoms with favorable absorption edges in the resist, (b) optimizing the use of the absorbed energy by including in the resist radicals that are especially sensitive to radiation, and (c) optimizing the chemicals, concentrations, and times used in resist development. It is not clear how much room remains for the improvement of resist sensitivity to x-rays.

The spatial resolution attainable in an x-ray resist exposure depends, as does the exposure time, on both the source and resist characteristics. Resolution as a function of source photon energy has already been examined and it was concluded that photon energies near 250-600 eV are optimum for PMMA.^{5,13} Lower photon energies (longer wavelengths) involve diffraction effects, while higher energies produce more energetic, further traveling electrons. The intrinsic resolution of a particular resist varies from the limit set by exposure due to the photo and Auger electrons in slow resists to values roughly 100 times poorer in fast resists.

Some measurements of the spectra of electrons emitted by x-irradiated polymer surfaces have been made.¹⁴ However, the energies and intensities of x-ray stimulated electrons in resists are not well known. Measured ranges for many materials fall below 100 Å for electrons with energies below 1 keV.¹⁵ Hence, resist resolutions below 100 Å might be expected in the best case. In fact, spatial resolutions near, and somewhat better than, 100 Å have been observed.¹⁶ The nonuniformity (photon statistics) of x-ray exposures requires that a resist more sensitive than PMMA will have poorer spatial resolution.⁵ Roughly speaking, faster resists require fewer photons/cm² for exposure, and the graininess of such a less dense exposure results in poorer resolution. Faster resists are indeed found to exhibit poorer resolution than PMMA.⁸

In summary, sensitivities and exposure times vary widely for x-ray exposure of polymer resists. It is not clear where the sensitivities of available resists stand relative to what is ultimately attainable. At the other extreme, resist resolution in an insensitive resist (PMMA) already approaches the limits set by the ranges of electrons excited during and following x-ray absorption. Thorough experimental studies of both resist sensitivity and resolution as functions of x-ray energy and development conditions remain to be made for a wide variety of resists. Exposure rate and temperature might also be relevant parameters, at least for a fundamental understanding of resist behavior.

ELECTRON IMPACT ON SOLIDS

Electron impact devices were the first to be developed and are now the most widely-used sources of x-rays. These devices consist of a source of electrons, a gap, and a target. The electrons may be ejected from the source (cathode) by thermal or field-emission effects, with heated filaments being most common. The gap, across which a high (keV) potential is applied to accelerate the electrons, is in a vacuum of at least 10^{-5} Torr. The x-ray source size (anode target area), which is typically a few mm², depends on electron focusing in both the source and the gap. Spectral intensities from all practical electron impact sources depend on the electron energy and current, the anode material, and the take-off angle from the target (due to self-absorption effects). The absolute x-ray intensity available from a given focal spot size is limited by space charge effects at low voltages (< 1 keV) and by anode heat dissipation at higher voltages (> few keV). The energetic electrons produce

uncollimated x-rays in the anode by two basic mechanisms: (a) bound-to-bound electron transitions, which follow the production of core-hole vacancies, give x-ray lines, and (b) free-to-free transitions, which are due to the curvature of incident electrons in the nuclear coulombic field (electronic bremsstrahlung), yield the x-ray continuum. Typically, only about 1% or less of the incident electron energy is converted into x-ray line and continuum energy in an electron impact source.

Spectra due to electron impact on solid targets can be obtained on an absolute basis either by a calculation or by measurement with calibrated spectrometers. In the past 10-15 years, several fairly efficient methods to compute x-ray spectra have been implemented. They range from Monte Carlo techniques¹⁷ to fast running transport-equation codes.¹⁸ Reliable measurements of x-ray tube output have become available during the same time period. Both energy-dispersive methods, e.g., Si(Li) detectors, and wavelength-dispersive devices, e.g., crystal spectrometers, have been employed. Examples of computed and measured spectra from a sealed commercial x-ray tube are given in FIGURE 2.¹⁹ Thin-window sealed tubes provide useful intensity only down to about 3 keV. Hence, windowless electron-impact

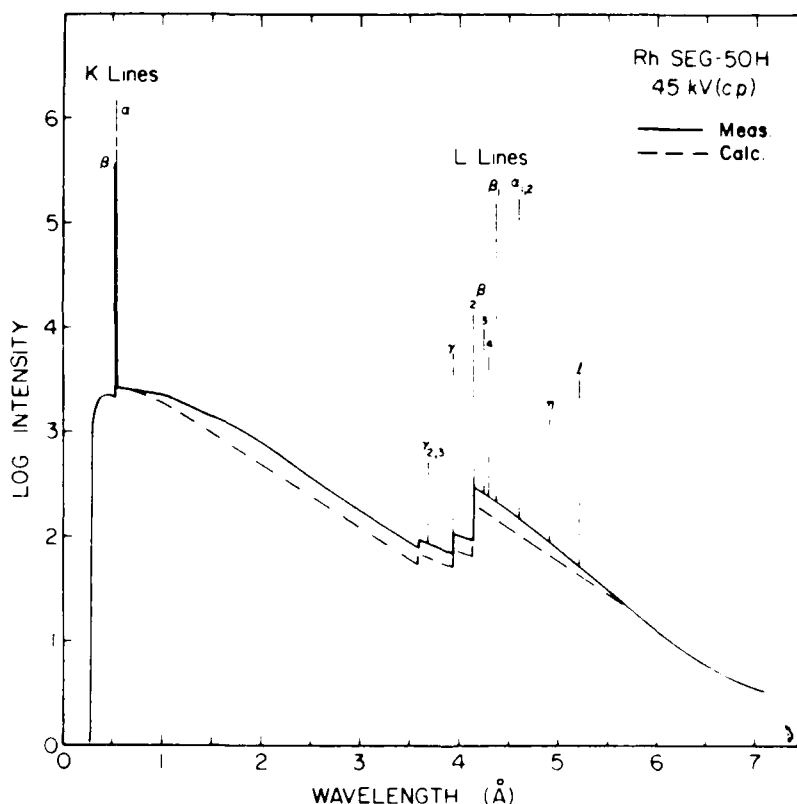


FIGURE 2. The measured and calculated spectral distribution for a Rh target x-ray tube on the same absolute basis. See Birks¹⁹ for units.

sources are usually used for resist exposures. Their spectra are quite easily calculated, but little data is available.

Electron impact x-ray sources for resist exposure can be grouped into two categories: Stationary anode sources that either have interchangeable anodes or are sealed commercial x-ray tubes and rotating anode devices. The latter sources yield higher x-ray intensity because they spread the electron beam heat load over much larger areas than do stationary target devices.

Fixed anode devices have been widely used to expose resists. The first x-ray source to be used for such work was an electron beam evaporator operated at a power too low to melt the stationary Al target.²⁰ Such windowless devices, which are readily available in the electronics industry, continue to be used for research, since they provide adequate exposure and solid angle (area) and useful, albeit long, exposure times. An Al target evaporator operated at 8 keV and 50 mA (0.4 kW) in a 1 mm spot can expose PMMA in 20 min at a distance of 3 cm.²¹ A specially designed, continuously pumped, stationary Pd anode x-ray source has been designed to expose the negative resist DC1PA in 4 min at 50 cm with 4 kW in a 3 mm spot.²² Sealed window x-ray tubes do not require constant pumping and are widely available commercially. Their size permits them to be mated with mask alignment equipment (FIGURE 3).²³ However, the relatively hard x-ray spectrum of sealed

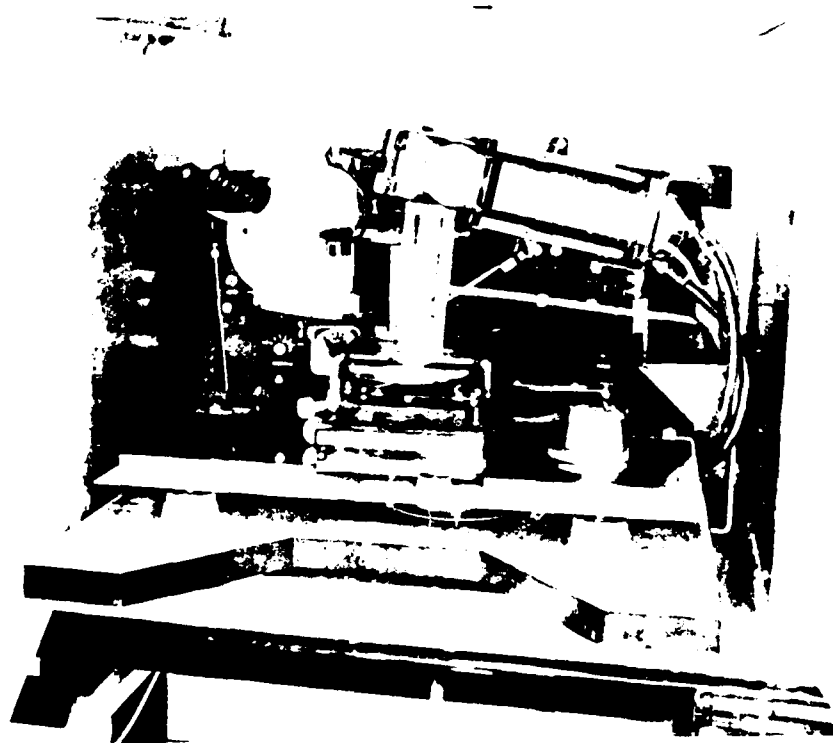


FIGURE 3. The Westinghouse steady state x-ray lithography alignment and exposure system.²³

x-ray tubes (due to window absorption) requires longer exposure times. With a commercial Rh anode tube operated at 20 keV and 40 mA (0.8 kW), it takes 60 min to fully expose poly(butene-1) sulfone (PBS) 28 cm from the anode.²⁴ The exposure of a slow resist, such as PMMA, takes prohibitively long with such a source.

Rotating anode sources generally dissipate powers about ten times greater than those for stationary targets.²⁵ Such devices are available commercially, but they do not offer easy anode interchangeability. Rotary vacuum seals can be bought now for construction of special rotating anode sources that have demountable anodes, oil-free high vacuum (to preserve target surface cleanliness) and large exposure areas with no windows. Schematic drawings of specially designed rotating anode sources were presented recently by Wardly *et al.*⁶ and Stover.²⁶ A review of x-ray sources, most of which involve rotating anodes, was provided by Hughes and Fink.⁷ Exposure times as short as 1 min at practical source-resist distances (40 cm) have been realized with fast resists.

In summary, a wide variety of electron impact devices are now in use for resist exposure, primarily for research production of microelectronics and other devices. At one extreme are relatively simple commercial evaporator and sealed x-ray tube systems for use in research work, where the time required to obtain an exposure is not critical. At the other extreme are complex, custom-designed stationary and rotating anode systems that have exposure times (with resists faster than PMMA) that may be acceptable for production line uses. The cost of electron-impact sources is roughly in the $\$2 \times 10^4$ – 10^5 range. High-power rotary anode sources are about a factor of five more expensive than most stationary target sources.

SYNCHROTRON RADIATION

Magnetic bremsstrahlung produced by the curved motion of energetic electrons in a magnetic field is called synchrotron radiation, after the machines in which it was first observed. Such radiation from synchrotrons and, especially, storage rings, is being widely employed now for many fundamental studies and technological projects.^{27–9} The spectral (continuous and intense), spatial (collimated to a few mrad), and temporal (pulses about 1 ns wide) characteristics of synchrotron radiation, along with its strong polarization, account for the intense general interest in synchrotron radiation.

The absolute synchrotron radiation spectra computed for a large storage ring are shown in Fig. RE 4.³⁰ Note that increasing the beam energy extends the spectrum into the x-ray region but does not increase the longer wavelength spectral intensity. Use of alternating magnetic devices, called "wigglers," increases both the higher energy cutoff and the overall intensity. Synchrotron radiation spectra are straightforward to compute but there is little absolute spectral data with which to compare. The spectrum of uncollimated emission from a rotating Cu anode x-ray tube is also given in Fig. RE 5. The high intensity and good collimation favor synchrotron radiation over x-ray tubes for exposure of photoresists.

Sources of synchrotron radiation, although expensive, are already numerous and several are under construction.^{27–9} They range from 0.2 GeV devices about 2 m in diameter to an 18 GeV storage ring, which is almost 400 m in diameter. Fig. RE 5 shows the 0.25 MeV storage ring at the National Bureau of Standards, which has a diameter of 1.68 m.³¹ Beam currents fall in the range from 10^{-3} to 1 A, with cross sections typically 1×4 mm.

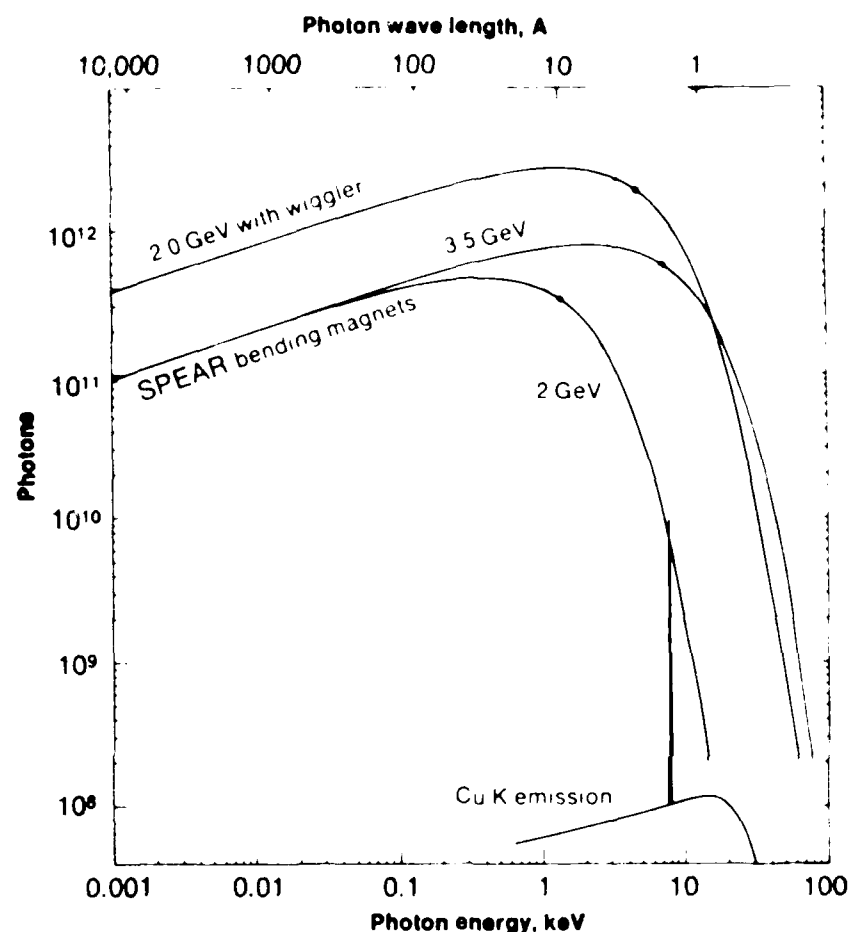


FIGURE 4. The computed intensity (photons $\text{sec}^{-1} \text{mrad}^{-1} \text{mA}^{-1}$ 1% passband width) of synchrotron radiation at 2 and 3.5 GeV, and at 2 GeV with a wiggler. The approximate emission spectrum of a rotating copper anode x-ray tube is also shown.³⁰

The initial studies of resist exposure with synchrotron radiation were done by a U.S.-German collaboration at DESY in Hamburg³² and a French group at ACO in Orsay.³³ More recently, other groups at Japanese^{34, 35} and U.S.³⁶ synchrotron radiation sources have been active in this field. Greatly increased use of synchrotron radiation for resist exposures is anticipated as additional dedicated storage rings begin operation.

The times required for synchrotron radiation exposure of PMMA are known from experiments already done with relatively low-current storage rings. Most exposures were performed at distances of 10–40 m from the source using broad-band (filtered but not monochromated) radiation. Exposure times for PMMA have

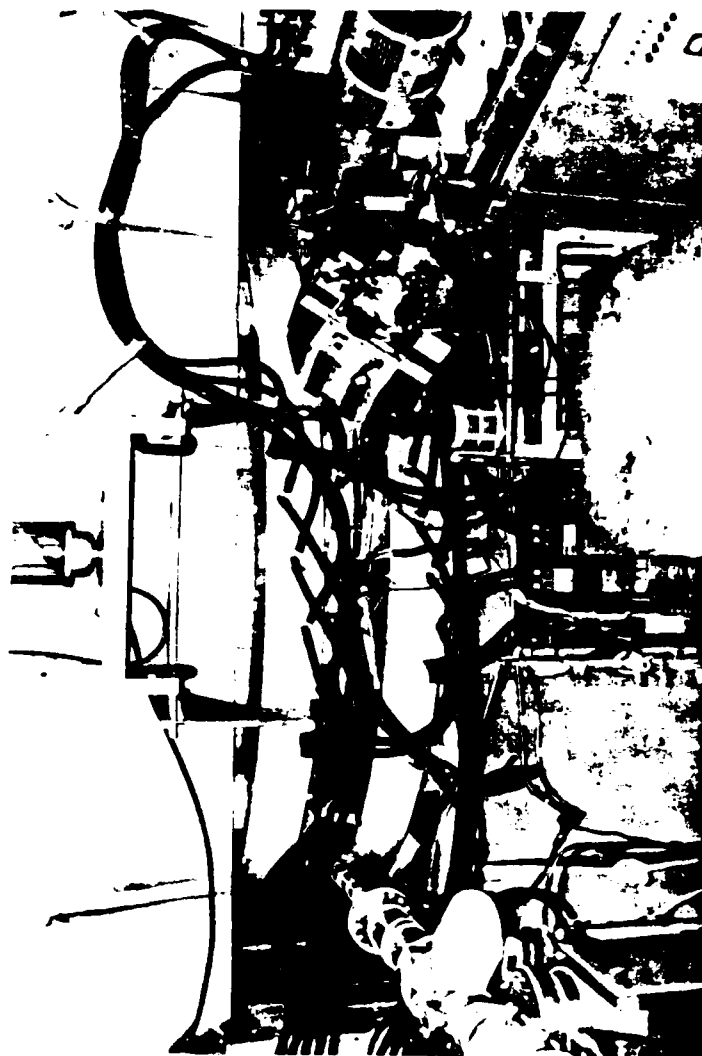


FIGURE 5. A photograph of the SURF storage ring at the National Bureau of Standards.³¹ The electrons are injected at the right and one synchrotron radiation beam line is visible on the left. The orbital diameter of the electrons (in the vacuum torus out of sight between the magnet pole pieces) is 1.68 m.

ranged from about 10^2 to 10^4 s, depending strongly on the stored electron current, which was usually < 0.1 A.³²⁻⁶ It is projected that newer machines, with 0.1-1 A currents, will require exposure times less than 100 s for PMMA.^{32, 37, 38} Betz *et al.* performed a trade-off analysis to assess the characteristics of an optimum storage ring for x-ray lithography.³⁸ They concluded that a 0.9 GeV, 0.5 A source could expose PMMA through realistic masks in 1-10 s. Only one exposure of a resist was performed with monochromatized synchrotron radiation; Pianetta *et al.* found that the time required for PBS was a factor of 10^3 longer than that for broad-band radiation.³⁶

In summary, resist exposures with synchrotron radiation have had two purposes: high-resolution radiography of biological systems and replication of masks for the production of structures, principally microelectronics.^{5, 16, 39} High-resolution radiography (x-ray microscopy) has been done with better than 100 Å resolution using PMMA. Microelectronics production with synchrotron radiation is attractive because of the excellent collimation, which permits comfortable mask-resist separations and prolongs mask life. However, the limited vertical exposure dimension and, especially, the size and expense of synchrotron radiation sources are drawbacks to industrial use. Storage ring facility costs fall approximately in the $\$10^6$ - 10^7 range, but they can simultaneously serve 10 to 20 exposure stations.

PLASMA SOURCES

Solids heated to about 10^3 K are termed "red hot." Continued heating produces "white hot" temperatures. Additional energy input produces melting and then vaporization. At around 10^4 K, atomic collisions are sufficiently violent to produce ionization (plasma formation), a state that could be called "uv hot," since the primary emission at that temperature is in the ultraviolet region. Temperatures of 10^5 K produce extreme uv radiation, while matter in the 10^6 - 10^7 K regime is "x-ray hot." Plasmas that emit x-rays consist of highly ionized atoms and energetic (keV) electrons. Depending on the atomic number (composition) of material in the plasma, dozens of electrons may be removed from each atom.⁴⁰

X-ray emission from multimillion degree plasmas is due to three mechanisms: (a) bound-to-bound transitions, often following collisional excitation, which give discrete lines, (b) free-to-bound, or recombination, transitions, which yield continua to the high-energy side of each ionization energy, and (c) free-to-free, or bremsstrahlung, transitions, which yield a continuum. Spectra from x-ray hot plasmas vary widely, depending on the relative importance of the three mechanisms in a particular source and the plasma composition, geometry, and heating details for various sources. Absolute measurements and calculations of x-ray spectra from plasmas are rare since much information on the emitting plasma can be obtained from relative spectra. FIGURE 6 exhibits the emission spectra of a laser-heated plasma on an absolute basis over a relatively wide photon energy range.⁴¹ It consists of those lines and recombination continua below 1 keV that were not resolved in either the measurement or calculation and of a steeply falling continuum at higher energies. The relatively high intensity in the 0.1-1 keV region, which is characteristic of very hot plasmas, makes them useful for the exposure of photoresists. Also, plasmas emit intense radiation over a large solid angle (2π to 4π), which permits simultaneous exposure of relatively large areas of resist. Their small size, often on the order of 1 mm, is also important.

Methods of heating plasmas to x-ray emission temperatures can be grouped into two categories: beam-heated plasmas and electrical-discharge plasmas. The impact

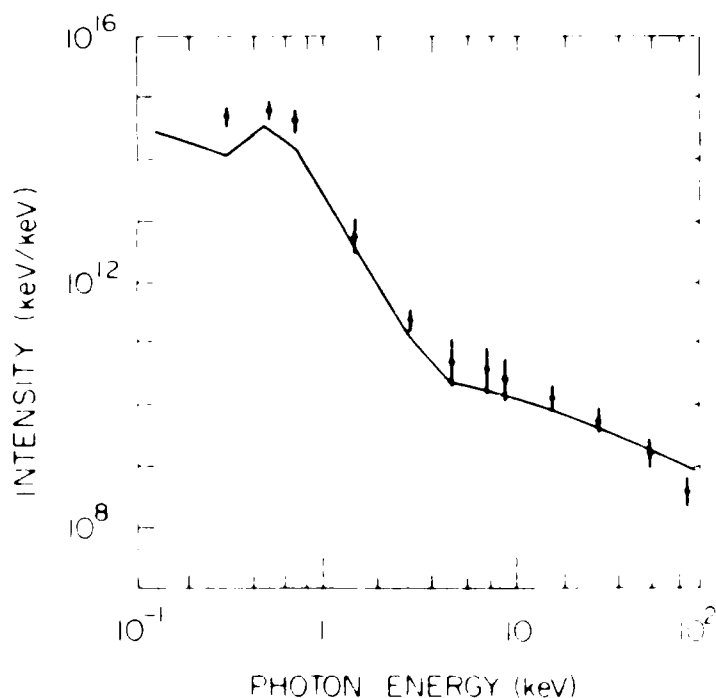


FIGURE 6 The x-ray spectrum from a laser-heated plasma (CH) measured (points) and computed (solid line) on an absolute basis.⁴¹ Lines and edges below 1 keV are not resolved.

of high power density ($> 10^{12}$ W/cm²) beams of photons, electrons, or ions on solid targets produces temperatures above 10^5 K.⁴² Laser beams have produced 10^6 – 10^7 K temperatures, but electron and ion beam heating has yet to yield x-ray hot plasmas. Relatively modest-sized lasers will produce million degree plasmas. Many devices in which plasmas are heated by electrical discharges are available. Both beam and discharge heated plasmas can produce submicrosecond bursts of x-rays.

Only recently have plasma x-ray sources been used in x-ray lithography and microscopy. Nd glass laser systems were employed in the initial work,^{43,44} one of them is shown in Figure 7.⁴⁵ Submicrosecond exposure times for replication of masks with single or multiple shots were demonstrated with fast resists. The sensitivity of PBS to such short exposure times was found to be similar to its sensitivity to long-term exposures.⁴⁶ Potential problems with the use of laser plasmas for routine exposure of resists were examined.⁴⁶ It was found that debris from the target can be eliminated by the use of thin targets and simple shields. The response of masks to repeated pulsed heating, which may be a problem with plasma sources, must be investigated experimentally. Optimization of the x-ray intensity from laser plasmas in order to reduce laser costs has been examined⁴⁷ and a production line facility roughly designed.⁴⁸ X-ray microscopy with 100 Å resolution using laser-heated plasmas has not been done, but it appears to be feasible.⁴⁸

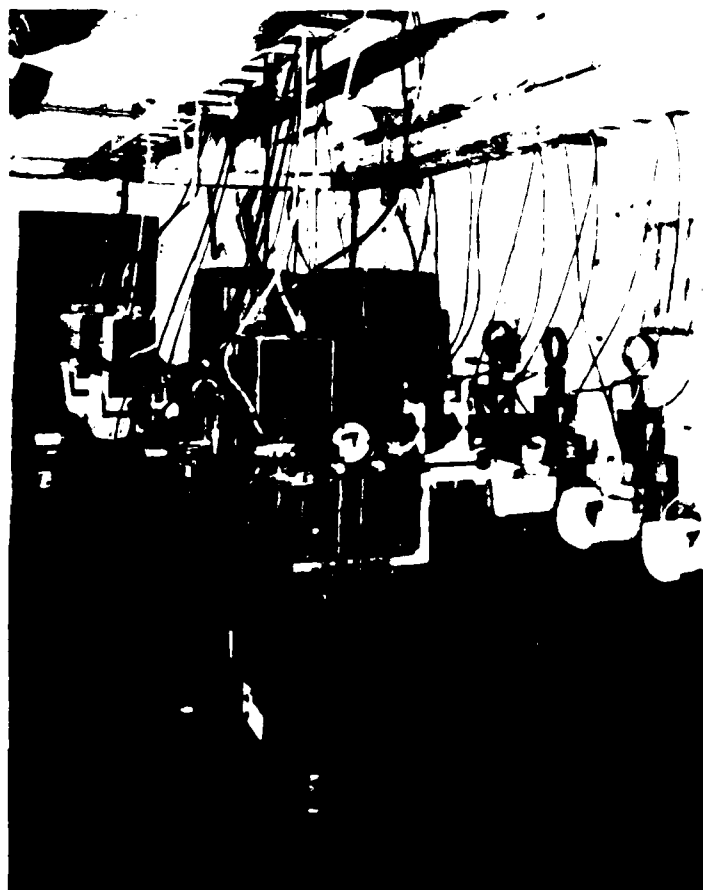


FIGURE 7. The Nd glass laser system⁴⁵ that was employed in early flash x-ray lithography experiments at NRI. The oscillator (nearest camera) and two amplifiers are in box-like structures mounted on the concrete beam. The capacitors, which power the flash lamps, are on the right.

One electron heated plasma source has been employed for photoresist exposure. McCorkle and Vollmer⁴⁹ built a device in which a plasma is first created by discharging a capacitor along the inside of a plastic tube 1–2 mm in diameter (a "sliding spark"). Then an electron beam is used to heat the plasma to a temperature near one-half million K. Soft x-rays up to about 400 eV are emitted largely from carbon ions, in ~ 100 ns pulses.^{50,51} The radiation was used to produce relief contact microradiographs of biological specimens on PMMA placed 22 cm from the source tube. Resolution of 300 Å was exhibited.⁵² No information on the use of beam heated sliding spark plasmas for the replication of masks has been published.

In summary, several studies employing plasmas as x-ray sources for lithography and microscopy have been performed in the last two years. Work with lasers is

more advanced now than research using electron-heated plasmas. Small lasers and discharge sources appear convenient for x-ray microscopy, while larger devices are needed to produce adequate intensity for practical single-shot replication of masks. Designs for production line x-ray facilities have been conceptualized for laser-heating but not for discharge devices. Debris from in and near the plasma and low repetition rates can be problems in the routine use of plasma x-ray sources, but these can be overcome. The long-term response of masks to pulsed heating due to x-ray absorption remains to be measured. Lasers adequate for heating plasmas to expose resists cost approximately $\$2 \times 10^5$, while small electron-heated plasma devices involve about one-tenth that expense.

TABLE I
SOURCE CHARACTERISTICS, SIZES, AND COSTS OF X-RAY DEVICES USED FOR
EXPOSURE OF PHOTORESISTS*

	Electron impact sources		Synchrotron radiation	Plasma sources	
	Static anode	Rotary anode	sources	Nd lasers	Electrical discharge
Spectral character	Lines and continuum		Continuum only	Strong lines and weak continuum	
Photon energy range	3 to > 10 keV (sealed source) < 0.1 to > 10 keV (windowless)		UV to > 50 keV	Most intense < 1 keV	
Source size (mm ²)	1-20		5	0.2	0.2
Emission solid angle (sr)	10^{-2}		10^{-5}	6	0.1
Exposure area (cm ²)	< 50		0.1-5	< 200	< 20
Emission time	Continuous emission		Steady, pulsed emission	$< 10^{-6}$ s	
Time between pulses (s)			10^{-8} - 10^{-6}	10^3	30-60
PMMA exposure time (s) [†]	10^4		10^2 - 10^3 (present sources) 10^{-1} - 10^2 (New sources)	$< 10^{-6}$	
Device size (m)	1 × 1	2 × 2	‡	2 × 5	1 × 1
Device cost (\$)	2×10^4	10^5	10^6 - 10^7	2×10^5	2×10^4
Other factors	Vacuum or helium atmos- phere used in the expo- sure regions			Exposures in vacuum to date	

*Only approximate or typical values are given. The data are from references cited in the text.

†The exposure times for electron-impact and synchrotron radiation sources are for full exposure of PMMA. Plasma sources usually produce relief structure in PMMA with a single shot.

‡Storage ring radii are in the 1-100 m range, with machines adequate for resist exposure having 1-10 m radii.

DISCUSSION

Three types of x-ray sources have been used to expose photoresists for mask replication and microscopy, and were first reported in the years indicated: electron impact devices (1972), synchrotron radiation sources (1976), and high temperature plasmas (1978). The mechanisms, spectra, and other characteristics of such sources, and their use in resist work, were reviewed above. TABLE I gives a summary of the salient features, including aspects of the radiation field (spectral, spatial, and temporal characteristics), as well as approximate source sizes and costs. No one source stands out as clearly advantageous for all resist exposure work. Electron impact devices are accessible but require long exposures. Synchrotron radiation is not conveniently available but has outstanding collimation as well as attractive exposure times. Very hot plasmas are the newest and least familiar sources for x-ray lithography and microscopy. Plasma sources can be small and cheap, but they require resists faster than PMMA for full exposure in a single shot. However, plasma radiation can produce high-resolution relief exposures in PMMA in less than a microsecond. Hence, they should prove useful for stop-motion studies of live biological specimens.

The x-ray sources used to date for resist exposures in no way exhaust the list of possible x-ray sources. It is anticipated that other electron-heated plasma sources will be employed in mask replication and microradiography. Furthermore, there is still much room for optimization of the sources already used. In particular, the use of multiple-pass laser amplifiers, short wavelength excimer lasers, and, possibly, repetitively-pulsed laser systems will reduce the size and cost of lasers for plasma radiation resist exposures.

Another type of research needed concerns the direct comparison of available x-ray sources. If the same masks were employed to produce a given set of test circuits by each of the three major types of x-ray sources, then the relative advantages and disadvantages of each source would be more quantitative. Factors concerning the practical use of various sources, as well as the structural character, electrical performance, and radiation hardness of the devices produced, could then be compared directly. Such a comparison could have significant industrial as well as scientific impact.

ACKNOWLEDGMENTS

It is a pleasure to recognize continual collaboration on x-ray lithography with M. C. Peckerar (Advanced Technology Laboratory—Westinghouse), R. R. Whitlock (Radiation Technology Division—NRL), J. R. Greig, J. M. McMahon, and R. E. Pechacek (Plasma Physics Division—NRL), and L. R. Hughey (Far UV Section—National Bureau of Standards).

REFERENCES AND NOTES

1. BARTOLINI, R. A., H. A. WEAKLEIM & B. F. WILLIAMS. 1976. *Opt. Eng.* 15(2):99.
2. DELZENNE, G. A. 1979. *In* *Advances in Photochemistry*. I. N. Pitts, Jr. *et al.*, Eds. 11:1. Wiley, New York.
3. COSLETT, V. E. & W. E. NIXON. 1960. *X-Ray Microscopy*. University Press, Cambridge.
4. NAGEL, D. J. & C. M. DOZIER. 1977. *In* *High-Speed Photography*. M. C. Richardson, Ed. SPIE 97:132.

5. SPILLER, E. & R. FEDER. 1977. *In* Topics in Applied Physics. H. J. Queisser, Ed. 22 (X-Ray Optics):35. Springer-Verlag, Berlin.
6. WARDLY, G. A. R. FEDER, D. HOFER, E. E. CASTELLANI, R. SCOTT & J. TOPALIAN. 1978. *Circuits Manufacturing* January:30-40.
7. HUGHES, G. P. & R. C. FINK. 1978. *Electronics* November:99-106.
8. TAYLOR, G. N. 1979. *In* Stanford Synchrotron Radiation Laboratory Report 79/02:93-109.
9. MALDANADO, J. R. 1979. *In* Stanford Synchrotron Radiation Laboratory Report 79/02:117-130.
10. SHAVER, D. C., D. C. FLANDERS & H. I. SMITH. 1979. *In* Stanford Synchrotron Radiation Laboratory Report 79/02:131-142.
11. WHITLOCK, R. R. (Naval Research Laboratory). Unpublished results.
12. BIGGS, F. & R. LIGHTHILL. 1971. Sandia Laboratories Report SC-RR-710507.
13. GUDAT, W. 1977. DESY SR-77/21.
14. CLARK, D. T. 1977. *In* Advances in Polymer Science. H. J. Cantow *et al.*, Eds. 24:126. Springer-Verlag, Berlin.
15. DUKE, C. B. 1978. *J. Vac. Sci. Technol.* 15(2):157.
16. FEDER, R., E. SPILLER, J. TOPALIAN, A. N. BROERS, W. GUDAT, B. J. PANESSA, Z. A. ZADUNAISKY & J. SEDAT (1977. *Science* 197:259.) employed synchrotron radiation. B. PANESSA-WARREN (This volume.) used a carbon-target electron impact x-ray source.
17. MURATA, K., T. MATSUKAWA & R. SHIMIZU (1971. *Jpn. J. Appl. Phys.* 10(6):678.) describe a Monte Carlo computation of x-ray line intensities. R. C. PLACIOUS (1967. *J. Appl. Phys.* 38(5):2030.) gives Monte Carlo continuum calculations performed by H. J. Berger and S. Seltzer.
18. BROWN, D. B., D. B. WITTRY & D. F. KYSER (1969. *J. Appl. Phys.* 40(4):1627.) describe transport equation x-ray line intensity calculations. D. B. BROWN, J. V. GILFRICH & M. C. PECKERAR (1975. *J. Appl. Phys.* 46(10):4537) include transport equation calculations of bremsstrahlung spectra.
19. BIRKS, L. S. 1972. *Anal. Chem.* 44(5):557R.
20. SPEARS, D. L. & H. I. SMITH. 1972. *Electron. Lett.* 8(4):102.
21. SMITH, H. I. 1977. *In* Surface Wave Filters. H. Matthews, Ed.:165. Wiley, New York.
22. MALDANADO, J. R. 1979. *In* Stanford Synchrotron Radiation Laboratory Report 79/02:13-23.
23. PECKERAR, M. C., C. J. TAYLOR & P. D. BLAIS. 1978. *Proc. IEEE Intl. El. Devices Mtg.*:588. IEEE, Piscataway, N.J.
24. PECKERAR, M. C. Private communication.
25. YOSHIMATSU, M. & S. KOZAKI. 1977. *In* X-Ray Optics. H. J. Queisser, Ed.:9 Springer-Verlag, Berlin.
26. STOVER, H. L. 1978. Hughes Research Laboratory Report ECOM-77-2669-1.
27. WINICK, H. & A. BIENENSTOCK. 1978. *Annu. Rev. Nucl. Sci.* 28:33.
28. KUNZ, C., Ed. 1979. *Synchrotron Radiation*. Springer-Verlag, Berlin.
29. *IEEE Trans. Nucl. Sci.* 1979. NS-26 (No. 3, Part 2):3779-3867 contains many recent articles on synchrotron radiation sources and uses.
30. HODGSON, K. O. & S. DONIACH. 1978. *Chem. Eng. News* 21 August:26.
31. RAKOWSKY, G. & L. R. HUGHEY. 1979. *IEEE Trans. Nucl. Sci.* NS-26(3):3845.
32. SPILLER, E., D. E. EASTMAN, R. FEDER, W. D. GROBMAN, W. GUDAT & J. TOPALIAN. 1979. *J. Appl. Phys.* 47(12):5450.
33. FAY, B., J. TROTEL, Y. PETROFF, R. PINCHAUX & P. THIRY. 1976. *Appl. Phys. Lett.* 29(6):370.
34. ARITOME, H., T. NISHIMURA, H. KOTANI, S. MATSUI, O. NAKAGAWA & S. NAMBA. 1978. *J. Vac. Sci. Technol.* 15(3):992.
35. NISHIMURA, T., H. KOTANI, S. MATSUI, O. NAKAGAWA, H. ARITOME & S. NAMBA. 1978. *Jpn. J. Appl. Phys.* 17 (Suppl. 17-1):13.
36. PIANETTA, P., R. BURG, J. KIRZ, H. RARBACK, M. MALACHOWSKI & J. WM. MCGOWAN. 1979. Stanford Synchrotron Radiation Laboratory Report 79/01.
37. NEUREUTHER, A. R. 1979. *In* Stanford Synchrotron Radiation Laboratory Report 79/02:24-40.

38. BETZ, H., F. K. FEY, A. HEUBERGER & P. TISCHER. 1979. IEEE Trans. Electron Devices **ED-26**(4):693.
39. SPILLER, E., R. FEDER & J. TOPALIAN. 1977. Phys. Technol. January:22.
40. NAGEL, D. J. 1975. In *Advances in X-Ray Analysis*. W. L. Pickles *et al.*, Eds. **18**:1.
41. HAAS, R. A., W. C. MEAD, W. L. KRUEER, D. W. PHILLION, H. N. KORNBLUM, J. D. LINDL, D. MACQUIGG, V. C. RUPERT & K. G. TIRSHILL. 1977. Phys. Fluids **20**(2):322.
42. NAGEL, D. J. 1979. IEEE Trans. Nucl. Sci. **NS-26**:1228.
43. NAGEL, D. J., M. C. PECKERAR, R. R. WHITLOCK, J. R. GREIG, & R. E. PECHACEK. 1978. Electron. Lett. **14**(24):78.
44. MALOZZI, P. J., H. M. EPSTEIN & R. E. SCHWERZEL. 1979. In *Adv. in X-Ray Analysis*. G. J. McCarthy *et al.*, Eds. **22**:267.
45. GREIG, J. R. & R. E. PECHACEK. 1977. NRL Memo Report 3461.
46. PECKERAR, M. C., J. R. GREIG, D. J. NAGEL, R. E. PECHACEK & R. R. WHITLOCK. 1978. In *Proc. Symp. on Electron and Ion Beam Sci. and Technology*. R. Bakish, Ed. 432. Electron. Chem. Soc. Princeton.
47. NAGEL, D. J., R. R. WHITLOCK, J. R. GREIG, R. E. PECHACEK & M. C. PECKERAR. 1978. In *Developments in Semiconductor Microlithography III*. R. L. Ruddell, Ed. SPIE **135**:46.
48. NAGEL, D. J., J. M. McMAHON, R. R. WHITLOCK, J. R. GREIG, R. E. PECHACEK & M. C. PECKERAR. 1978. Jpn. J. Appl. Phys. **17** (Suppl. 17-2):472.
49. McCORKLE, R. A. & H. J. VOLLMER. 1977. Rev. Sci. Instrum. **48**(8):1055.
50. McCORKLE, R. A. 1978. J. Phys. B **11**(14):L407.
51. McCORKLE, R. A., J. ANGILELLO, G. COLEMAN, R. FEDER & S. J. LAPLACA. 1979. Science **205**:401.

DISCUSSION

DR. G. SCHMAHL: Is it possible to give a number with which to compare the plasma output and the simple x-ray source? Let's say, number of photons per pulse per square milliradian per second.

DR. D. J. NAGEL: Yes. Efficiencies for the conversion of laser light to x-rays and hard ultraviolet radiation can range up to around 30%. If you have a 100 Joule laser, one which is intermediate in size and expense and within the reach of many laboratories, then you can get a few tens of Joules of radiation emitted into 2π sr in a pulse that is less than one microsecond long. For such lasers, a time of 15 minutes between pulses is typical. Single-shot exposures are possible, so multiple pulses are not necessary.

DR. N. M. CEGLIO: I'd like to take exception to the multiple-pulse concept. I think the reason you have low repetition rate lasers now is that lasers designed now are not designed for this particular application. The technology that's most advanced is that for neodymium lasers, ruby lasers, and CO₂ lasers. There are, however, many other lasers. Even for neodymium lasers, these slow repetition rates really apply only to the heating of the glass, which then compromises your ability to focus that beam to very small spots. But you don't really need very small spots. A 100 or 200 μ m spot is not anywhere near the diffraction limit, so you could even push those lasers beyond their design repetition rates.

So those of you who are thinking of a laser as an option should not let your concepts be limited by the repetition rate because, just over the horizon, rare gas halide lasers are being developed for laser isotope separation. These are going to operate mainly in uv, which is much better for coupling to x-ray conversion. Also,

they're going to operate at a thousand pulses per second, and they're going to operate at hundreds of Joules. The technology for these things currently exists, but only in the laser isotope separation program, and so they're being developed for the laser fusion program. And those people aren't thinking about your problem.

NAGEL: I couldn't agree with you more. No one has published even a design study on building a laser specifically for resist exposures. We have done some work on it, and come to the conclusion (based on the measurements of CO₂ lasers and of the short pulses, and so forth) that it is better to go with single shots with near-term technology. Of course, the laser system you're referring to is not the kind of relatively modest laboratory system that is within our financial reach, but approaches a small synchrotron source.

DR. J. KIRZ: Just from a back-of-the-envelope estimate, there appears to be a significant danger of the kind that you've already alluded to, that is, if you are talking about making a single shot exposure on PMMA, in particular, where you know that an exposure takes on the order of a Joule per square centimeter, and you absorb that in a thickness of about a micrometer, I cannot escape the conclusion that the temperature rise, just of the caloric input, is going to be several hundred degrees. Now PMMA undergoes a phase transition at around 200 degrees, and it is very hard for me to see how you are going to compensate for the fact that you might undergo a phase transition both going up and coming down. Will you be able to register the pattern correctly?

NAGEL: I don't know yet. I am concerned about the same problem. And it may be that the necessity of staying below the resist "thermal response envelope" as the laser parameters are varied will force us to go to multiple shot lasers. But there's no data on that yet.

DR. R. A. McCORKLE: I have a few comments about that. We've done some work with single shot exposures in PMMA, both near the limit where we damage the PMMA and where we think we have valid registration in the PMMA. What we think is that—and this is backed up by some calculations that Dr. Sayre has done—one can expect something on the order of 300 Å resolution information in single shot exposures. In fact, we think we've seen that, or something very close to that. We don't think that higher resolution information can be developed by the single shot method.

My other point is that you can beat this 1 J/cm² limit somewhat by using softer radiation. As I indicated yesterday, in the 23–44 Å region, the absorption is again much higher in the resist. So, for information of a biological nature, where you can etch and make shallow exposures, you can use quite a bit less energy per cm² and still make a sufficient exposure to get 300 Å resolution.

KIRZ: Less energy is absorbed by a thinner layer, and, as a result, caloric input is going to be comparable.

McCORKLE: That's right. And in test patterns we do see an image prior to etching.

NAGEL: Yes, we've seen the same. You can just flash-imprint it.

UNIDENTIFIED SPEAKER: I just want to clarify that statement. Dr. McCorkle's wavelength is very well suited for that because the absorption takes place in a tenth of a micrometer. The heat penetrates about one micrometer. So he gains a factor of ten. Heat travels a micrometer in a nanosecond, so heat affects a larger volume than does absorption. That is true in the region around the carbon edge. For microscopy that's very nice. But if you want to make an exposure on the other side of the carbon edge, where the absorption rate is also on the order of a micrometer, then the heat associated with the same exposure level as before is much higher, because the heat cannot travel away. So Dr. McCorkle has a special system, and you won't be able to get that at another wavelength.

NAGEL: Of course, we claim the same advantage, because we can manipulate the spectrum by changing the target.

McCORKLE: I would like to say that we have also found that, by using a somewhat broad-band emission, we minimize artificial confusing information, at least that apparent to the human eye, in producing images of biological specimens. The diffraction pattern seems to wash out. I'm sure that there's information hidden in there, but the loss of the diffraction effects does give a rather nice picture.

DR. D. K. BOWEN: I'd like to emphasize once again that the number of photons you need for an image depends directly upon the contrast, and the contrast depends exactly on how you choose the wavelength. So it's not just a matter of the thermal dissipation, it's a matter of what information you get out of the photons you put in. And if you choose monochromatic radiation near absorption edges, preferably with differential techniques on either side, then you gain enormously. You can gain factors of ten or more in contrast, and this will cut down, again, by factors of ten or more, the number of photons that you need. These techniques are well worth investigating.

So I don't know how well you can peak the radiation from a plasma source.

I wondered, too, if, for some applications, it's really worthwhile having a very small source to get certain collimation effects, as everyone knows. Is there any possibility of having a relatively simple magnetic field arrangement around the plasma source to get a magnetic pinch to keep the plasma from expanding too much?

NAGEL: We've done experiments with up to 100 kilogauss applied fields, which narrowed the sideways expansion, but it elongates the expansion the other way. So I don't think that's a good idea.

In regard to the question, how tightly can we sweep up the photons into a narrow range by choosing elements, like carbon and boron, that predominantly emit K-shell radiation? We can put the energy in relatively narrow bands on one side or the other side of the carbon edge.

DR. J. W. MCGOWAN: You brought up the point, which was a very good one, that the garbage, essentially, comes back and floods the mask. What about the question of the electrons that come back from a number of different sources? The standard electron source impacts onto an anode, and there are an awful lot of secondary electrons there. Certainly, there are a lot of secondary electrons in the laser plasma. Now, I wonder what kind of damage those secondary electrons do.

NAGEL: I've wondered too. I don't have an answer. But I can say the following: the plasma tends to blow off, just because of the pressure, normal to the target. Now the bulk of the electrons and ions tend to stay together for charge neutrality reasons. So you can sit off to the side and dodge most of the electrons. But it is important to sort that problem out, and one can do it by applying magnetic fields and not doing differential experiments in order to separate photon, electron, and ion effects. They have been done for laser fusion applications, but not for resist exposure.

Radiation effects in MOS devices caused by x-ray and e-beam lithography

M. Peckerar, R. Fulton, and P. Blaise

Westinghouse Electric Corporation, Baltimore, Maryland 21203

D. Brown and R. Whitlock

Naval Research Laboratory, Washington, D.C. 20375

(Received 13 June 1979; accepted 28 September 1979)

In this study we have found that electron-beam and x-ray irradiations of metal (or polysilicon)-oxide-semiconductor devices performed at typical PBS or PMMA exposure levels create temperature-bias-stress (TBS) instability. Experimental results can be most reasonably explained by assuming that exposure to both of these types of ionizing radiation causes mobilization of positive charge in the insulator. The positive charge is forced closer to the semiconductor-gate-oxide interface during the positive bias phase of the TBS test. This damage mechanism was found in HCl, H_2/O_2 , and dry grown oxides. HCl oxides exhibited the effect the least of the three oxide types studied. N_2 anneals performed at 500 and 900°C, and H_2 anneals performed at 500°C (all for 30 min) did not substantially reduce TBS instability. A 900°C anneal in H_2 for 30 min did create a marked reduction in the TBS-induced instability.

PACS numbers: 73.40.Qv, 61.80.Cb, 61.80.Fe, 81.40.Ef

I. INTRODUCTION

It has been realized for sometime that radiation doses in excess of a megarad are frequently absorbed in sensitive gate oxides during the x-ray or e-beam fabrication of metal-oxide-semiconductor (MOS) parts.^{1,2} For example, a typical exposure dose for PMMA is 500 J/cm². For a unity density resist film, this corresponds to a 50 Mrad exposure. A faster resist such as PBS requires a 1 Mrad exposure dose. As is shown below, for typical polysilicon gate structures, energy deposition in the gate oxide generally approximates the resist exposure dose for both x-ray and e-beam exposures. Since such doses have a marked effect on the resist, it is not too surprising to find that the oxide layer undergoes damage as well.

Observations of damage patterns following room-temperature ⁶⁰Co irradiation of biased gate devices indicate that the damage effects include a charging of the insulator and the production of insulator traps. Charging results as mobile electrons move out of the biased insulator, leaving the relatively immobile positive holes behind. For aluminum gate devices, this positive charge can be removed by annealing.³ For unbiased gate devices subjected to ⁶⁰Co irradiation, there is little charging, although traps are still produced for both the biased and unbiased cases. Attempts to anneal leave many residual trapping centers (primarily electron traps), which can become charged during operation.^{3,4} In addition, there is a general increase in fast interface state density.⁵

In this paper, we present results of high field temperature bias stress (TBS) testing of MOS and polysilicon gate-oxide-semiconductor (POS) structures. These structures have been irradiated to levels characteristic of x-ray and e-beam lithography. Various anneals were attempted to remove positive charging and residual trapping centers. Following anneals, high field TBS tests were employed as an accelerated

life test. The high field TBS tests indicate the existence of a positive charge instability other than that previously discussed with respect to irradiations performed on devices under bias. The experimental TBS results can be most reasonably explained by assuming that the x-ray and e-beam radiations mobilize positive charge in the oxide. The source of this positive charge is, at present, not known. The high fields and elevated temperature of the positive gate bias stress test forces the charge to the oxide-semiconductor interface where it has its largest effect on threshold and flatband voltages. TBS-induced flatband shifts as large as 2 V have been encountered in 500 Å oxides. Nitrogen anneals performed at temperatures as high as 900 °C failed to alleviate this problem. Hydrogen anneals at 500 °C (which we consider the highest safe sintering temperature for aluminum gates) also failed to significantly reduce the problem. Hydrogen anneal at 900 °C did significantly alleviate the problem for polysilicon gates.

EXPERIMENTAL SET-UP

The test structures were 0.5-mm-diam capacitor dots. A schematic of the POS structure used is shown as Fig. 1. In addition, an MOS structure (in which the only layer above the gate oxide was 1000 Å of aluminum) was also used. Dry oxides, steam (H_2/O_2) oxides and HCl oxides were examined in this study. Oxidation temperatures were 900 and 1000 °C. Each oxide received a 5 min dry N_2 anneal in the oxidation furnace tube (at oxidation temperature) before withdrawal and deposition of the gate. The thin film structures were irradiated using exposure levels typical of x-ray or e-beam lithography.

X-ray irradiations were performed in a vacuum chamber containing the sample and x-ray source. A 1/2 mil Kapton layer (simulating a mask) protected the samples from stray electrons

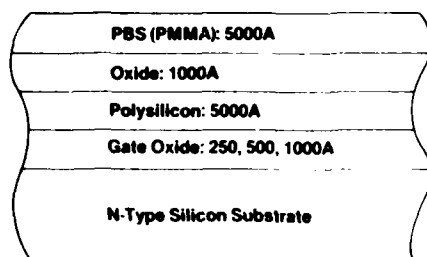


FIG. 1: Layer structure of the polysilicon-gate capacitor used in this study.

coming from the source. Dosimetry was provided both by films (Kodak No-Screen and T) and by $\text{CaF}_2\text{:Mn}$ thermoluminescent detectors (TLD's). The x-ray source was electron excited by perpendicularly incident electrons. Aluminum and silver targets were used. The x-ray take-off angle was 30° , measured from the anode surface normal. The amount of stray x-ray scattering within the vacuum chamber was measured with film by occluding the source with a lead shield held midway between the film and the source. Scattering intensity was not more than about 10% of the primary source intensity.

Electron-beam irradiations were performed in a Cambridge scanning electron microscope. The beam was set to raster scan over the region of interest until the time integrated specimen current indicated that the required number of charges at 25 KeV were incident on the sample. For PMMA, this was 10^{-5} C/m^2 . After irradiation, visible light photolithography was used to define half-millimeter diameter capacitor dots on the POS or MOS structure.

Anneals were performed on all samples (except for controls) following irradiation and capacitor dot photo-definition. For the N_2 anneals, the heat-up, anneal and cool-down phases were performed in N_2 . For the H_2 anneal, heat-up was done in N_2 , while the anneal and cool-down were done in H_2 ambient.

The TBS tests were performed after sweeping an initial room temperature C-V curve from +6 to -12 V. Next, the capacitor sample was heated to 200°C and a positive bias (either 15 or 20 V) was applied for 5 min. A capacitance voltage plot was then swept on the device after it was cooled to room temperature. The device was reheated to 200°C and

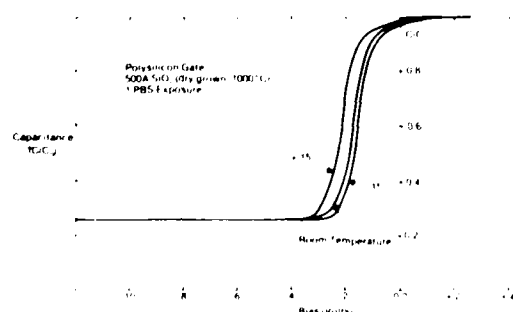


FIG. 2: Typical C-V plots obtained during temperature-bias-stress testing of capacitors after irradiation (1 PBS exposure performed with an Al K α source at 10 keV). Largest TBS shift occurred for the +15 V bias case. Specimen was not annealed prior to our following TBS test.

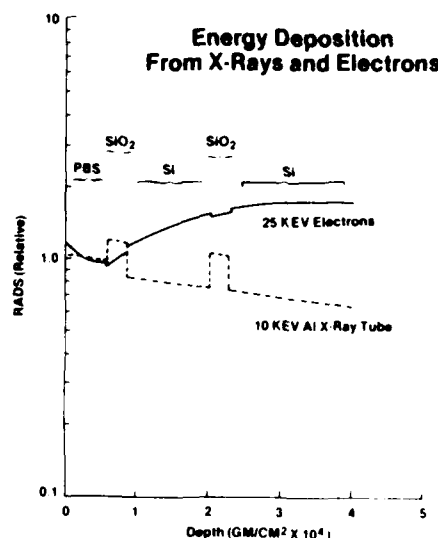


FIG. 3: A comparison of energy deposition for the x-ray (10 keV Al K-line) and e-beam (25 keV accelerating potential) exposure of PBS on the structure shown in Fig. 1.

a negative bias (15 or 20 V) was applied for 5 min. The device was cooled and a C-V curve was swept. The TBS instability was taken as the difference in flatband voltages (ΔV_{FB}) between the positive and negative bias C-V curves. No attempt was made to anneal out TBS-induced flatband shifts.

EXPERIMENTAL RESULTS

A typical set of C-V plots taken during the TBS test of irradiated capacitors is shown as Fig. 2. Similar curves were obtained, whether from electron beam or x-ray irradiation. A large negative shift is encountered following positive stress at elevated temperature. This cannot be caused by electron injection (which would create a negative shift). The most likely mechanism is the forcing of positive charges, made mobile by ionizing radiation, away from the gate-oxide interface and toward the oxide-semiconductor interface. Changes in interface state density can also cause this effect, as shown below, however, the density of interface state increase does not support this hypothesis. A 2 V flatband shift in a 500 Å oxide corresponds to $2.6 \times 10^{12} \text{ charges/cm}^2$ forced to the oxide semiconductor interface from the gate.

The reason for this TBS-induced flatband shift is the large amount of energy deposited in the gate/insulator by the incident ionizing radiation. In Fig. 3 we see the calculated results for energy deposition in the various layers of the POS structure for e-beam and x-ray irradiation. The electron energy deposition was arrived at using the transport electron program (TEP),⁶ which applies Boltzmann's equation to the electron transport problem. For the x-ray energy deposition, the SLABS program⁷ was used, which also accounts for secondary fluorescence in each layer. The deposition curves are normalized to the deposition midway in the resist film. We see that there is a slight increase in the deposition ($\sim 10\%$) in the gate oxide over the resist-midpoint-deposition for Al K-line source. There is about a 50% increase in gate-oxide-deposition over the resist-midpoint-deposition for the 25 keV e-beam case.

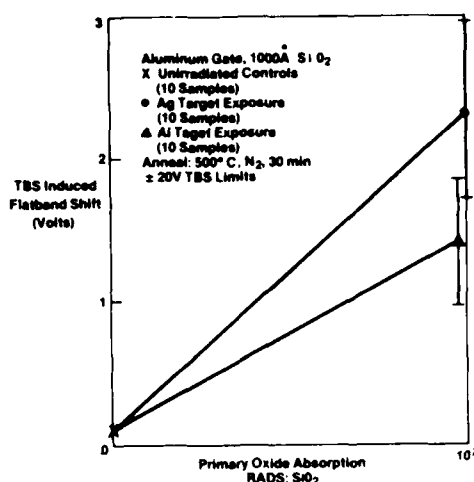


FIG. 4: Temperature-bias-stress induced flatband shift as a function of primary radiation dose for Ag, and Al soft x-ray exposures

In Fig. 4 we see a graphic summary of the TBS instability present in the aluminum gate, 1000 Å oxide capacitor following x-ray exposure. Both aluminum K-line and silver L-line results are shown; a 10 Mrad dose was absorbed in the oxides for both the silver and the aluminum cases. Unirradiated controls are compared to irradiated samples. Significant TBS instability was introduced during both the aluminum as well as silver x-ray exposure. There was a considerable spread in the data for radiation exposed samples, as indicated by full range error bars, which represent the extremes of the data. TBS instability distributions for silver and aluminum exposures overlap. These results were obtained on samples which underwent 500°C N₂ anneals for half an hour.

A similar result was obtained for the polysilicon gate devices (as seen in Fig. 5). In this figure, dry, steam, and HCl oxides were compared. No post-radiation anneal was performed. HCl oxides gave the best result. Exposure levels were chosen to be consistent with PBS and PMMA exposures. A full range error bar for 5 samples of this HCl oxide exposed to 1 PMMA exposure is included. Figure 6 illustrates the effects of 500 and 900°C anneals on samples similar to those used to obtain Fig. 4. Nitrogen anneals performed at 500 and 900°C had no real effect on the TBS stability TBS-induced flatband shifts

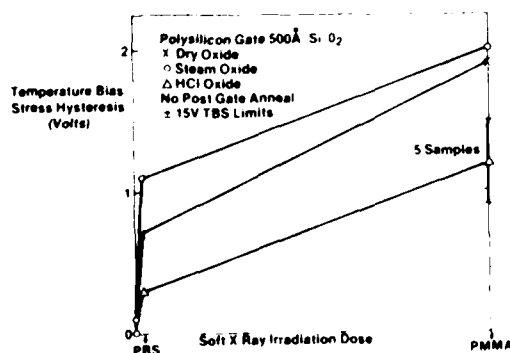


FIG. 5: Temperature bias stress as function of x-ray irradiation dose of various types of oxide

J. Vac. Sci. Technol., Vol. 16, No. 6, Nov./Dec. 1979

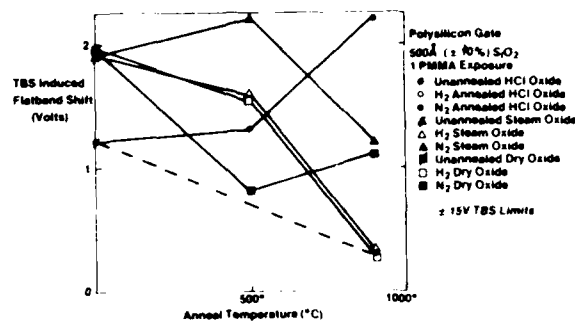


FIG. 6: Results of annealing polysilicon gate, soft x-ray-irradiated capacitors in N₂ and H₂ at 500° and 900°C

ranged between 1 and 2 V. The same was true for H₂ anneal at 500°C. Only the 900°C anneal done in hydrogen significantly reduced TBS instability.

We have observed this same effect occurring in *e*-beam irradiation. These results are shown in Fig. 7 for PMMA-level exposures done with *e* beam and x rays (Al K-line exposure). The postradiation TBS instability was essentially the same in both cases. There did appear to be some difference in control samples, probably due to a slight difference in the way controls were selected. The *e*-beam system employed accepted small samples (~1 cm²). A shielded region near the irradiated region was used as the control. There was some possibility that this region was not shielded as well as a similar control used in the x-ray case. In any event, H₂ anneal at 900°C brought about TBS stability for both x-ray and *e*-beam irradiation.

The effect of x-ray and *e*-beam irradiation on fast interface states was also studied. Prior to irradiation high/low frequency interface state measurements were performed. These measurements indicated the samples used in this study has ~5 × 10¹⁰ states/eV cm² near midgap. In Fig. 8 we see the growth of the ac conductance peak height (indicating a growth of fast interface states) resulting from both x-ray and *e*-beam damage. Conductance peaks almost double following PMMA-level exposures from Ag-L-line or *e*-beam irradiation. High/low frequency C-V plotting also indicated a doubling in the number of states. Such a small amount of increase could not account for the over 2 × 10¹² occupied states implied by TBS test results. Also, since the greatest shift is in a negative direction after positive bias, holes would have to be injected

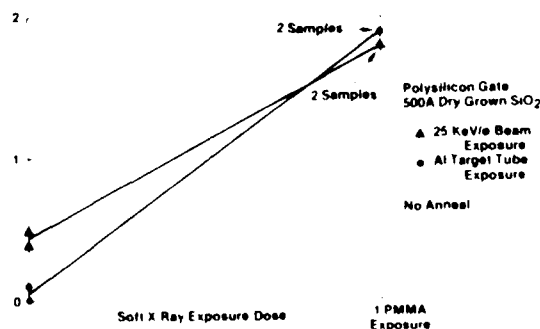


FIG. 7: Comparison of temperature bias instability created by *e* beam (25 keV/e) and x-ray (Al K-line) exposures

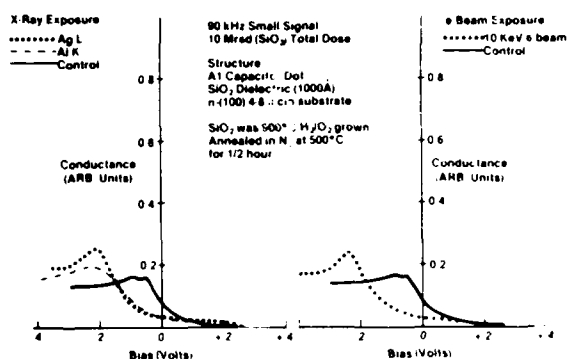


FIG. 8 Effect of x-ray and e-beam exposures on conductance peak height

into the insulator from the gate and migrate to the interface to produce the observed result. This is unlikely. Thus, the TBS charging mechanism is most likely a bulk phenomenon. However, it should be pointed out that we were unable to observe the interface-state density accurately near the band edges with the equipment at hand. Such states tend to remain occupied and could appear as a fixed charge. This mechanism explaining TBS instability cannot be fully ruled out at present.

CONCLUSIONS

Both x-ray and e-beam irradiations typical of those encountered in x-ray and e-beam lithography create damage in MOS structures which is not annealable at 500°C in H₂ or N₂ ambients. The pattern of the damage observed is the same in both the e-beam and x-ray case. A reasonable explanation for these results would be that positive charge is mobilized in the insulator and forced closer to the oxide-semiconductor surface during TBS high field stress test. HCl oxides appear to exhibit somewhat less (but not negligible) instability compared to dry or steam oxides. An N₂ anneal at 900°C for one-half hour does not alleviate this problem, but a 900°C anneal for one-half hour in H₂ does. X-ray and e-beam radiation-damaged samples demonstrated marked increase in fast interface states densities.

¹K. F. Galloway and S. Mayo, *J. Appl. Phys.* **49**, 2586 (1978).

²T. H. Nung, *J. Appl. Phys.* **49**, 4077 (1978).

³S. E. Bernacki and H. J. Smith, *IEEE Trans. Electron Devices* **ED-22**, 421 (1975).

⁴J. M. Aitken, *IEEE Trans. Electron Devices* **ED-26**, 372 (1979).

⁵P. J. Balk, *J. Electrochem. Soc.* **112**, 185C (1965).

⁶D. B. Brown, J. V. Gilfrich, and M. C. Peckerar, *J. Appl. Phys.* **46**, 4357 (1975).

⁷D. B. Brown, U. S. Naval Research Laboratory (private communication).

RADIATION HARDNESS OF LSI/VLSI FABRICATION PROCESSES*

B. L. Hughes
Naval Research Laboratory
Washington, D. C. 20375

Abstract

Candidate large-scale and very large scale integrated (LSI/VLSI) circuit fabrication processes have been partitioned, and representative MOS capacitors irradiation-bias stressed and characterized. Laser annealing for implantation activation of polysilicon films has been found to provide MOS devices with greater radiation-hardness than those which are furnace annealed. Pre-gate processes (those processes performed before the deposition of the gate-electrode, which is either aluminum or polysilicon) involving ionizing radiation, such as X-ray lithography, cause increased MOS irradiation-bias sensitivities, even though post-fabrication, pre-irradiation characteristics reveal no differences from standard, non-radiative processing. These deleterious effects can be eliminated when both high temperature (800°C) pre-gate annealing and aluminum sintering (450°C) operations are performed. Since the aluminum sintering operation releases atomic hydrogen into the gate oxide, reducing the radiation damage, other oxide hydrogenation techniques may prove beneficial for those cases where aluminum is not available, such as in polysilicon gate structures.

Introduction

In order to achieve the reduced feature sizes required for VLSI device fabrication, new and modified processes will most likely be utilized. X-ray and electron beam lithographies, laser and electron beam annealing, low pressure CVD, sputter deposition, and reactive ion etching (RIE) are likely candidate processes for routine use in fabricating future VLSI circuits. The X-ray or electron beam lithographies, as well as RIE, are needed to define submicron size patterns; laser and electron beam annealing provide the local heating needed to activate implants and form metal/semiconductor contacts; LPCVD provides for superior uniformity, high purity and excellent step coverage.

Most of the above processes involve exposing the device structures to high doses of ionizing radiation. For typical X-ray and electron resists, the calculated doses of radiation for SiO_2 layers range from 80 Krad to 40 Mrad (SiO_2) for X-rays and 1 to 20 Mrad (SiO_2) for electrons.² In typical RIE operations the SiO_2 layers are exposed to bombardment by positive ions and electrons with energy approximately 1 keV, soft X-rays, and UV light.

It is well known that such radiative-processing bombardment of SiO_2 layers causes radiation damage in MOS structures.³ However, it has been reported that routine heat treatments during post-exposure processing recover the structures to their pre-bombardment condition.^{4,5,6} The remaining question is then whether the bombarded MOS structures have recovered sufficiently such as to not realize increased sensitivity to operational stresses such as irradiation-bias. The present work addresses this question of latent defects for a variety of VLSI processes, and attempts to determine possible cures in eliminating observed deleterious effects.

*Work supported by the Defense Nuclear Agency under Subtask TD033.

Experiment

In characterizing the radiation-hardness of the various VLSI processes, it was decided to explore the possible effects by using MOS capacitors fabricated with radiation-hardened oxides. Gate oxides were grown in dry oxygen at 1000°C without a high temperature post-oxidation N_2 anneal. Since hardened silicon on sapphire devices use lower temperature pyrogenic oxidations, 925°C pyrogenic oxides were also used in this work. HCl/O_2 oxidations, electron beam aluminum deposition and forming-gas sinter operations, often used in the semiconductor industry, were not used for this study because of the acknowledged enhanced radiation sensitivity inherent to these techniques. Filament or induction-heated sources for aluminum deposition and nitrogen sinter operations were utilized. This work utilized 4-8 $\Omega\text{-cm}$, n-type (100) silicon substrates for all experiments.

X-Ray Lithography

The X-ray lithography experiment used PBS (polybutane-1-sulfane) positive resist coated over $\text{Al/SiO}_2/\text{Si}$ structures. The SiO_2 was grown to 700 \AA in dry O_2 at 1000°C . An X-ray line at 1.6 keV was used to expose the resist.⁷ For this experiment, using 5000 \AA of PBS resist, a dose of 10^7 rads (SiO_2) was deposited in the exposed oxide regions. Since it is the field region that is exposed to X-rays for a positive resist, additional aluminum gates were deposited over these regions and sintered at 500°C for 30 minutes in N_2 .

After the sintering operation, both the control and X-ray exposed samples had identical inversion voltages (V_i) of -1.2 volts. However, after a worse-case irradiation-bias stress of 10^7 rad (Si) at +10 volts, the control and X-ray exposed samples shifted in V_i (mean values) at -2 and -5 volts, respectively. These V_i values observed from MOS C-V curves include the effects of interface-states, oxide space charges and lateral non-uniformities (LNU). No attempt was made to partition these interface parameters for the various processes used in this work.

Laser Annealing

A major concern in fabricating high speed VLSI devices is that of minimizing the resistivity of polysilicon films used to interconnect the myriad of devices on integrated circuits. Nearly all commercial vendors presently use n^+ polysilicon for these regions. A highly attractive, emerging technique found to reduce the resistivity of such polysilicon films is laser annealing.⁸ This present work compares laser annealing to furnace thermal annealing in terms of both the resulting resistivity and radiation hardness. Polysilicon films were deposited using the pyrolysis of SiCl_4/H_2 at 800°C . These films were deposited on 700 \AA of dry-oxygen (1000°C) grown silicon dioxide. The polysilicon films were implanted with 150 keV phosphorous ions to a dose of $5 \times 10^{15} \text{cm}^{-2}$. The thermally-annealed, ion-implanted polysilicon films were treated in N_2 at 1000°C for only 30 minutes to minimize thermal-induced oxide traps which would increase MOS radiation sensitivity. However, as such, the sheet resistivity was severely compromised in the thermal activation of the phosphorous implantation by the realization of a final value of 100 ohms per square. For the laser annealed

ion-implanted polysilicon films, a final sheet resistivity of 35 ohms per square was observed. A scanned, 15 watt, CW argon ionlaser was used to anneal in a non-melting mode. It was also observed that irradiation-bias stressing (10^6 rad-Si, + 10 volts) caused greater degradation in MOS structures fabricated using thermally annealed samples ($\Delta V_i = -17$ volts) than those with laser annealed polysilicon ($\Delta V_i = -6$ volts).

Sputter Deposition

Sputter deposition of aluminum directly on silicon dioxide was used to form the gate electrodes for MOS structures on one half of a wafer while the other half provided the control samples where filament deposited aluminum was used. A Varian, Type S, dc magnetron sputter gun was used to deposit the sputtered aluminum. For an irradiation bias stress of 10^6 rad(Si) at + 10 volts the V_i for the control sample changed -2 volts whereas the samples prepared using sputtered aluminum gate-electrodes changed on the average -12 volts for the same stress. Such large radiation-induced shifts are not observed if the sensitive gate-oxide regions are covered with polysilicon gate electrodes during the operation of sputter deposition of aluminum interconnection patterns. Such sputter deposition is now used routinely for other metallization systems, as well; for example, titanium and platinum depositions in trimetal, sealed-junction CMOS devices (again these devices have been found to be more radiation sensitive than CMOS devices fabricated with standard filament aluminum).

High Pressure Oxidation

In order to reduce the temperatures and times needed to fabricate VLSI circuits, high pressure oxidation is now being explored. A Gasonics Hipox system was used to grow 700 Å of SiO_2 at 700°C; a wet O_2 ambient at 10 atm was utilized. The irradiation bias-stress (10^6 rad-Si, + 10 volts) caused an inversion voltage shift of -26 volts, whereas a control (also grown in wet O_2 but at 925°C and 1 atm) shifted -6 volts. The reason for the much larger shift on the high pressure oxide is not understood, and further work is being pursued.

Low-Pressure CVD

Using 25% SiH_4 in N_2 at 650°C and 0.5 Torr for the LPCVD case and 760 Torr for the APCVD, 0.5 μm polysilicon films were grown on radiation-hard oxides (900 Å SiO_2 grown at 925°C pyrogenic). These films were implanted with 3×10^{15} boron ions cm^{-2} at 70 keV, and activated at 850°C, 30 minutes in N_2 . The polysilicon films were stripped by wet chemical means and aluminum gates were deposited and sintered (using the standard procedure mentioned above). With identical pre-stress inversion voltages, these samples shift in V_i -9 volts for the LPCVD case and -7 volts for the APCVD devices. The oxide control sample (without silicon deposition and activation heat treatments) shifted only -4 volts, thus again pointing out the deleterious effects of post-oxidation processing and heat treatments.

Reactive-Ion Etching (RIE)

Polysilicon/oxide samples as processed in the above section were etched in an IPC barrel-type reactor at 60 watts using a CF_4 + 5% O_2 plasma at 0.5 Torr. The polysilicon films deposited by LPCVD techniques (described above) were completely removed on half of the 2-inch wafer exposing the radiation-hardened silicon dioxide films, the etching was terminated (removing at most 50 Å of SiO_2 in the operation). Aluminum gates

were then deposited (using In-Source techniques) and sintered (450°C, 30 minutes in N_2). The RIE samples shifted in V_i -13 volts after irradiation-bias stress (10^6 rad-Si, + 10 volts), whereas the control portion of the wafer where the polysilicon was etched using wet chemical means shifted -9 volts for the same stress. Obviously, the concomitant ionizing radiation during RIE operations causes latent damage (with pre-irradiation-bias stress values of V_i the same as control samples) which is then reactivated during subsequent irradiation-bias stressing to produce large shifts in V_i .

Pre-metal Irradiation Treatment

In order to study MOS samples with known pre-metal radiation exposures, silicon dioxide films grown on silicon wafers were exposed to precise doses of cobalt-60 gamma radiation. A convenient, representative dose of 13.5 Mrad(Si) was exposed to a lot of wafers, each of which was then studied from the standpoint of the effect of subsequent processing on the radiation damage. The silicon dioxide films were grown in dry O_2 at 1000°C to a thickness of 700 Å prior to cobalt-60 irradiation. After irradiation (no bias/no gate electrode) the wafers were annealed 30 minutes in N_2 at various temperatures (400°C-1000°C), and some wafers were also sintered 30 minutes in N_2 at 450°C after gate-metallization (In-Source deposited aluminum). The following table indicates the effect of subsequent irradiation-bias stress (10^6 rad-Si, + 10 volts):

Table I
Irradiation-bias Stress Effects on
Pre gate-metal Irradiated Samples

Process	$-\Delta V_i$
800°C anneal + no sinter (V_i initial = -4.0 v)	6 volts
800°C anneal + sinter (V_i initial = -1.0 v)	2 volts
400°C anneal + sinter (V_i initial = -1.1 v)	3 volts
1000°C anneal + sinter (V_i initial = -1.2 v)	17 volts

From the above table it can be seen that the -2 volts hardness of the control process (no pre-gate irradiation) is retained only after both an 800°C N_2 anneal and an aluminum sinter operation. Since aluminum is not present in the gate regions of silicon gate circuits, an even higher temperature anneal was assessed. However, for annealing at 1000°C in N_2 reverse annealing is observed to such a large extent that this treatment can be eliminated as a possible remedy.

Discussion

From the above investigations, it is apparent that the aluminum sintering operation plays a major role in reducing irradiation-bias stress effects in pre-gate irradiated MOS structures. It is well known that the aluminum sintering operation releases atomic hydrogen into the silicon dioxide layer where the hydrogen transport mechanism possesses a 0.3 eV activation energy.^{10,11}

The atomic hydrogen introduced during the aluminum sintering operation is easily transported through channels in the silicon dioxide structure to the silicon/silicon dioxide interface where passivating Si-H bonds are formed.¹² For hydrogen introduced into oxides at temperatures above 600°C, deleterious SiOH bonds^{13,14,11} are formed throughout the bulk of the oxide, thus accounting for the observation

of increased radiation sensitivity, even though hydrogen is present during processing (as in the case of polysilicon deposition at high temperature using SiH_4).

It is apparent from this work that for silicon gate devices a method to hydrogenate the oxides at low temperature is necessary to remove the damage caused by radiative-processing. Ion implantation, hydrogen plasma bombardment, and high pressure-low temperature permeation are possibilities which should be explored. Since metal silicides (polycides) are being considered for very low resistivity interconnects in place of polysilicon, molybdenum or tungsten should be explored as agents to release the needed atomic hydrogen into the oxide regions.

Conclusions

As a result of the present experimentation, it is seen that advanced LSI/VLSI processing techniques will definitely impact MOS radiation hardness. Laser annealing activation of ion-implanted polysilicon is advantageous in providing both low resistivity and improved radiation hardness. However, the radiation sensitivity of MOS structures is aggravated by X-ray and electron beam lithographies, pre-gate plasma processing, sputter deposition, low pressure chemical vapor deposition of polysilicon, and high pressure oxidation.

Furthermore, experimentation in annealing pre-gate radiation damage indicates that the atomic hydrogen released during the sintering operation is highly effective in reducing this damage.

Acknowledgements

The author wishes to thank the efforts of P. R. Reid, J. F. Gibbons, T. J. Magee, I. Lagnado, D. J. Nagel, and M. C. Peckerar for assistance in sample preparation.

References

1. See Joint Special Issue on VLSI, IEEE Trans. Electron Devices, ED-26, April 1979.
2. K.F. Galloway, IEEE Trans. Nucl. Sci. NS-25, No. 6, 1469 (1978).
3. R.A. Gdula, IEEE Trans. Electron Devices, ED-26, No. 4, 644 (1979).
4. H.L. Stover, P.A. Sullivan, J.H. McCoy, F.L. Hause, H. Yuan, and E. E. Harari, Electro. Chem. Soc. Extended Abs, 78-1, abstract 384 (1978).
5. R.C. Henderson, T. Reiner, and P.J. Coppen, IEEE Trans. Electron Devices, ED-25, 408 (1978).
6. M.C. Peckerar, D.J. Nagel, R.E. Pechacek, J.R. Greig, R.R. Whitlock, ECS Meeting (May 1978), Abstract 368.
7. D.J. Nagel, R.R. Whitlock, J.R. Greig, R.E. Pechacek, M.C. Peckerar, SPIE vol. 135, Developments in Semiconductor Microlithography III, 1978.
8. A. Gat, L. Gerzberg, J.F. Gibbons, T.J. Magee, J. Peng, and J.D. Hong, Appl. Phys. Lett. 33, 775 (1978).
9. E.E. King (Naval Research Laboratory), private communication.
10. B.E. Deal, E.L. MacKenna, and P.L. Castro, J. Electro Chem. 116, No. 7, 997 (1969).
11. A.G. Revesz, J. Electro Chem. 126, No. 1, 122 (1979).
12. A.G. Revesz, J. Non-Cryst. Solids 4, 347 (1970).
13. R.W. Lee, Phys. Chem. Glasses 5, 35 (1964).
14. C.T. Sah, IEEE Trans. Nucl. Sci. NS-23, No. 6, 1563 (1976).

Ultraviolet and x-ray lithography

D. J. Nagel

Naval Research Laboratory, Washington, D. C. 20375

ABSTRACT

Characteristics of the generation and absorption of ultraviolet and x-ray lithography are examined for their effects on lithographic reproduction of fine-scale features. *Direct-write*, *projection*, *proximity* and *contact* x-ray lithography are studied. Reviewed topics are given to x-ray lithography, especially the wide variety of potential, solid and plasma x-ray sources. Reference is also made to other aspects of x-ray lithography, namely masks, resist's and alignments, as well as the x-ray exposure systems.

Introduction

A range of almost 10^9 exists between the smallest features which can be seen by the unaided eye (1 mm) and the size of atoms (0.1 nm). Atomic structures on a scale of 0.1 nm have long been made, for example, by engraving. Organic chemists produce molecular structures ranging in dimensions upward from near 0.1 nm to atoms in the case of long polymeric chains. In recent years, the gap between what is visible and can be made by hand and the scale of atoms and molecules is being closed by a variety of lithographic techniques. The situation is indicated in Figure 1. Semiconductor microelectronics have dimensions approaching two decades below visible features, it may be possible to push the minimum dimensions of some devices to near 0.1 nm. Fine lines have already been made by photon (x-ray), electron and ion lithographies on the scale of 100 nm. Further reductions in structural dimensions may be possible, although scattering and other effects set to limit minimum line widths.

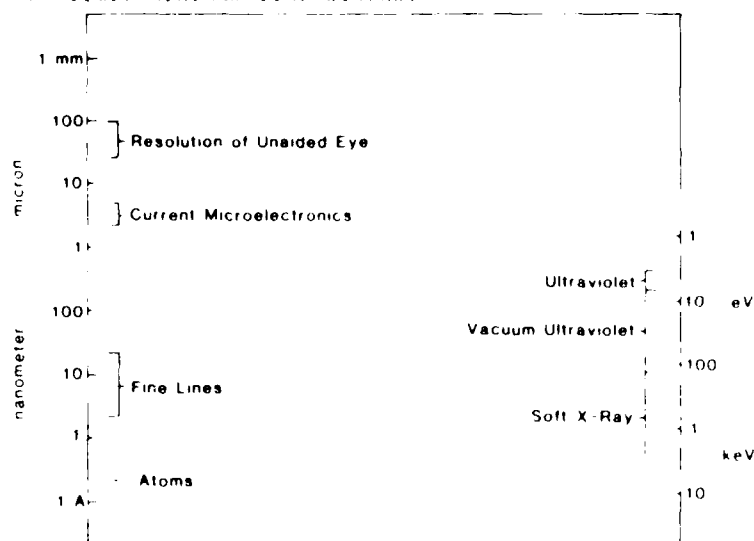
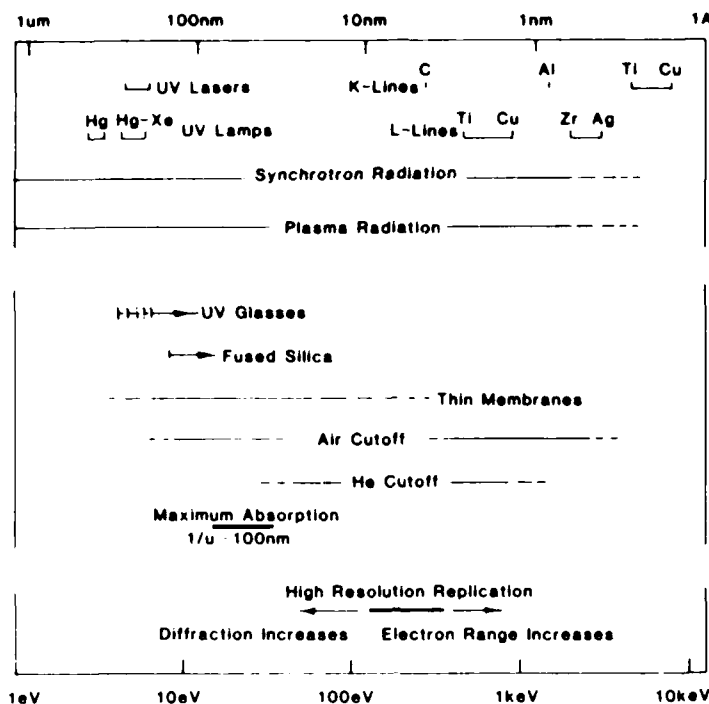


Fig. 1. Range of sizes relevant to atomic and atomic structure reproduction. The range of sizes which lithographically are made is from 1 mm (eye) downward. The finest features of current production microelectronics (regions of the electron microscope) are shown. X-ray lithography are indicated on the right, with the photon energies corresponding to the wavelengths on the left axis.

Some characteristics of making fine-scale structures are given. 10^4 to 10^5 times more energy is required to make a structure of 100 nm than the greatest depth of a 1 mm structure. The energy is used to break bonds and to create particles. Wavelengths are more carefully controlled and variations in the exposure of the surface of a lithographic mask are more critical than in the case of a 1 mm structure. The wavelength of the radiation is more critical than in the case of a 1 mm structure. The wavelength of the radiation is more critical than in the case of a 1 mm structure. The wavelength of the radiation is more critical than in the case of a 1 mm structure.

Some figures of merit of the various lithographic techniques are given. The energy of the radiation is a key factor in the choice of the lithographic technique. The energy of the radiation is a key factor in the choice of the lithographic technique.



1. Major types of UV and x-ray sources (top), including UV lasers and lamps, electron-impact sources of K and L x-rays, and synchrotron and plasma radiation sources. Spectral regions of absorption (center) for glasses and thin membranes used as mask supports and for ambient gases. Maximum absorption for most materials occurs around 20 eV (60 nm) where the photon "range" is commonly near 100 nm. Best resolution in resist replicas (bottom) is obtained near 200 eV (6 nm).

Absorbing materials for masks are readily available for all photon energies, with chromium being commonly used in the UV region and gold in the x-ray region. The maximum absorption coefficient for many solids falls near 20 eV with 100 nm photon mean free paths being characteristic in that region. The resolution of photo resists is best in the region near a few hundred eV. Diffraction effects at longer wavelengths, and the greater electron mean free paths and reduced mask contrasts which are associated with higher photon energies combine to determine the energy range for optimum resolution.

Having surveyed these general considerations, the three classes of photon lithography shown in Figure 2 will be discussed in more detail in the following sections. UV and x-ray lithography are quite similar, but practically distinct because high absorption coefficients of solids in the 10 to around 100 eV region preclude useful masks. Practically, there are three main spectral regions for UV and x-ray lithography, as determined by absorption in the source-to-resist path: (1) below 6 eV where refractive and reflective optical components are readily available and air transmits, (2) around a few hundred eV where resolution is optimum but a vacuum path and fragile masks are required, and (3) in the 1 to few keV range where, although sources and masks are problems, He paths can be used. It is interesting that nature permits the best resolution in the second region which is the most difficult technically due to the need for vacuum paths and thin mask supports.

Direct-write Ultraviolet Lithography

Maskless lithographic techniques employing computer-controlled focused beams are attractive although they tend to be slow. In the past few years, major attention has been given to the use of focused UV lasers to induce localized chemical reactions in an ambient gas which result in deposition on or removal of materials from a nearby solid. Hopefully, such methods will prove to be practical ways to introduce metal lines onto, or dope or etch windows in microcircuits during manufacture. Resist preparation, diffusions, implantations and etching steps can possibly be avoided by the use of direct-write lithography. Work aimed at development of such capabilities is briefly reviewed in the following paragraphs.

Deposition of a wide range of metals on many substrates by laser or photochemistry has received most attention. Frequency-doubled cw Ar ion lasers at 257.2 nm have been employed to deposit Al, Cd and Sn as metals in lines about 2 μ m wide²⁷ from atmospheres containing metal alkyls, e.g., Al(CH₃)₃. Repair of lithographic masks by this technique has been demonstrated²⁸. Simultaneous use of the Ar ion laser fundamental to heat the substrate while the harmonic photolyzed a gaseous alkyl produced Cd-doped InP²⁹ and Zn-alloyed Al³⁰. A pulsed ArF laser at 193.0 nm was employed to introduce Cd or Sn into InP³¹. Most recently, a cw CuI hollow cathode laser (200-270 nm) broke down carbonyls of Cr, Mo and In, e.g., Cr(CO)₆, and produced deposits on polished and oxidized silicon wafers and on quartz³².

Removal (etching) of InP and GaAs with micron spatial resolution was demonstrated by use of cw 257.2 nm radiation in halogen-containing reactants such as Cl₂ or Br₂³³. Photo etching of GaAs in a reactive liquid with a mercury lamp was employed a decade ago to check the distribution of dopants³⁴. Lasers with visible wavelengths have been used for gas-phase etching of Si^{28,35}.

Most of the work related to potential direct-write UV techniques has been reviewed in detail³⁶. Several tasks are clearly needed before UV laser photo reactions can be employed in production of devices. Greater versatility in materials deposited and driven into substrates is needed. Additional work on the active mechanisms (not discussed here) is desirable in order to optimize deposition or etching. Determination of tolerances in parameters such as laser power and focus is required for process design. A proof-of-principle demonstration of an operative microcircuit would further enliven interest in direct-write UV lithography.

Conventional and Deep Ultraviolet Lithography

Direct-write UV lithographic techniques are now in the research stage. In contrast, the other two classes of patterning with photons indicated in Figure 2, namely projection and proximity/contact, form the basis of conventional current microelectronics production. Near UV sources in the 3-4 eV (300-400 nm) region are widely used in what is called "optical" lithography because ordinary techniques and components (e.g., lenses) are employed. Methods for optical lithography are outlined in the next paragraph. Deep or far UV lithography employs photons in the 4-6 eV (200-300 nm) range (i.e., up to the air cut off at about 6 eV). Recent research on deep UV lithography is mentioned later in the section.

Optical lithographic methods can be classified according to the spacing between the mask and resist. The contact method was first employed when line widths were large. It still finds use for research, but routine contact between mask and wafer introduces defects in the mask. Proximity printing, with the mask close to the wafer, prolongs mask life while keeping penumbral blurring within limits acceptable for intermediate line width (several μ m). Projection printing offers both good mask life and resolution approaching 1 μ m. Projection can be accomplished in static, continuous scanning or step-and-repeat modes. Projection printers commonly employ demagnifications of 1:1, 1:5, or 1:10. Reviews of optical lithography^{37,38} and its resolution limits³⁹ are available. Commercial projection lithography devices were reviewed recently⁴⁰.

The use of wavelengths shorter than 300 nm is attractive because diffraction effects are reduced and ordinary optical methods can be employed^{39,40}. The characteristics of deep UV lithography have been explored for the past six years^{41,42}. Line widths as fine as 0.3 μ m have been produced by contact methods⁴³. A commercial proximity deep UV printer is available with 2 μ m resolution⁴⁴. The source in a commercial 1:1 projection printer was modified for deep UV exposure of 1 μ m lines 1 μ m apart⁴⁵. A new-deep UV 1:1 projection system capable of exposing 60-70 wafers per hour with 0.3 μ m alignment accuracy was developed⁴⁶.

Mercury-containing lamps are employed as near-UV sources for optical lithography. Xe-Hg lamps are usually employed in deep UV work, although a deuterium lamp was also used^{47,48}. Many sources of UV radiation exist which are potentially applicable to deep UV lithography⁴⁹.

Reviews of resists for conventional UV lithography are available^{44,45}. The action of energetic UV radiation on resists has similarities to x-ray exposure of resists. In both cases, electrons can be excited across the band gaps due to photon absorption. Work on resists for deep UV lithography has been summarized^{49,50}.

X-Ray Lithography

Both optical and deep UV lithographies provide experience which is directly useful

in the development of x-ray lithography tools, especially in the areas of alignment and automation. However, there are major differences in sources, masks and resists. Aspects of x-ray lithography will be discussed in the remainder of this review. Many surveys of x-ray lithography are available^{32,33}.

X-Ray Sources

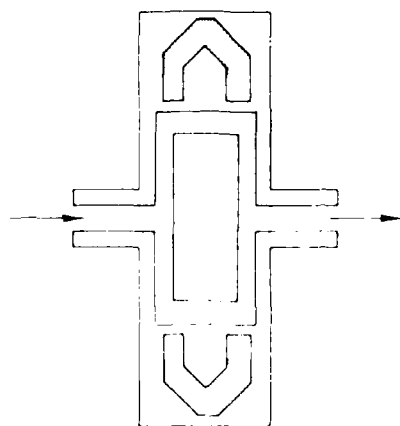
The three types of x-ray sources which have been employed for exposure of photoresists are discussed in this section. Emphasis is given to recent work, although plasma sources are surveyed more generally. Recent reviews of x-ray lithography sources are available^{32,33}.

Electron-Impact Sources

Electron bombardment of solids was the first source employed for x-ray lithography. Such sources are relatively cheap but they are not as intense as desired. A great deal of work on source optimization has been done in order to reduce resist exposure times. Both stationary and rotating anode sources have been studied.

Fixed-anode x-ray sources are limited in the power they can dissipate via thermal conduction and water cooling. Ordinary planar anodes do not provide intensities adequate for exposures of useful resists in less than one minute. Recently a new type of fixed-anode x-ray source was applied to x-ray lithography³⁴. A conical depression in the anode is excited near its apex by electrons from a circular cathode. High-pressure water forced parallel to the metal-vacuum interface sweeps bubbles of vapor due to boiling away from the electron impact point. In an ordinary anode, such bubbles would not move, and hot spots would develop due to the poor thermal characteristics of the vapor. Exposure times of about 20 sec are possible with a Pd anode and special resists. A fixed diamond anode source of soft x-rays is under development^{35,36,37}. The high thermal conductivity and strength of diamond makes possible dissipation of high input powers.

Rotating-anode sources distribute the heat load over greater areas and, hence, can run at higher powers³⁸. Such sources have been widely used for x-ray lithography. It is not clear that rotating-anode generators have reached their limits. It may be possible to store energy at a high rate during short, intermittent lithographic exposures, and to dissipate it gradually between exposures. A potential way to do this is indicated in Figure 4. Energy could be stored in heating and melting material in a cavity within a hollow annulus, and removed slowly with conventional water cooling. The high pressure due to centrifugal force would retard boiling. Fabrication and materials compatibility are evident problems. Al, which is rather insoluble in w, has favorable thermal properties. A full thermal analysis is needed in order to assess the potential of a melt-anode x-ray source, and to choose materials. It may be that little improvement over ordinary rotating-anode tubes is possible if the surface temperature is the limiting factor.



Schematic cross section through the axis of revolution of a section of the rotating anode of a potential x-ray tube cooled by water. The water is in contact with the anode with relatively low melting point material is contained in a cavity within the annulus as a temporary heat reservoir. The thin wall section could be in the center of the horizontal face. (From ref. 39).

the absolute spectra of both fixed and rotating-anode x-ray sources have been computed by a variety of techniques with useful accuracy. Experimental spectra are available for very few electron-impact sources of interest for lithography.

Storage ring sources

Synchrotron radiation from electron or positron storage rings is extremely intense, giving good pattern definition in exposures which can be an order of magnitude better than electron-impact sources. Hence, there is significant interest in developing synchrotron radiation for x-ray lithography despite the relatively high cost of storage rings.

The initial experiments in this area were performed in the late 1960's and early 1970's, then, there has been a relatively low level of work. The last consistent effort was in Japan. Very recently, a new beam line for lithography was installed in the storage ring in the U.S.A. A photograph of that beam line is shown in Figure 1. It will be employed for resist characterization and production of patterned substrates.



Fig. 1. Photograph of the lithography beam line recently installed at the Stanford Linear Accelerator. The storage ring at the top contains a series of standing wave resonators. The exposure chamber is a cryogenic chamber, which is cooled by liquid nitrogen and is used for resist characterization and patterned substrates.

Work is still active in synchrotron-radiation x-ray lithography, but the focus is on the development of several storage rings for lithography. It is expected that work in the next few years will show the advantages of storage rings for x-ray lithography, but it will be some time before a storage ring is built.

Plasma sources

Low-pressure plasmas are preferential for lithography, but the development of exposure times with equipment of intermediate complexity is a major problem. Under intense irradiation is a potential process.

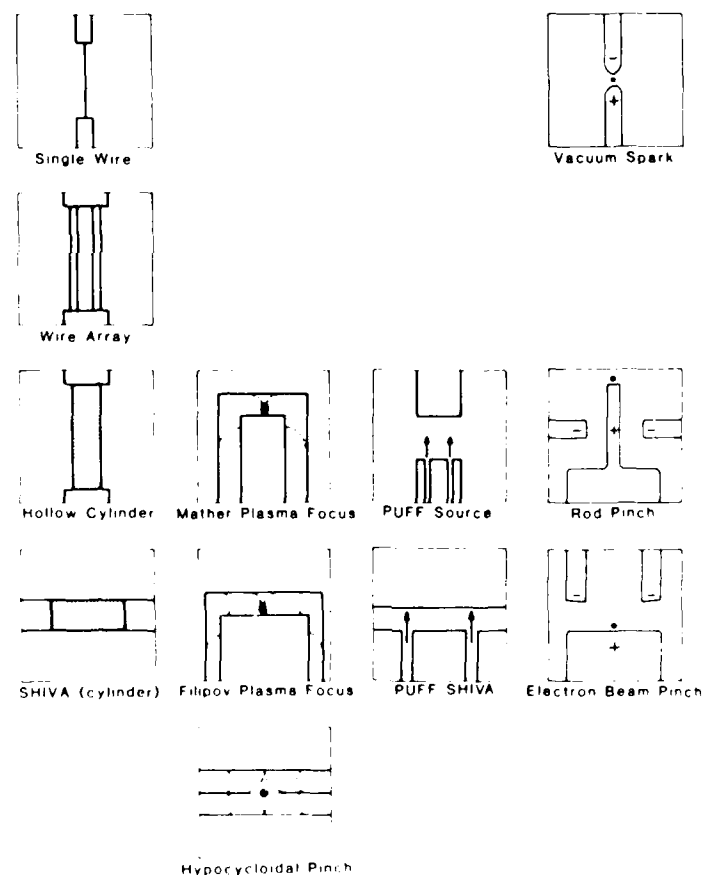
Low-pressure plasmas are produced by discharges of gases in a vacuum. The development of these plasmas is still in progress. Some of the most interesting work in this area has been done in the past few years. The sources have been developed for use in lithography, but they have not yet been used for lithography. There are also some other sources of interest in this area.

Low-pressure plasmas are produced by discharges of gases in a vacuum. The development of these plasmas is still in progress. Some of the most interesting work in this area has been done in the past few years. The sources have been developed for use in lithography, but they have not yet been used for lithography. There are also some other sources of interest in this area. The development of these plasmas is still in progress. Some of the most interesting work in this area has been done in the past few years. The sources have been developed for use in lithography, but they have not yet been used for lithography. There are also some other sources of interest in this area.

SPR-100-100 Ultraviolet and Vacuum Ultraviolet Systems, 1985-1986

Plasmas heated by electron discharges can be produced in devices indicated schematically in Figure 6. Detailed discussion of each of these plasma x-ray sources will be available in a review now being prepared^{6,7}. Here only general characteristics will be outlined, with reference to use of some of the sources for resist exposure. The sources are arranged in Figure 6 in columns depending on the origin of the material which forms the plasma. Similar geometries are arrayed side-by-side. The left column shows sources which have low-mass solids placed between the electrodes before each shot. Plasmas are formed by cylindrical implosions. Such devices are bright sources of x-rays above 1 keV but inconvenient operationally, especially if multiple-shot exposures are required. Injection of liquids (by pressure or electrohydraulically) immediately prior to the discharge may make repetitive operation feasible. Sources in the next column begin with a low-pressure fill gas which supports a propagating discharge sheath that collapses ("focuses") to produce the hot plasma. A plasma focus was used recently in trial resist exposures^{6,8}. The two-sided machine (hypocycloidal pinch) is attractive since resists could be exposed over a relatively large solid angle. Repetitive pulsing of such devices is possible. The next class of source begins with an inter-electrode vacuum into which a hollow gas is injected ("puffed") before the discharge. Such sources, which have been used to expose resists^{6,9}, are attractive because they are efficient and can be operated in a repetitively-pulsed mode. The final grouping of sources involves induction of a vacuum breakdown, with plasmas being formed from the anode material. The vacuum spark produces energetic x-rays but is erratic. The other anode-material sources emit only subkilovolt radiation with relevant intensity.

A great deal of work on plasma sources for x-ray lithography could be done. Based on the results to date, laser-plasma, "putt" and plasma focus x-ray sources should be studied further. If subkilovolt sources prove interesting for step-and-repeat VUV lithography, many plasma sources will be of potential use.



6. Schematic cross sections of sources of dense millimeter-degrees plasmas which are intense sources of uv radiation and soft x-rays. (see text for a discussion of the differences (from column to column) and similarities (within column rows).)

X-Ray Masks

Masks for x-ray exposure of resists consist of three components: a support, an x-ray-transparent membrane and a patterned absorbing material. The frame must be rigid and permit easy handling. The membrane should be transparent in the visible region (to permit optical alignment) as well as in the x-ray region. It must also be relatively easy to produce and handle, flat and dimensionally stable. The absorber must provide adequate contrast. Gold up to about 500 nm thick is almost universally employed as the absorber. A review of x-ray masks is available⁷.

Research on x-ray masks has centered on production of thin (few nm), often large (several cm) membranes. Many materials have been employed, including elements (Be, Si, and Ti), compounds (Al₂O₃ and SiC), polymers (mylar and polyimide) and layered materials (SiO₂ with Si₃N₄ and BN with polyimide). Work on masks is discussed in the x-ray lithography reviews cited above. Recent efforts on specific mask materials are also described. Various methods have been employed to determine the distortion and stability of x-ray masks^{7,74}.

Step-and repeat x-ray exposures are clearly desirable from the viewpoint of producing and using x-ray masks. Small area masks for, say, 1 to 12 chips would be flatter, less vulnerable to distortion and more stable than the large-area masks needed for full-wafer exposures. Such an approach requires a bright x-ray source, of course. This is one of many examples of coupling between design of components for x-ray lithography.

X-Ray Resists

Most x-ray resists are organic polymers which experience chain scission or cross linking due to ionization by energetic electrons produced by photon absorption. These changes in molecular weight alter the solubility of the polymer, making it possible to produce surface relief by exposure to suitable solvents after irradiation. Some progress has been made toward understanding the behavior of resists in terms of their fundamental electronic structure⁷⁵. A recent review of resist research is available⁷⁶.

The characteristics of ideal x-ray resists have been enumerated⁷⁶. Briefly, a high molecular weight improves sensitivity at the expense of resolution. Incorporation of atoms having absorption edges located favorably relative to the source spectrum improves absorption and sensitivity⁷⁶, as does the design of resists which efficiently use the absorbed energy⁷⁶. A narrow distribution of molecular weights favors high contrast and good edge definition. Many other properties of resists, e.g., adhesion and process resistance, are also important⁷⁷.

The unavoidable sensitivity-resolution trade-off has been discussed in terms of photon statistics (shot noise)⁷⁸. A statistical approach to defects⁷⁹ has also been formulated^{81,82}. Data on the sensitivities and resolutions of x-ray^{46,83,90} and related electron^{81,82} resists have been tabulated and discussed.

Inorganic resists are also being explored for x-ray and other lithographies⁷⁶. AgCl-covered As₂Se₃ was found to be x-ray sensitive⁸⁴. Ge-Se glasses doped with Ag respond to UV and electron irradiation so they are probably also x-ray sensitive⁸⁵. Inorganic resists are non-swelling and compatible with dry processing. However, they are usually developed with solvents, similar to organic resists⁸⁶.

Dry, plasma development of resists is attractive in order to avoid wet-chemical processing altogether^{76,80,85}. Changes in plasma-driven reaction rates, say, with oxygen, and the attendant production of volatile products due to lithographic exposures make plasma development possible. Either positive or negative replicas of a mask may be produced after x-ray exposure, depending on plasma conditions.

Multi-level resist systems have been employed to achieve good resolution and step coverage simultaneously⁸⁰. One scheme involves electron-beam patterning of the top resist followed by x-ray exposure of the second, thicker resist⁸⁰.

Mask-Wafer Alignment

The ability to overlay a mask with patterns already on a wafer to a precision of around 2% of the narrowest line is needed for all but single-level x-ray lithography tasks. That is, devices like bubble memories can be produced by one lithographic procedure but microelectronic devices commonly require several mask levels.

Alignment is discussed in most reviews on x-ray lithography. The range of techniques to sense the relative position of a mask and wafer have been enumerated⁸⁸. Most methods employ visible light to achieve alignment. Transparent masks can be aligned to accuracies less than 50 nm⁸⁸, while an optical transfer method has been used to align opaque masks to about 500 nm⁸⁸. Various patterns allow alignment precisions, for transparent masks, which are a small fraction of an optical wavelength. These include Moire patterns⁸⁹, uniform gratings⁹⁰, and Fresnel zone patterns⁹¹. Alignment accuracies of less than 50 nm have been achieved with the last two techniques. X-rays have been suggested for mask alignment^{92,93} in addition to the use of optical methods.

Some mask alignment techniques for x-ray lithography involved human observation and manual positioning. Automatic position sensing and mask-wafer motion has also been employed with accuracies below 100 nm⁹⁴. Step-and-repeat systems with automatic alignment at the 100 nm level are also possible⁹⁵. Optical tests for alignment accuracy are discussed in most papers on alignment. Electrical alignment tests are also employed⁹⁶.

X-Ray Exposure Systems

A great deal of work on systems for x-ray lithography has been reported in the past three years⁹⁷⁻⁹⁸. A summary of initial systems was published late in 1978⁹⁹. Both fixed and rotary⁹⁹ anode sources were employed in the earlier devices. Additional work with stationary⁹⁹ and rotary¹⁰⁰ sources was reported recently. A step-and-repeat x-ray system is presently under development.

In general, all x-ray lithography systems developed to date are experimental in nature. Production-line use of any of them is unlikely. However, many of the components from these systems might find use, when suitably integrated into industrial machines.

Summary and Discussion

The status of UV and x-ray lithographic techniques can be summarized. The new direct-write photon methods are in the early stages of research. It is difficult to assess their potential now, although the process simplifications they offer are attractive. Presently, near UV lithography is the work horse of the microelectronics industry. Deep UV lithography may come to be widely employed through evolutionary changes in equipment and techniques.

X-ray lithography has advanced significantly in the decade since its development. Major use of x-ray lithography has been projected, beginning in a few years¹⁰¹. However, a great deal of work remains to develop production-line x-ray machines. Improvements in sources and resists would be valuable. Demands on x-ray masks will be alleviated by the use of step-and-repeat exposure schemes with realignment prior to each exposure.

Radiation effects in the oxides of MOS devices can result from the use of x-rays to pattern devices¹⁰². The nature and consequences of such process-associated effects are being actively investigated now. If lithographic-induced radiation effects are deleterious, it will be necessary to find ways to mitigate or avoid the problem.

X-ray lithography is closely related to x-ray microscopy, the study of small structures with x-rays. Two approaches to microscopy are available. In the first, the object is simply radiographed with a high-resolution recording medium, commonly a resist. This form of x-ray microscopy is very closely related to x-ray lithography, a specimen is substituted for the mask. In the second approach to x-ray microscopy, a fine beam is scanned sequentially over the object of interest, and its transmission is measured with ordinary x-ray detector. Fine x-ray beams can be produced with apertures or by use of x-ray focusing optics. The submicron-diameter x-ray beams of interest in scanning x-ray microscopy are conceivably of interest for direct-write x-ray lithography.

Acknowledgements

Continual collaboration with colleagues at SRC (M.C. Recker of the Solid State Devices, K.L. Williams and J. Kite of the Optical Probes Branch and R.K. Whitlock of the Condensed Matter Physics Branch) and useful interactions with persons at other institutions are gratefully recognized.

References

1. Microstructure Science, Engineering and Technology, National Academy of Sciences, Washington, DC (1979).

2. Proc. of NSF workshop on Opportunities for Microstructure Science, Engineering and Technology (19-22 Nov 1978, Airlie, VA) National Science Foundation, Washington, DC.
3. E.D. Wolf and J.M. Ballantyne in N.G. Einspruch (Editor) VLSI Electronics: Microstructure Science, Vol. 1, Academic Press, New York (1981) pp. 129-183.
4. F.W. Voltmer in N.G. Einspruch (Editor) VLSI Electronics: Microstructure Science, Vol. 1, Academic Press, New York (1981) pp. 1-40.
5. R.F.W. Pease, Contemp. Phys. 22(3), 265-290 (1980).
6. J.P. Scott, Sol. St. Tech., 20(5) 43-7 (May 1977).
7. K.L. Seliger, J.W. Ward, V. Wang and K.L. Kubend, Appl. Phys. Lett. 34(5) 310-2 (1979).
8. L. Csepregi, F. Iberl and D. Eichinger, Appl. Phys. Lett., 37(7) 630-2 (1980).
9. G. Stengl, K. Kartna, H. Loschner, P. Wolf and R. Sacher, J. Vac. Sci. Tech. 16(6) 1883-5 (1980).
10. W.L. Brown, T. Venkatesan and A. Wagner, Sol. St. Tech., 24(6) 60-7, (Aug 1981).
11. B.J. Lin and T.H. P. Chang, J. Vac. Sci. Tech., 16(6) 1009-11 (1979).
12. J.P. Reeksten and J.H. McCoy, Sol. St. Tech., 24(6) 66-73 (Aug 1981).
13. A. Broers, Phys. Today (Nov 1979) pp. 38-45.
14. M.J. Bowden, J. Electrochem. Soc. 128(5) 1950-2140 (1981).
15. R.K. Watts and J.H. Bruning, Sol. St. Tech., 24(5) 99-105 (May 1981).
16. M.P. Lepselter and W.F. Lynch in N.G. Einspruch (Editor) VLSI Electronics: Microstructure Science, Vol. 1, Academic Press, New York (1981) pp. 83-127.
17. B.L. Henke in D.F. Attwood and B.L. Henke (Editors) Proc. Topical Conf. on Low Energy X-ray Diagnostics, Am. Inst. of Physics, New York (1981).
18. R. Feder, E. Spiller and J. Topalian, Polymer Engr. and Sci., 17(6) 365-9 (1977).
19. W. Gudat, DESY Report SR-77/21 (Dec 1977).
20. T.F. Deutsch, D.J. Ehrlich and R.M. Osgood Jr., Appl. Phys. Lett. 32(1) 10-12 (1979).
21. D.J. Ehrlich, R.M. Osgood Jr., D.J. Silversmith and T.F. Deutsch, IEEE ED. Dev. Lett., EDL-1(6) 101-3 (1980).
22. D.J. Ehrlich, R.M. Osgood Jr. and T.F. Deutsch, Appl. Phys. Lett. 36(11) 916-8 (1980).
23. D.J. Ehrlich, R.M. Osgood Jr. and T.F. Deutsch, Appl. Phys. Lett. 38(6) 599-101 (1981).
24. T.F. Deutsch, D.J. Ehrlich, R.M. Osgood Jr., and Z.W. Liaw, Appl. Phys. Lett. 36(10) 847-9 (1980).
25. R. Solanki, P.K. Boyer, J.E. Mahan and G.L. Collins, Appl. Phys. Lett. 35(7) 572-4 (1981).
26. D.J. Ehrlich, R.M. Osgood Jr. and T.F. Deutsch, Appl. Phys. Lett. 39(8) 693-6 (1980).
27. F. Kuhn-Kuhnenfeld, J. Electrochem. Soc., 119(8) 1063-8 (1972).
28. L.L. Sveshnikova, V.I. Donin and S.M. Repinskii, Sov. Phys. Tech. Phys. 13(4) 223-4 (1977).
29. D.J. Ehrlich, R.M. Osgood Jr. and T.F. Deutsch, Appl. Phys. Lett. 35(11) 1000-2 (1981).
30. D.J. Ehrlich, R.M. Osgood Jr. and T.F. Deutsch, IEEE ED. Dev. Lett. EDL-1(6) 101-3 (1980).

SPIE Vol. 279 Ultraviolet and Vacuum Ultraviolet Systems, 1981

31. M.C. King in W.G. Einspruch (Editor) VLSI Electronics, Microstructure Science, Vol. 1, Academic Press, New York (1981) pp. 41-61.
32. F.H. Dill, IEEE Trans. on El. Dev. ED-22(7) 440-4 (1975).
33. J.H. Brunning, J. Vac. Sci. Tech. 17(5) 1147-55 (1980).
34. D.A. Doane, Sol. St. Tech., 23(8) 101-14 (Aug 1980).
35. B.J. Lin, J. Vac. Sci. Tech., 12(6) 1317-20 (1975).
36. Y. Mimura, T. Onkubo, T. Takeuchi and K. Sekikawa, Jap. J. Appl. Phys. 17(3) 941-50 (1978).
37. A.M. Vosnichenov and H. Herrmann, El. Lett. 17(2) 61-2 (1981).
38. D.O. Massetti, M.A. Hockey and D.L. Merriam in J. Bey (Editor) Developments in Semiconductor Microlithography v. 3, SPIE Vol. 221 (1980) p. 32.
39. T. Matsuzawa and H. Tomioka, IEEE El. Dev. Lett. EDL-2(4) 90-1 (1981).
40. S. Iwamatsu and K. Asanami, Sol. St. Tech., 23(5) 61-65 (May 1980).
41. J.A.R. Sampson, Techniques of Vacuum Ultraviolet Spectroscopy, Wiley and Sons, New York (1967).
42. L.F. Thompson and K.E. Kerwin in K.A. Muggins et al. (Editors) Ann. Rev. Mat. Sci. 6, 267-300 (1976).
43. A.J. Bowden and L.F. Thompson, Sol. St. Tech., 22(5) 72-82 (May 1979).
44. S.A. Chandross, R. Ketchum, C.W. Wilkins Jr. and K.L. Bartless, Sol. St. Tech., 24(8) 51-5, Aug. 81.
45. H.L. Smith, D.M. Spears and S.R. Bernacki, J. Vac. Sci. Tech., 16(4) 913-7 (1979).
46. J.S. Greenleif, IEEE Trans. on El. Dev. ED-22(7) 434-9 (1975).
47. J.H. McCoy, Circuits Manufacturing (Nov. 77) pp. 33-44.
48. R. Spiller and K. Feder in H.-J. Queisser (Editor) Topics in Applied Physics, X-ray Optics, Springer-Verlag, Berlin (1977) p. 33.
49. G.R. Hughes and K.G. Rink, Electronics (9 Nov 73) pp. 99-100.
50. G.A. Wardly, K. Feder, D. Hofer, E.H. Castellan, K. Scott and J. Topalian, Circuits Manufacturing (Jan 75) pp. 30-32.
51. K.K. Watts, Sol. St. Tech., 21(5) 66-71 (May 1978).
52. D.C. Jager, Annals of New York Acad. of Sci., 342, 233-51 (1980).
53. A.F. Reemert and D.C. Janders, to be published.
54. J.W. Lacharas, Proc. of Ninth Premier University Government Industry Conference, Symposium on Research and Development in Solid State Electronics, pp. 111-120.
55. G.W. Nelson and W.L. Wolff, J. Appl. Phys. 49(11) 5960-7 (1978).
56. G.W. Nelson, J. Appl. Phys. 48(8) 3011-14 (1977).
57. H. Roth, H. H. and G. S. in H. J. Queisser (Editor) Topics in Applied Physics, X-ray Optics, Springer-Verlag, Berlin (1977) p. 33.
58. J.W. Brown and J. L. Green, J. Vac. Sci. Tech. 16(4) 913-7 (1979).
59. J.W. Brown, J. Vac. Sci. Tech. 16(4) 913-7 (1979).
60. J.W. Brown, J. Vac. Sci. Tech. 16(4) 913-7 (1979).
61. J.W. Brown, J. Vac. Sci. Tech. 16(4) 913-7 (1979).
62. J.W. Brown, J. Vac. Sci. Tech. 16(4) 913-7 (1979).

61. L.R. Hughey, R.T. Williams, J.C. Rife, D.J. Nagel and M.C. Peckerar, *Nucl. Instr. and Methods* (1982).
62. H. Winick in H. Winick and S. Doniach (editors) *Synchrotron Radiation Research*, Plenum Press, New York (1981) pp. 27-60.
63. D.J. Nagel, K.R. Whitlock, J.R. Greig, R.E. Peckacek and M.C. Peckerar, in R.M. Ruddell (Editor) *Developments in Semiconductor Microlithography IV*, SPIE, Vol. 155 (1978) pp. 46-53.
64. K.A. McCorkle, J. Angilello, G. Coleman, R. Feder and S.J. LaPlaca, *Science* 203, 401-2 (1979).
65. D.J. Nagel, *Appl. Phys. Rev.*, To be published.
66. K.A. Gutcheck and J.J. Murrar in E. Spiller (Editor) *High Resolution Soft X-Ray Optics*, SPIE, Vol. 316 (1982).
67. S.M. Matthews, R. Stringfield, I. Roth, R. Cooper, W. P. Economou and D.C. Flinders, To be published.
68. J.S. Pearlman and J.C. Riordan, *Proc. 16th Symp. on Electron, Ion and Photon Beam Technology* (26-9 May 1981).
69. J.R. Maldonado in C.R. Dammiller (Editor) *Stanford Synchrotron Rad. Lab. Report 79/02* (1979) pp. 117-30.
70. D. Maydan, G.A. Coquin, H.J. Levinstein, A.S. Sinha and, D.A. K. Wang, *J. Vac. Sci. Tech.* 16(6) 1959-61 (1979).
71. L. Cseprgi and A. Heuberger, *J. Vac. Sci. Tech.* 16(6) 1962-4 (1979).
72. P. Parrens, E. Tabouret and E.C. Tacussel, *J. Vac. Sci. Tech.* 16(6) 1965-7 (1979).
73. W.D. Buckley, J.F. Nester and H. Windischmann, *Electrochem. Soc. Trans.* 1119-120 (1981).
74. K.R. Nicholas, I.J. Stemp and H.R. Brockman, *J. Electrochem. Soc.* 128(1), 6-9-14 (1981).
75. M. Tsuda, S. Oikawa and A. Suzuki, *Polymer. Engr. and Science*, 17(6) 359-5 (1977).
76. M.J. Bowden, *Sol. St. Tech.* 24(6) 2355/73-87 (June 1981).
77. G.A. Taylor, G.A. Coquin and G. Somers, *Polymer Engr. and Science*, 17(6) 351-4 (1977).
78. M.J. Bowden, *Critical Rev. in Sol. St. and Mat. Sci.* 10(3) 113-56 (1980).
79. G.A. Taylor in C.R. Dammiller (Editor) *Stanford Synchrotron Rad. Lab. Report 79/02* (1979) pp. 93-109.
80. G.A. Taylor, *Sol. St. Tech.* 73-89 (May 1981).
81. M. Hatzakis, *Applied Polymer Symposium Ser. 34*, Wiley and Interscience, New York, 73-86.
82. L.P. Thompson, *Sol. St. Tech.* 17(2) 127-30 (May 1977).
83. K.D. Selwitz and M.J. Bowden, *J. Electrochem. Soc.* 128(1), 15-18 (1981).
84. A. Yoshikawa, G. Oishi, H. Sugita and H. Nakagawa, *Electrochem. Soc. Trans.* 1117-18 (1979).
85. D.M. Toller, *Sol. St. Tech.* 13(1) 69-71 (May 1977).
86. M. Hatzakis, *J. Mater. and Chem.* 1(1) 1-10 (1981).
87. H.K. Rothmann, *J. Vac. Sci. Tech.* 16(6) 1968-70 (1979).
88. W.D. Buckley, *Elect. Engr. and Science*, 17(6) 355-6 (1977).

SPIE Vol. 294, *Microphotography and Microlithography*, 1981, pp. 1-10

89. M.C. King and D.H. Berry, Appl. Opt., 11(11) 2455-9 (1972).
90. S. Austin, H.I. Smith and D.C. Flanders, J. Vac. Sci. Tech., 15(3) 984-6 (1978).
91. B. Fay, J. Frotel and A. Frichet, Vac. Sci. Tech., 16(6) 1954-8 (1979).
92. D.L. Spears and H.I. Smith, Sol. St. Tech., 15(7) 21-6 (July 1972).
93. J.H. McCoy and P.A. Sullivan, Sol. St. Tech., 19(9) 59-64 (Sept 1976).
94. S. Yamazaki, S. Nakayama, T. Hayasaka and S. Ishihara, Vac. Sci. Tech., 15(3) 987-91 (1978).
95. H.L. Stover, Sol. St. Tech., 24(5) 112-120 (May 1981).
96. D.S. Perloff, I.F. Hasan, D.H. Hwang and J. Frey, Sol. St. Tech., 24(5) 126-140 (May 1981).
97. G.P. Hughes, J. Vac. Sci. Tech., 15(3) 974-6 (1978).
98. P. Marsh, New Scientist, 82 (1157) 712-5 (1979).
99. M.P. Lepseiter, IEEE Spectrum (May 1981) pp. 26-9.
100. W.D. Buckley and G.P. Hughes, J. Electrochem. Soc., 128(5) 1106-1111 (1981).
101. T.M. Lyszczarz, D.C. Flanders, N.P. Economu and P.D. DeGraft, Proc. 16th Symp. on Electron, Ion and Photon Beam Technology (26-9 May 1981).
102. M. Peckerar, R. Fulton, P. Blaise, D. Brown and R. Whitlock, J. Vac. Sci. Tech., 16(6) 1658-61 (1979).

RADIATION EFFECTS INTRODUCED BY X-RAY LITHOGRAPHY IN MOS DEVICES

M. C. Peckerar, C. M. Dozier, D. B. Brown, D. Patterson
and D. McCarthy
Naval Research Laboratory, Washington, DC 20375

D. Ma
Sachs/Freeman, Associates
Bowie, MD 20715

ABSTRACT

The effects of low energy ionizing irradiation on MOS structures, with doses typical of those encountered in x-ray lithography, were studied in capacitors and transistors. The capacitor studies indicated the irradiations induced a slow trapping instability and an increase in surface state density. This surface state density increase was partially annealed at 450 C in N_2 after 1/2 hour. Transistor threshold shifts were largely annealed away under these conditions. However, a shift of 250 mV was observed in 1000 Å oxides which was not annealed away. In the 250 Å case, 50 mV remained after anneal. Even in the thinnest oxides studied (250 Å oxides) increases in subthreshold swing as large as 35% were encountered. This degradation was only partially annealed away under the conditions listed above. No channel length dependence to the effect was uncovered (down to 1 μ m channel length).

I. INTRODUCTION

State-of-the-art microelectronics lithographic procedures rely on x-ray, deep-UV and e-beam exposure tools. During the course of these procedures, radiation sensitive MOS devices are subjected to ionizing radiation. The effect of this radiation on

- a. device properties
- b. device stability
- c. device radiation tolerance

may present a critical obstacle to the application of these techniques. The full nature and extent of the damage introduced is still unknown.

Previous work in this area has roughly outlined the nature of the problem. Aitken¹ has shown that e-beam lithography creates positive charges and "neutral-traps" which are fully annealable only at temperatures greater than 550 C. While the threshold shifting in MOSFETs caused by e-beam damage was not large (< 400 mV), hot electron trapping effects were enhanced.² Peckerar et al.³ reported a substantial increase in positive charge instability caused by both x-ray and e-beam lithography in MOS capacitor structures. They also noted increase in fast interface states. Chen et al.⁴ have reported a radiation softening due to the e-beam lithographic exposures.

In this paper, the effects of soft x-ray exposures on MOSFETs and on MOS capacitors are reported. This work differs from previous work in that the effects of x-rays rather than electrons are studied. Systematic studies of geometrical (i.e., "size") effects are presented. Also, a broader range of device parameters are analyzed. Specifically, in addition to threshold shifting, data on subthreshold leakage and transistor transfer characteristics are presented. These data shed light on interface damage effects.

It is shown below that the primary residual damage which remains after 450 C anneal is in interface damage. Prior to annealing, but after x-ray exposure, capacitors demonstrate slow trapping be-

instability.^{5,6} This is indicative of traps near (but not at) the oxide-semiconductor interface. Anneals at 450 C remove this instability; anneals at 300 C do not. Residual interface damage affects subthreshold leakage and to some extent, mobility related transistor parameters. We estimate the increase in interface charge at threshold to be approximately 6×10^{10} states/cm². We observed no transistor channel length dependence to the effect. In going from 10 μ m gate width to 5 μ m gate widths, there appeared to be a *reduction* in the observed radiation effect.

In the paper below, the experimental procedures used and details of device characterization are given. Next, capacitor data are presented, followed by transistor data. Finally, data are analyzed and conclusions are presented.

II. EXPERIMENTAL DETAILS

All substrates used in this experiment were p -type silicon (100) wafers. The resistivity range was 3-5 Ω -cm. All gate oxides were dry-grown at 1000 C in polysilicon furnace tubes with a "white-elephant" cap to prevent nitrogen back-streaming. Field oxides were 4000 Å thick, steam grown at 1000 C. The test devices (capacitors included) were fabricated using an n -MOS self-aligned polysilicon gate process. The field oxide was *not* self-aligned (i.e., a field-oxide-cut etch was employed). In-source (inductively-heated) evaporated aluminum was used as a final interconnect layer. No threshold controlling implants were employed.

For capacitor flatband determination, 1 MHz C-V plots were taken. Temperature-bias-stress (TBS) stability data were also taken with a 1 MHz C-V measuring tool. The stress conditions were +10 volts for 5 minutes at 300 C followed by cooling to ambient and C-V sweep, then -10 volts for 5 minutes at 300 C followed by cooling to ambient and a second C-V sweep. The difference in flat band voltages between the two sweeps is referred to as the TBS instability. It is an indication of charge instability in the insulator. It can also be viewed as an accelerated life test. G-V plots for interface state studies were made at 1 kHz.

Transistor characteristics were measured in the low field region (prior to saturation). The source-drain bias was 100 mV. Threshold was obtained by linear extrapolation of the conductance-gate voltage plot to zero source-drain conductance.

X-ray dosimetry was done using TLDs. The standard x-ray dose administered was that required to expose COP (co-polymer of methyl methacrylate). COP is a commercially available x-ray resist. The COP exposure dose corresponds to 5 Mrad in a 1000 Å oxide adjacent to a polysilicon gate.

III. EXPERIMENTAL RESULTS

1. Capacitors

The purpose of this study was to establish radiation effects mechanisms and to study annealing behavior. The standard COP exposure dose was employed throughout. The oxide used was 1000 Å thick. Four radiation induced effects were observed. These are discussed below.

The first observed effect was flatband voltage shift. A substantial negative shift in the flat band voltage was observed. The shift was highly dependent on the applied bias during irradiation. For the polysilicon gate devices irradiated to 5 Mrad (SiO₂) observed shifts were -5 to -8 V (using 2.5 MV/cm fields) and -0.5 to -2.6 V (using no applied bias). The shift showed sublinear dependence on dose with indication that the shift saturates in the neighborhood of 10 Mrad. For the Λ gate devices the shift was substantially annealed out at room temperature after 2 days and was essentially completely annealed after 1/2 hour at 300 C. The polysilicon gate devices irradiated to 5 Mrad did not show a room temperature annealing. About 1/3 of the flat band shift was annealed out after 1/2 hour at 300 Å. The observed flat band shifts after such an anneal were -5 V at 2.5 MV/cm bias (gate positive).

substrate ground) and -0.8 to -1.8 V with no applied bias. The behavior of the polysilicon gate capacitors after a 300 C anneal is shown in Fig. 1. These shifts were reduced to less than 0.1 V by 450 C or 550 C anneals for devices unbiased during irradiation.

All devices had TBS instabilities of less than 0.1 V prior to irradiation. Following irradiation TBS instabilities were observed. The measured values for polysilicon gate capacitors after an irradiation of 5 Mrad ranged from 0.20 to 0.50 V (average 0.45 V) for large applied bias during irradiation and an average of 0.30 V for no bias. Similar results were observed for Al gate capacitors. For all tests the $+10$ V TBS curve lay to the right of the -10 V curve. This is the opposite of the effect observed by Peckercar et al.³ The reason for this difference is discussed below. The effect reported here has been called a slow-trapping instability.^{5,6} Replacing the 300 C anneal for 1/2 hour by a 450 C or 550 C anneal, removed measurable TBS instability for devices irradiated without bias.

Two types of interface effects were noted. First, prior to annealing a substantial radiation induced peak in the A-C conductance (G-V) curve was observed. The peak height was dose dependent. Most of the data could be fit by the (dose)^{2/3} dependence suggested by Winokur and Boesch.⁸ No bias dependence was observed. This is consistent with the interface states observed by Winokur et al.⁹ but is not consistent with the interface states observed by Winokur and Boesch.⁸ In addition, a radiation induced softening of the capacitors was observed. The devices were irradiated, annealed, and then re-irradiated. The G-V peak height was 50% larger following the second irradiation.

Second, following a 300 C anneal for 1/2 hour, the G-V peak described above was substantially annealed. The remaining peak, which was roughly 1/5 as large as the peak prior to annealing, behaved differently and thus presumably represented a different type of interface state. Specifically, it showed a dependence on the bias applied during irradiation. The dependence was small, roughly that observed for the TBS instability described above. These may be related. The slow-trapping instability has previously been associated with a growth in interface states.¹⁰

2 Transistors

Transistors with gate oxides ranging from 280 Å to 1000 Å were prepared. The following parameters were studied: threshold voltage (V_T), conductance (g_n), conductance slope (slope of the g_n vs gate voltage plot) and subthreshold swing factor (S). Threshold voltage shifts are encountered after irradiation due to bulk and interface charging effects. In the low-field regime (before the transistor enters saturation), the conductance slope (designated as g_{slope}) is approximately:¹¹

$$g_{slope} = \mu_n C_o (W/L) \quad (1)$$

where

μ_n = electron mobility

(W/L) = transistor width-to-length ratio (W/L)

C_o = oxide capacitance

Degradation in g_{slope} is caused by drop in μ_n . This lowering of μ_n comes about due to increase surface scattering attributed to interface damage or to interface charge or to Coulombic centers near the interface. The subthreshold swing factor is defined as

$$S = dV_g/d(\log I_D) \quad (2)$$

where

V_g = gate voltage

I_D = drain-source current measured below threshold

Degradation in subthreshold sensitivity can also be explained in terms of interface state growth. Consider the following expression for the reciprocal of substrate swing (the subthreshold sensitivity factor)¹²:

$$\frac{d \log (I_{DS})}{d V_g} = \frac{q}{k T} \frac{C_{ox}}{C_{ox} + C_b + C_{ss}} \quad (3)$$

where:

- q = electron charge,
- k = Boltzmann constant,
- C_{ox} = oxide capacitance,
- C_b = bulk capacitance,
- C_{ss} = interface state capacitance

Increase in C_{ss} makes it more difficult to reduce I_{DS} for a given gate voltage swing. The interface state term prevents the gate from controlling bulk and interface leakage.

The total amount of threshold shift is strongly dependent on oxide thickness. This is indicated in Fig. 2. The threshold shift is given as a function of channel width for the three oxide thicknesses studied. All oxides received a 450 C N_2 anneal for 1/2 hour. While the 1000 Å data ranged from 200 to 300 mV in post-irradiation shift, the 500 Å data averaged about 175 mV. The 250 Å oxides were between 50 and 75 mV after anneal. The shifts were negative, corresponding to positive insulator charging. A trend was observed relating channel width to threshold shift. In 3 out of 4 of the oxide thicknesses studied, the narrowest gate has the least threshold shift.

The g_{slope} term also demonstrated marked oxide thickness dependence. The 1000 Å oxides always showed most significant degradation. A typical post 450 C N_2 anneal result is shown in Fig. 3. For the widest channel studied (50 μm), almost 50 % degradation in μ_s is encountered, according to Eq. (1). Channel widths less than 10 μm exhibited less effect. For 280 Å oxides, the degrading effect (although present to some extent) was almost completely annealed away (see Fig. 4). There was no observable trend relating channel length to g_{slope} degradation. This is seen quite clearly in Fig. 5.

For all oxides studied, there was a degradation in S . Even in the thinnest oxide, degradation of subthreshold leakage was observed after 450 C anneal. This is seen in Fig. 6, where subthreshold swing is plotted against channel width. Degradation ranges from 10% to 35%.

Co^{60} total dose experiments were also performed on the transistors studied. These data are presented in Fig. 7. Again, the width dependent trend could be observed. The narrowest channels (<10 μm) showed least degradation. Early small degradation was encountered after 10 Krad exposure for the 5 μm wide channels (always less than about 200 mV). Somewhat larger degradation was encountered for the wide devices (in one case about 450 mV). Since these data were obtained under bias, it is difficult to compare these data with the soft x-ray results. The soft x-ray results were obtained with the gates unattached during irradiation. These results are shown to illustrate that the width dependent trend observed was present even in gate-biased irradiation.

IV. DISCUSSION

The initial x-ray lithographic exposure causes larger amounts of positive charge to be present in the insulator. Low temperature anneals (300 C in N_2) significantly reduce the number of chargeable centers in the insulator. However, even after such an anneal, slow trapping instabilities still are observed in capacitors. This indicates the presence of bulk trap sites near the oxide-semiconductor interface. After 450 C anneals in N_2 for 1/2 hour, this instability is no longer observed. However, growth in the G-V interface state peak is still not annealed away. Thus, the bulk oxide charges and bulk oxide traps seem to disappear after anneal, leaving the interface region as the most significantly damaged area. This is consistent with the capacitor post irradiation post anneal flat band in the oxide being less than 10

mV, while transistor threshold shifts are larger (200-300 mV). Thresholds are more sensitive to interface charging effects. This is also consistent with the fact that the most severely degraded transistor properties (g_{slope} and S), are largely determined by interface quality.

Analysis of Fig. 2 yields more information on the amount and distribution of insulator charge. Replotting the threshold shift vs oxide thickness data for a given channel width on a log-log scale yields best fit straight lines whose slope is always less than 1.5. Simple electrostatic considerations¹¹ indicate a uniform bulk charging mechanism would yield a quadratic dependence of the ΔV_t vs oxide thickness curve. This would give a slope 2 on the log-log plot. A fixed interface charge would yield a linear ΔV_t vs t_{ox} curve (slope 1 on log-log scale). The best model explaining the observed data would be that the V_t shift is dominated by the interface charge, with a small second order component due to residual bulk charge.

Based on this approach, we have fit that data to an expression of the form

$$\Delta V_t = at_{ox} + bt_{ox}^2 \quad (4)$$

where:

t_{ox} = oxide thickness

a = surface charge related constant

b = bulk charge related constant.

As shown in Grove¹¹

$$a = \frac{Q}{\epsilon_{ox}} \quad (5)$$

where:

Q = interface charge present at threshold.

ϵ_{ox} = permittivity of the oxide.

A table showing the interface charge present at threshold for each channel width studied is given in Table 1. The bulk term data, b , is such that it never caused more than a 20% change in ΔV_t . These data are small and are not given here.

Table 1 — Surface Charges Induced
by Soft X-Rays

Channel Width (μm)	Surface Charge ($\# / cm^2$)
5	3.4×10^{10}
10	7.8×10^{10}
20	5.9×10^{10}
30	6.9×10^{10}
50	6.8×10^{10}
Group	6.2×10^{10}

Ref Dose = 1.5×10^{17} electrons/cm²

X-ray energy = 0.1 keV, $\lambda = 12.4$ nm, $\lambda_{Si} = 0.357$ nm

Interfacial area =

$L = 4 \mu m$

Inspection of Table 1 indicates the narrowest channel had least interface charge growth. Interface charge growth ranged from 3×10^{10} states/cm² to 7×10^{10} states/cm². It is interesting to note, that the growth in interface states obtained from degradation in S (Fig. 5 and Eq. (2)) averages 1×10^{11} states/cm² over the range of studied widths shown in Fig. 5. This is obtained by assuming an initial interface charge of 1×10^{10} states/cm² (as inferred from G-V peak height analysis on capacitors).

Production of interface states during irradiation has been analyzed by McLean.¹³ The model proposed involves the transport of radiation-mobilized bulk-resident ions to the oxide-semiconductor interface. This model implies a t_{irr}^2 dependence to the threshold shift data. In this study, the quadratic dependence was not observed. This is probably due to immobilization of liberated ions by the anneal prior to measurement. Immobilized ions cannot drift to the interface to cause interface states production. Ions may still be implicated in the interface state growth observed here. These ions would come from the immediate vicinity of the damaged interface and would not contribute added thickness dependence.

No length dependence to the radiation effects was observed in threshold shift or in g_{slope} degradations. Since the source and drain nodes were grounded and the gate was unattached during irradiation, one might not expect a large field in the oxide or a field which changed significantly with channel length. The n^+ source-drain implant further acts as a "guard-ring" to prevent field variation along the gate length. This does not mean that there is *no* field in the oxide during soft x-ray lithographic irradiation. There may be residual charges due to the processing environment. There may also be work function potential drops across the insulator. As in standard narrow channel modeling, the field near the width extremes is less than in the center of the channel. Reduced field creates less radiation induced insulator charging. For narrow channels, this effect is more obvious. Thus, one would expect that the radiation effect would be less for narrow channels. Data derived here supports this observation. Data has appeared in the literature⁴ which indicated opposite effects can be observed for MOSFETs of similar dimensions. This data was obtained on self-aligned field MOSFETs. In the self-aligned field case, a part of the radiation-soften field oxide becomes a part of the active FET.¹⁴ Also, the local stress present near the self-aligning nitride boundary may cause even further softening of the oxide around the field boundary. In these cases, the width-extremes of the FET would become very soft. For narrow-channel devices, this region would dominate, explaining the observed results on self-aligned field devices done in other laboratories.⁴

As mentioned above, previous work indicated that soft x-ray irradiations enhanced the mobilization of positive charge.³ This was not observed in the present experiment. The emphasis of the work in Reference 3 was to study the influence of oxidation conditions on radiation response. Many of the oxidations employed were not of the type suitable for radiation-hard processes. To mobilize ionic charge and create positive charge instability, ionic centers must be present in the oxides. The oxides used in the study presented here apparently did not have these ionic centers present. This underlines the fact that oxides grown in different laboratories and under different conditions may exhibit different radiation responses.

V. CONCLUSIONS

The conclusions drawn from this work in soft x-ray exposure are similar to those drawn previously by Aitken. The damage levels observed here are not so severe as to preclude IC technology utilizing x-ray lithography. However, care must be taken in device modeling to account for lithography-induced parameter shifts.

Specifically, care must be exercised in accounting for interface related effects. At threshold, we usually observe charges amounting to about 6×10^{10} states/cm². This tends to reduce electron mobility. For thin oxides ($t_{\text{ox}} \approx 250 \text{ \AA}$), the most severe degradation is in subthreshold leakage. Increase of as much as 35% in subthreshold swing was observed. In high-density VLSI, power dissipation is (in many cases) dominated by subthreshold swing. In such cases, x-ray lithography would cause large increases in power dissipation. This increase must be accounted for to assure device functionality and reliability.

REFERENCES

1. Aitken, J., IEEE Jour. Sol-St. Circ., **SC-14**, 294 (1979).
2. T.H. Ning, P.W. Cook, R.H. Dennard, C.M. Osburn, S.E. Schuster, and H. Yu, IEEE Jour. Sol-St. Circ., **SC-14**, 283 (1979).
3. M. Peckerar, R. Fulton, P. Blaise, D. Brown and R. Whitlock, J. Vac. Sci. Technol. **16**, 1658 (1979).
4. J.Y. Chen, R.C. Henderson, D.O. Patterson, and R. Martin, IEEE Trans. ED Lettrs., **EDL-3**, 13 (1982).
5. K.O. Jeppson and C.M. Svensson, J. Appl. Phys. **48**, 204 (1977).
6. S.R. Hofstein, Solid State Electronics **10**, 657 (1967).
7. This dose in the SiO₂ gate is corrected for interface enhancement. The dose in thick SiO₂ was 3 Mrad.
8. P.S. Winokur and H.E. Boesch, Jr., IEEE Trans. Nuc. Sci., **NS-27**, 1647 (1980).
9. P.S. Winokur, H.E. Boesch, Jr., J.M. McGarrity, and F.B. McLean, IEEE Trans. Nuc. Sci., **NS-24**, 2113 (1977).
10. A. Goetzberger, A.D. Lopez, and R.J. Strain, J. Electrochem. Soc. **120**, 90 (1973).
11. Grove, A.J., *Physics and Technology of Semiconductor Devices*, Wiley, New York (1967).
12. Gesch, H., Leburton, J.P., Dorda, G.E., IEEE Trans. ED., **ED-29**, 915 (1982).
13. McLean, F.B., IEEE Trans. Nuc. Sci., **NS-27**, 1651 (1980).
14. F.Z. Custode, M. Tam, IEDM Technical Digest, 760 (1980).

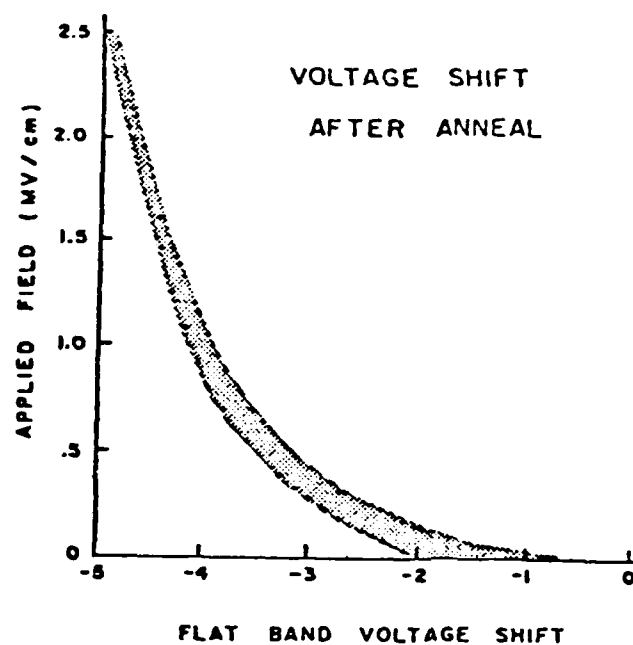


Fig. 1 — Flatband shifts in 1000 Å gate oxide polysilicon capacitors as a function of insulator field. All capacitors received 300 C anneals in N_2 for 1/2 hour. As expected, the larger biases created larger flatband shift. The bar represents the full range flatband variation for 5 capacitors. Unbiased devices did show unannealed shifts after 5 Mrad (SiO_2) exposures.

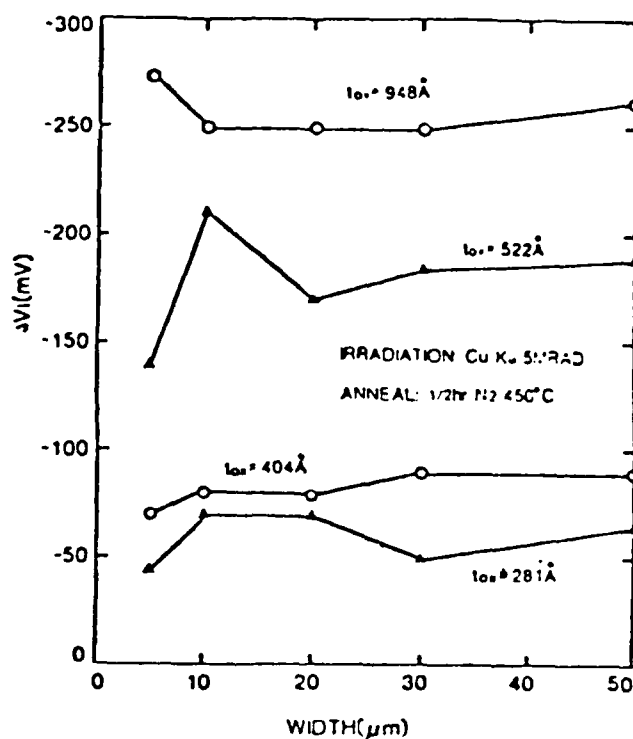


Fig. 2 — Threshold shifts, as a function of W_{geom} for transistors of different oxide thickness. A strong dependence of threshold shift on oxide thickness is observed. There is a weak channel width dependence. In all cases (except the 948 Å case) the 5 μm width had least unannealed V_t shift.

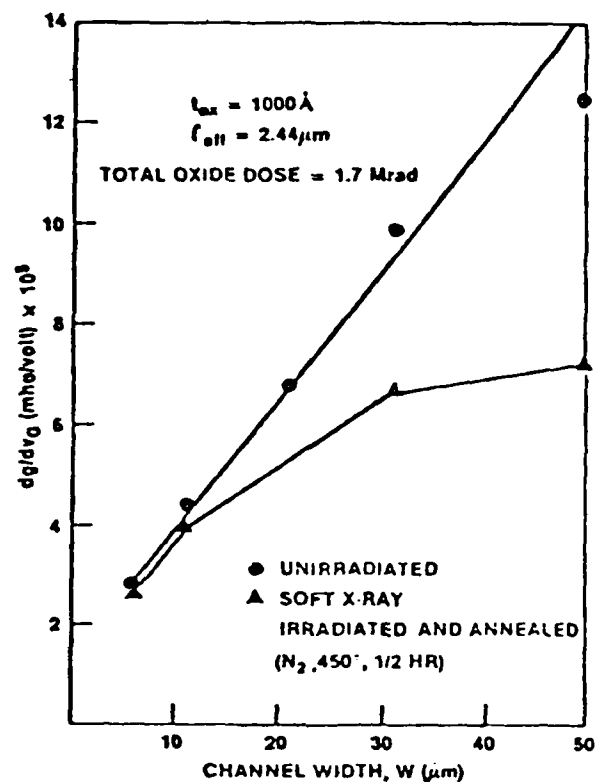


Fig 3 — Marked degradation in κ_{slope} noted for the wide channel devices. This large degradation is seen in 1000 Å oxides only

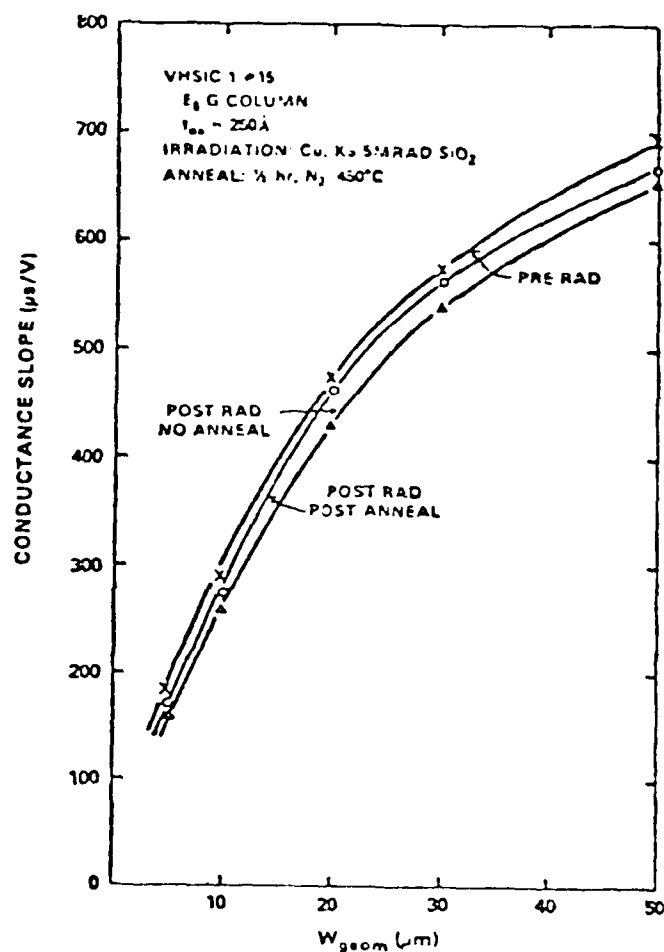


Fig 4 — Conductance slope showed little post-anneal degradation regardless of width for the 250 Å gate oxide sample. Results here represent an average of 3 devices

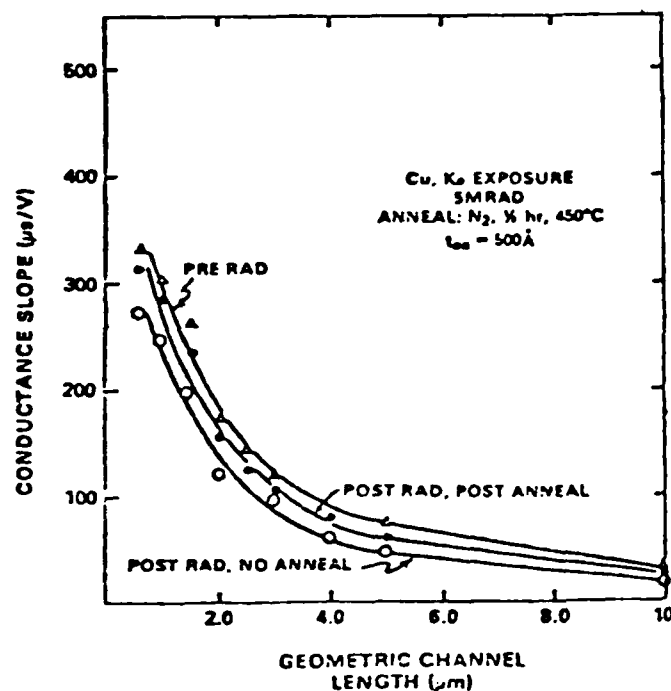


Fig. 5 — There is no apparent g_{slope} degradation as a function of channel length devices to $1\ \mu\text{m}$. This was true for $1000\ \text{\AA}$ and $250\ \text{\AA}$ oxides. At $1000\ \text{\AA}$, some unannealed g_{slope} degradation was noted. Channel width was $5\ \mu\text{m}$ in all cases.

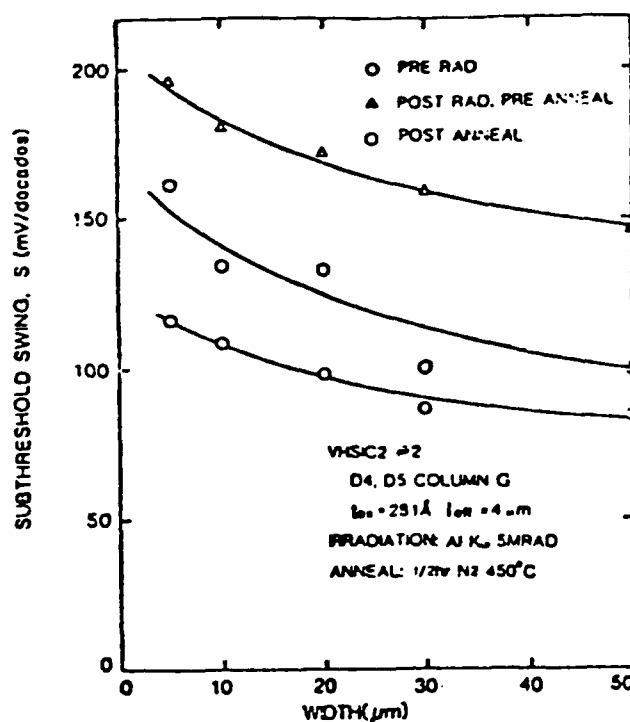


Fig. 6 — For $281\ \text{\AA}$ oxides some significant unannealed degradation in subthreshold sensitivity was observed. Results here represent an average of 3 devices.

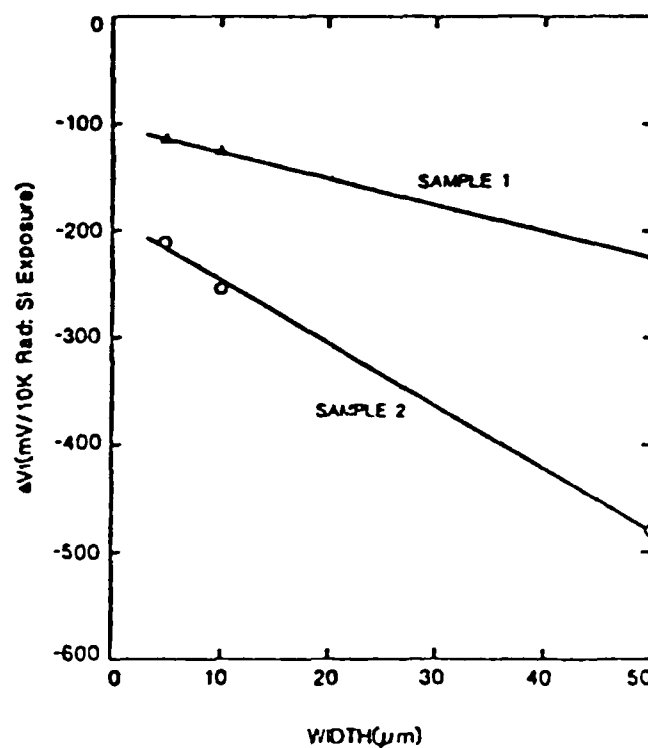


Fig. 7 — Threshold shift following $10\ \text{krad}\ \text{Co}^{60}$ irradiation. A $5\ \text{volt}$ bias was employed. Two chips from separate wafers were studied, each chip was irradiated separately. The gate oxide was $1000\ \text{\AA}$ thick.

Repetitively pulsed-plasma soft x-ray source

David J. Nagel, Charles M. Brown, M. C. Peckerar, Marshall L. Ginter,
J. A. Robinson, Thomas J. McIlrath, and P. K. Carroll

A 10-Hz Nd:YAG laser system with 0.6-J, 25-nsec pulses was used to produce plasmas which emitted strongly in the soft x-ray region. Spectral, temporal, and spatial characteristics of these plasma emissions are presented together with an application of the source to soft x-ray lithography.

I. Introduction

Lasers with low pulse repetition rates (less than $\sim 10^{-1}$ Hz) have produced high temperature plasmas when tightly focused on solid targets. Early studies¹⁻⁶ showed that such plasmas yield short, bright pulses of radiation with wavelengths extending into the x-ray region. More recent studies⁷⁻²¹ have expanded the characterization of these plasmas' short-wavelength outputs and have initiated tailoring of the plasma conditions and target materials to achieve desired types of radiative output (e.g., continuum emissions, enhanced soft x-ray emissions). In particular, plasmas generated on rare-earth targets have been developed as XUV continuum sources for absorption spectroscopy^{11,12} and their use as radiometric transfer standards has been proposed and currently is under investigation.^{12,14,15,21} A number of ways in which the usefulness of these light sources might be enhanced, including the use of high pulse rates, have been suggested.⁸ The present work describes a high repetition rate (10-Hz) pulsed plasma source of short-wavelength radiation, presents observations of the spectral, temporal, and spatial characteristics of the source's vacuum ultraviolet (VUV) and soft x-ray (SXR) outputs for selected targets, and illustrates initial results obtained from the utilization of the source for x-ray lithography. Expanded descriptions of our observations are available in a Naval Research Laboratory technical note.²²

P. K. Carroll is with University College Dublin, Physics Department, Belfield, Dublin, Ireland; M. L. Ginter, J. A. Robinson, and T. J. McIlrath are with University of Maryland, Institute for Physical Science & Technology, College Park, Maryland 20742; the other authors are with U.S. Naval Research Laboratory, Washington, D.C. 20375.

Received 16 September 1983.

II. Experimental Procedures

The laser employed in this work was an International Laser Systems (ILS) Nd:YAG laser which produces 25-nsec FWHM pulses of 1.06- μ m radiation with energies up to 0.8 J and repetition rates up to 10 Hz. These pulses were focused by a glass lens ($f \approx 300$ mm) through a Pyrex window onto cylindrical targets. Radiation emitted by the plasma passed from a target chamber through a 19-mm diam aperture into an experimental chamber, where the plasma was viewed perpendicular to the laser beam. The experimental arrangement is illustrated and discussed in greater detail elsewhere.²²

The source chamber, target drive, and experimental chamber have been described previously.¹⁵ Briefly, target cylinders ~ 16 -mm diam $\times \sim 70$ mm long were attached to a stepping-motor-driven screw, and the target drive usually was set so that a fresh area of target material advanced to the laser's focal position before each laser pulse.^{14,15} Targets of graphite (C), Teflon (CF₂), Al, steel (Fe), brass (Cu, Zn), Sn, Yb, Hf, and U were utilized in various phases of our experiments.

The laser produced single-mode pulses which could be tightly focused. Damage craters were used as indicators both of proper laser operation and of attainment of best focus. Crater diameters were ~ 130 μ m for low power shots on refractory targets and on plastic tape, which is an upper bound on the minimum focal spot diameter. For 25-nsec, 0.6-J pulses focused to 130 μ m the lower bound on the averaged irradiance would be $\sim 2 \times 10^{11}$ W/cm²/pulse. For a perfect lens and a TEM₀₀ beam we estimate the spot diameter would be ~ 30 μ m, which places an upper bound on the irradiance of $\sim 5 \times 10^{12}$ W/cm²/pulse for the same pulse power and duration.

Spectra were recorded in the 30–1.4-nm (40–900-eV) range. In the longer wavelength region ($\lambda > \sim 3$ nm), spectra were obtained using a 1-m grazing-incidence spectrograph²³ with a 10- μ m entrance slit and a 1200-lines/mm grating. A rubidium acid phthalate

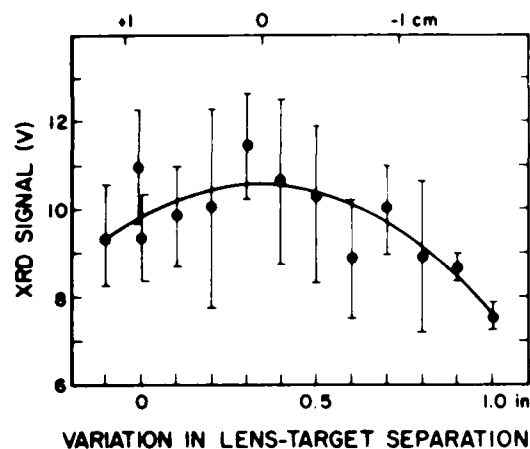


Fig. 1. Variation of x-ray diode signal (volts) with focusing lens to target distance for an aluminum target irradiated with 500 mJ/pulse at a 10-Hz pulse rate. A point represents the average of five output pulses with the error bar indicating one standard deviation.

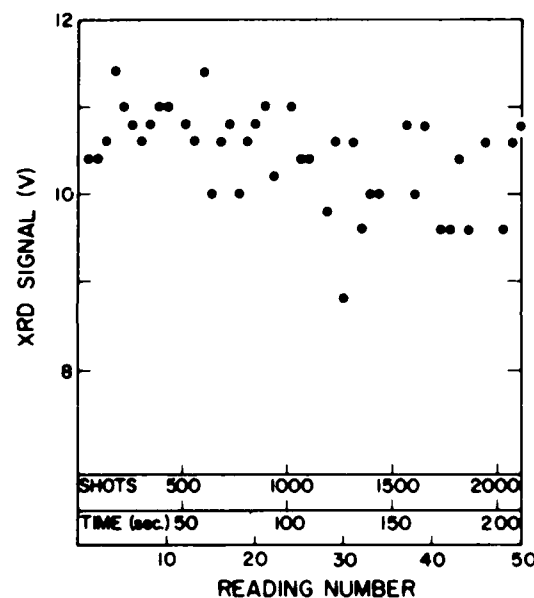


Fig. 2. Variation of x-ray diode signal (volts) with time for plasma pulses produced from a rotating aluminum target irradiated with 500 mJ/pulse at 10 Hz. Readings were taken of the output at 4.2-sec intervals (see text).

crystal spectrograph²³ was used in the shorter wavelength region. Both instruments used Kodak 101 film to record spectra. In addition, short-wavelength (~ 2.5 –80-nm bandpass) images of the plasma were recorded on 101 film using a pinhole camera (50- μ m pinhole covered by a 0.5- μ m Al film). Time histories of the soft x-ray (SXR) emissions were recorded using an x-ray diode²⁴ (active area ~ 0.5 cm²) with an Al (actually Al₂O₃) photocathode covered by a 1- μ m thick polypropylene filter. An x-ray diode (XRD) so filtered has most of its response in the 14–4.3-nm (90–284-eV) XUV region.²⁴ A silicon PIN diode behind 13 μ m of beryl-

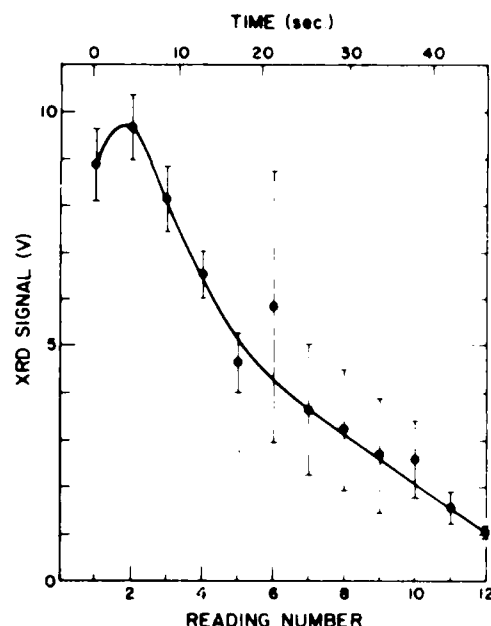


Fig. 3. Variation of x-ray diode signal (volts) with time for plasma pulses produced from a stationary aluminum target. Irradiation and readings as described for Fig. 2. Points represent three run averages with one standard deviation error bars.

lium was tried but failed to sense emission in its <1.2 -nm (>1 -keV) bandpass.

III. Results

The time variation of the XUV emission measured with the XRD was similar to that of the laser pulse (25-nsec FWHM). Typical variations in the source's XUV intensity with lens-to-target separation, with time, and with multiple pulses on a single target spot are illustrated in Figs. 1–3, respectively, for 0.5-J laser pulses on aluminum targets. It can be seen from Fig. 1 that the filtered XRD output is not strongly dependent on focal conditions, which is similar to previous observations at longer VUV wavelengths^{14,15,21} but different from the more stringent dependence on focal conditions observed²⁵ in the production of harder x rays. Data in Fig. 2 are values taken from a storage oscilloscope which sampled the XRD output at 4.2-sec intervals as the laser pulsed at 10 Hz and the target rotated to provide a new target area to the laser before each pulse. The scatter in Fig. 2 is significantly greater than variations in the laser's output in similar conditions and there appears to be a gradual decrease in the XRD output with time. In Fig. 3 data were taken at 4.2-sec intervals as in Fig. 2, but the target was stopped and the laser allowed to strike the same target spot at 10 Hz.

While the data presented in Figs. 1–3 are specific to aluminum targets, the trends illustrated are encountered in the other target materials studied. The slow decrease in apparent output with time noted specifically in Fig. 2 may be due to slight coating of the detector window by evaporated materials (see below). The initial rise and eventual fall in output for multiple pulses

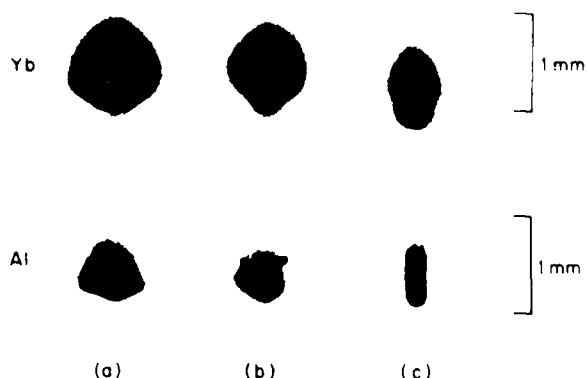


Fig. 4. Pinhole photographs in XUV radiation from two targets irradiated from the top of the figure with (a) 10 pulses at 600 mJ/pulse, (b) 20 pulses at 300 mJ/pulse, and (c) 240 pulses at 25 mJ/pulse.

on a single spot shown in Fig. 3 may be due to initial confinement followed by increased obscuration of the plasma in a deepening damage crater. Pinhole camera images in Fig. 4 show that the plasma plumes producing 2–80-nm radiation from fresh target surfaces were smaller than 1 mm in extent for the laser pulse energies available.

Representative examples of spectra obtained from several target materials with the grazing incidence and crystal spectrographs appear in Figs. 5 and 6, respec-

tively. The spectra illustrated in Fig. 5 required exposure times in the 2–12-sec range at 10 Hz, while the spectrum in Fig. 6 required an exposure time of 100 sec. For the target materials studied, the $\lambda > 3$ -nm spectra taken with the present laser system do not differ appreciably from analogous spectra obtained using higher peak power (1–5-J/pulse) lasers with lower pulse repetition rates.^{2,9,13,16}

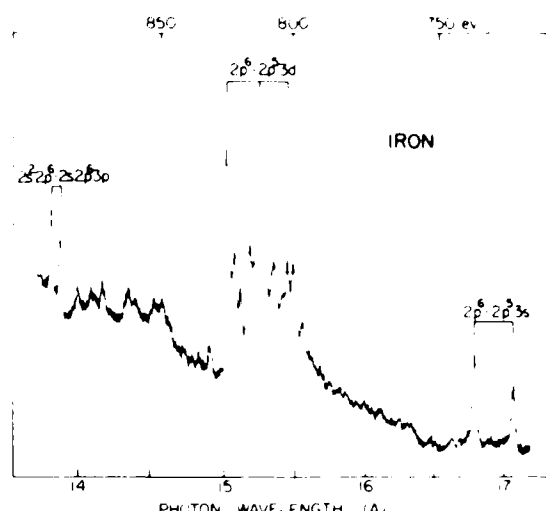


Fig. 6. Densitometer trace of the Ne-like iron spectrum obtained from the plasma source (steel target) using a crystal spectrograph.

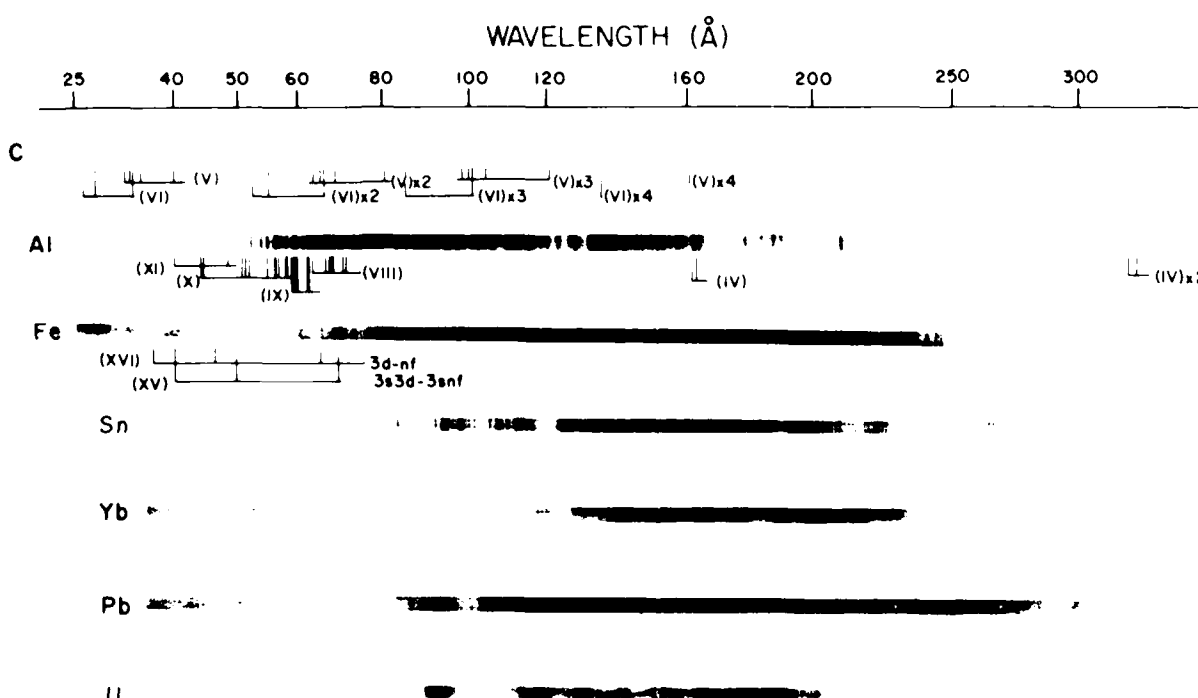


Fig. 5. Typical spectra obtained from the plasma source using a 1-m grazing incidence spectrograph. The target elements appear at the left of each spectrum and the higher orders (x order number) of several ion stages (Roman numerals) are indicated below the spectra for C, Al, and Fe (from steel).

Figure 5 illustrates the variety of VUV emissions available from the source using low, intermediate, and high atomic number (Z) target materials. Low Z materials such as carbon provide sparse but well-defined emission spectra from hydrogenlike and heliumlike ions. The C VI and C V spectra are apparent in all orders up to sixth in the top band of the figure. The aluminum spectrum contains lines from numerous stages of L -shell ionization and represents an example of complex line emissions. The still more complex Fe spectrum is representative of the emissions observed using intermediate Z target materials, which tend to display compacted line spectra overlaying weak continua. Finally, high Z materials tend to produce continua overlaid by weak and sometimes sparse line spectra. The Yb spectrum in Fig. 5 is typical of the rare earth continua⁹⁻¹⁵ which in part results because open $d^n f^m$ configurations⁹ are predominant in the electronic structures of the ions produced in these plasmas. The rare-earth continua generated using higher energy per-pulse lasers are adequate⁹⁻¹³ for use as background continua in absorption spectroscopy, and our lower per-pulse energy system produces comparable results.²²

Figure 7 illustrates the variation of the source's XUV output with laser pulse energy for several elements using the filtered XRD as the detector. The per pulse laser energy threshold for production of measurable XRD signals was in the 25–50-mJ range. As can be seen in Fig. 7, the targets with the lowest (C) and highest (U) atomic numbers produce approximately linear increases in XRD signal with increasing laser energy, while SXR outputs from targets of intermediate Z elements saturate or possibly decrease at the higher per-pulse energies. The per-pulse XUV intensity did not vary significantly for operation at 1 or 10 Hz. Spectra taken²² as the per-pulse energy was increased showed that the ionization stage of the emitters also increased, reflecting an anticipated collateral increase in plasma temperature.

Damage craters produced by the laser were largest in materials which vaporize readily and crater depths increased with increasing per pulse energy. Crater depth also was found to depend on the laser's pulse repetition rate, possibly because of the laser's mode of operation. In the ILS system the amplifier flashlamps are pulsed continuously at 10 Hz regardless of the Pockels-cell-controlled laser output rate. For laser rates <10 Hz, low energy ($\sim 9\text{-}\mu\text{J}$) superradiant pulses from the amplifier rods reach the target from the flashlamp pulses between laser firings and produce minicraters into which the laser pulse subsequently falls. Although the superradiance-produced cratering is very small, this prepulse alteration of the target surface affects the size and depth of the crater produced by the lasing pulse. Figure 8 shows reproductions of scanning electron micrographs of craters in aluminum produced when the laser was run at 1-, 5-, and 10-Hz rates. Substantially deeper craters are produced at the lower rates, with a collateral increase in material ablated from the target.

Target debris and vaporization products generated together with the plasmas can be a significant consid-

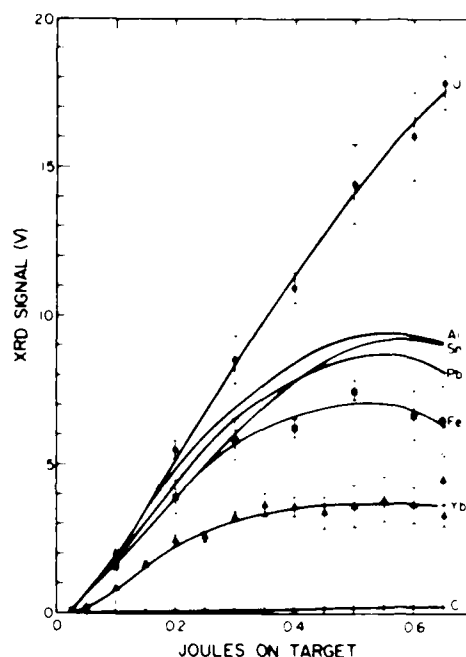


Fig. 7. Dependence of soft x-ray output on laser pulse energy and target material for 10-Hz pulse rates. Data points (shown for C, Yb, Fe, and U only) are averages of five or more pulses while error bars represent one standard deviation.

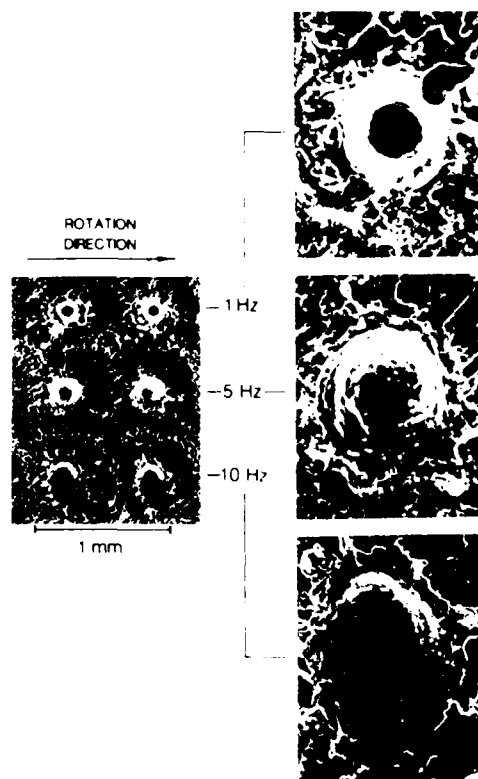


Fig. 8. Scanning electron micrographs of craters in aluminum produced at 1-, 5-, and 10-Hz main pulse repetition rates (see text). The right-hand panels are 5 \times enlargements.

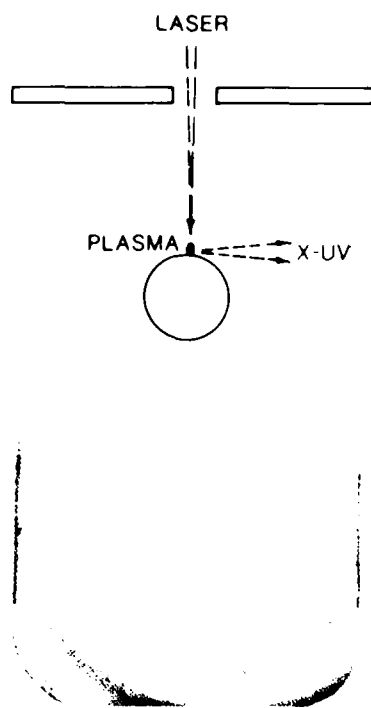


Fig. 9. Relative positions (top) of the target and the plastic ablation product catcher in the photograph (bottom) which shows interference fringes produced by a thin film of ytterbium (see text).

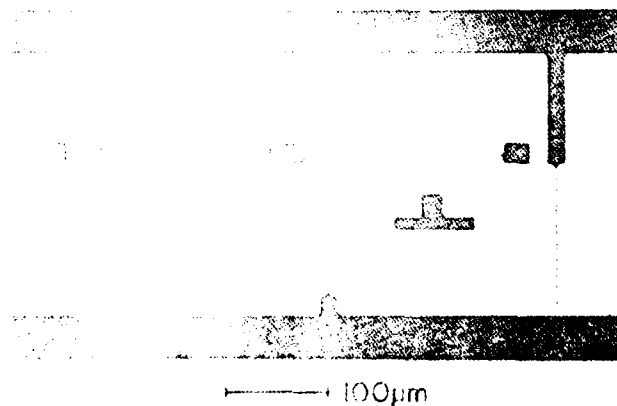


Fig. 10. Photomicrograph of a replica in photoresist of the gate level mask for a large-scale dynamic shift register made using soft x rays from the source operating at 10 Hz.

eration in applications using a laser plasma light source. The ablation products are distributed over a wide cone angle with deposition found even at right angles to the incident laser beam. An example of the pattern of ablation products observed above a Yb target is shown in Fig. 9. The debris in Fig. 9 was collected on a flat plastic sheet, with a hole to admit the laser beam, placed 5 cm from the focal spot on the target. Interference rings produced by varying thicknesses of vaporized yt-

terbium are clearly visible in the figure, while a small amount of particle debris in a central ring near the target normal is less evident.

Experiments were performed to investigate the source's utility for SXR lithography. We used the positive resist polybutene sulfone (the resist was spun on 50-mm diam silicon wafers in layers 0.3 μm thick and baked by conventional procedures) and mask patterns of 0.7- μm thick gold on 2- μm polyimide membranes. Photoresist coated wafers were masked, exposed to light with restricted wavelengths (see below) from the plasma light source, and then developed by conventional techniques. Figure 10 reproduces the photomicrograph of a portion of a test chip showing the gate level from a large-scale dynamic shift register made by this process using a 20-min exposure at 10 Hz employing a steel target. The source's output wavelength distribution and mask absorption combined to limit our resist exposing wavelengths primarily to the $\sim 8\text{--}4.3\text{-nm}$ (150–284-eV) region,²² which is near the 5-nm region suggested²⁶ as having potentially the best compromise of resolution to contrast for masked photoresist based lithographs.

IV. Summary

We have employed a modest energy, high repetition rate laser as a driver for a laser-plasma light source and have presented data on the following: (1) the characteristics of the source's SXR output as functions of laser focus, source operation time, number of pulses per target spot, target material, laser energy, and driver pulse repetition rate; (2) the plasmas' spectral output in the 30–1.4-nm region, with emphasis on conditions generating predominantly many line or predominantly continuum spectra; (3) laser-produced damage of the target and ablation of target vapor and debris; (4) the lithographic preparation of test chips using the light source and $\sim 8\text{--}4.3\text{-nm}$ radiation.

Helpful discussions with T. W. Barbee, Jr., M. Morris, and W. C. Martin are gratefully acknowledged, as is the technical assistance of N. Baldwin, K. Hudson, P. Isaacson, and M. Rebbert. This work was partially supported by the National Science Foundation under grants PHY-80-16657 and CPE 8119250A01 to the University of Maryland.

C. M. Brown is in the E. O. Hulbert Center for Space Research.

References

1. B. C. Fawcett, A. H. Gabriel, F. E. Irons, N. J. Peacock, and P. A. H. Saunders, *Proc. Phys. Soc. London* **88**, 1051 (1966).
2. A. W. Ehlers and G. L. Weissler, *Appl. Phys. Lett.* **8**, 89 (1966).
3. C. Breton and R. Popoulet, *J. Opt. Soc. Am.* **63**, 1275 (1973).
4. P. J. Malozzi, H. M. Epstein, R. G. Jung, D. C. Applebaum, B. P. Fairand, and W. J. Gallagher, in *Fundamental and Applied Laser Physics*, M. S. Fred, A. Javan, and N. A. Kurnet, Eds. (Wiley-Interscience, New York, 1973), p. 165.
5. D. J. Nagel, P. E. Burkhalter, C. M. Dozier, J. F. Holzrichter, B. M. Klein, J. M. McMahon, J. A. Stamper, and R. R. Whitlock, *Phys. Rev. Lett.* **33**, 743 (1974).
6. P. G. Burkhalter, D. J. Nagel, and R. R. Whitlock, *Phys. Rev. A* **9**, 2331 (1974).

7. C. G. Mahajan, E. A. M. Baker, and D. D. Burgess, *Opt. Lett.* **4**, 283 (1979).
8. P. K. Carroll, *Extended Abstracts of the Fourth International Conference on Vacuum Ultraviolet Radiation Physics* **3**, 56 (1980).
9. P. K. Carroll and G. O'Sullivan, *Phys. Rev. A* **25**, 275 (1982).
10. G. O'Sullivan and P. K. Carroll, *J. Opt. Soc. Am.* **71**, 227 (1981).
11. P. K. Carroll, E. T. Kennedy, and G. O'Sullivan, *Appl. Opt.* **19**, 1454 (1980).
12. P. K. Carroll, E. T. Kennedy, and G. O'Sullivan, *Opt. Lett.* **2**, 72 (1978).
13. P. K. Carroll and E. T. Kennedy, *Phys. Rev. Lett.* **38**, 1068 (1977).
14. G. O'Sullivan, J. Roberts, W. Ott, J. Bridges, T. Pittman, and M. L. Ginter, *Opt. Lett.* **7**, 31 (1982).
15. G. O'Sullivan, P. K. Carroll, T. J. McIlrath, and M. L. Ginter, *Appl. Opt.* **20**, 3043 (1981).
16. P. Nicolasi, E. Jannitti, and G. Tondello, *Appl. Phys. B* **26**, 117 (1981).
17. R. M. Gilbert, J. P. Anthes, M. A. Guisnow, M. A. Polmer, R. R. Whitlock, and D. J. Nagel, *J. Appl. Phys.* **51**, 1449 (1980).
18. D. J. Nagel, R. R. Whitlock, J. R. Greig, R. E. Pechacek, and M. C. Peckerar, *Proc. Soc. Photo-Opt. Instrum. Eng.* **135**, 46 (1978).
19. R. D. Bleach and D. J. Nagel, *J. Appl. Phys.* **49**, 3832 (1978).
20. D. J. Nagel, M. C. Peckerar, R. R. Whitlock, J. R. Greig, and R. E. Pechacek, *Electron. Lett.* **14**, 781 (1978).
21. M. Kuhne, *Appl. Opt.* **21**, 2124 (1982).
22. D. J. Nagel, C. M. Brown, M. C. Peckerar, M. L. Ginter, J. A. Robinson, T. J. McIlrath, and P. K. Carroll, *Memorandum Report 5201* (Naval Research Laboratory, Washington, D.C., 1983).
23. The 1-m spectrograph is discussed in NRL Memorandum Report 4732 by R. D. Bleach, P. G. Burkhalter, and D. J. Nagel. The lighttight window on the slitless crystal ($2d = 2.66\text{-nm}$) spectrograph was $2\text{-}\mu\text{m}$ polypropylene coated with $0.2\text{-}\mu\text{m}$ of aluminum.
24. R. K. Day, P. Lee, E. B. Saloman, and D. J. Nagel, *J. Appl. Phys.* **52**, 6965 (1981).
25. T. N. Lee and D. J. Nagel, *J. Appl. Phys.* **46**, 3789 (1975).
26. E. Spiller and R. Feder, in *X-Ray Optics*, H. J. Queisser, Ed. (Springer, New York, 1978), pp. 35-92.

Chapter 6

Plasma Sources for X-Ray Lithography

D. J. NAGEL

Naval Research Laboratory,
Washington, D.C.

I. Introduction	147
II. X-Ray Lithography	148
III. X-Ray Source Requirements	149
IV. Electron-Impact X-Ray Sources	149
V. <i>Synchrotron X-Radiation Sources</i>	149
Plasma X-Ray Sources	149
A. General Considerations	149
B. Discharge-Heated Plasma Sources	150
C. Laser-Heated Plasma Sources	150
VII. Conclusion	151
Appendix: X-Ray Source Characterization	152
References	153

I. INTRODUCTION

Interest in the production of fine-scale structures with dimensions of about $1\ \mu\text{m}$ or less cuts a wide swath through science and technology [1-4]. *Active devices* are of greatest interest, with microelectronic circuits having overwhelming commercial importance [5]. Attention to other classes of active microdevices is increasing as electronic device patterning and processing techniques are applied to produce active acoustic and other mechanical microdevices [6]. *Passive microstructures* can channel radiation and orient matter. For example, diffraction grating plates are employed in x-ray optics to disperse spectra and focus radiation [7]. Fine-scale coded

147

0022-3099/80/0000-0000\$01.00/0

apertures and test patterns are used in plasma diagnostics and other areas [8]. Micropatterns on a surface provide a means of orienting cells [9]. In short, there are already numerous reasons for producing submicrometer structures, and the list is growing rapidly.

Production or replication of microdevices and structures can be accomplished by a wide variety of lithographic techniques. These can be categorized according to the means of pattern definition and the type of energy that actually produces the pattern, as indicated in Fig. 1 [10]. The sensitive material in which the pattern is produced can be irradiated with photons in the few-electron-volt-to-the-few-kilo-electron-volt region, electrons usually in the 5–50-keV range or ions in the 20–200-keV range. The actual pattern can be produced by programmed motion of a focused beam, by a projected image, or by the radiation that passes through a nearby mask. Of the photon techniques, ultraviolet (optical) projection lithography is very important commercially, although the optical proximity technique is still widely used. Focused electron-beam (direct-write) lithography is well developed, and machines are commercially available. Focused and masked ion-beam lithographies are still under development. Direct-write electron- and ion-beam lithographies offer submicrometer resolution but are too slow for mass production of chips. However, they will be used for production and repair of masks for X-ray and flood-ion-beam lithographies. General reviews of lithographic techniques are available [11–20].

The relentless drive for smaller and denser integrated circuits, with the attendant benefits of higher speeds, lower cost per function, and greater yields, will make the use of high-resolution (submicrometer) lithography a necessity if current trends continue. Present commercial linewidths of about

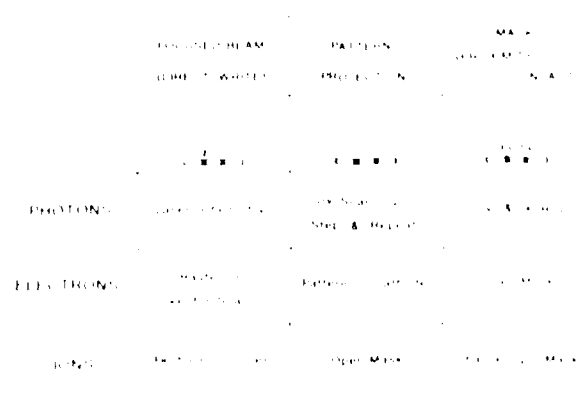


Fig. 1. Lithographic techniques arranged by the method of pattern formation and the quanta that cause resist exposure. (From Nagel [10].)

$1\text{ }\mu\text{m}$ are far from the limiting resolution of resists, which is near $0.01\text{ }\mu\text{m}$. Optical lithography continues to advance, but diffraction provides a fundamental barrier to its use for linewidths below about $0.1\text{ }\mu\text{m}$. This is most easily seen for proximity printing, in which the diffraction angle for radiation of wavelength λ and linewidth D is approximately $\theta = \lambda/D$. The resulting blurring at the resist is $B = \theta S$, where S is the mask-to-resist separation. Typically, $\lambda = 0.3\text{ }\mu\text{m}$ and $S = 30\text{ }\mu\text{m}$, so $B = 3\text{ }\mu\text{m}$ for $D = 3\text{ }\mu\text{m}$. The use of high-quality lenses and small fields for projection printing is necessary to reduce diffraction blurring. Photoresist nonlinearities ameliorate diffraction effects, but the point remains that optical lithography may not be commercially useful at linewidths below around $0.75\text{--}0.5\text{ }\mu\text{m}$ even though it can produce smaller lines with special care.

It is conceivable that despite the availability of lithographic techniques with resolution below $0.1\text{ }\mu\text{m}$ and other appropriate characteristics, very fine scale microcircuits will not attain widespread usage and commercial importance. As discussed in other chapters in this volume, appropriate dry processing methods must be available to transfer the lithographically produced patterns during VLSI circuit production. Single-event upset due to cosmic rays or radiation from packaging may set a practical limit on circuit dimensions [21]. Substrate defects are increasingly important as device dimensions shrink [22,23]. Even in the absence of these limitations, other factors will eventually halt further reduction of integrated circuit dimensions below around $0.01\text{ }\mu\text{m}$. Interactions between devices and noise are among the ultimate problems [23,24]. However, structures with scales below $0.1\text{ }\mu\text{m}$ will be of use in other areas of science and technology, no matter what the size limits on microcircuits turn out to be. It is presumed here that there is a window between roughly 0.5 and $0.01\text{ }\mu\text{m}$ where circuits and structures will be produced by techniques other than optical lithography [24a].

Of all the lithographic techniques now in use or under development, only proximity printing with short wavelength (x-ray) photons is treated in this chapter. It is believed by many people that x-ray lithography will eventually supplant both proximity and projection ultraviolet lithographies as the primary commercial replication tool. Several major companies have invested heavily in x-ray lithography research and development. Even if optical lithography remains in use for linewidths near $1\text{ }\mu\text{m}$, x-ray lithography may be the technique of choice for mass production of critical, leading-edge submicrometer circuits for computers, memories, signal processors, and other major applications. At present, x-ray lithography is being employed commercially with relatively low brightness sources. The plasmas discussed in this chapter may find use as second-generation x-ray lithography sources in 5 to 10 years.

Background information on x-ray lithography is provided in the next section. Then the focus is narrowed to sources of x rays for lithography. These fall into three major classes [25,25a]: electron-impact devices, accelerator and storage ring sources of synchrotron radiation, and multimillion-degree plasma sources. Each is discussed in turn. Electron-impact devices are already employed in prototype and early production x-ray lithography systems. Intense research is now being done on higher-brightness synchrotron radiation and plasma sources. Much smaller and cheaper synchrotron-radiation sources than are now being used for research may be developed in the next decade. If so, they could find routine use by large companies. Plasma sources may be small and low-cost enough to find widespread use. Major problem areas for both synchrotron radiation and plasma sources are summarized in the final section. The Appendix is a discussion of techniques for measurement of the spectral, spatial, and temporal characteristics of x-ray lithography sources.

II. X-RAY LITHOGRAPHY

The potential of x-ray lithography has long been recognized. The initial demonstration was performed by Spears and Smith [26] over a decade ago. Presently envisioned advantages of x-ray lithography include [27]

1. high resolution (compared to optical lithography),
2. excellent edge definition and linewidth control (negligible standing-wave or proximity effects),
3. high throughput (compared to direct-write techniques),
4. good step coverage and insensitivity to particulate contaminants (which promote high yield),
5. variable magnification (to compensate for process-induced linear wafer distortion), and
6. intermediate equipment cost (optical < x ray < electron beam).

Also, x-ray lithography may be operationally similar to optical lithography in terms of alignment of the mask and wafer and its exposure. This facilitates the training of processing personnel for hybrid lithography wherein conventional exposures are made for most wafer levels and x-ray lithography is employed for only a critical level, e.g., the gate level in an MOS process [28,29].

The advantages of x-ray lithography must be quite compelling because it does require new sources, masks, and resists compared to the familiar optical techniques. Further, since commercial x-ray exposure stations have

AP-A188 313

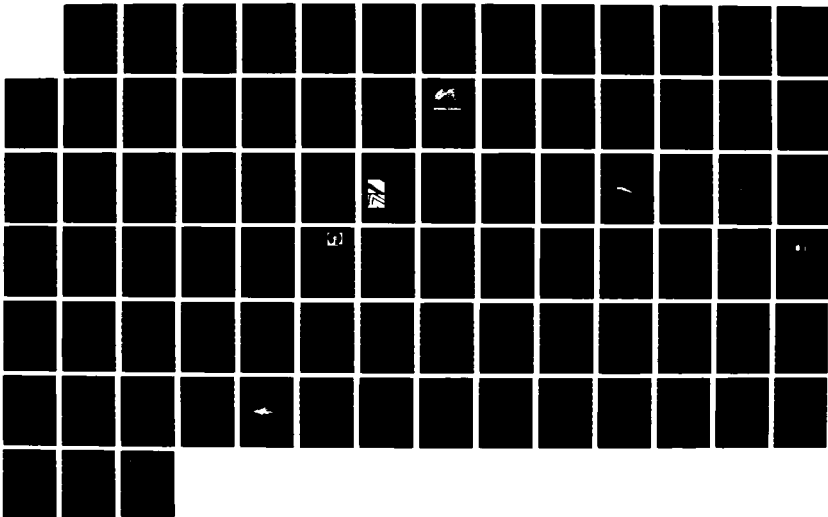
X-RAY LITHOGRAPHIC RESEARCH: A COLLECTION OF NRL
CONTRIBUTIONS(U) NAVAL RESEARCH LAB WASHINGTON DC
R R WHITLOCK 24 AUG 87 NRL-MR-5731

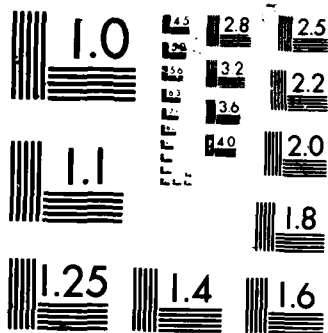
2/2

UNCLASSIFIED

F/G 13/8

ML





become available only recently, work in this arena has generally required local development of alignment systems. Each of the components needed for x-ray lithography is reviewed in the remainder of this section, with emphasis on constraints imposed by x-ray absorption.

X-ray lithography is dominated by the wavelength-dependent characteristics of sources and of absorbers (ambient gases, mask membranes, and photoresists), as indicated in Fig. 2. The absorption characteristics of mask membranes define three regions for lithography with photons [30]. The peak absorptivity for materials is near a photon energy of 20 eV (60 nm), where the x-ray mean free path is only 0.1 μm . Optical (UV and deep-UV) lithographies are done in the 3–6-eV range for which convenient transparent materials, such as thick silica glasses, are available for mask substrates. It is necessary to move to the opposite side of the peak absorptivity to do x-ray lithography. If a thin plastic mask support is employed, it is possible to work in the region from about 100 eV to the carbon K edge at 284 eV. This X-UV region may eventually be used for step-and-repeat exposures through small-area masks. However, the thrust of current x-ray lithography

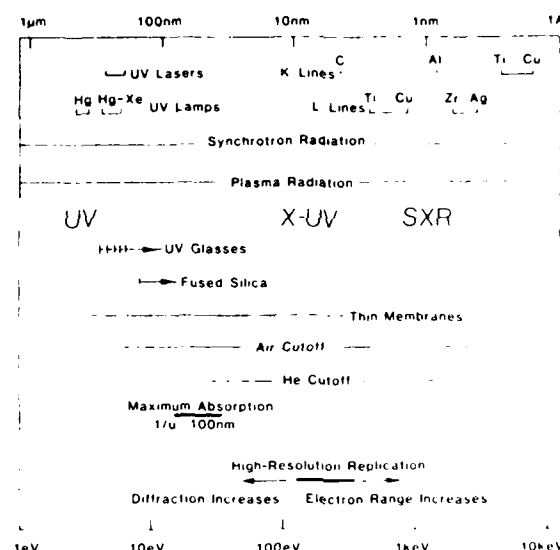


Fig. 2. Wavelength-dependent factors that influence ultraviolet and x-ray lithography. Regions of source emissions are shown at the top for UV lasers and lamps and electron-impact sources of K and L x rays, plus synchrotron and plasma radiation. Ranges of heavy absorption for various materials are shown in the center. Maximum absorptivity occurs around 60 nm (20 eV) for most materials, where mean free x-ray paths are typically 100 nm. Best x-ray lithographic resolution is obtained near 6 nm (200 eV). Three regions of interest for lithography are indicated: UV = optical and deep-UV regimes, X-UV = region below the carbon K edge, and SXR = soft x-ray range of primary use for x-ray lithography. (From Nagel [10].)

work involves use of photons with energies of about 1 to a few keV, for which stable large-area masks are available for full-wafer exposure.

X-ray sources provide wavelengths throughout the region of interest for lithography. Electron-impact sources emit K or L x-ray lines at the energies indicated in Fig. 2. Their continuum radiation is relatively weak and lithographically useless. Synchrotron radiation continua extend to a maximum useful energy dependent on the orbiting electron energy (~ 1 GeV) and the magnet bending radius (about a few meters). For example, radiation useful for x-ray lithography from a 0.7-GeV machine with a 2-m bending radius cuts off at about 3 keV. Plasma radiation consists of intense lines and continua, the wavelengths of which are determined by the plasma composition and temperature. Additional information on each of these three classes of sources will be given in Sections IV–VI.

Masks are a major problem in x-ray lithography. Mask membranes no thicker than a few micrometers are required for x-ray lithography so that they will transmit an adequate fraction of the incident soft x rays. A wide range of membrane materials has been tried: elements (Be, Al, Si, and Ti), compounds (Al_2O_3 , SiC, and Si_3N_4), polymers (Mylar, Kapton, and polyimide), and layered materials (SiO_2 with Si_3N_4 and BN with polyimide). References to mask-development work have been cited by Nagel [10] and Levinstein [31]. Although various groups still favor alternative mask materials, there is growing interest in the BN–polyimide combination [32–34]. The BN provides dimensional stability, while the polyimide provides toughness. The combination is transparent and hence easier to align than opaque metallic membranes; BN–polyimide membranes 100 mm in diameter are available commercially. Whatever the membrane material, gold about $0.5\text{ }\mu\text{m}$ thick is almost universally used as the absorber in x-ray masks.

New photoresists had to be developed for x-ray lithography. Attention was given both to increasing x-ray absorption by addition of appropriate elements to the resist [35] and to efficient use of the absorbed energy for producing cross-links or broken bonds [36]. References to x-ray resist work prior to 1981 have been given by Nagel [10]. For a recent review of lithographic resists, see Hatzakis [37]. Certain resists are being heavily used in major United States x-ray lithography programs now. The negative resist DCOPA [38] exposed in an O_2 -containing ambient [39] is employed at Bell Laboratories [31], Perkin-Elmer Corporation [27] and Intel Magnetix [34] used the negative Eastman Kodak EK88 resist [40]. Resists that can be plasma developed [41] will find increasing use.

Alignment of masks and resist-covered wafers can be accomplished manually. However, the overlay accuracy and speed required of high-throughput x-ray lithography systems necessitate automatic alignment. A wide variety of schemes, cited by Nagel [10], has been considered. In most

cases, the mask-wafer combination is horizontal and remains so when it translates under an electron-impact x-ray source. Synchrotron-radiation sources and some plasma source configurations require the mask and wafer to be nonhorizontal during exposure. In such cases, additional development work is needed. A means to scan a mask-wafer combination through a synchrotron radiation beam was employed in a recent study [42]. An aligner that will work in a nearly vertical plane is being developed for use at a storage ring [43]. Alignment locks have also received attention. They hold the aligned mask and wafer together during exposure of several wafers at once [44,45]. A simple lock including magnetic and mechanical clamps has been employed at this laboratory [46].

Several full x-ray systems consisting of sources, with appropriate masks and resists, plus means for alignment, have been built. French, Japanese, and United States systems are commercially available now. Fencil and Hughes [27] have shown both prototype full-wafer and projected step-and-repeat systems.

X-ray lithography has often been reviewed. Many of the general lithographic surveys already cited [11-20] contain sections on x-ray lithography. Reviews that focus specifically on x-ray lithography are numerous [25a,27,47-60d].

III. X-RAY SOURCE REQUIREMENTS

Attention is now restricted to x-ray sources for lithography. Desirable performance characteristics for x-ray lithography, such as high resolution, are related to desirable source characteristics, such as collimation, in this section. Some of the characteristics of actual sources, including spectrum and intensity, are sketched here. Later sections give more details on the characteristics and usage of electron-impact, synchrotron-radiation, and plasma sources. The goals of this and succeeding sections are (1) to outline what is needed from a production viewpoint; (2) to examine what this demands of x-ray sources, that is, what would be the characteristics of a source ideal for x-ray lithography; and (3) to assess what is available now and expected in the foreseeable future in comparison to what would be ideal.

The demands of lithographic replication and the characteristics of x-ray sources are complex. Lithographic processes must offer three main performance features: resolution, throughput, and yield. The desired pattern has to be produced with adequately fine features and steep sidewalls, with high contrast, in a process-compatible resist. The number of levels exposed per hour, whether by full-wafer or step-and-repeat approaches, must be sufficient to meet production demands. Yield is dramatically important, so

factors such as step coverage and dust insensitivity are important. In general, the lithographic equipment must be compact, cheap, reliable, and safe.

The characteristics of x-ray sources are also numerous. High emission intensity is of paramount importance, with high efficiency of x-ray generation (and usage) also important. The spectral character (lines or continuum) must be considered. The range of emitted photon energies is critical because of its influence on absorption before and within the resist, including attainment of adequate contrast. The spectrum also determines unwanted absorption in the wafer that can produce radiation damage. Spatial characteristics include source size, important for resolution, and emission solid angle, which determines the collimation and exposure area. Temporal variation in x-ray emission is important since it influences mask and resist behavior. Steady or high-frequency pulsed sources are best since large, infrequent pulses cause undesirable thermal cycling of masks. A matrix relating the lithographically desirable performance features listed in the preceding paragraph to the x-ray source characteristics enumerated here could be constructed. It would show many interactions. For example, resolution is influenced by the source spectrum, size, and collimation, while the spectrum affects yield and equipment cost as well as resolution.

Resolution and throughput are primary but competing measures of performance for x-ray lithography systems. A detailed discussion of resolution in terms of modulation transfer functions (dependent on penumbra and mask contrast) is available [27]. A useful summary of resolution in relation to exposure time circa 1979 was given by Brewer [13] for several lithographic systems. The intrinsic resolution and exposure requirements are reciprocally related for photoresists as for photographic film. In a similar manner, the linewidth tends to be inversely related to the exposure time for lithographic systems with uncollimated x-ray sources.

Throughput (wafer levels per hour) varies inversely with $N(I_X + I_A)$, where N is the number of subfields per level (1 for full-wafer exposure) and I_X and I_A the resist exposure time and alignment time for each subfield. Resist exposure time T_X is simply related to resist, source, and system characteristics as follows:

$$A \left(\frac{\text{J}}{\text{cm}^2} \right) = E (\text{J}) \times \frac{\eta (\%) }{100} \frac{1}{\Omega (\text{sr})} \frac{4\pi (\text{sr})}{4\pi R^2 (\text{cm}^2)} \frac{T (\%) }{100}$$

where A is the resist sensitivity, typically about 0.01 J/cm^2 dependent on the volume energy deposition (joules per cubic centimeter) and resist absorption coefficient (per centimeter) [56]; E the energy provided to the source; η the production efficiency for the x-ray band of interest; Ω the solid angle into which x-rays are emitted; R the source-to-resist distance (approximately the source-to-mask distance); and T the fractional x-ray transmission of compo-

nents or gases between the source and resist. For electron-impact and synchrotron-radiation sources,

$$E = T_x (\text{sec}) \times P (\text{J/sec}),$$

where P is the source power consumption. For pulsed plasma sources,

$$E = T_x (\text{sec}) \times R (\text{shots/sec}) \times E (\text{J/shots}) = M (\text{shots}) \times E (\text{J/shot}).$$

These equations show for a given resist sensitivity \mathcal{S} , what exposure time (T_x) is required for a given source (P or RE and Ω) and system (R and T). Alternatively, they show what resist sensitivity and source intensity are required to achieve a desired exposure time.

Efficiency of radiation production (η) and usage (Ω , T , and resist absorption) are closely related to source characteristics. Synchrotron-radiation production is highly efficient. That is, most of the kinetic energy supplied to the orbiting electrons is emitted as synchrotron radiation. However, usage is poor because only a small fraction ($< 10\%$) of the overall emitted radiation is collected from present sources, the remainder being lost onto the vacuum chamber walls and components. Plasma x-ray production efficiency falls in the $10^{-1}\%$ range, while electron-impact sources are less than 0.1% efficient for the x-ray lines of interest. Collection efficiency is poor ($\sim 0.1\%$) for the uncollimated plasma and electron-impact emission. The high production efficiency values indicate part of the reason for current research interest in second-generation synchrotron- and plasma-radiation sources.

The ideal x-ray lithography source would produce radiation only in a narrow spectral band of interest. This would obviate absorption of unwanted long wavelengths in ambient gases, windows, or the mask. Mask heating is especially undesirable. Short wavelengths reduce mask contrast and deposit energy in the wafer, leading to radiation-induced changes in microcircuit performance. Materials for electron-impact and plasma sources can be chosen to place x-ray lines in the spectral region of interest. For synchrotron radiation, however, filtration and/or mirrors must be used to obtain the desired spectral band.

An optimum source would emit highly collimated radiation so that the mask-wafer separation and wafer flatness are less critical. Synchrotron radiation nicely approximates a collimated source. However, electron-impact and plasma sources must be distance collimated. The penumbral width at the wafer is $(S/R)X$, where S is the mask-wafer separation, R the source-to-mask distance, and X the x-ray source size. For typical values of $S = 30 \mu\text{m}$ and $R = 30 \text{ cm}$, X has to be on the order of 1 mm for the penumbra to be about $0.1 \mu\text{m}$. Electron-impact and plasma sources can be made with few-millimeter or smaller cross sections.

Discussion of desirable x-ray source features must give separate attention

to plasma sources because of their temporal characteristics. Electron-impact sources operate steadily, while x rays come from storage rings in small pulses at a high rate (megahertz). Plasmas, in contrast, necessarily emit bright pulses at relatively low repetition rates. Plasma sources that operate in or near the 10–100-Hz range appear favorable. They will be discussed in Section VI.

X-ray sources for lithography must be compatible with production requirements and environments. In particular, the source must mate with an aligner in such a way that clean, vibration-free operation is possible. Exposure of the wafer in an ambient gas, e.g., He, at 1 atm (rather than in a vacuum) is also most desirable.

Size and capital cost are major factors. Electron-impact sources are small (0.1-m³ head with 0.5-m³ power supply) and relatively cheap (<\$100,000). Plasma sources promise to have similarly small emission heads, with a few cubic meters being required for the energy source. They might cost about \$200,000. Storage rings now in use are designed for multiple purposes. They are tens of meters in diameter and cost several million dollars for x-ray emission above about 1 keV. Prospects for more compact and less expensive storage rings will be discussed in Section V.

The reliable, low-cost, and safe operation of x-ray sources must also be ensured. Electron-impact devices now in the early x-ray exposure systems have been operated for a few thousand hours without failure. Reliabilities and operating costs of storage ring and plasma sources are very important open questions. Radiation safety is not a problem with x-ray lithography sources. That is, x-ray shielding is readily accomplished. The same is true for optical safety in the case of plasma sources heated by high-power lasers. In all x-ray systems, electrical safety tends to be somewhat more problematic. That is, adequate attention must be paid to the possibility of high-voltage arcs. Of course, this is even more true for higher-voltage ion implanters that have been operated safely in production environments for many years.

IV. ELECTRON-IMPACT X-RAY SOURCES

An electron-impact source was used in the first x-ray lithography tests in 1971 [26]. Sources in all first-generation x-ray lithography systems also depend on x-ray production by impact of energetic electrons on solids. The fixed and rotating anode sources being employed are described briefly in this section.

Stationary-anode sources are mechanically convenient but relatively limited in their power-dissipation capabilities. That is, if the cooling water in the

anode is kept below the boiling point, power dissipation is limited to around 1 kW. Recently, a fixed-anode source in which the water boils and the bubbles are rapidly swept away was developed [61,61a] on the basis of concepts originated at Livermore [62]. The design permits operation near 6 kW in a compact source with a spot of effective size near 3 mm. This source is commercially available. Production of complex 1- μm NMOS chips by multilevel x-ray lithography with such a stationary-anode source was reported recently [63]. Twelve 75-mm wafer levels per hour can be exposed with a 17-mJ/cm² resist. Fifty wafer levels per hour are projected when a dry-developed resist is incorporated into the process [64].

Rotating-anode sources spread the incident energy over a greater area, leading to smaller temperature rises or higher power dissipation [65]. Power levels exceeding 10 kW are possible but at the price of vacuum-seal maintenance and the introduction of rotation-induced vibration. A rotating anode was employed in the prototype source used to make the first commercial chips by x-ray lithography [66].

It appears that both fixed- and rotating-anode electron-impact sources are adequately reliable (> 1000-hour operation) for the initial commercial exposure stations. Exposure times are about 1 min with practical resists. This is adequate for early submicrometer full-wafer exposures. However, the step-and-repeat x-ray systems envisioned for submicrometer production in the 1990s will require sources brighter than any expected electron-impact device [67].

V. SYNCHROTRON X-RADIATION SOURCES

The first photoresist exposures with synchrotron radiation were performed in 1975 by a United States group working at a German facility [68]. Since that time, both synchrotron and storage-ring sources of synchrotron radiation have been employed in a wide variety of tests in Japan, France, the Soviet Union, and the United States. Despite the large capital cost of synchrotron radiation sources, interest in their use for x-ray lithography is increasing steadily [69]. For example, many of the beam lines at the new BESSY synchrotron radiation source in Berlin are devoted to lithography. A short synopsis of recent advances and expectations for synchrotron radiation lithography is given in this section.

Operating microcircuits were produced with synchrotron radiation for the first time recently [42]. An electron synchrotron was used to make NMOS transistors with gate lengths as small as 1.5 μm . Exposures were made by rotating cartridges containing wafer and mask pairs through the

4 × 30-mm beam in a vacuum chamber. Threshold voltages were measured for devices made by both synchrotron x radiation and optical lithographies. No x-ray-induced shifts were observed. The exposure times (6 sec at one position for PMMA) measured in this recent Japanese study translate into fifty 125-mm wafer levels per hour for a sensitive resist exposed to x rays from a 1-GeV, 0.1-A storage ring in step-and-repeat fashion.

A major effort by IBM in x-ray lithography is under way on a beam line at the National Synchrotron Light Source (NSLS), a storage ring designed to carry 1 A at 0.7 GeV [70,70a]. Wavelengths in a band around 1 keV (12 Å) are deposited in the resists. An oscillating mirror is used to scan the strip of radiation across the wafer. Eight-minute exposures of PMMA over 25 × 50 mm are possible at 0.2 A and 0.75 GeV. A step-and-repeat system will be installed on the lithography beam line at the NSLS [43].

The synchrotron-radiation sources currently in use for lithographic research are large, multipurpose sources. Recently, the conceptual design of a tabletop storage ring was published [71]. That source, called Klein-ERNA, is a 0.57-m-diameter toroid placed entirely within the poles of a 5-T (tesla) superconducting magnet. Radiation with useful intensities up to 1–2 keV would result for 0.43-GeV electron energies. Hence, such a source would be useful for x-ray lithography. A compact storage-ring source is expected to be built first at the BESSY facility. Design studies are being made for compact storage rings within either electromagnets or superconducting magnets [71a]. Such synchrotron-radiation sources could approach the price of electron-beam direct-write exposure systems (about \$2–3 million), especially if several such rings were built. Another more distant possibility is a small synchrotron-radiation lithography source based on wigglers rather than the conventional bending magnets [72]. The utility of both wigglers and undulators as sources of synchrotron radiation for x-ray lithography was examined recently [73]. It is conceivable that future compact synchrotron-radiation sources could be oriented with a vertical orbital plane, with aligned mask-wafer combinations moving rapidly through the beam on a horizontal track. In any event, present synchrotron x-radiation lithography research is providing exciting results with significant promise.

VI. PLASMA X-RAY SOURCES

A. General Considerations

The foregoing information on x-ray lithography and alternative sources was provided to set the stage for a more detailed discussion of plasma sources. That is, x-ray lithography is competing with other lithography

methods and plasma sources are competing with electron-impact and synchrotron sources. The focus is now narrowed to hot, dense plasmas produced by either electrical discharges or laser beams. Plasmas that efficiently emit x rays are contrasted in the next paragraph with the cold, dilute plasmas used for dry processing of microelectronics. Then, the production and x-ray emission of multimillion-degree dense plasmas are outlined. Motivations for using repetitively pulsed plasma sources for x-ray lithography are discussed next. General concerns with plasma x-ray lithography, including mask life and source reliability, are also examined.

Plasmas are now a familiar part of microelectronics production. But the plasmas used for thin-film deposition, etching, and resist development are very different from those of interest here. The two classes of plasmas are contrasted in Fig. 3. Dry processing plasmas are relatively low in temperature and density. Electron temperatures of a few electron volts are typical (1 eV is equivalent to 11,600 K). Velocity distributions of the electrons and ions in such plasmas are usually not in equilibrium. That is, the ions are cold

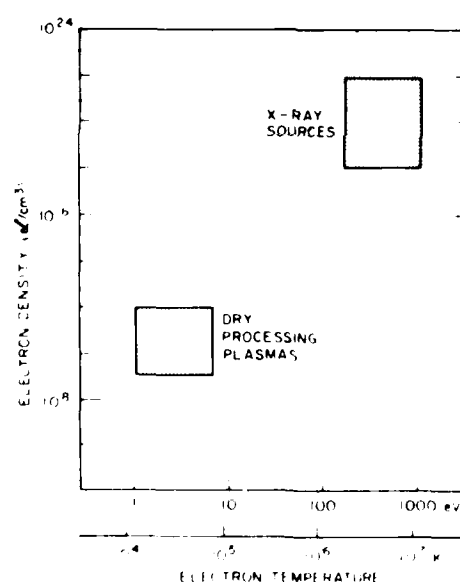


Fig. 3. Two types of plasmas are employed in current and projected microelectronics production. Electron temperatures and densities are shown for dry processing plasmas now in use and for hot, dense x-ray source plasmas that may be used in second-generation x-ray exposure stations.

compared to the electrons. Ion bombardment is critically important to processes such as sputtering and reactive-ion etching. Ion-impact energies are determined not by the thermal velocity distribution within the plasma, but rather by ion acceleration across the plasma-sheath potential created by loss of energetic electrons from plasma-edge regions. The electron density of dry processing plasmas is low due to the low pressure of the ambient gas and the relatively low degree (fraction) of ionization at low temperatures.

X-ray source plasmas have temperatures that correspond to x-ray emission energies, typically 0.1–1 keV or about 10^6 – 10^7 K. In order to emit x-ray efficiently, they must be dense as well as hot. Discharge-heated plasmas of interest for lithography have densities that range from around 10^{18} to 10^{22} e/cm³. Laser-heated plasmas have effective densities that depend inversely and quadratically on the laser wavelength. For densities greater than a critical value, the plasma no longer transmits laser light, so that efficient absorption and short wavelength reradiation occur. The commonly used Nd laser ($\lambda = 1.06 \mu\text{m}$) has a critical density of 10^{21} e/cm³. For future ultraviolet lasers with $\lambda = 0.1 \mu\text{m}$, the critical density is near 10^{23} e/cm³, a value typical of solids. Because of the high temperatures and densities in x-ray-source plasmas, the electrons and ions tend to be in equilibrium. Hence, ions expand outward with significant kinetic energies. The expanding and recombining plasma material constitutes a vapor source that can coat masks. Methods to defeat plasma and target debris are discussed later in this section.

Spectra emitted by plasmas depend on the elements present and the conditions of excitation. Each ion in source plasmas commonly has several to dozens of electrons removed due to incessant bombardment by energetic plasma electrons. This same bombardment excites electrons with appropriate binding energies to still-bound levels, after which electron decay and x-ray emission occur. The precise wavelengths emitted are sensitive to the atomic number and degree of ionization of material in the plasma [74]. High-temperature plasmas also emit continua due to Bremsstrahlung and recombination processes, but conditions can be chosen so that most of a lithographic exposure is due to lines of the desired wavelengths.

The intensities of line emission depend on the plasma and atomic characteristics as follows [75]:

$$I \left(\frac{\text{W}}{\text{cm}^2} \right) = \frac{n_e^2}{\sqrt{T_e}} \sum_{Q,N} \frac{g_N^Q}{Q} \exp \left(-\frac{\lambda_N^Q}{T_e} \right),$$

where T_e and n_e are the plasma-electron temperature and density, respectively, and g_N^Q the transition oscillator strength and λ_N^Q the x-ray energy for ionization state Q and transition N . This equation shows that while increasing the electron temperature tends to increase intensity, the electron density

is dominantly important. That is, the temperature must be sufficient to produce the ion stage that will emit wavelengths of interest. This sets lower limits on required discharge currents and laser-beam intensities. Overheating is actually deleterious since the electron level of interest will be totally ionized and the excitation-emission sequence producing the desired wavelengths will not occur efficiently. A computed plasma spectrum from a discharge-heated plasma is shown in Fig. 4 [76].

Emission times from x-ray source plasmas are usually in the 10–100-nsec range for discharge heating and the 1–10-nsec range for laser heating. These short times are dictated by the difficulty in concentrating and sustaining sufficient energy to keep the material x-ray hot in competition with cooling by radiation and ion expansion. Plasma sources are usually about 1 mm in diameter. The small sizes are due to having inadequate energy available to heat a large plasma volume to x-ray temperatures as well as to the dynamics of plasma heating. The spatial distribution of plasma x-ray emission extends over large solid angles. It is not uniform due to opacity effects but varies smoothly with angle.

X-ray sources with intensity sufficient to expose photoresists in a single shot are available. However, they are not optimum for x-ray lithography. Such sources are large and expensive due to energy storage requirements. Exposure times of 10 sec or shorter are needed for high throughput due to alignment and other wafer-handling overheads. Further, plasma sources usually have significant shot-to-shot variability. In fact, plasma sources considered to be reproducible still vary by 10% in x-ray emission from shot to shot. Hence, exposure control is problematic. Finally, mask absorption of

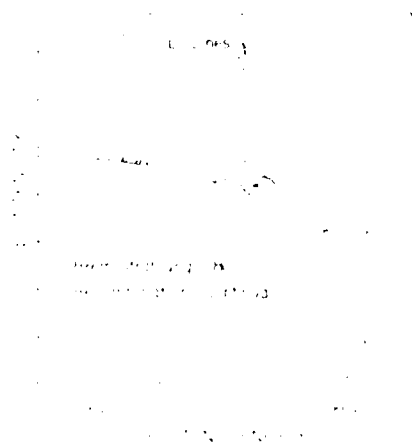


Fig. 4. Computed emission spectrum from argon heated by an electrical discharge. (From Davis *et al.* [76].)

the energy required for single-shot exposure leads to major thermal spikes in the mask temperature history [77]. A computational analysis of mask heating due to x-ray absorption is available [78]. The associated thermal cycling is expected to degrade mask quality, although there are no data on plasma-x-ray-induced mask behavior.

The problems just enumerated are all relieved by the use of repetitively pulsed (i.e., cw) plasma sources rather than large single-shot devices. Less energy per shot and smaller energy storage devices are needed. Adequately short (<10-sec) exposures should still be possible with better than 1% fluence control. And mask absorption would be less per shot so that temperature spikes would be smaller. Masks could be thermally clamped to the wafer, which would act as a heat sink, if exposures were made in even 1 Torr of ambient helium to provide a mask-to-wafer heat conduction path. That is, cw pulsed x-ray sources used with a gas in the mask-wafer area should obviate mask thermal problems. Again, however, there is no experimental information on this topic since repetitively pulsed sources are only now being developed and employed for x-ray lithography.

Thermal stresses are not the only concern for mask life with plasma x-ray sources. Debris from the plasma and nearby solids can coat or damage masks. Atomic vapor due to expansion of recombined plasma ions can produce an absorbant thin film on x-ray masks. Such vapor covers a wide solid angle for all plasma sources. Its distribution has not been measured for discharge-heated plasmas, but it is expected to cover 4π sr. In the case of laser-heated plasmas, the distribution tends to span the 2π sr in front of a solid target. Vapor deposition at angles near the target surface has been measured to be markedly less than that near the target normal [77]. Solid laser targets pose another problem, namely, production of particles of target material. The plasma that still exists near the target after the laser pulse and x-ray emission have ceased vaporizes material from even the most refractory targets. Small molten droplets are blown out in rather well defined angles as a crater is produced in the target [77,79]. This problem is largely overcome by use of thin targets (less than the crater depth, which is typically $100\text{ }\mu\text{m}$). Then little debris forms, and the debris that is produced blows out the back of the target, generally normal to the film [77]. Both plasma vapor and any residual debris from laser targets can be defeated by the use of a thin plastic sacrificial shield over the mask in a roll-to-roll configuration. Although it remains to be demonstrated, it is expected that vapor and debris will not limit the use of plasma x-ray lithography sources.

Reliability is a major concern for all lithographic sources. Electron-impact sources have already proven sufficiently reliable for prototype production exposure stations. Large, multiuse storage rings become increasingly reliable with use over a period of 1 to 2 years. However, no projections can

yet be made for the reliability of compact synchrotron-radiation sources now being designed. The situation is even more open for repetitively pulsed plasma x-ray sources. High-power pulsed-electron generators are required both to heat plasmas directly by their currents and to produce inverted populations for laser action. Ten-kHz electron-power sources are commercially available for excitation of gas lasers [80], but they have not yet been adapted to discharge heat plasma x-ray sources or to pump high-power short-wavelength lasers sufficiently energetic to produce x-ray intensities adequate for lithography. The reliability of other components of plasma x-ray sources remains to be demonstrated. Magnetically actuated high-pressure values that admit gas for discharge-heating in an x-ray source chamber must have adequate mean times between failures. Laser flash lamps (for solid-state laser rods) and electron-beam sources (for gas lasers) also require additional engineering for commercially relevant long lives. It appears that for both discharge and laser heating, production-line x-ray lithography will stress x-ray source components more than other present uses of such technology.

In summary, plasma sources do have drawbacks such as thermal cycling of masks and debris. However, such problems can be overcome so that the advantages of plasma x-ray emission can be realized. The high intensity available from plasma sources provides the main attraction. Favorable spectra, with little hard radiation, and small source sizes are also important. Plasma x-ray-source development involves two major considerations: (1) choice of the plasma composition and attainment of electron temperature that will produce wavelengths of interest and (2) attainment of a high electron density that gives intense emission. The source of high power to heat plasmas is the primary engineering consideration. Direct heating with electrical discharges and heating due to absorption of laser beams are considered in the next two subsections.

B. Discharge-Heated Plasma Sources

Many different geometrical configurations have been developed to heat and confine plasmas with electron currents. Of all, linear electrical discharges are most useful for lithography. They are simple and produce high-temperature, compact plasmas with adequate densities. The initial cool plasma is generated by electron passage through the source. The magnetic field produced by the high electrical currents (much greater than 100 kA) interacts with the current and plasma material to pinch the plasma and heat it to the 10^6 – 10^7 -K range prior to explosive expansion and dissipation. Because cylindrical coordinates (r, θ, Z) are appropriate for the

geometry of these sources, with the plasma along the Z direction, they are termed *normal type*. Such sources produce multiple-point or rodlike plasma regions with temperatures and densities sufficient for intense x-ray emission. Various types of discharge-heated plasma x-ray sources are discussed in this subsection, with emphases on those that have shown or promise utility for lithography.

The first resist exposures with discharge-heated plasmas were done with a small two-stage device [81]. The plasma was created within a few-millimeter-diameter hole through an insulator and then heated by a pulse of electrons from a nearby pointed electrode. The source was very compact and offered significant promise. However, attempts to employ later models of this device have not resulted in reliable operation.

Most types of Z-pinch source geometries are shown in schematic cross sections in Fig. 5 [10]. Sources with somewhat similar geometries are arranged in rows, while the columns distinguish the different ways in which the plasma is generated. In the left column, the plasma is formed from solid materials placed between the electrodes. Next are sources in which a low-pressure ambient gas present well before the discharge is ionized and pinched. The third column involves sources in which a gas is admitted ("puffed") into the interelectrode vacuum immediately prior to the discharge. Sources that consume their electrodes to produce the plasma are presented in the fourth column. Low repetition rates and irreproducibility rule out sources in the first and last columns, respectively, for x-ray lithography. Puff devices that are most developed as lithography sources are discussed next. Then features and potential advantages of gas-filled plasma focus and hypocycloidal pinch sources are examined. When used for lithography, mesh or hollow anodes are usually employed in Z-pinch sources in order to permit near-axial x-ray egress from the source region and to reduce debris generation from electrode vaporization. Solid electrodes are shown in the schematics of Fig. 5.

Puff sources are attractive for lithography because they are bright, are relatively reproducible, and offer the possibility of repetitive-pulse operation. Single-shot puff sources of widely different sizes were developed during the late 1970s. Giant, near-megajoule, near-terawatt pulsed-power sources were used to drive puff loads [82]. Also, much smaller 10-kJ capacitor banks were employed with similar heads [83]. Only the latter are of interest for x-ray lithography, and attention will be limited to them.

Early x-ray measurements from small puff systems showed them to have emission characteristics useful for x-ray lithography. Pinhole photographs [83,84] revealed millimeter-size source cross sections. Spectral measurements showed that various wavelengths of interest could be generated by use of different inert gases [84]. Photoresist exposures were demonstrated by two

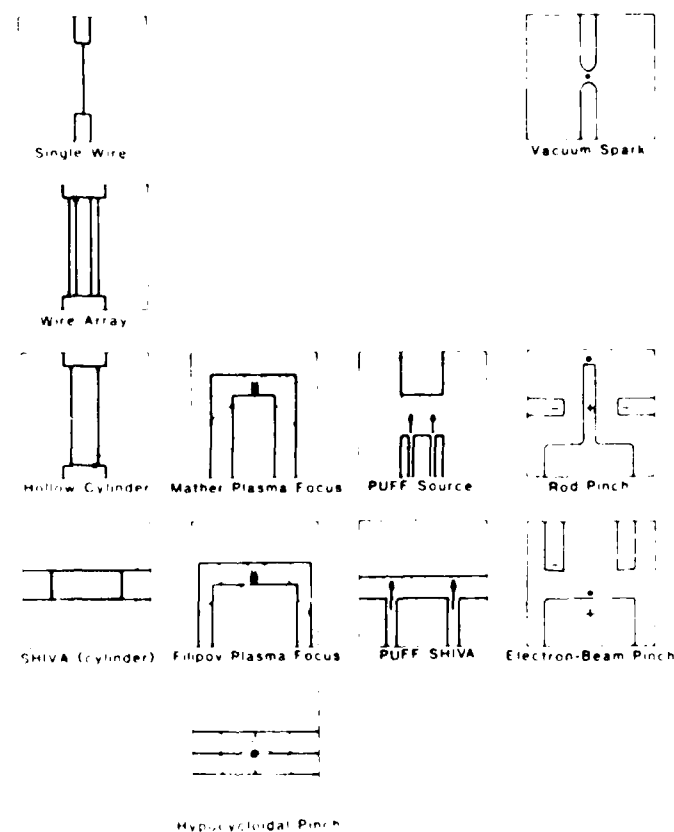


Fig. 5. Schematics of axial cross sections for various electrical-discharge-heated dense plasmas. Unique polarities are indicated. Current flow at two different times is shown by dotted lines in sources initially filled with low-pressure gas. Flow of gas prior to the discharge is shown by arrows for "puff" devices. See the text for discussion. (From Nagel [10].)

companies, Physics International and Maxwell Laboratories, through the use of small puff sources [85–88]. About three dozen shots were required to expose intermediate-sensitivity resists in these initial measurements. Figure 6 is a micrograph of a resist pattern produced with a puff source [89].

The same two companies that did the early lithographic work with experimental puff sources now sell models subsequently engineered for routine use. Depending on the working gas, x-ray photon energies in and near the 0.3–3-keV ranges are available from plasmas 1 mm in diameter. Approximately 10–100-J pulses of x rays are produced per shot in the x-ray lines of interest. The puff sources now on the market can fire only once



Fig. 6. Scanning electron micrograph of $0.25\text{ }\mu\text{m}$ lines and $1\text{-}\mu\text{m}$ spaces produced at 20 cm in DC OPA trilayer resist with x-rays from 35 kV pull plasma discharge. (From Pearlman and Riordan [89].)

about every 10 sec. Their ultimate commercial impact will hinge on the development of power supplies and valves for reliable multi-hertz operation.

Plasma x-ray sources that are filled with gas well ahead of the discharge also have potential for x-ray lithography. The ambient gas can impede flow of debris from the plasma region to the mask and also provide thermal coupling of the mask and wafer. Dense plasma focus machines have long been studied as sources of x-rays [90]. Recently, such a device was used to produce $1\text{-}\mu\text{m}$ lines in FBM resist [91]. The hypocycloidal pinch in essentially two plasma focus devices back to back [92]. In it, the x-ray-emitting focus occurs away from the electrode surfaces; this tends to reduce debris production compared to the usual dense plasma focus configurations. The

shot-to-shot reproducibility of gas-filled Z-pinch plasma x-ray sources is still in question. Also, like puff sources, the plasma focus and hypocycloidal pinch have not yet been engineered for cw operation. These sources would require high-average-power electrical systems similar to puff devices, but gas valving is simpler for the sources that are initially gas filled.

One way in which a discharge-heated plasma source could be mated to a wafer aligner is shown in Fig. 7 [87]. The box, approximately 1 m³, would contain the electrical storage and pulse-forming components and the vacuum chamber for the source. X-ray passage through a thin window at the bottom of the box into a He-filled column is envisioned. The concept in Fig. 7, though developed for a puff source, could also be employed for plasma focus and hypocycloidal pinch sources.

C. Laser-Heated Plasma Sources

X-ray sources produced and heated by laser pulses are not as advanced toward commercialization as discharge-heated plasma sources. However, they show significant promise and are being developed and studied intensively. Work to date and current directions are discussed in this subsection. The manner in which plasmas transmute long-wavelength laser radiation into short-wavelength x radiation is sketched first for both solid and gas targets. Then the various types of high-power lasers germane to x-ray-source

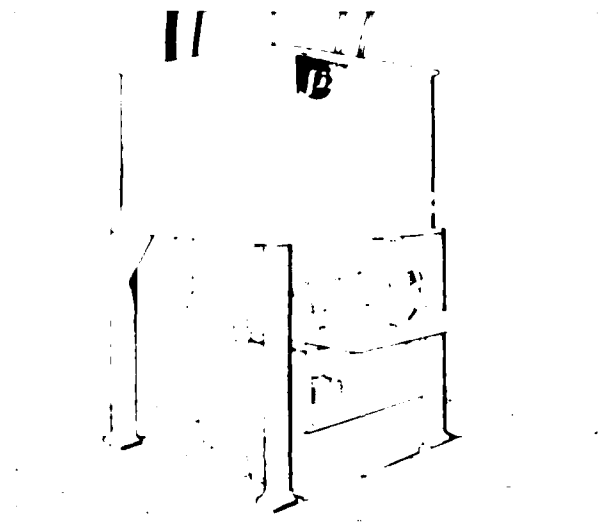


Fig. 7. Schematic of a discharge plasma x-ray source integrated with a mask-wafer aligner (From Matthews and Cooper [87].)

production are listed. Most work to date has been done with Nd solid-state laser systems, so results obtained with them constitute the bulk of the discussion. The potential of excimer gas lasers is outlined. Finally, possible configurations for production-line laser-plasma x-ray lithography exposure stations are considered.

When a high-power laser pulse encounters a solid target in a vacuum, its leading edge produces a plasma at the target surface. The electron density varies from its value in a solid ($\sim 10^{23}$ e/cm³) to less than 10^{19} e/cm³ over about 1 mm from the target. Laser light is little absorbed in the low-density plasma until it reaches the critical density, beyond which the plasma is opaque. Laser energy arriving at the critical region is primarily absorbed, although some scattering also occurs. The plasma electrons heated by photon absorption cause ionization and excitation of target material streaming outward through the dense and hot critical absorption region. This behavior is little modified by the presence of a low-pressure ambient gas in the target region so long as the gas breakdown threshold is not exceeded. That is, a laser-heated plasma x-ray source will operate in a few-Torr ambient of He, which provides debris suppression and mask cooling [93]. High-pressure gas jets can also be used as laser targets [94]. It was shown that escape of 2000-psi gas through a 0.1 mm orifice into a vacuum produced a convenient soft x-ray source when irradiated axially with a high-power laser. Such a source used in a pulsed mode might provide soft x-rays with relatively little debris if a reliable valve is developed. Gas-target laser plasma sources have not been used for x-ray lithography.

Both solid and gas laser systems are relevant to present x-ray lithography research and development. In general, solid-state lasers tend to be less attractive than gas systems because of cooling requirements. This limits the average laser power and hence the average x-ray power. However, extensive work has gone into high-power solid-state lasers, especially those based on lasing in Nd at 1.06 μ m. Applications range from laser fusion to pumping of tunable dye lasers. The availability of Nd systems has led to their almost exclusive use in early laser plasma x-ray lithography work. The CO₂ gas laser at 10.6 μ m is also well developed, but the wavelength is so long that the low critical density gives poor x-ray production efficiencies. At 10^{14} W/cm², CO₂ lasers produce about 20 times less x-ray intensity near 1 keV than do Nd lasers. Excimer lasers are attractive because they are gas systems and have wavelengths in the 0.15–0.35- μ m range, which should produce x-rays efficiently. X-ray lithography work with excimer-laser plasmas is expected in the near future. Beam divergence and focusability of excimer lasers are major questions. If focal spots less than 0.1 mm in diameter cannot be obtained, then the short wavelengths of excimer lasers cannot be utilized for efficient x-ray production.

The wavelengths and intensity of x-ray emission from laser-heated

plasmas depend on both laser and target parameters. Variations with pulse length, beam quality (focusability), and target composition have been summarized for Nd lasers [95,96]. In short, pulse lengths in or near the 1–10-nsec range with 1–10 J or more that can be focused to less than 10^{-4} cm² are required. That is, irradiances on target in the 10^{13} – 10^{15} W/cm² range are needed to achieve plasma temperatures in the 0.1–1-keV range, which are best for emitting wavelengths of use for x-ray lithography. The efficiency of useful x-ray production is strongly dependent on the target composition. Optimum emission results when the plasma electron energy distribution and plasma ion-binding energies are properly matched. Conversion efficiencies of 10% into 2π sr for 1-keV lines have been demonstrated. That is, 10% of the incident laser energy can be emitted by the plasma as soft x-rays.

Exploration of laser-plasma x-ray lithography has been pursued in parallel programs at the Battelle Columbus Laboratories and the Naval Research Laboratory during the past 5 years. In both places, work began with relatively large low-repetition-rate (10^{-3} -Hz) Nd-glass systems capable of emitting up to about 100 J in pulses near 10 nsec in length [97,98]. Single-shot exposures of an intermediate-sensitivity resist (COP) at 10 cm were demonstrated [97].

The third harmonic ($\lambda = 0.35 \mu\text{m}$) of a Nd laser was employed recently to replicate fine scale patterns [99]. Single 1-nsec, 35 J pulses were adequate to produce plasmas that emitted sufficient x-rays to expose PBS at 10 cm. A pattern in the resist with $0.5\text{-}\mu\text{m}$ lines is shown in Fig. 8. The PBS required less exposure with 1-nsec pulses of x rays compared to steady exposures. This sensitization may be due to heating of the resist by x-ray deposition.

The need for repetitively pulsed laser-plasma sources for x-ray lithography is clear. Current Nd systems that produce 10 J or more can only be fired at rates of about 10^{-2} Hz or less. For 10% conversion and a source-to-wafer distance of 30 cm, only about 0.1 mJ/cm²/shot is available. Hence, more than 10 shots are needed and even with full-wafer exposures, throughputs of only a few levels per hour would result.

The initial lithographic work with a high-repetition-rate laser system was recently completed [93]. A 10-Hz ILS Nd:YAG system that produced up to 0.8 J in 25-nsec pulses was used to irradiate targets across the periodic table (C–U). Spectral, spatial, and temporal source characterization measurements were performed. X-ray wavelengths as short as 13 Å were observed, and COP resist was exposed through a $2\text{-}\mu\text{m}$ polyimide mask membrane for 20 min at 10 Hz with Fe radiation at 7 cm from the source. For the irradiance achieved in this work, the conversion efficiency into kilo-electron-volt x rays is only about 10^{-5} [100]. Measurement of the spectrum transmitted by $2 \mu\text{m}$ of polyimide showed that the resist was exposed with photons in the 100–284-eV range.

A 10-Hz Nd laser capable of producing harmonics at 0.53 and $0.35 \mu\text{m}$



Fig. 8. Scanning electron micrograph of the replica of a $0.45\text{-}\mu\text{m}$ transmission grating in PBS resist exposed with x rays from a single laser-heated plasma. (A $10\text{-}\mu\text{m}$ -long scale is shown.) (From Yaakobi *et al.* [99].)

was employed recently to produce X-UV-emitting plasmas [101]. The beam divergence of the system used did not permit tight focusing. Hence, relatively low plasma temperatures and long wavelength ($< 400\text{-eV}$) emission resulted. Small beam divergence as well as high peak and average powers are needed for x-ray production with lasers. Presently available, high-repetition-rate commercial Nd lasers are insufficient for practical x-ray lithography.

The Nd lasers used to date for x-ray lithography have been produced for other purposes. In most of them, the pulse makes only a single pass through the amplifiers, so that efficient energy extraction is not achieved. Only now are laser systems being designed and built with the aim of producing x-ray-emitting plasmas. In about a year, 10-Hz Nd systems that produce 10 J per 25-nsec pulse (100 W average power) should be available in the laboratory [102]. These will contain slab laser amplifiers rather than cylindrical rods. Multiple-bounce paths through the slab between the parallel walls should give improved energy extraction. If adequate beam quality is achieved, irradiances near 10^{14} W/cm^2 will result. Then useful average x-ray

powers of 10 W would be available. Exposure of a resist requiring 10 mJ/cm^2 at 30 cm would require only 10 sec with such a laser. This system could be employed in a prototype laser-plasma x-ray exposure station. As with repetitively pulsed, discharge-heated plasma sources, reliability over hundreds of hours is a primary question.

Excimer lasers are promising as drivers for production of x-ray-emitting plasmas. Their short wavelengths ($0.15\text{--}0.35 \mu\text{m}$) are efficiently absorbed in target plasmas, and the associated high critical electron densities favor intense x-ray emission. Furthermore, gas excimer lasers might allow higher repetition rates and average powers than do solid-state lasers. Commercially available KrF excimer lasers ($\lambda = 2485 \text{ \AA}$) currently produce energies of about $0.5\text{--}1 \text{ J}$ in 15-nsec pulses at rates of $10\text{--}20 \text{ Hz}$ (average powers up to 20 W). An excimer system that yields 1 J per pulse at 100 Hz (100 W average power) has been marketed recently. Measurements of X-ray spectra and intensities from plasmas heated by excimer lasers are needed. If such lasers give promising results, engineering of higher-average-power excimer systems specifically for x-ray production will be indicated.

The work with 10-Hz lasers to date has involved the use of solid-cylindrical targets that move to place fresh material at the focus prior to each shot. Such a source would not be practical in a commercial system. Several possible automatic target changers have been discussed. One of them is shown schematically in Fig. 9. A coating of $5 \mu\text{m}$ of target material on $5\text{-}\mu\text{m}$ -thick Mylar would produce the same x-ray intensity as a thick target but with much less debris. Proper rotation and translation would lead to efficient usage of the target foil.

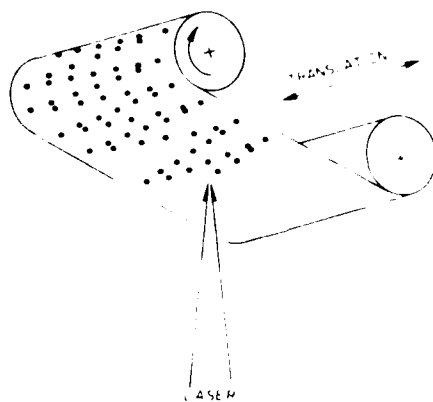


Fig. 9. Schematic of a roll-to-roll metal-coated plastic laser-target x-ray source. Sideways translation with a mechanism not shown distributes the laser shots. Actual shot density would be much greater than indicated.

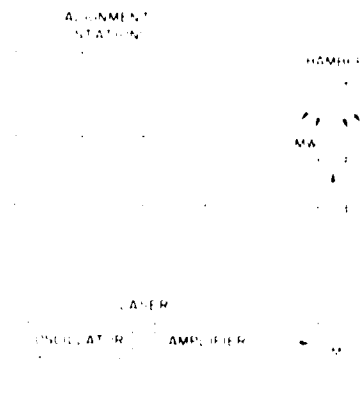


Fig. 10. Elevation-view schematic of a laser and exposure facility for replication of multiple mask-wafer (MW) combinations aligned and locked together at nearby stations prior to transfer into the exposure chamber. The laser pulse, turned by mirror M, is focused by lens L onto target T in a chamber evacuated by pump P. (From Nagel *et al.* [45].)

There are at least two approaches to integration of a laser-plasma x-ray source with wafer-handling equipment. The more conventional is to use standard horizontal alignment hardware and translate the mask-wafer combination under the x-ray source [27]. Another approach is shown schematically in Fig. 10. In this case, masks and wafers would be aligned and locked together with devices discussed in Section II. They would then be placed in the laser-plasma exposure chamber. Several alignment locks could be exposed simultaneously to take advantage of the unique small, nearly equiaxed nature of laser-heated plasma sources. Of course, debris shields and emission uniformity are among the concerns for this approach.

VII. CONCLUSION

In the past decade, x-ray lithography has moved from a laboratory demonstration to the production line use of prototype equipment. It is difficult to estimate the costs but over \$30 million may have been spent on x-ray lithography research and development during that period. A brief history and upbeat projection for x-ray lithography are shown in Fig. 11 [27]. Problems with x-ray lithography have been assessed and are being overcome. For example, early concerns that lithographically produced radiation damage would severely limit the use of x-ray exposures were shown to be important but not fatal [103]. The many advantages of x-ray

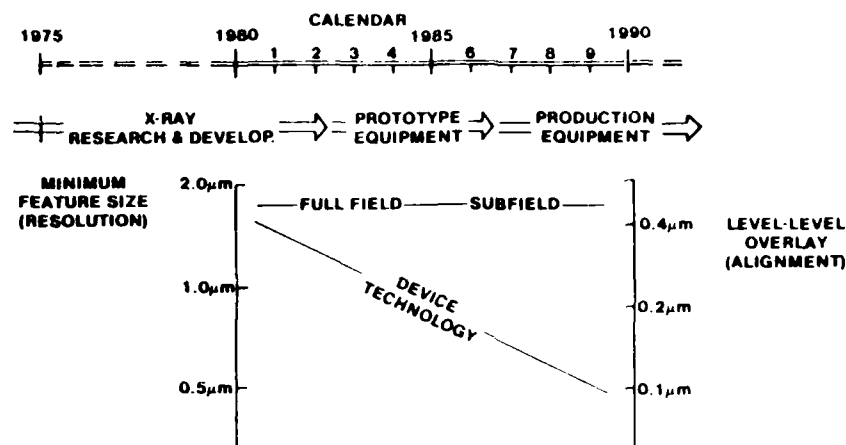


Fig. 11. History and projected development of x-ray lithography in both full-wafer and step-and-repeat modes. (From Fencil and Hughes [27].)

lithography (especially resolution, throughput, and yield) bode well for its future.

Electron-impact sources will probably be subject to little further engineering development. They are now being used to produce 1-Mbit bubble memory devices with 1.2- μm minimum feature size at Intel Magnetics [66]. That company recently announced a new commercial 4-Mbit bubble memory chip with 0.75- μm features [104]. Full-wafer exposures are providing valuable experience in the commercial use of x-ray lithography. Adequate intensity for submicrometer step-and-repeat schemes remains a major concern with electron-impact sources.

Synchrotron radiation sources for x-ray lithography are being intensively studied now. Large multipurpose storage rings are employed to demonstrate capabilities, while compact special-purpose rings are being designed for lithography. Operating microcircuits but not commercial devices have been made with synchrotron x radiation. System costs and long-term performance are areas of concern for x-ray lithography with synchrotron x-ray lithography.

Two types of low-repetition-rate discharge-heated plasma sources (the puff and dense plasma focus devices) and both low- (10^{-3} -Hz) and medium- (10-Hz) rate Nd laser plasma sources have been used for resist exposure demonstrations. Microelectronic devices have yet to be produced with plasma x-ray sources. A great deal of source engineering remains for both discharge and laser sources. Efficiency, repetitive pulsing, and reliability are major concerns for discharge sources. Adequate beam energy and quality, as

well as reliability, are among the development challenges for laser-plasma sources.

There are foreign as well as United States programs in x-ray lithography with electron-impact and synchrotron sources. Curiously, work on lithography with x rays from plasmas seems to be confined to the United States. In a decade, it should be clear which of the various plasma sources is commercially viable. The situation may be similar to that for the internal combustion engine for which from among a plethora of designs (reciprocating versus rotary, gasoline versus diesel, etc.), several alternative types have found niches in the marketplace.

APPENDIX. X-RAY SOURCE CHARACTERIZATION

It is necessary to measure the spectral output, source size, and spatial distribution as well as the time variation of x-ray sources for lithography for two purposes:

- (1) the specification of x-ray sources and exposure stations and
- (2) the monitoring of source output.

Both vendors and users of x-ray lithography equipment will need hardware and techniques (possibly standards) to set specifications and check actual output at procurement. And during routine processing, users of x-ray sources will have to monitor source output to ensure adequate performance. Approaches to measuring the various source characteristics for these reasons are outlined in this appendix. In general, the techniques apply to electron-impact and synchrotron radiation as well as plasma sources.

Spectra of electron impact [106] and synchrotron radiation [107] sources can be calculated with useful accuracy, but it is still necessary to measure their output because of time-dependent window or mirror contamination and other possible malperformance (e.g., current loss from the focal spot or shift in the electron orbit). Scanning flat-crystal spectrometers are useful for both impact and orbiting electron sources [108]. Plasma-source spectra are not predictable quantitatively. For a rapidly pulsed cw plasma source, a scanning spectrometer can be used, but in general, a convex curved-crystal spectrograph that records a wide range of wavelengths simultaneously on photographic film must be used [109].

The spectrometers and spectrographs employed for source characterization are suitable for bench testing of x-ray sources during development or prior to installation in exposure stations. That is, they are too bulky to check spectra with the source in an aligner system. Figure 12 shows how a compact

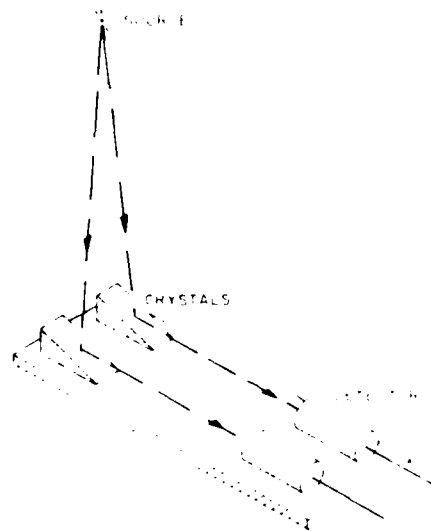


Fig. 12. Schematic concept for a low-profile spectral intensity monitor for insertion in aligners to determine x-ray intensity at two wavelengths. (From Nagel and Whitlock [110].)

spectral monitor could be made for use in an exposure station [110]. By appropriate choice of crystal (see, for example, Gilfrich *et al.* [111]) or multilayer (see, for example, Barbee [112]) dispersion elements, wavelengths of interest will be diffracted at 90° into the detectors. Such a device could be inserted periodically to test the absolute output of a production source at two wavelengths.

Determination of x-ray source sizes is best done with simple, cheap pinhole cameras. In situ monitoring of source size can be accomplished easily if provision is made to swing the pinhole into the exposure column, say, one-quarter of the way from the source to the wafer position. Then a $3\times$ -magnified image of the source will result. Recording could be done quickly with a sensitive photographic film in a light-tight cassette with a thin, x-ray-transmissive window. Removal of the pinhole and use of an insensitive film [113] or dyed plastic [114] would permit determination of the x-ray source uniformity. Both film [115] and plastic dosimeter materials [116] can be calibrated for quantitative dose determination.

The time variation of x-ray emission is of interest for two reasons. With plasma sources, the submicrosecond intensity variation is a sensitive indicator of source performance. For all sources, long-term intensity degradation must be assessed. Many simple, broad-band detectors are available for pulse-shape and drift determinations. Silicon $p-i-n$ diodes have response

times as short as 1 nsec. Simple scintillator-fiberoptic-photodetector systems should be useful monitors.

Development, testing, and calibration of source characterization tools for x-ray lithography largely remain for the future. Plasma diagnostics instrumentation is useful but inadequate. It is expected that x-ray sensors tailored to lithographic needs will be commercially available in several years.

ACKNOWLEDGMENTS

Continued collaboration and helpful discussions with M. C. Peckerar are enjoyed. His comments and those of D. M. Brown on the manuscript are appreciated. Recent collaborations with C. M. Brown on lithography with x rays from plasmas heated by repetitively pulsed lasers, with C. L. Marquardt and R. L. Williams on the dependence of X-UV emission on laser wavelength, and with R. R. Whitlock on characterization of x-ray lithography sources have also been pleasant and productive. Useful conversations with or receipt of information from R. L. Byer, J. Davis, R. Dukhart, C. Feneil, C. Gilman, R. M. McIntosh, J. Pearlman, E. J. Petersen, J. P. Silverman, G. Wakalopoulos, and B. Yaakobi are greatly appreciated. E. C. Cox and B. Throckmorton are thanked for expert typing.

REFERENCES

1. "Microstructure Science, Engineering and Technology," National Academy of Sciences, Washington, D.C., 1979.
2. *Proc. NSF Workshop Oppor. Microstructure Sci. Eng. Tech.*, November 1978, 19-22, Airlie, Virginia, National Science Foundation, Washington, D.C.
3. F. D. Wolf and J. M. Ballantyne, in "VLSI Electronics: Microstructure Science" (N. G. Einspruch, ed.), Vol. 1, pp. 129-183, Academic Press, New York, 1981.
4. F. W. Voltmer, in "VLSI Electronics: Microstructure Science" (N. G. Einspruch, ed.), Vol. 1, pp. 1-40, Academic Press, New York, 1981.
5. A. Reisman, *Proc. Inst. Electr. Eng.* **71**, 550 (1983).
6. J. B. Angel, S. C. Terry, and P. W. Barth, *Sci. Am.* **248**, 44 (1983).
7. H. I. Smith, in "Low Energy X-Ray Diagnostics—1981" (D. T. Attwood and B. L. Henke, eds.), p. 223, Am. Inst. Phys., New York, 1981.
8. N. M. Ceglio, in "Low Energy X-Ray Diagnostics—1981" (D. T. Attwood and B. L. Henke, eds.), p. 210, Am. Inst. Phys., New York, 1981.
9. B. L. Grammura and G. A. Rozgonyi, in "Molecular Electronic Devices" (E. L. Carter, ed.), Marcel Dekker, New York, 1984 [in press].
10. D. J. Nagel, in "Ultraviolet and Vacuum Ultraviolet Systems" (W. R. Hunter, ed.), *Proc. Soc. Photo Opt. Instrum. Eng.* **279**, 98 (1981).
11. H. I. Smith, *Proc. IEEE* **62**, 1361 (1974).
12. A. Broers, *Phys. Today* **32**, 38-45 (1979).
13. G. R. Brewer, in "Electron Beam Technology in Microelectronic Fabrication" (G. R. Brewster, ed.), pp. 1-58, Academic Press, New York, 1980.
14. R. Newman (ed.), "Fine Line Lithography," North-Holland Publ., Amsterdam, 1980.

15. M. J. Bowden, *J. Electrochem. Soc.* **128**, 195C-214C (1981).
16. R. K. Watts and J. H. Bruning, *Solid State Technol.* **24**(5), 99-105 (1981).
17. M. P. Iepselter and W. T. Lynch, in "VLSI Electronics: Microstructure Science" (N. G. Einspruch, ed.), Vol. 1, pp. 83-127, Academic Press, New York, 1981.
18. R. K. Watts, in "Very Large Scale Integration" (D. F. Barbe, ed.), pp. 42-88, 295, Springer-Verlag, Berlin, 1982.
19. D. A. McGillis, in "VLSI Technology" (S. M. Sze, ed.), p. 267, McGraw-Hill, New York, 1983.
20. N. P. Economu, *Proc. IEEE* **71**, 601 (1983).
21. E. L. Petersen, *IEEE Trans. Nucl. Sci.* **NS-30**, 1638 (1983).
22. J. R. Monkowski, *Solid State Technol.* **24**, 44 (1981).
23. P. K. Chatterjee, *Proc. 1980 IEEE Int. Symp. Circuits Systems*, Vol. 1, p. 253.
24. R. W. Keyes, *Science* **195**, 1230 (1977).
- 24a. J. P. Lazzari and P. Parrens, in "Electron-Beam, X-Ray, and Ion-Beam Techniques for Submicron Lithographies II" (P. D. Blais, ed.), *Proc. Soc. Photo-Opt. Instrum. Eng.* **393**, 213 (1983).
25. D. J. Nagel, *Am. J. Acad. Sci.* **342**, 235 (1980).
- 25a. A. Heuberger and H. Betz, in "Electron-Beam, X-Ray, and Ion-Beam Techniques for Submicron Lithography II" (P. D. Blais, ed.), *Proc. Soc. Photo-Opt. Instrum. Eng.* **393**, 221 (1983).
26. D. L. Spears and H. I. Smith, *Electron. Lett.* **8**, 102 (1972).
27. C. R. Fencil and G. P. Hughes, in "Submicron Lithography" (P. D. Blais, ed.), *Proc. Soc. Photo-Opt. Instrum. Eng.* **333**, 100 (1982).
28. B. J. Lin and T. H. P. Chang, *J. Vac. Sci. Technol.* **16**, 1669 (1979).
29. J. P. Reeksten and J. H. McCoy, *Solid State Technol.* **24**(8), 68 (1981).
30. L. R. Hughey, R. T. Williams, J. C. Rife, D. J. Nagel, and M. C. Peckerar, *Nucl. Instrum. Methods* **195**, 267 (1982).
31. H. J. Levinstein, *Proc. Tutorial Symp. Semiconductor Technol. Electrochem. Soc.* **82**, 5 (1982).
32. D. Maydan, G. A. Coquin, H. J. Levinstein, A. K. Sinha, and D. N. K. Wang, *J. Vac. Sci. Technol.* **16**, 1959 (1979).
33. D. I. Brors, in "Submicron Lithography" (P. D. Blais, ed.), *Proc. Soc. Photo-Opt. Instrum. Eng.* **333**, 111 (1982).
34. B. R. Triplett and R. F. Hollman, *Proc. IEEE* **71**, 585 (1983).
35. G. N. Taylor, G. A. Coquin, and S. Somekh, *Polym. Eng. Sci.* **17**, 420-429 (1977).
36. M. J. Bowden, *Crit. Rev. Solid State Mat. Sci.* **8**, 223 (1979).
37. M. Hatzakis, *Proc. IEEE* **71**, 570 (1983).
38. J. M. Moran and G. N. Taylor, *J. Vac. Sci. Technol.* **16**, 2014 (1979).
39. J. M. Moran and G. N. Taylor, *J. Vac. Sci. Technol.* **16**, 2020 (1979).
40. Z. C. H. Tan, C. C. Petropoulos, and F. J. Ranner, *J. Vac. Sci. Technol.* **19**, 1348 (1981).
41. G. N. Taylor, I. M. Wolf, and J. M. Moran, *J. Vac. Sci. Technol.* **19**, 872 (1981).
42. T. Kimura, K. Mochizuki, N. Tsumita, H. Obayashi, A. Mikami, and H. Kanzaki, in "Electron-Beam, X-Ray, and Ion-Beam Techniques for Submicron Lithographies II" (P. D. Blais, ed.), *Proc. Soc. Photo-Opt. Instrum. Eng.* **393**, 2 (1983).
43. J. P. Silverman, IBM, Yorktown Heights, New York, private communication (1983).
44. G. A. Wardly, R. Feder, D. Hofer, E. F. Castellani, R. Scott, and J. Topalian, *Circuits Manufacturing*, p. 30 (January 1978).
45. D. J. Nagel, J. M. McMahon, R. R. Whitlock, J. R. Greig, R. F. Pechacek, and M. C. Peckerar, *Jpn. J. Phys. Suppl.* **17-2**, 472 (1978).
46. D. J. Nagel and D. Ma, Naval Res. Lab., Washington, D.C., unpublished (1983).

47. D. I. Spears and H. I. Smith, *Solid State Technol.* **15**, 21 (1972).
48. H. I. Smith, D. I. Spears, and S. E. Bernacki, *J. Vac. Sci. Technol.* **10**, 913 (1973).
49. D. Maydan, G. A. Coquin, J. R. Maldonado, S. Somekh, D. Y. Lou, and G. N. Taylor, *IEEE Trans. Electron Devices* **ED-22**, 429 (1975).
50. J. S. Greeneich, *IEEE Trans. Electron Devices* **ED-22**, 434 (1975).
51. E. Spiller, R. Feder, J. Topalian, E. E. Castellani, I. Romankiw, and A. Heritage, *Solid State Technol.* **19**, 62 (1976).
52. J. H. McCoy, *Circuits Manufacturing*, pp. 35-44 (November 1977).
53. H. I. Smith, in "Surface Wave Filters" (H. Matthews, ed.), pp. 165-217, Wiley, New York, 1977.
54. R. Feder, E. Spiller, and J. Topalian, *Polym. Eng. Sci.* **17**, 385 (1977).
55. G. P. Hughes, *Solid State Technol.* **20**, 39 (1977).
56. E. Spiller and R. Feder, in "Topics in Applied Physics: X-Ray Optics" (H. J. Queisser, ed.), p. 35, Springer-Verlag, Berlin, 1977.
57. G. P. Hughes and R. C. Fink, *Electronics* **51**, 99-106 (1978).
58. G. A. Wardly, R. Feder, D. Hofer, E. E. Castellani, R. Scott, and J. Topalian, *Circuits Manufacturing*, pp. 30-40 (January 1978).
59. R. K. Watts, *Solid State Technol.* **22**(5), 68 (1979).
60. R. K. Watts and J. R. Maldonado, in "VLSI Electronics: Microstructure Science" (N. G. Einspruch, ed.), Vol. 4, p. 55, Academic Press, New York, 1982.
- 60a. A. R. Heureuther, in "Synchrotron Radiation Research" (H. Winick and S. Dourach, eds.), Chapter 7, Academic Press, New York (1982).
- 60b. C. R. Fencie and G. P. Hughes, in "Electron-Beam, X-Ray, and Ion-Beam Techniques for Submicron Lithography II" (P. D. Blais, ed.), *Proc. Soc. Photo-Opt. Instrum. Eng.* **393**, 87 (1983).
- 60c. A. P. Neukermans, in "Electron-Beam, X-Ray, and Ion-Beam Techniques for Submicron Lithography II" (P. D. Blais, ed.), *Proc. Soc. Photo-Opt. Instrum. Eng.* **393**, 93 (1983).
- 60d. W. I. Novak, in "Electron-Beam, X-Ray, and Ion-Beam Techniques for Submicron Lithography II" (P. D. Blais, ed.), *Proc. Soc. Photo-Opt. Instrum. Eng.* **393**, 106 (1983).
61. J. R. Maldonado, M. E. Poulsen, I. F. Saunders, E. Vratny, and Z. Zacharias, *J. Vac. Sci. Technol.* **16**, 1942 (1979).
- 61a. B. Teslie, A. Neukermans, I. Simon, and J. Foster, *J. Vac. Sci. Technol.* **B1**, 1251 (1983).
62. J. I. Gaines and R. A. Hansen, *Nucl. Instrum. Methods* **102**, 7 (1972).
63. M. P. Uepselter, D. S. Alles, H. J. Levinstein, G. I. Smith, and H. A. Watson, *Proc. IEEE* **71**, 640 (1983).
64. I. N. Fuls, in "Submicron Lithography" (P. D. Blais, ed.), *Proc. Soc. Photo-Opt. Instrum. Eng.* **333**, 113 (1982).
65. M. Yoshimatsu and S. Kozaki, in "Topics in Applied Physics: X-Ray Optics" (H. J. Queisser, ed.), pp. 9-33, Springer-Verlag, Berlin, 1977.
66. B. B. Triplett and S. Jones, in "Submicron Lithography" (P. D. Blais, ed.), *Proc. Soc. Photo-Opt. Instrum. Eng.* **333**, 118 (1982).
67. N. P. Economu and D. C. Elanders, *J. Vac. Sci. Technol.* **19**, 868 (1981).
68. E. Spiller, D. E. Eastman, R. Feder, W. D. Grobman, W. Gudat, and J. Topalian, *J. Appl. Phys.* **47**, 15450 (1976).
69. W. Grobman, in "Handbook on Synchrotron Radiation" (E. E. Koch, D. E. Eastman, and Y. Tarte, eds.), Vol. 1, North-Holland Publ., Amsterdam, 1983.
70. J. P. Silverman, R. D. Haelbich, W. D. Grobman, and J. M. Warlarmon, in "Electron-Beam, X-Ray, and Ion-Beam Techniques for Submicron Lithography II" (P. D. Blais, ed.), *Proc. Soc. Photo-Opt. Instrum. Eng.* **393**, 99 (1983).

- 70a. R. P. Haelbig, J. P. Silverman, W. D. Grobman, J. R. Maldonado, and J. M. Warlaumont, *J. Vac. Sci. Technol.* **B1**, 1262 (1983).
71. U. Trinks, F. Nolden, and A. Jahnke, *Nucl. Instrum. Methods* **200**, 475 (1982).
- 71a. W. G. Grobman, *J. Vac. Sci. Technol.* **B1**, 1257 (1983).
72. H. Wmick and A. Bienenstock, *Phys. Today* **36**, 49, (1983).
73. A. R. Neureuther, K. J. Kim, A. C. Thompson, and E. Hoyer, to be published.
74. R. L. Kelly and I. J. Palumbo, Naval Res. Lab. Rep. 7599, Washington, D.C. (1973).
75. D. Mosher, *Phys. Rev.* **A10**, 2330 (1974).
76. J. Davis, R. Clark, and P. Kepple, Naval Res. Lab., Washington, D.C., unpublished (1983).
77. M. C. Peckerar, J. R. Greg, D. J. Nagel, R. F. Pechacek, and R. R. Whitlock, *Proc. 153rd Meet. Electrochem. Soc., Seattle, Washington* (May 1978).
78. H. A. Hyman, A. Ballantyne, H. W. Friedman, D. A. Reilly, R. C. Southworth, and C. I. Dym, *J. Vac. Sci. Technol.* **21**, 1012 (1982).
79. S. Ariga and R. Sigel, Max-Planck-Institut für Plasma Physik Rep. IV/81, Cologne, West Germany (March 1975).
80. G. Wakalopoulos, Electro-Optical Energy Systems, Los Angeles, unpublished (1983).
81. R. A. McCorkle, J. Angilello, G. Coleman, R. Feder, and S. J. LaPlaca, *Science* **205**, 401-402 (1979).
82. C. Stallings, K. Childers, I. Roth, and R. Schneider, *Appl. Phys. Lett.* **35**, 524 (1979).
83. J. Shiloh, A. Fisher, and N. Rostoker, *Phys. Rev. Lett.* **40**, 515 (1978).
84. P. G. Burkhalter, J. Shiloh, A. Fisher, and R. D. Cowan, *J. Appl. Phys.* **50**, 4532 (1979).
85. G. Dahlbacka, S. M. Matthews, R. Stringheld, I. Roth, R. Cooper, B. Ecker, and H. M. Sze, in "Low Energy X-Ray Diagnostics—1981" (D. T. Attwood and B. L. Henke, eds.), p. 32. Am. Inst. Phys., New York, 1981.
86. J. S. Pearlman and J. C. Riordan, *J. Vac. Sci. Technol.* **19**, 1190 (1981).
87. S. M. Matthews and R. S. Cooper, in "Submicron Lithography" (P. D. Blais, ed.), *Proc. Soc. Photo-Opt. Instrumen. Eng.* **333**, 136 (1981).
88. S. M. Matthews, R. Stringheld, I. Roth, R. Cooper, N. F. Economou, and D. C. Flanders, "Semiconductor Microlithography VI," *Proc. Soc. Photo-Opt. Instrumen. Eng.* **275**, 52 (1981).
89. J. Pearlman and J. Riordan, Maxwell Laboratories, San Diego, California, and G. Georgio and A. Zacharias, AT&T Bell Laboratories, Murray Hill, New Jersey, unpublished (1983).
90. J. W. Mather, *Methods Exp. Phys.* **98**, 187 (1971).
91. R. A. Gutcheck and J. J. Murray, in "High Resolution Soft X-Ray Optics" (F. Spiller, ed.), *Proc. Soc. Photo-Opt. Instrumen. Eng.* **316**, 196 (1981).
92. J. H. Lee, *Phys. Fluids* **20**, 313 (1977).
93. D. J. Nagel, C. M. Brown, M. C. Peckerar, M. I. Ginter, J. A. Robinson, I. J. McIlrath, and P. K. Carroll, *Appl. Optics* (1984) (to be published).
94. G. Charais, D. C. Slater, E. J. Mayer, J. A. Tarvin, G. E. Busch, D. Sullivan, D. Musinski, D. T. Matthews, and L. Koppel, in "Low Energy X-Ray Diagnostics—1981" (D. T. Attwood and B. L. Henke, eds.), p. 270. Am. Inst. Phys., New York, 1981.
95. D. J. Nagel, R. R. Whitlock, J. R. Greg, R. F. Pechacek, and M. C. Peckerar, in "Semiconductor Microlithography III," *Proc. Soc. Photo-Opt. Instrumen. Eng.* **135**, 46 (1978).
96. H. M. Epstein, D. J. Mallozzi, and B. L. Campbell, *Proc. Soc. Photo-Opt. Instrumen. Eng.* **385** (to be published).
97. P. J. Mallozzi, H. M. Epstein, and R. F. Schwerzel, in "Advances in X-Ray Analysis"

- (G. J. McCarthy, C. S. Barrett, D. E. Leyden, J. B. Newkirk, and C. O. Rudd, eds.), Vol. 22, p. 267. Plenum, New York, 1979.
98. D. J. Nagel, M. C. Peckerar, R. R. Whitlock, J. R. Greig, and R. E. Pechacek, *Electron Lett* **14**, 781 (1978).
 99. B. Yaakobi, H. Kim, J. M. Sources, H. W. Deckman, and J. Dunsmuir, *Appl Phys Lett* **43**, 686 (1983).
 100. R. D. Bleach and D. J. Nagel, *J Appl Phys* **49**, 3832 (1978).
 101. D. J. Nagel, C. Marquardt, and R. T. Williams, Naval Res. Lab., Washington, D.C., unpublished (1983).
 102. R. L. Byer, Stanford Univ., Stanford, California, private communication (1983).
 103. M. C. Peckerar and R. E. Neidert, *Proc IEEE* **71**, 657 (1983).
 104. W. Andrews, *Electronic Engineering Times* (November 1982).
 105. B. B. Triplett and S. Jones, in "Submicron Lithography" (P. Blais, ed.), *Proc Soc Photo-Opt Instrumen Eng* **333**, 118 (1982).
 106. D. B. Brown and D. J. Nagel, in "Low Energy X-Ray Diagnostics—1981" (D. T. Attwood and B. L. Henke, eds.), p. 253. Am. Inst. Phys., New York, 1981.
 107. G. K. Green, Brookhaven Nat. Lab. Rep. 50595, Upton, New York (1977).
 108. J. S. Thomsen, in "X Ray Spectroscopy" (L. V. Azaroff, ed.), p. 26. McGraw-Hill, New York, 1974.
 109. D. J. Nagel, *Rev Sci Instrum* **54**, 1797 (1983).
 110. D. J. Nagel and R. R. Whitlock, Naval Res. Lab., Washington, D.C., unpublished (1983).
 111. J. V. Gilfrich, D. B. Brown, and P. G. Burkhalter, *Appl Spectrosc* **29**, 322 (1975).
 112. T. W. Barbee, Jr., in "Low Energy X-Ray Diagnostics—1981" (D. T. Attwood and B. L. Henke, eds.), p. 131. Am. Inst. Phys., New York, 1981.
 113. J. Vierling, Naval Res. Lab. Rep. 6679, Washington, D.C. (July 1968).
 114. L. Chalkley, *J Org Chem* **26**, 408 (1961).
 115. C. M. Dozier, D. B. Brown, L. S. Birks, P. B. Lyons, and R. F. Benjamin, *J Appl Phys* **47**, 3732 (1976).
 116. J. M. Shaw and M. Hatzakis, IBM Rep. RC8892 (#39013), Yorktown Heights, New York (1981).
-
111. J. V. Gilfrich, D. B. Brown, and P. G. Burkhalter, *Appl Spectrosc* **29**, 322 (1975).
 112. T. W. Barbee, Jr., in "Low Energy X-Ray Diagnostics—1981" (D. T. Attwood and B. L. Henke, eds.), p. 131. Am. Inst. Phys., New York, 1981.
 113. J. Vierling, Naval Res. Lab. Rep. 6679, Washington, D.C. (July 1968).
 114. L. Chalkley, *J. Org. Chem.* **26**, 408 (1961).
 115. C. M. Dozier, D. B. Brown, L. S. Birks, P. B. Lyons, and R. F. Benjamin, *J. Appl. Phys* **47**, 3732 (1976).
 116. J. M. Shaw and M. Hatzakis, IBM Rep. RC8892 (#39013), Yorktown Heights, New York (1981).

Soft x-ray lithography using radiation from laser-produced plasmas

P. Gohil, H. Kapoor, D. Ma, M. C. Pekerar, T. J. McIlrath, and M. L. Ginter

Plasmas formed by focusing 0.6-J pulses from a 10-Hz Nd:YAG laser onto solid targets were used as soft x-ray sources for lithographic studies. Results of exposing masked photoresists to plasma radiation produced using steel, copper, and tungsten as targets are presented.

I. Introduction

Laser-produced plasmas have proven to be excellent sources of short wavelength radiation with a wide variety of applications in the XUV and soft x-ray regions. In this work we report results which extend earlier¹ preliminary x-ray lithographic studies performed using a high-repetition-rate plasma light source.² The laser-driven light source and experimental chamber have been described in detail previously.^{1,2} Briefly, the laser is an International Laser System (ILS) Nd:YAG laser ($\lambda = 1.06 \mu\text{m}$), which consists of a Q -switched oscillator cavity and three amplifier sections operated at a repetition rate of 10 Hz. Laser pulses were 25-nsec FWHM with energies typically in the 630–670-mJ range for the majority of the experiments described below. The laser beam was steered to an evacuated source chamber by dielectrically coated mirrors and was focused on the surface of metal targets within an evacuated light source chamber by a convex glass lens with $f = 310 \text{ mm}$ (see Fig. 1). Light emitted from the plasma produced by the focused laser pulse passes from the source chamber through an $\sim 20 \text{ mm}$ diam. aperture into an experimental chamber containing the object being irradiated, in the present case masked photoresist-coated substrates and/or x-ray photodiodes, with the

center line from the experimental chamber aperture to target being at nearly right angles to the laser beam (see Fig. 1).

II. Experimental Conditions and Procedures

The irradiance of a driver pulse is determined from the laser parameters listed above and the focal spot size on the target surface. The focal spot size (focused beam waist) for the system in Fig. 1 was measured using a reticon diode array (resolution $17 \mu\text{m}$) placed in the focal plane of the lens. To protect the reticon the incidence laser intensity was reduced $\sim 10^{-7}$ by reflection of the beam off optical flats followed by passage through neutral density filters. The measured FWHM beam diameter was $170 \mu\text{m}$, as can be seen from the reproduction of a typical oscillograph of the reticon's output appearing in Fig. 2. Use of standard beam profile formulae for a TEM_{00} spatial mode³ leads to a theoretical minimum spot size from our lens and laser of $60 \mu\text{m}$ with a confocal beam parameter of 14 mm . Previous measurements¹ of target crater diameters for low power pulses on refractory targets and on plastic tape provide an independent estimate of $\sim 130 \mu\text{m}$ for the focal spot diameter. Since the $\sim 170 \mu\text{m}$ images obtained on the reticon could be larger than the on-target images because of aberrations introduced by the intensity reduction optics (see above), 170 and $60 \mu\text{m}$ seem reasonable upper and lower bounds, respectively. Thus, for 25 nsec, 0.65-J pulses with focal spot diameters of 60, 130, or $170 \mu\text{m}$, the averaged incidence irradiance on a target surface normal to the incident beam would be 9.2×10^{11} , 1.8×10^{11} , or $1.1 \times 10^{11} \text{ W cm}^{-2}$ pulse.

The light source uses cylindrical metal targets ($\sim 16 \text{ mm}$ diameter) attached to a programmable stepping motor driven screw which can provide, among other options, a fresh area of target material for each laser pulse. The plasma producing laser pulses usually are focused on the target surface somewhere in the octant between normal incidence (θ in Fig. 3) and an in-

T. J. McIlrath and M. L. Ginter are with the University of Maryland, Institute for Physical Science & Technology, College Park, Maryland 20742 while M. C. Pekerar and D. Ma are with U.S. Naval Research Laboratory, Washington, D.C. 20375. P. Gohil is now with University of California, Lawrence Berkeley Laboratory, Berkeley, California 94720 and H. Kapoor is now with GTE Communication Systems, Reston, Virginia 22096.

Received 24 November 1984

0003-6935/85/132024-00\$02.00/0

© 1985 Optical Society of America

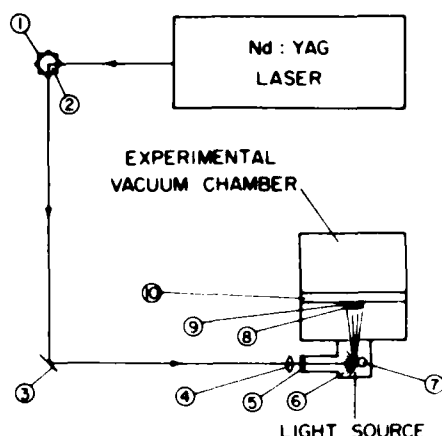


Fig. 1. Schematic diagram of experimental arrangements. Light from a laser is deflected and height adjusted with three mirrors (1,2,3) focused by a glass lens (4) through a Pyrex window (5) onto a cylindrical metal target (7) to produce a plasma plume (6). Radiation from the light source chamber passes into the experimental chamber through a mask (8) onto a photoresist coated wafer (9) held in an alignment mount (10).

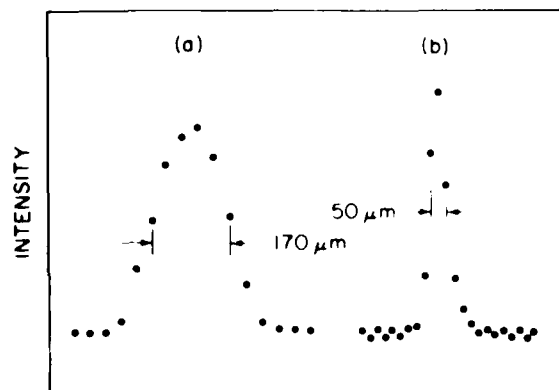


Fig. 2. Plots of the observed spatial distributions of the 1.064 μm beam (a) and 0.6328 μm reference beam (b) at the focus of an $f = 310\text{-mm}$ lens. Data points are from 17 μm wide detector elements on 17- μm centers for 0.6328 μm and from 17 μm elements on 34 μm centers for 1.064 μm . Calculated values for $2\omega_0$ ($1/e^2$ full width) are 100 μm (1.064) and 88 μm (0.6328).

cidence angle of 45° to the target surface's normal (L'' in Fig. 3). The choice of focal spot positioning on the target is determined by the experimental conditions desired, because both the intensity of the light and the quantity of ablation products from the target observed^{1,2,4} in the direction of the experiment (E in Fig. 3) increase as the focused driver ray proceeds from L to L'' . For the lithographic exposures described below, an angle of incidence of $\sim 27^\circ$ (L' in Fig. 3) was chosen as a compromise between a reduced soft x-ray throughput to the wafer surface and an intolerable level of target debris in the experimental chamber containing the wafer. The elongation of the focal spot image in one direction produced by striking the target surface at 27° to the cylinder's normal leads to almost negligible de-

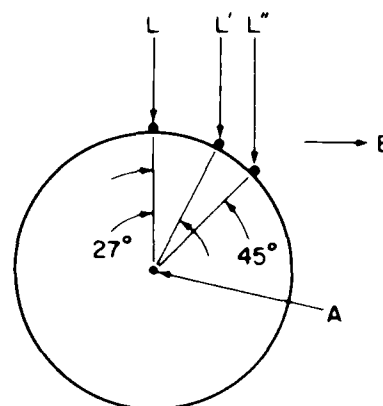


Fig. 3. Schematic diagram of laser focal spot positions on the target surface. The target cylinder rotates about axis A, which is perpendicular to incident laser rays (L, L', L'') and to the plasma light exiting from the source to the experimental chamber in direction E .

creases in the averaged per pulse radiation discussed in the preceding paragraph (i.e., a drop from 1.8×10^{11} to 1.6×10^{11} $\text{W}/\text{cm}^2/\text{pulse}$ for the 130- μm diameter normal incidence example, etc.).

Lithographic reproductions of circuit patterns were made by exposing masked photoresist-coated wafers placed ~ 15 cm from the focal spot on the target to radiation from the plasma. The photoresist used was a copolymer of polyglycidyl methacrylate and ethyl acrylate (COP), which was spun to a thickness of 4700 \AA on the surface of 76-mm diameter silicon wafers. COP is a negative photoresist with a sensitivity⁵ of 15 mJ/cm^2 corresponding to the energy per unit area required to form bonds between molecules in the photoresist. Masks consisted of polyimide membranes overlaid with circuit patterns in gold.

The polyimide membrane used for mask construction was made by forming a thin layer of polyimide on a glass surface spinning at 4000–5000 rpm and by subsequent removal of the glass with hydrogen fluoride solutions. The transmission of the 1.5- μm thick membrane was measured at the National Synchrotron Light Source (NSLS), Brookhaven National Laboratory, using the VUV storage ring. Using calibrated dosimeter film FWT 60-20,⁶ the transmission, integrated over the $\sim 44\text{--}100\text{-\AA}$ effective bandpass⁷ of the membrane, was found to be 70%. To complete a mask, circuit patterns in a 0.5- μm thick layer of gold were formed on the polyimide film.

In each experiment the photoresist-coated wafer was placed ~ 10 μm behind the mask in a kinematic mount designed to allow precise alignment of both mask and wafer. The mounted mask/wafer assembly then would be inserted in the experimental chamber and the light source and experimental chamber (see Fig. 1) evacuated to ~ 0.050 Torr. Targets of copper, steel, or tungsten were used with the optical arrangements discussed above to expose the masked resists for times ranging from 15 to 60 minutes at pulse repetition rates of 10 Hz. After exposure, the mask and wafer were separated, the

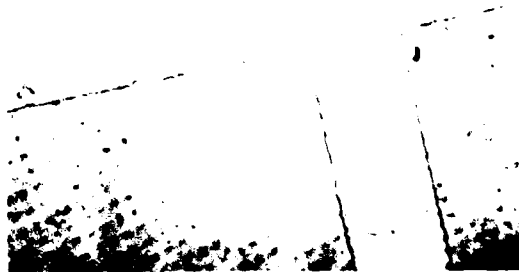


Fig. 4. Photograph of a developed COP photoresist exposed through a mask for 1 h using a Cu target (see text). The smallest element is $\sim 19 \mu\text{m}$ wide, while the small spots result from imperfections in the microscope optics and are not a product of the lithography.



Fig. 5. Photograph of a scanning electron micrograph of a developed COP photoresist exposed as in Fig. 4. The top figure is a $\times 5$ enlargement of a portion of the lower panel, with the longer of the three white lines in the lower right-hand corner of the top figure being $10 \mu\text{m}$ in the photograph. The small spots result from imperfections in the mask and not from the lithography.

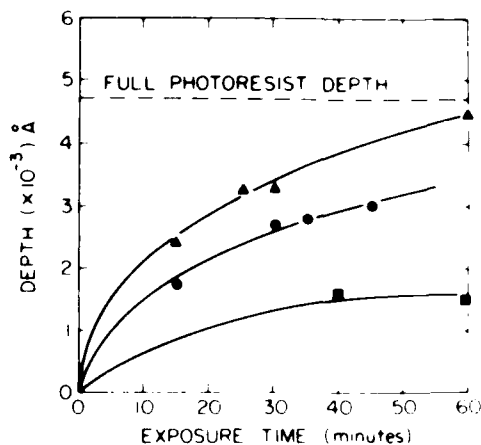


Fig. 6. Depth of photosensitized (etchable) resist as a function of exposure time to pulsed laser plasma radiation produced at a repetition rate of 10 Hz (see text). Triangles, circles, and squares represent data points for Fe (steel), Cu, and W targets, respectively.

exposed resist was removed from the wafer by developing, and the resulting lithographs were studied by detail.

III. Results and Discussion

The developed photoresists were examined using both optical and electron microscopy. Figures 4 and 5 are reproductions of typical optical and electron microscope photographs, respectively, illustrating the clarity of sidewall profiles (average vertical wall uniformity better than $0.3 \mu\text{m}$) obtained from lithographs in COP resists exposed using a copper target. The small spots in Fig. 4 result from dust particles in the microscope optics while the small indentations apparent in Fig. 5 result from pinholes in the mask. The depth of the resist removed on development corresponds to the depth photosensitized and, therefore, to the amount of radiation received by the resist which is effective in bond formation. The depths of development of photoresists exposed for different times using Cu, Fe (steel), or W targets were measured with an electron microscope, and the results are summarized in Fig. 6.

The radiations observed from the plasma source and targets employed in this work are most intense in the $\sim 30\text{--}500 \text{ Å}$ region,^{1,2} so that it seems likely that resist exposures resulted primarily from radiation transmitted in the short-wavelength ($\sim 44\text{--}100 \text{ Å}$) effective bandpass (see above) of the polyimide mask substrate. In these wavelength regions, the emissions from Cu and Fe (steel) targets are predominantly dense line spectra overlaying weaker continua (spectra of focused plasmas from Cu targets become predominantly continuous near 50 Å) while the emissions from W targets are almost exclusively continuous with very few discrete spectral lines observable.^{1,2} As can be seen from Fig. 6 it appears that radiation from Cu and Fe (steel) targets is at least twice as effective in exposing our masked COP lithographs as the continuous emission from W, with Fe being slightly superior to Cu. The relative ordering of

Fe > Cu > W for exposure efficiency may have a slightly greater spread than implied by Fig. 6, since the quantities of ablation products produced by these targets fall in the order W > Fe > Cu. Thus, a system which reduces or stops the migration of ablation products from the targets into the experimental chamber might lead to greater differences between the efficiencies of Fe and Cu, etc. than those reported in Fig. 6.

The same masks and similar COP-coated silicon wafers were exposed⁷ at NSLS and developed by the same procedures as the lithographs discussed above. The sole object of these experiments was the direct comparison of analogous lithographs prepared using different light sources. We find that (1) the lithographs exposed using the plasma light source were uniformly exposed over their entire area while the lithographs exposed using the electron storage ring light source (NSLS) were much less uniform, (2) to produce exposures comparable with those obtained in the most intense positions of the beam from NSLS requires ~10 times more elapsed time using the laser plasma source, and (3) there were no obvious differences in the quality of the lithographs (wall and surface uniformity, etc.) made using either light source.

The total soft x-ray output of the laser plasma light source currently in use can be increased (1) by increasing the repetition rate of the laser, (2) by using focusing optics with soft x-ray reflective coatings, (3) by increasing the energy per pulse at the same repetition rate, and/or (4) by reducing the quantity of ablation products from the target which travel to the experiment. All four of these approaches will be incorporated in future efforts to produce a laboratory light source for soft x-ray lithography which is at least as intense and of significantly better intensity uniformity per steradian than

can be obtained from the current generation of synchrotron light sources.

This work was supported in part by the Air Force Office of Scientific Research under contract AFOSR 4900-83-C-0130. P. Gohil acknowledges support from the Science and Engineering Research Council (UK) in the form of a postdoctoral research fellowship.

References

1. D. J. Nagel, C. M. Brown, M. C. Peckerar, M. L. Ginter, J. A. Robinson, T. J. McIlrath, and P. K. Carroll, "Repetitively Pulsed-Plasma Soft X-ray Source," *Appl. Opt.* **23**, 1428 (1984).
2. G. O'Sullivan, P. K. Carroll, T. J. McIlrath, and M. L. Ginter, "Rare-Earth Plasma Light Source for VUV," *Appl. Opt.* **20**, 3043 (1981).
3. M. Kogelnik and T. Li, Proc. "Laser Beams and Resonators," *IEEE* **54**, 1312 (1966).
4. G. O'Sullivan, J. Roberts, W. R. Ott, J. Bridges, T. L. Pittman, and M. L. Ginter, "Spectral Irradiance Calibration of Continuum Emitted from Rare-Earth Plasmas," *Opt. Lett.* **7**, 31 (1982).
5. G. N. Taylor, "X-Ray Resist Materials," *Solid State Technol.* **73** (May 1980).
6. *Radi-Chromic Reader* (Far West Technology, Goleta, Calif. 93077).
7. H. Kapoor, M.S. Thesis (Electrical Engineering), U. Maryland, College Park, Md. (1984).
8. P. Gohil, V. Kaufman, T. McIlrath, and M. Ginter, "Very High Resolution Photographic Studies of Continua from Laser Produced Plasmas Between 50 and 550 Å," *Appl. Opt.* (to be submitted).
9. M. Kuhne and B. Wende, "Spectral Radiant Power Measurements of VUV and Soft X-Ray Sources," *X-Ray Microscopy*, G. Schmahl and D. Rudolph, Eds. (Springer, Berlin, 1984), p. 30.

LASER-PLASMA SOURCES FOR X-RAY LITHOGRAPHY

D.J. Nagel
Naval Research Laboratory
Washington DC
USA

The status of characterization and engineering of laser-heated plasma sources for x-ray lithography is reviewed.

INTRODUCTION

A hierarchy of competitions is in progress to determine which lithography tool will be dominant for microcircuit production in the 1990's:

- * X-ray lithography is projected to gradually supplant optical lithography as commercial linewidths approach $0.5 \mu\text{m}$.
- * Bright x-ray sources suitable for step-and-repeat replications onto large wafers will be preferred over current x-ray tubes which expose entire medium-size wafers.
- * Storage ring sources of synchrotron radiation and dense, multimillion degree plasmas are candidate second generation x-ray lithographic sources.
- * Both electrical discharges and laser beam plasma x-radiation sources are now being commercialized for lithography.
- * High peak and average power solid-state (notably Nd) and gaseous (excimer) laser systems are both being considered for production line systems.

This paper briefly updates a review of plasma sources for x-ray lithography (1) by summarizing recent advances and current efforts devoted to development of x-ray exposure tools with laser-heated plasma sources. The possibility of subkilovolt x-ray lithography is examined in the next section. Continuing research on characterization of laser-plasma x-radiation is then sketched. Current efforts to design laser and exposure systems with appropriate features are described in the next two sections. Development of reliable pulsed lasers with adequately-high peak and average power, and of exposure stations which prevent target debris from degrading masks, is both necessary and challenging.

SUBKILOVOLT X-RAY LITHOGRAPHY

Most research and commercial x-ray lithography systems operate in the 1 to 4 keV region (12 to 3 \AA wavelengths) because lines from convenient x-ray tube anode materials occur in this range. However, as shown in Figure 1, resist absorption is low above 1 keV, while absorption is high in the subkilovolt region, down to the oxygen and carbon K-absorption edges at 284 eV and 532 eV. Furthermore, the x-radiation from laser-plasmas is most intense in the subkilovolt region.

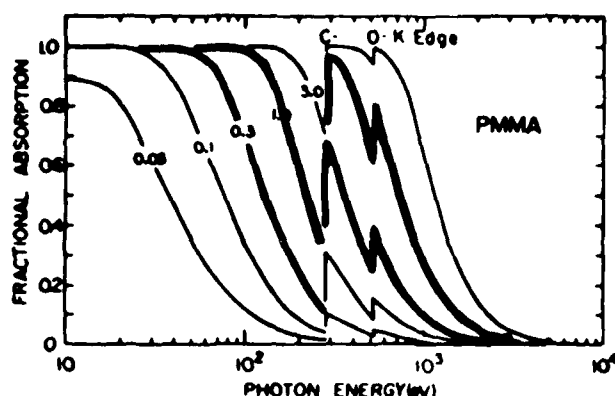


Figure 1
The fractional x-ray absorption of PMMA layers
of the thicknesses indicated (μm)(2)

Above 1 keV, where large area transparent masks have already been developed for use with x-ray tubes, laser-plasma intensity decreases rapidly with photon energy. Lasers with peak powers exceeding 10^{10} watts are needed to achieve irradiance values of 10^{14} W/cm² required for 10% efficiency of conversion of laser light into x-rays above 1 keV (emitted into 2π sr). Lasers with 10^9 watt pulses will not produce radiation above 1 keV with adequate efficiency, but will provide irradiances exceeding 10^{13} W/cm² which give conversion fractions exceeding 10% for subkilovolt x-radiation.

There are two reasons why x-ray lithography below 1 keV has been little studied. The same diffraction effects which require x-ray rather than ultraviolet wavelengths in the first place, set a lower (upper) limit on x-ray energies (wavelengths). For diffraction of wavelength λ past an edge, the blurring B at a distance S (the mask-wafer separation) is approximately $B = \sqrt{S\lambda/2}$. If B is to be less than $0.5 \mu\text{m}$ (or $0.1 \mu\text{m}$) for $S = 25 \mu\text{m}$, λ must be less than 200\AA (8\AA). Also, window and mask absorption are severe in the subkilovolt region.

Small area (few cm²) step-and-repeat masks with plastic membranes could be used below the C K-edge, but they would have to be very thin ($< 3000 \text{\AA}$). Diffraction effects are large enough to make this region of little interest anyway.

Above the carbon edge, resist absorption is favorable and diffraction is tolerable for nearer-term line widths, but masks are still a problem. Metal membranes about $0.5 \mu\text{m}$ thick are being examined for use in this region. Their opacity to optical wavelengths requires an alternative alignment strategy.

The 0.5–1 keV region is attractive because laser plasma intensities and x-ray absorption are still high in this region (for short exposure times), diffraction is adequately low and transparent masks should be available.

Increasing attention will be given to x-ray lithography with subkilovolt photon energies because high intensities are available from plasmas which can be produced by lasers with lower peak powers, a major engineering advantage.

X-RAY CHARACTERIZATION

The spatial and temporal, as well as spectral properties of laser-plasma x-ray emission must be known for design of lithography systems. These depend on the laser wavelength, pulse energy and length, focal area and the target composition and geometry. Many quantitative studies of plasma x-ray emission have been made since 1970 with "single pulse" (low repetition rate) lasers made for purposes other than lithography. In the recent past, such work has been extended to use of small lasers with more relevant repetition rates of a few Hz or greater. X-ray characterization work continues at many laboratories in the U.S.S.R., Israel, the F.R.G., France, the U.K., Canada, the U.S. and Japan with both single pulse (low average power) and multi-Hertz (high average power) lasers.

Another major recent trend in laser-plasma x-ray studies has been the use of short wavelength laser pulses. These can be obtained as harmonics of the fundamental 1.05 μm wavelength from Nd solid-state lasers, or as laser lines near 0.25 μm from excimer gas lasers. Figure 2 shows that short laser wavelengths are preferentially absorbed by the target in the 10^{13} to 10^{15} W/cm^2 range. Scattering (non absorption) of the incident laser energy is wasteful, just as is the transmission of x-ray energy through the resist which was discussed above. Recent work has also shown that short laser wavelengths also favor efficient x-ray production. Figure 3 gives such data in various x-ray energy bands for λ , $\lambda/2$ and $\lambda/4$ pulses from a large Nd laser.

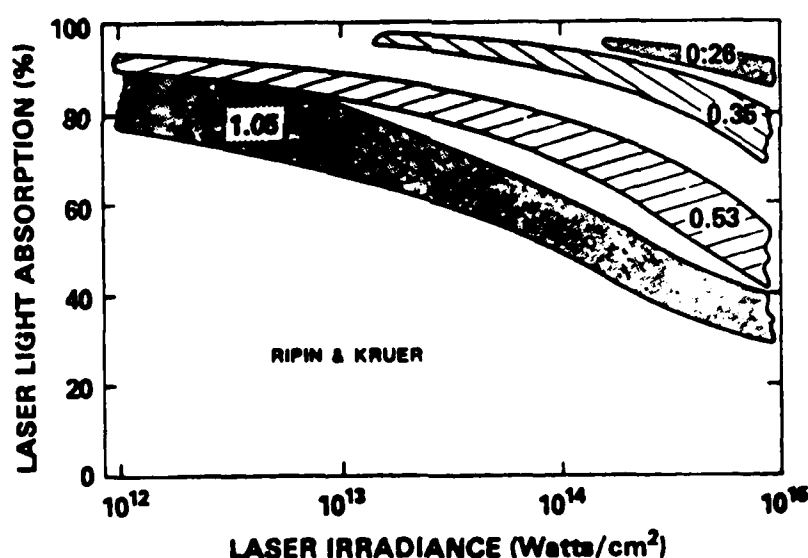


Figure 2

The percent laser light absorption for the laser wavelengths indicated (μm). The bands include data taken with different targets at different laboratories (3).

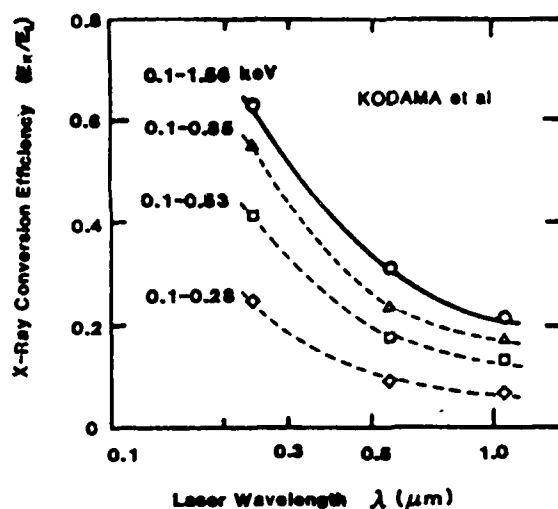


Figure 3

The fraction of incident laser energy converted to x-ray energy in the indicated bands for gold targets irradiated at $7 \times 10^{13} \text{ W/cm}^2$ (4).

X-ray characterization measurements will continue to be of high interest for several years, especially for excimer and high average power laser systems. The motivation comes not only from the x-ray lithography potential, but also because laser-plasmas are uniquely bright sources of soft x-radiation with a wide range of uses (5).

LASER ENGINEERING

Laser characteristics required for x-ray lithography are reasonably clear now: several joule, few nanosecond pulses ($>10^9$ watt peak power) with beam divergence low enough to produce focal spots of $100 \mu\text{m}$ or less with average laser powers exceeding about 100 W. As already discussed, the pulse energy, duration and focusability are needed to achieve 10^{13} W/cm^2 on target to produce plasma temperatures adequate for 10% or greater conversion efficiencies from laser light to useful x-rays. The 100 W average laser power then translates into 10 W of x-rays, or about $10 \text{ mJ/cm}^2/\text{sec}$ for 30 cm plasma-resist separation. With a resist requiring 100 mJ/cm^2 and 7 exposure subfields per wafer, throughputs exceeding 40 wafer levels per hour can be anticipated.

Various laser systems may ultimately find use for lithography, but it is adequate now to concentrate on the status and development prospects for solid Nd and gaseous excimer systems. In general, Nd lasers produce high quality, low divergence beams which can be focused to spots on target less than $100 \mu\text{m}$ in diameter. That is, they have peak powers and irradiances adequate for x-ray production. However, Nd systems do not provide high enough average powers now. Present commercial systems produce multi-joule nsec single pulses, or about 1 J in 25 nsec pulses at 10 Hz. Lasers are now being designed to yield several joule, few nsec pulses at rates of 10 to 100 Hz. They use multiple-bounce slab or multi-pass rod geometries which efficiently extract energy from the pumped lasing medium. Athermal glasses, which do not form effective lenses when they become hot, are

also receiving attention. The challenge for Nd systems engineers includes not only achieving high average powers, but also reliability. Flash lamps life is a major consideration since 10 Hz is equivalent to 6×10^6 shots/week.

The inverse situation prevails for excimer laser systems now. KrF lasers with 100 W average power (1 J pulses at 100 Hz) are commercially available. However they generally have poor beam quality and relatively low irradiance ($< 10^{12}$ W/cm²). Excimer systems, which can be operated near 10 Hz with a low-divergence pulses injected and amplified, have become available. Characterization of x-ray emission from plasmas produced by injection-locked excimer systems is expected. Excimer lasers are attractive because they can be electrically pumped (no flash lamps) and have a gaseous gain medium (a lessened heating problem). However, reliability remains to be demonstrated.

The situation for design of laser systems is summarized with respect to high peak power and irradiance (Figure 4) and regarding high average power (Figure 5). Multi-Hertz nanosecond-pulse Nd and excimer systems generally fall below the required irradiance region. Large Nd systems have ample irradiance but they have low average power and are far too expensive for commercial lithography.

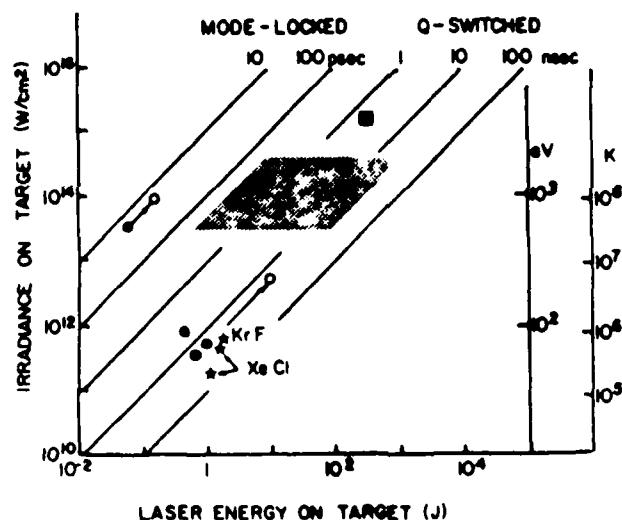


Figure 4

Irradiance on target for low (■) and high (●) repetition rate Nd and excimer (★) lasers which exist (solid circles) or are under development (open circles) as a function of pulse energy and duration relative to the region for efficient x-ray production (shaded). Plasma temperatures (in eV and K for Nd laser pulses are indicated on the right-hand scale (5).

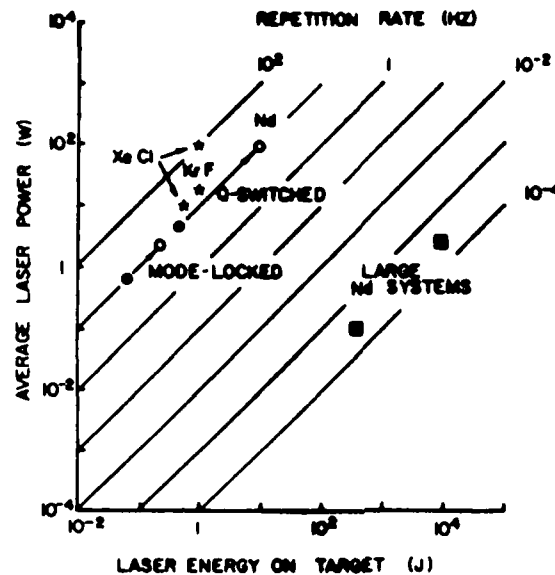


Figure 5

Average laser power as a function of pulse energy and repetition rate.
The symbols are the same as in Figure 4 (5).

EXPOSURE SYSTEM ENGINEERING

The laser is the most formidable design challenge for a laser-plasma lithography system. However, engineering of the system which will contain the target and means to protect masks from target debris also has its demands. This is especially true because the high average power lasers will operate near 10 to 100 Hz for x-ray lithography, requiring the availability of fresh target material.

It has been shown that about one hundred 0.5 J can be placed on the same spot of a thick target before the crater deepens to trap the x-ray emission (6). Even in this case, however, a mechanism to move pristine material to the focus must be provided, be it as a gas, liquid or solid. Gas jets irradiated with pulsed lasers are good x-ray sources and have only high vapor pressure, easily pumped residue (7). Liquid targets are self healing but produce relatively much debris (8). Solid targets, if thick, also yield excessive vapor and high velocity droplets (9). Thin sheet or tape targets offer reduced extraneous material, and much of it is blown out the back of the target foil by the plasma pressure (10).

The amounts of vapor arising from the recombined plasma, which expands normally to the target surface (11) and droplets, which are blown out at approximately 45° to the normal (10), depend on laser and target characteristics. Both types of debris produce unacceptable mask damage (absorptive coating or punctures).

Many methods are available to prevent debris, even the low amounts produced by thin targets, from reaching the mask. They include the use of thin, sacrificial roll-to-roll shields, if the x-ray energy is high enough for transmission (11);

high speed shutters which allow x-ray but not debris passage (12); and, employment of a low pressure the gas in the target area, which slows down the vapor and allows it to be pumped (13). The He also serves to thermally clamp the mask, which absorbs significant x-ray power, to the wafer, but it can also transmit damaging shock waves (14).

Repetitively pulsed lasers offer two advantages beyond high average power. Thermal spikes in the mask due to x-ray absorption at the gold-membrane interface are lessened compared to single-shot exposures, which should promote mask stability. Also, single-shot exposure control is problematic due to variations in the laser output or plasma emission. The system outlined in Figure 6 can be used, with an optical or mechanical shutter, to give exposure constancy to a few percent or better.

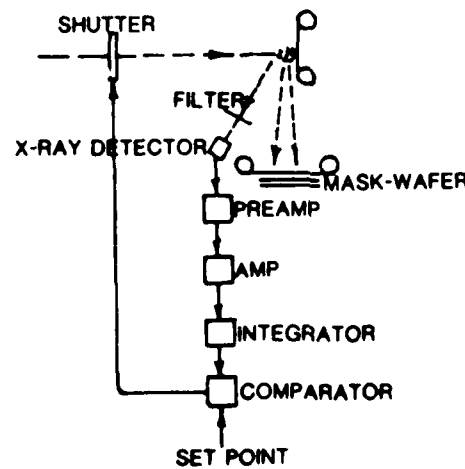


Figure 6
Schematic of an exposure control system for x-ray lithography
with a high rate (> 10 Hz) laser system.

The design requirements to bring light onto the target not too far off the normal, to permit transit of x-rays from the plasma to the wafer, to stop debris and to monitor exposures are all being faced as practical laser-plasma aligners are being brought to market.

SUMMARY

Laser-heated plasmas appear to be a viable source for x-ray lithography. Characterization of their output remains a major activity, even though much is already known. The output of plasmas heated by excimer lasers is receiving significant current attention. Meanwhile, serious engineering of high peak and average power systems for lithography, and the required exposure chambers is occurring. Commercial x-ray lithography systems with laser-plasma sources may be available in a few years.

Acknowledgement: T. Mochizuki is thanked for a preprint of reference (4).
Mrs. A.M. Verweij is thanked for the expert typing.

REFERENCES

- [1] D.J. Nagel in D.M. Brown and N.G. Einspruch (Editors): *VLSI Electronics; Microstructure Science*, vol. 8, Academic Press, New York (1985), p. 137-170
- [2] D.J. Nagel, *Annals of the New York Academy of Sciences*, 342, 235-51 (1980).
- [3] B.H. Ripin and W.L. Kruer, *NRL Memorandum Report* 5225 (June 1984).
- [4] R. Kodama, K. Okada, N. Ikeda, M. Mineo, K. Tanaka, T. Mochizuki and C. Yamanaka, to be published.
- [5] D.J. Nagel in *X-Ray Lithography and Applications of Soft X-Rays to Technology*, *Spie Vol.* 448 (1984) p. 17-24.
- [6] D.J. Nagel, C.M. Brown, M.C. Peckerar, M.L. Ginter, J.A. Robinson, T.J. McIlrath and P.K. Carroll, *Applied Optics* 23, 1428-331 (1984).
- [7] R.W. Lee, D.L. Matthews, L. Koppel, G.E. Busch, G. Charatis, M.J. Dunning and F.J. Mayer, *J. Applied Physics* 54, 4909-15 (1983) page 02 Ru1ssgg 7965 Unc1as
- [8] R.M. Jopson, S. Darack, R.R. Freeman and J. Bokor, *Optics Letters*, 8, 265-7 (1983)
- [9] S. Ariga and R. Sigel, *Max-Planck Inst. fur Plasma Physik Report* IV/81 (March 1975).
- [10] M.C. Peckerar, J.R. Greig, D.J. Nagel, R.E. Pechacek and R.R. Whitlock in R. Bakish (editor) *Electron and Ion Beam Science and Technology*, *Electrochemical Society Proc. Vol.* 78-5 (1978) p. 432-43.
- [11] C.L. Marguardt, R.T. Williams and D.J. Nagel: *Mat. Res. Soc. Proc.* 38, 325 (1985).
- [12] A.L. Hoffman, G.F. Albrecht and E.A. Crawford, *J. Vacuum Science and Technology B*3, 258-61 (1985).
- [13] M. Kuhne and H.-C. Petzold, *Optics Letters*, 9, 16-8 (1984).
- [14] B.H. Ripin, J.A. Stamper, and E.A. McLean, *NRL Memorandum Report* 5279 (March 1984).

LASER PROCESSING OF HIGH-TECH MATERIALS AT HIGH IRRADIANCE

The major applications of lasers to the processing of high technology materials are briefly enumerated. It is found that the majority of these applications rely upon the direct thermal effects of irradiating the material with laser light. Several other important interactions of high irradiance lasers with materials are examined. The need for survey and evaluation of the capabilities of lasers to generate shocks for materials processing is underscored. Emphasis is placed on applications and potential applications of secondary processing, in which the particle or photon emissions of a laser-produced plasma are employed in the materials processing steps. The demonstrated feasibility of using x-ray pulses from laser-produced plasmas for x-ray lithographic fabrication of microelectronics and microstructures is briefly reviewed. The possible application of laser evaporative deposition to the fabrication of novel materials, such as multilayers, superlattices, quantum devices and microstructures, is proposed.

INTRODUCTION

The majority of commercial applications of lasers for materials processing involve directly focusing the laser light onto the material, thereby locally raising the temperature of the material to promote the desired process. The disposition of absorbed energy in high irradiance laser-matter interactions, schematically indicated in Figure 1, includes melting, vaporization, light emission, and, at sufficiently high irradiances, plasma formation, the initiation of thermal and shock waves going into the target, and the emission of x-ray and UV photons as well as charged particles (electrons and ions) directed away from and into the material. Most of these major components of the interaction are either being used or are contemplated for use in materials processing applications, generally at low irradiances. Process control with lasers, at 8% of the laser marketplace in 1983, commands almost twice the market share of all materials processing with lasers.¹

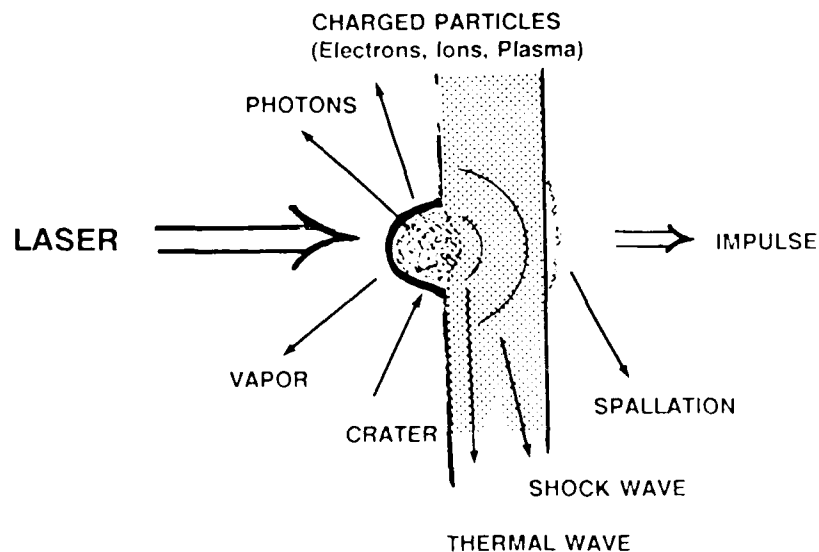


Fig. 1 Interaction of a high power pulsed laser with condensed matter.

In the first section, this paper will enumerate many applications of lasers to the processing of high-technology materials. Thereafter, three sections will emphasize laser-driven shocks, x-ray lithography with x-ray emitting laser-produced plasmas, and the laser irradiated solid target as an evaporative coating source.

MATERIALS PROCESSING

As it stands today, the area of materials processing with lasers has received a strong impetus from the success of laser shaping, joining, and modification of metals.^{2,3,4} Shaping includes drilling, cutting, bending, laser assisted machining (turning and milling) and direct laser machining. Joining includes bonding, welding of various types (spot, seam, butt), brazing and soldering.

Surface modification treatments of metals encompass transformation hardening, surface alloying, injecting a refractory material into a surface melt layer, post processing of electroplated layers, post processing of plasma sprayed layers, and marking. Laser heat treatment for surface hardening has progressed beyond the original goal of wear reduction and has achieved increases in strength and fatigue life, improved lubrication, tempering, creation of surface carbide, etc. The importance of materials modification by "advanced, precisely controlled processing techniques, which beneficially change the alloy structure during either consolidation or joining," has been emphasized as a remaining route which may lead to structural (as distinguished from surface) properties which are increasingly difficult to obtain by alloy development alone.⁵ Laser processing is playing a role in the development of this new technology, e.g., with techniques to build up structures from laser-processed layers. A graph of power density regimes for metal processing with CO₂ lasers is available in the literature.⁶

Another class of economically important materials, semiconductors, has also been intensely investigated to determine the suitability of laser processing. Silicon has received the greatest attention, but many other materials, including GaAs, (Al,Ga)As, InSb, CdTe, HgTe, InP, GeSe, Cu-In-Se, CuInSe₂, and CdS, have not been neglected.^{7,8,9,10,11} In the large, these investigations and applications are related to the microelectronics industry, with more forward looking aspirations for integrated optic devices.

Laser annealing of semiconductors, perhaps the most actively pursued process for these materials, now encompasses more than its initial scope, the heating and recrystallization of ion implantation-damaged Si wafers. Annealing seats the implanted dopant at lattice sites and also heals macroscopic defects caused by ion bombardment. Removal of defects and precipitates arising from high temperature processing, epitaxial regrowth of evaporated Si on crystalline Si, crystallization of polysilicon, and the formation of metal silicide conducting paths, a form of laser-induced chemical change, are also included under the banner of laser annealing. In addition, the melting and regrowth process can be used to incorporate dopants and to tailor the profile of dopants in the regrown material in a manner different than is attainable by ion implantation. A related thermal process, the selective absorption of the 9.25 micron line of CO₂ by SiO₂, allows the topographic smoothing of silicon oxide features on a wafer.

Another technique addressed to semiconductor processing is laser chemical vapor deposition (LCVD). In LCVD, laser light promotes the deposition of reactants from a vapor phase onto a substrate. Since its inception about half a decade ago, LCVD has progressed to having demonstrated epitaxial growth of deposited films. LCVD has also accomplished writing a pattern of desired composition onto the substrate for local doping, for conduction paths, or for mask definition and repair. Materials deposited include metals, insulators, semiconductors (both elemental and compound), and polymers. Although the writing rate is up to 10,000x greater than in planar vapor reactions (a geometric effect which varies with feature size), the disadvantage of serial operation remains. The chemical reactions may be induced thermally (pyrolytically) or by direct chemical reaction from photon absorption in the gas (photolytically); the latter offers wavelength selectivity among reactions and

can operate satisfactorily at lower temperatures, yielding less stress on the substrate.¹² Other examples of reactions locally induced by lasers have been demonstrated, e.g., electroplating and chemical etching.

Additional types of materials for which laser processing is being researched include chemicals (IR photochemistry, photodissociation, photoisomerization, catalysis, photopolymerization, and vibrationally enhanced reactions), biological materials, isotopes (laser isotope separation for nuclear fission fuel), and hydrogen isotopes (inducing thermonuclear fusion reactions).

SHOCKS

As an introduction to shock processing of materials, the following sections will successively consider some of the effects which shocks produce in materials, methods of producing or driving shocks in solids, and comments on applications using those effects. The motivation for this overview¹³⁻¹⁶ is to examine the field of shock generation and to review and assess the suitability of lasers as a driver for shocks, both for research and for commercial applications.

Shock waves in materials are compressive. Like acoustic waves, which travel at the sound speed, shock waves are a manifestation of atomic movements. Since the material in and behind the shock front is compressed to a higher pressure, and because sound speed increases with pressure, the shock travels at a greater speed than the sound speed in the uncompressed material. However, the shock travels at a speed below the sound speed in the compressed material behind the front (for stable shocks in nonreactive media). The shock speed increases with the compression, i.e., with the amplitude of the shock. Thus, the highest amplitude portion of a high amplitude compression wave overtakes the lower amplitude components, resulting in a shock front at which uncompressed material is immediately adjacent to the region of highest compression the pressure, density, temperature, and some physical properties of the material change across this sharp front in a nearly discontinuous fashion. In part, these changes result from the violence of the atomic motions associated with shock waves, which can be sufficiently strong to melt or even ionize the material. Compressions as small as a few percent and up to a factor of 2 are not uncommon, with values as high as 6 having been reported. The distance over which the discontinuity takes place can be a few microns for dense, ionized material; experiments in condensed matter at room temperature anticipate probing shock fronts with micron resolution, and profiles with submicron dimensions are not unheard of. Dissipative losses, such as compression heating, decrease the amplitude of the shock as it traverses the material. The removal of the driving force initiates a decompression (rarefaction) wave which can quickly overtake the shock, thus limiting the duration of the highly compressed condition of the material. As a rule of thumb, an unconfined laser-generated shock in a homogeneous solid decays only after about twice the laser pulse duration.¹⁷ Many of these calculated profiles of a shock wave as it develops¹⁸ as shown in Figure 2, together with a photograph of a shock wave at late time in a plastic target.¹⁹ The unit of pressure adopted in this article and in much of the literature is the Pascal (Pa), $1 \text{ Pa} = 1 \text{ Newtons sq. meter}$, ($1 \text{ psi} = 6894.8 \text{ Pa}$, $1 \text{ standard atmosphere} = 101,325 \text{ Pa}$, and $1 \text{ bar} = 0.1 \text{ MPa}$.)

Two areas of research which benefit from shock investigations in condensed matter are astrophysics and geology. The understanding of stellar interiors is also dependent upon the study of matter at high densities, pressures, and temperatures. It has been proposed that thermonuclear fusion reactions, such as take place in stars, might be induced in the laboratory by a high velocity impact (impact fusion), a technique which has long been used to generate shocks; a somewhat related approach to fusion involves the convergent implosion of spherical or cylindrical shells, which also must take transient shock pressures into consideration. The impact of micrometeoroids on spacecraft is a further problem which can be addressed by shock experiments. The behavior of hydrogen at high pressures may be important to the study of the planets Jupiter, Saturn, and Uranus, which are constituted primarily of that element. Geologic interest in the state of matter in the core of the earth, where static pressures are 300-400 GPa and the temperature is about 5000 degrees Kelvin, has been directed to laboratory shock experiments which momentarily achieve temperatures and pressures in that range.

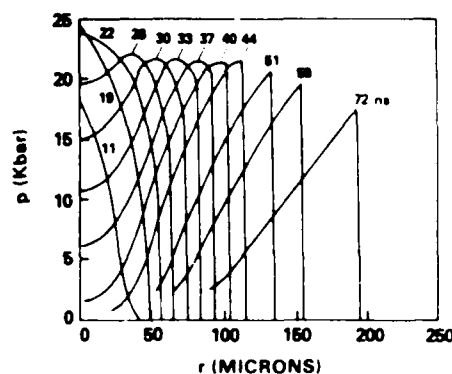


Fig. 2 Development of laser-driven shock in plastic: (a) calculated, 20 nsec laser, confined target;¹⁷ (b) experimental, 5 nsec, unconfined.^{17,28}

The overall breadth of scientific interest in shock processes in condensed matter is perhaps best surveyed in the light of the many effects which shock waves produce.

SHOCK EFFECTS

The passage of a shock wave results in compression heating, one of the most important effects of the shock. While high static pressures can be applied in the presence of a heat sink, if necessary, the transient nature of shocks does not allow heat dissipation sufficient time to prevent the attainment of elevated temperatures. The arrival of the rarefaction wave, on the other hand, is associated with expansion cooling, but residual thermal energy remains in the material. The net result of the atomic motions associated with the shock wave and the thermal history can include chemical breakdown, chemical synthesis, defect formation, phase changes, twinning, precipitation, recrystallization, melting, ionization, and plasma production.

Shocks also can produce mass motions on a larger, micron scale. For shock waves which traverse an interface, particularly at an angle, these motions can include hydrodynamic instabilities of fluidized materials; after shock treatment, the interface of two solid materials can resemble breakers at an ocean shore. Such effects allow the bonding or cladding of metals essentially without diffusion across the interface, which constitutes the most important commercial process for metal working with explosives. In crystalline materials, shocks can produce comminution, the reduction of crystal structure into crystallites of powder dimensions. The shock may also rotate the crystallites about, into a distribution of orientations.

The release of electrons, production of defects, and the reduction of particle size in shocked materials can strongly influence the chemistry¹⁴ of the shocked state, and has been a focus of research. Shock induced defects are cited as having significant effects on compressional, mechanical, electrical, optical, thermodynamic, chemical, and structural processes in shock loaded solids.

A further example of morphological change induced by a shock is the removal of material at a free surface in the path of a shock. The reflection of the shock from the surface induces a tensile stress which can be sufficient to exceed the material's strength. This dynamic fracture of material is called spallation. Although spallation is most easily diagnosed in macroscopic samples, the processes must also take place on the microscopic level, e.g., in powders.

Shocks not only can produce powders and rip a material apart, they have been used in the compaction and sintering of powders. Precision parts of dissimilar materials such as aluminum and steel can be fabricated from admixtures by this means. Admixtures of powders may also be induced to

chemically react by the passage of a shock front. The production of defects in shocked materials is related to catalytic activity; accordingly, defect production in and the catalytic behavior of shocked powders, which have large surface areas, is a matter of investigation. In general, the powder sizes which have been used are larger than the thickness of the shock front.

Phase changes in condensed matter have been induced by shock waves, e.g., the conversion of graphite to diamonds, martensitic transformations in stainless steel, and phase transformations in ceramic powders. Of particular interest is the design of a shock treatment which permits recovery of the sample. The largest number of metallurgical recovery experiments have been concerned with fee metals. Hardening in metals is related to defect production, phase transformation, and morphology. All of these have been studied in shock treated metals. Several review articles on the metallurgical effects of shock waves are cited in references.²⁰

Polymerization by shock waves has also been studied for various organic substances. The existence of a pressure threshold has been demonstrated in acrylamide, 5 GPa being insufficient; multiple shocks have been shown to be effective in enhancing polymerization.

Magnetic effects might be suspected to be influenced by shock passage, and indeed a few observations have been made in this area. Piezoelectric effects of shocks have been seen in the 0.01-0.9 GPa range, and piezoresistive effects in the 1-14 MPa range. Refractive index changes have been charted in the 5-50 GPa range.

The compression of atoms into close proximity to one another is necessarily influenced by the interatomic potentials, and studies have been addressed to this topic. The potentials gained from shocks, in which the material likely is at elevated temperatures, has a greatly disturbed lattice and may even be ionized, may not be directly applicable to the modelling of materials at room temperature and below.

Pressure ranges over which many of these effects have been experimentally investigated are displayed in Figure 3. Chemical experiments have also been conducted at much lower ranges, e.g., 0.5-2, MPa. Many of the effects are limited by the onset of melting at very high pressures, and thus cannot be investigated by the highest shock pressures available. For example, defect structures can be annealed out by a shock or thermally-induced melting. At yet higher pressures, the thermal radiation emitted by a free surface of the material signals the arrival of the shock front.

SHOCK DRIVERS

The methods and machines for driving shocks in solid materials may be compared on the basis of the peak shock pressures which have been produced and measured (or inferred by suitable means) for each of the various drivers. Reported pressure ranges of experimentally measured shocks are shown in Figure 4 for several types of shock drivers operating in planar or nearly planar geometry. The maximum pressure attainable with a given driver will be dependent upon the material in which the shock is propagated, so that many materials will not be able to access the highest peak pressure of which the driver is capable. Furthermore, shocks dissipate energy as they propagate, with an attendant drop in pressure (see Figure 2, above). Techniques for generating converging shocks, e.g. shaped explosive charges, implosion of spherical or cylindrical shells, etc., are not included in the figure. The highest static pressure attained in the laboratory,²¹ 0.25 TPa (2.5 Mbar), was in a diamond anvil cell, a device which presses a sample between two gem quality diamonds having facets a fraction of a millimeter in diameter;²² higher pressures than this may be achieved in future laboratory experiments.

The drivers portrayed together in any one category in Figure 4 are not necessarily identical. For example, the data for chemically explosive drivers encompass the relatively simple sandwich structure ignited by an explosive lens, as well as the chemically explosive flyer plate driver, of which several variants exist. Overall planarity is not always achieved: the sample is generally held in a cavity in a metal plate, and radially propagating shock and release waves do get set up at the boundaries

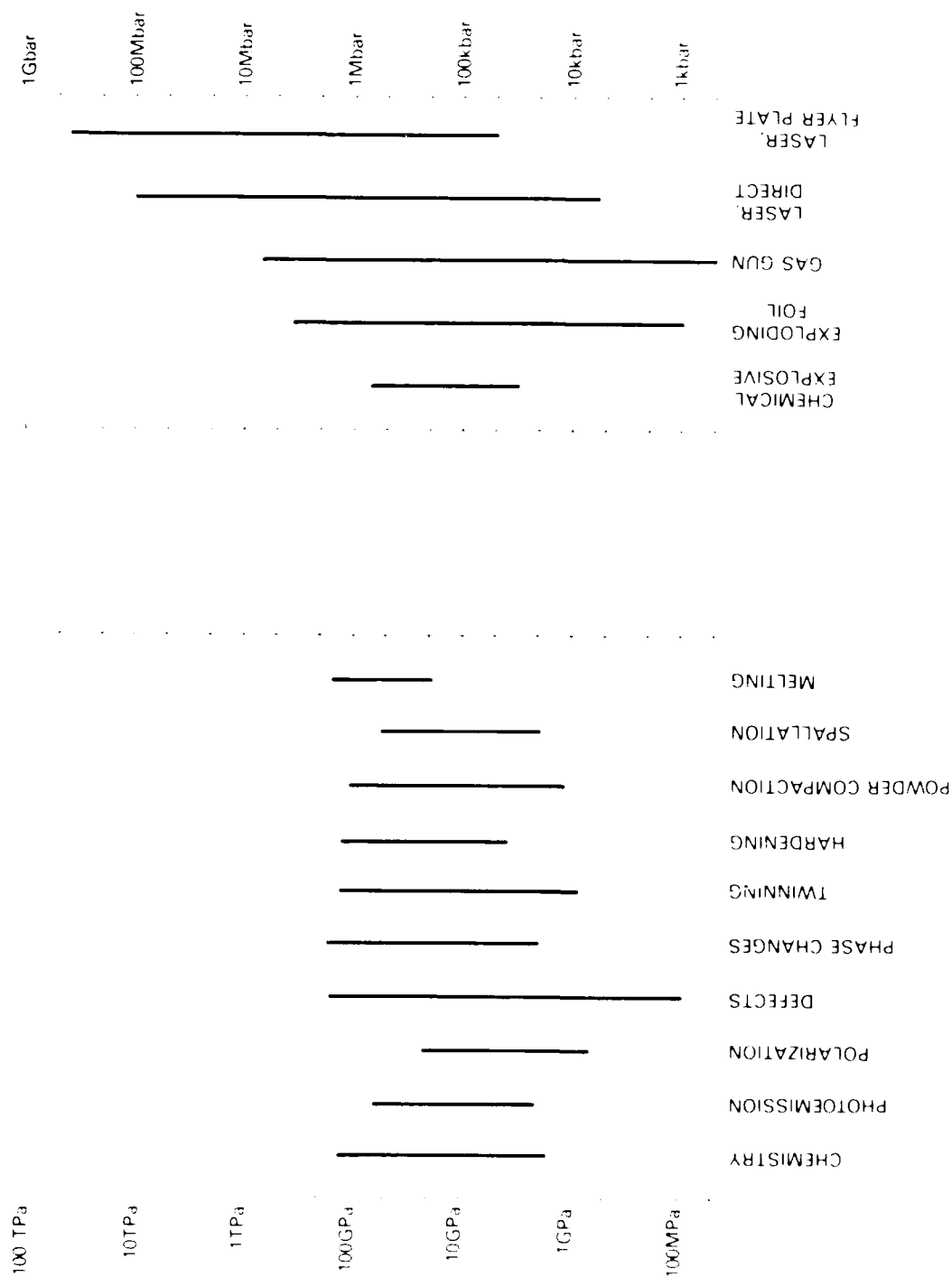


Fig. 4 Pressure ranges of shock drivers.

Fig. 3 Pressure ranges of experiments on shock effects.

of the sample cavity. Also, pressure is increased by multiple shocks passing both radially and axially through the sample. The pressures attained depend primarily upon the type of explosive used, on the details of the geometry of the device, and on the materials employed.

Chemicals are not the only way to initiate an explosion. A thin material can be made to explode in response to the sudden deposition of heat in it by a large pulse of electricity. In one such device, an aluminum foil is exploded to form a plasma, which expands and accelerates a tantalum flyer plate. (It is also possible to generate shocks without a flyer plate by this method, that is, the Ta impactor also has shocks generated within it.) Impact velocities of 30 km/sec have been achieved with this "electric gun."¹⁵ On the low end of the pressure range, an exploding foil apparatus has been constructed according to theoretical predictions of pressures of but a few hundred MPa, to be applied in experimental studies of dislocations in crystals.

Another instrument for generating shocks is the gas gun. A gas gun expels a projectile from a barrel by the force of expanding propellant gases. The expansion of compressed gases yields more reproducible results than gases produced by ignited powders. Since the velocity of the projectile is limited by the sound speed of the compressed gas, the highest projectile speeds are obtained with gases of low molecular weight. A light gas gun projectile includes the flyer plate and a carrier called a sabot. The flyer plate is accelerated by a comparatively low pressure (a fraction of a GPa) over a relatively long time (few msec), which does not disturb the initial thermodynamic state of the flyer plate—a significant advantage for this technique of driving shocks; the temperature rise of the projectile during acceleration and prior to impact is only about 1 degree Kelvin. Single stage light gas guns can yield about 1.5 km/sec with kilogram projectiles 10 cm in diameter. In a two stage light gas gun, the propellant gas is compressed and heated by a piston driven from a powder discharge; the projectile then can achieve higher velocities, e.g., up to about 8 km/sec.

The rail gun, or electromagnetic launcher, is a device in which the projectile essentially becomes the moving part of an electric motor. Velocities of 10 km/sec have been achieved, corresponding to shock pressures of about 1 TPa. A combined gas gun rail gun has been reported in the construction phase, with an anticipated velocity for a 1 gram projectile of at least 15 km/sec.

A comparison of various flyer plate drivers is given in Table 1. It is readily apparent that orders of magnitude can separate the various drivers, depending on the parameter of interest. The needs of a pilot research project might be quite different than those of a production line application. For instance, a gas gun may be very useful for studying the equation of state of a metal, and yet be totally irrelevant to the surface hardening of a manufactured item by shock treatment.

Table 1. Flyer Plate Parameters. The characteristics of projectiles, generally taking the highest speed and associated values. The drivers may be operated in parameter ranges other than those cited. The temperature shown is after acceleration and prior to impact, and is often design dependent.

	Thickness cm	Diam. cm	Highest Velocity km/sec	Mass kg	Momentum kg m/s	Kinetic Energy MJ	Temperature Rise deg. K
Exploding foil	0.03	0.8	30	0.003	7.5	0.1	
Gas Gun, 1 Stage	2.5	10	1.7	1.1	1600	1.2	1
Gas Gun, 2 Stage	1.5	2.8	8	0.2	160	0.6	
Laser	0.01	0.1	100	10^{-3}	1	8×10^{-7}	7×10^3
Rail Gun	0.1	1	10	0.03	120	2	

APPLICATIONS OF LASER-GENERATED SHOCKS

The pressure profile produced by a laser pulse incident upon a material is primarily dependent upon the irradiance (power per unit area) absorbed by the material, but is also a function of other parameters, such as the laser wavelength and the details of the laser pulse's temporal profile. The mechanism by which laser pulses generate shocks in condensed materials is the ablation (evaporation and removal) of material from the absorbing surface: the momentum carried off by the evaporated or ionized surface atoms is balanced by momentum imparted to the bulk material. This momentum transfer produces the compression wave. Representative values of resulting pressures are given in Figure 5 for Nd-doped pulsed glass lasers. The data below 10 GPa pertain to absorbers covered by transparent material, a technique (applicable only to irradiances for which the transparent surface does not ionize appreciably) which confines the vapor, lengthens and increases the pressure pulse, e.g., from 60 MPa for a free surface in vacuum to 700 MPa for a confined target near 1 GW cm^{-2} .



Fig. 5. Pressures from Nd lasers at 1.06 micron. Solid dots, and open triangles, are in vacuum; points below 10 GW cm^{-2} are for over-layered targets. Definitions of irradiance vary for the different data sets.

Laser irradiation has been employed both for the removal of and production of defects in silicon. Removal of defects is accomplished by laser annealing, during which a melt layer is formed (thermally, not by shock heating) at the surface of the silicon by the absorption of laser energy. The strength of laser annealing is that macroscopic defects such as dislocations, stacking faults, and precipitates are absent in the recrystallized layer, but the process also introduces defects (evidently point defects) which remain and are a disadvantage for some electron device structures.¹¹ At these irradiances, below about 100 MW cm^{-2} , defect production mechanisms other than shock generation are in view.¹² Intentional introduction of defects at higher irradiances has been pursued as a gettering technique, using repetitively pulsed Nd lasers which can focus to about 100 GW cm^{-2} . A pulsed laser beam is impinged directly onto the back surface of the semiconductor, typically in air, to create defects. Thermal processing allows unwanted impurities to migrate to the defects where they become trapped; the laser-damaged back layer, with the impurities, may then be chemically removed. Advantages of laser irradiation over mechanical means for gettering site production have been enumerated.

Defects in crystals affect not only their electrical properties, but also their x-ray diffraction properties. For this reason, x-ray diffraction is used to characterize shocked materials. It has been shown that the intensity of x-ray diffraction from an x-ray analyzing crystal is dependent upon the degree of perfection of the lattice. In some cases, higher diffraction efficiencies can be obtained by rendering the lattice "ideally imperfect," i.e., composed of small, disoriented crystallites. In lithium fluoride, an important x-ray analyzing crystal, the requisite disordering can be introduced by abrading and etching the surface of the crystal; however, for the more penetrating x-rays, which reach deeper than the 50 microns or so of disorder, the diffracted intensity reverts to the lower value typical of the perfect lattice. Mechanically flexing the crystal introduces sufficient disorder to yield the desired dependence of intensity with x-ray wavelength, but unfortunately at a reduced absolute value. The demonstrated ability of laser irradiation to harden metals (by introducing defects) to depths many times greater than 50 microns invites the shock processing of LiF x-ray analyzer crystals. Surface melting from direct irradiation may not be disadvantageous to the performance of analyzing crystals, and may possibly be reduced with a flyer plate technique.

The laser-accelerated flyer plate technique has already been employed to shock harden aluminum alloys, with peak pressures in the 5-15 GPa range. Shock waves produced by direct laser illumination has also induced surface hardening, and increased tensile and fatigue strengths: a single laser shot can produce a hardness the same as that of a heavily hammered surface in some materials. In certain materials, hardness increases with the number of shocks. Sheet samples of an aluminum alloy have been irradiated from two sides, and hardened throughout their 1.35 mm thickness, due to a shock-induced increase in dislocation density.

One might suppose that a longer pressure pulse, at constant pressure, would give the same hardening, and deeper. Experiments with exploding foil flyer plates at constant pressure and varying shock pulse duration in Cu-8.7%Ge reveal a more complicated result, showing a maximum in hardness.²⁸ This maximum is explained on the basis of the rates of twinning and dislocation production during the shock. Similar pulse length dependence for laser generated shocks would be expected in this material.

A list of possible industrial applications, once proposed (with suggested processing schedules) for other shock drivers²⁹ and largely applicable for the laser driver as well, includes tool steels, shafts, armor, punches, cutting tools, gun barrels, etc. Presently active industrial applications of shock processing by explosives,³⁰ some of which are obviously not relevant to the laser driver, include rock blasting (although direct cutting of rock with lasers has been investigated), metal bonding, modification of ceramic powders, and diamond synthesis.

The synthesis of stable and metastable phases of solid materials by shock treatment has been demonstrated, and attempts have been made to shock synthesize superconductors. Superconductors have no resistance, and therefore do not introduce resistive power losses into the transmission of electrical energy through them. The main difficulty is that they must be operated below a critical temperature which is, in all superconductors thus far fabricated, too low for economical use in power transmission. Many superconducting materials exist in a metastable phase. The ability of lasers induce phase changes by shock processing in a non contact fashion with good control, and even to shock wires in cylindrical geometry in a pulsed repetitive fashion, make this technology worth investigating more fully.

The higher irradiances are important in evaluating the equation of state of materials at high pressures, for which a uniform planar shock is best suited to the required precision. An advance in laser irradiation uniformity, and hence shock uniformity, has recently been achieved with Induced Spatial Incoherence, a technique for spatially and temporally homogenizing larger scale beam structures.³¹ This technique may be transferrable to other experiments and processes requiring a uniform, focused, but essentially planar, irradiation pattern.

X-RAY LITHOGRAPHY

The pervasive influence of the microelectronics industry on commercial activities of almost all sorts is widely recognized. The overall importance of the power of information retrieving and processing equipment is poorly estimated by considering only the magnitude of annual sales volume. The recognition of the role of this industry has resulted in its sustained growth; and yet, forecasts anticipate a levelling off in the near future. The growth of the industry has been directly linked to the continued diminution of sizes on microchips, illustrated in Figure 6:³² the smaller the feature sizes, the greater the number of elements per chip, and the greater the capability of the resulting circuit per unit cost³² and, generally, the greater the speed.

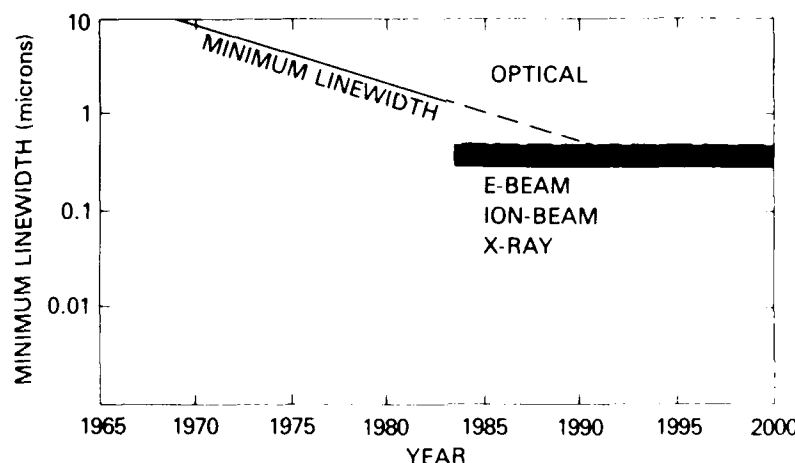


Fig. 6 -- Trend of linewidth in integrated circuits. Courtesy of R.T. Bate, Texas Instruments, Inc.

Present efforts to sustain growth and realize the next generation of improvement in processing power are therefore centered on techniques for further miniaturization of microcircuits. One major thrust in this effort is the attainment of commercially viable processes to produce smaller linewidth features on microchips, but with the same basic device structures as used heretofore. A more novel approach is to develop a totally new type of structure around quantum well devices.³² This paper will indicate ways in which processing steps with laser-produced plasmas might contribute to each of these major thrusts.

In this section, an introduction to lithographic concepts is followed by a brief summary of results of research performed at this Laboratory on the technical feasibility of attaining of small linewidths by x-ray lithography, using a laser plasma (LP) as an x-ray source. The principal advantages and limitations of this method are then outlined and areas of future work suggested, and lastly, the present status of commercial application is indicated.

LITHOGRAPHY CONCEPTS

Commercial fabrication of microcircuits includes patterning of thin films of different materials on the surface of a semiconductor, and patterning of relatively dilute concentrations of dopants near the surface. The patterning steps are performed by techniques conceptually similar to some originally employed in the printing of lithographs. Optical lithography for circuit manufacture involves placing a mask, i.e. a pattern of dark and light areas on the surface of a transparent substrate such as a glass plate, between a wafer of semiconductor material and a light source. The light exposes a photosensitive polymer layer called a photoresist which has previously been coated onto the semiconductor's

surface. Development of the exposed resist removes portions of the resist according to the pattern of exposure, the net result being a replication of the mask pattern in the polymer. Optical lithography is easily performed for feature sizes of 5 micrometers or greater, with successively greater care required as one approaches 1 micrometer, i.e. a few times the wavelength of visible light. Submicron lithography is performed with shorter photon wavelengths, or with electron beams or ion beams. Accordingly, lithography with x-ray photons is of interest, their wavelengths being orders of magnitude smaller than the visible. Applications of fine line fabrication outside the field of microelectronics, the comparison of electron, ion, x-ray, UV, and optical lithographies, the evaluation of the suitability for lithography of various types of x-ray sources, and other topics related to lithography have been well reviewed by Nagel,^{33,34,35} and will not be treated here in such detail.

LASER PLASMA X-RAY LITHOGRAPHY FEASIBILITY

In one suggested arrangement for a laser plasma (LP) x-ray lithography exposure facility, a high-power laser directs a pulsed beam into an exposure chamber and onto a target, typically at an irradiance near or above about 10^{13} W/cm² and in a focal diameter of a fraction of a millimeter. During the laser pulse, the target material is heated to a temperature sufficiently high to cause x-ray emission, about a million degrees Kelvin. The x-rays radiate away from the target in all directions, and pass through masks held in alignment with their respective semiconductor wafers. The conditions are chosen to produce x-rays which pass through the mask substrate, but not through the pattern defined on the mask. The mask substrate itself must be thin in order to achieve low x-ray absorption.

An early test of the feasibility of LP x-ray lithography was performed at this Laboratory,^{36,37,38,39,40} and exemplified many relevant characteristics of the x-ray source: source size, spectral content, emission efficiency, debris patterns, and submicron replication. A Q-switched Nd:glass laser put about 30 Joules onto an aluminum slab target in a 40 nsec pulse. The plasma emits visible, UV, and x-ray photons, as well as plasma particles (electrons and ions) and vapor. The full width at half maximum of x-rays near a kilovolt in energy was 15 nsec. An x-ray mask, composed of a gold pattern on a beryllium substrate, was held in close proximity to a silicon wafer coated with a resist. Kilovolt x rays exposed the resist through the mask, and the resulting patterns were developed by spraying with the appropriate solutions. Electrical tests⁴¹ were performed to assess radiation damage to the silicon by the x-rays.^{36,39,42}

The spatial distribution of x-rays emitted above 1 kilo-electron Volt (keV) was recorded with pinhole cameras of differing sensitivity and resolution. As shown in Figure 7, the highest intensity of x-ray emission originates in a region about 0.4 mm by 0.6 mm. Measurable x-radiation does arise from a much larger plume (Figure 7b). (Materials synthesis in such plumes is the subject of other work reported in these Proceedings.⁴³) The importance of the emission pattern to lithographic exposure levels, however, is more properly represented by the smaller size of the high resolution image. The penumbral blurring from this source is adequately small to attain line widths under one micron (see below) by placing the mask very near to the resist, i.e., within several tens of microns.

The spectra of LP x-ray sources above a kilovolt in photon energy are fairly distinctive, being composed of emission lines and continua, both of which are characteristic of the target material, its degree of ionization and other plasma properties. The spectrum of an aluminum target near 1 kilovolt, taken with the 40 nsec laser and given in Figure 8a, exhibits a cluster of lines about 1.6 keV which contain nearly 90% of the spectral energy above a keV, and lower-lying but nonetheless noticeable continuum contributions having low energy limits at the ionization energies of the various aluminum ions of which the plasma is composed. The continuum falls rapidly with a slope that depends on the plasma temperature; a very few photons are produced at high photon energies, and the number of these which are absorbed per shot by a wafer will fluctuate. A typical high energy LP continuum spectrum (obtained under other conditions) is indicated in Figure 8b. (The continuum of an electron impact x-ray source, such as an x-ray tube has an entirely different shape, with significant continuum levels all the way out to the accelerating energy of the electrons.) There is also an intense contribution predominantly below 1 keV, composed of lines and a differently shaped continuum. If a mask

substrate were so chosen as to allow longer wavelength, lower energy (e.g., visible) photons to expose the resist through the mask, loss of resolution by diffraction of these photons might result. This region of the spectrum was effectively absorbed by the Be mask substrate, and therefore did not contribute to the lithographic exposure.

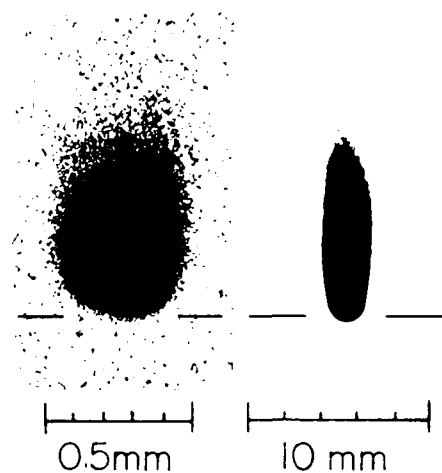


Fig. 7 X-ray images of an aluminum plasma (a) at high resolution (about 25 microns) showing the hottest region and (b) at low resolution (about 1 mm) showing the plume.

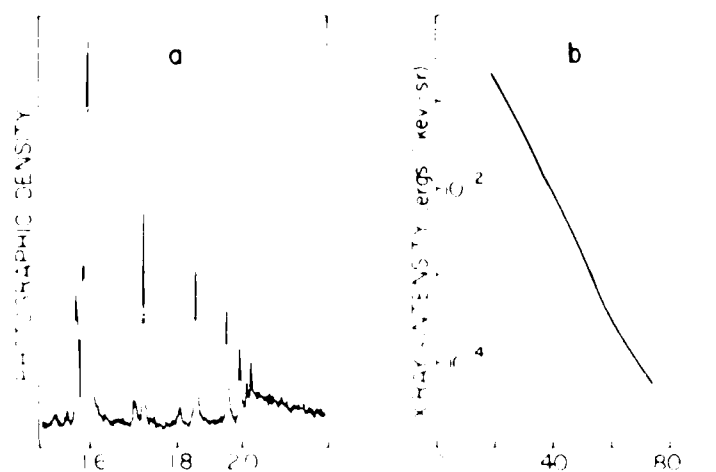


Fig. 8 Spectra from laser plasmas. (a) Trace of photographic density clearly reveals the weaker lines and the continuum above about 2.4 keV. Unfolded intensity is dominated by the 1.6 keV group of lines. (b) High energy continuum, taken under other conditions.

The beryllium mask substrate was nominally 25 microns thick, and the gold pattern 500 nm thick. At these thicknesses, the absorption in the gold (beryllium) would be at least 99% of the photon energy below 0.9 (0.8) keV, 82 (49)% at 1.6 keV, and 86 (9)% at 3.0 keV. It is desired that the substrate foil be uniformly absorbing across its area.⁴⁴ This absorption of photons in the mask and gold pattern produces heating, which in turn induces thermal expansion. According to a calculation³⁹ which does not account for any other heat loads or for thermal conduction, the heating produced by the 1.6 keV photons is but a couple of degrees in Be, although the heating of the gold would be over 100 degrees C. Warpage might result, and differential expansion between substrate and pattern could possibly delaminate the mask. However, when the patterned side of the mask is placed away from the source (as in this work), so that the substrate alone absorbs the abundant UV radiation, a significant additional heat load on the substrate does result. This effect may be used to render the temperatures of substrate and pattern more nearly isothermal. Also, thermal equilibration times are less than the laser pulse duration over distances of 1 micron (the thermal diffusivity of beryllium is 6×10^{-5} m²/s, and that for gold 10^{-4}). The gold pattern is evidently isothermal with a significant thickness of the substrate which may retard delamination. Thus, it is important to evaluate mask substrate and pattern heating, and to do so in the light of the details photon deposition and mask design.

Another attribute of laser-produced plasmas, the emission of target material itself, can be deleterious to the mask if care is not taken. The pattern of aluminum vapor and debris, which was emitted by these solid slab targets and caught on a glass plate, is reproduced in Figure 9. The majority of debris is confined within a well defined cone of fairly large half angle, 55 degrees in the present case.³⁹ Generally speaking, the debris emission prevents placing the mask in the region of most intense x-ray emission, when microcircuits are to be made. The amount of such debris can be reduced appreciably by suitable target design, e.g., a thin foil target which does not contain the large reservoir of meltable material of a slab target.³⁹ It is possible to fabricate the target of a disc sufficiently thin that it is completely vaporized by the laser pulse; this disc may then be held on a thinner, larger foil for mounting. Nonetheless, some target material will always be present and may proceed by line of sight toward the mask. Having taken measures to reduce the quantity and particle size of such material, it is anticipated that the material can be caught on another film which is interposed between the source and the mask. This catcher film, of course, must be appreciably transparent to the x rays which are to expose the resist. Likely as not, the catcher film will absorb the subkilovolt x rays, which then would not be available to thermalize the mask. While these considerations have been conceptualized, they remain to be rigorously demonstrated in practice.

Exposure of polybutene-1-sulfone (PBS) resist was performed at a distance of 5 cm from the source, by a series of 90 laser shots.³⁶ The mask and wafer were in close proximity to each other, 5 cm from the source at an angle of about 40 degrees from the incident laser beam, i.e., within the debris cone.³⁹ With this non-optimized system, the x-ray output of about a third of the shots was significantly below the norm, due largely to insufficient optical isolation of the laser from the target in the system as it was then configured. Part of the mask was covered by a series of Be filter layers with graded x-ray attenuation; the exposure behind this step wedge was quantified and the sensitivity of the resist determined (5 J cm^{-2}) and found to be in reasonable agreement with previous values from continuous wave x-ray exposures (14 J cm^{-2}). More recent results with a single shot, 1 nsec exposure of PBS by a laser produced plasma found the resist to be more sensitive than for steady exposures.⁴⁵ Partial exposure of the resist results in partial development, such that the topography of the resist receives the mask pattern in relief, but not to the extent that the valleys descend fully to the wafer. (A similar topographical effect can be expected in exposures by photons insufficiently penetrating to reach the full depth of the resist.) In a region of the mask subject to such a partial exposure, a relief pattern showing features of 0.75 microns (the narrowest structures on the mask) was recorded (see Figure 10), thus demonstrating the feasibility of producing fine lines by this method.

In addition to the mask exposure test, a concurrent exposure test was performed on MOS capacitors, to determine whether the ionizing lithographic exposure would induce electrically significant radiation damage. Capacitors consisting of 100 nm thick aluminum dots were evaporated onto a dry silicon oxide layer on the silicon substrate. These test structures were protected by an 18 micron Be

foil (i.e., thinner than the mask substrate), and placed 5 cm from the plasma. The radiation hardness of these wafers was found to be less than in wafers not subject to ionizing lithography.⁴² Capacitance/voltage curves³⁹ taken before and after irradiation yielded no change in shape and less of a shift than in similar tests following exposures by x-ray tubes and electron beams.⁴¹ It appears, however, that the presence of impurities in the oxide layer was the controlling factor in these findings, rather than the lithographies used.⁴⁶ The impurities can evidently be avoided by appropriate processing steps.



Fig. 9 — Debris pattern recorded on a glass plate placed in front of Al targets.

EVALUATION

The advantages and disadvantages of x-ray lithography in general, and of various plasma sources in particular, have been enumerated elsewhere.^{33,34,35} The advantage of greatest moment, of course, is the ability to attain finer resolution than with conventional optical methods. Some of the limits on this resolution vary with system design: source size, geometrical placement of components (source, mask, wafer), and the diffraction of photons which reach the resist. Other limits are more fundamental: smearing produced by energetic photoelectrons liberated in the resist by the x-ray absorption process, and effects produced by the inevitable damage sites which are formed by ionizing radiation (e.g., electrical power losses and leakage). A systematic comparison of the electrical side-effects of laser plasma x-ray lithography remains to be carried out; initial investigations are beginning to develop a partial view. It has been found that the electrical effects of lithography with ionizing radiations are dependent on the details of the structures and materials present at the time of irradiation; for this reason, radiation hardness tests on finished devices may not give the same effects as those undergoing processing, and effects may be different for different processing agendas. Thus, the evaluation of radiation effects is likely to remain a matter for further investigation, especially as processing techniques evolve. Research in this area should be conducted with repetition and verification until the controlling parameters are well understood. Mask heating remains a consideration which is deserving of further investigation. Protection from debris is clearly a need, the details of which must be worked out. Single shot lithographic exposures have been performed with LP x-ray sources, but the variability experienced in x ray output from these sources leads one rather to consider a multi-shot scheme.⁴⁷

In addition to reducing the heat load on the mask in a system with less energy per pulse, the precision in integrated exposure can be increased,⁴⁷ while reducing the cost of the laser. Such an approach has been demonstrated with a 10 Hz Nd laser,⁴⁷⁻⁴⁸ although the exposure time for presently available lasers is again too long⁴⁸ (15 to 60 min.) for a commercially attractive lithography system. The development of higher average power, repetitively pulsed lasers may have an impact here.³⁴ It has been pointed out that the 1 micron wavelength of Nd lasers is not optimal for x-ray lithography, and that a greater x-ray output would be expected from shorter wavelengths.³⁴ This expectation was recently corroborated experimentally with a KrF laser operating at 249 nm: a hundred shots exposed a less sensitive resist in under two minutes, a very inviting result.⁴⁹

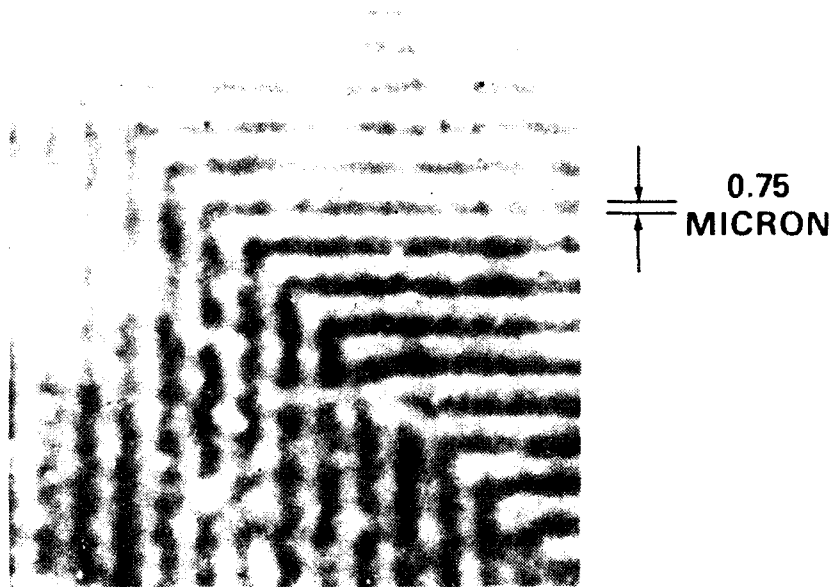


Fig. 10 — Submicron replication achieved by x-ray lithography with Al plasmas.³⁹

LITHOGRAPHY APPLICATIONS STATUS

X-ray lithography has proceeded through a number of phases of development. After initial investigations were made, devices were made in low quantities to serve demonstration, research, or customized purposes. Bubble memory devices with 1 micron features have been fabricated by x-ray lithography on a production line basis by Intel.⁵⁰ Although the center of gravity of the industry is still solidly in the optical lithography region, electron impact x-ray lithography systems⁵¹ and exposure sources are now on the market, e.g., Perkin-Elmer's new step-and-repeat unit and the Micronix flood exposure unit.⁵² In addition, electron discharge plasma sources are being offered for x-ray lithography by Maxwell.⁵² The laser plasma x-ray source has been under development by Spectra Technology, and an integrated x-ray lithography system employing a laser plasma x-ray source is being developed by Hampshire Instruments.⁵²

In summary, x-ray lithography is presently in its early phases of commercial productivity. The research performed on laser plasma x-ray sources is bearing fruit in the development, now in progress, of x-ray lithographic systems for the commercial market. Further advances in optimization of the laser plasma exposure system are anticipated to enhance the strength of this application of laser technology.

EVAPORATIVE COATING

Above laser densities of about 10^5 to 10^6 W/cm² impinging on a solid target, vapor and other forms of material begin to be expelled from the irradiated region. These other forms include expanding plasma (above about 10^8 to 10^9 W/cm²) and ejected liquid, e.g. globules. Various mechanisms are responsible for the ejection of liquid, including microexplosions beneath the surface, and the forcing out of liquid by the pressure pulse associated with laser-driven ablation. Despite the fact that the prospect of using laser-produced evaporation as a coating technique was pointed out early and has continued under investigation,⁵³ the technique has evidently not been competitive with the numerous alternative technologies. This is likely due in part to the perception that other coating systems offer better control, higher deposition rates, and superior coating uniformity over larger areas. It remains, then, to examine whether specialized uses for laser evaporative coating offer significant advantages over other means.

An example of coating quality for the higher irradiance regimes, where ejecta are emitted, is typified by Figure 9; the uniformity of the coating would obviously be poor over most, if not all, of the available solid angle. However, such results need not be taken as optimum. Carbon films produced by pulsed laser plasma deposition (about 1 J-pulse, 9 nsec, 10 Hz, Nd laser) were smooth in thickness down to micron distances laterally, although thickness did vary gradually on a scale of centimeters.⁵⁴ (Aluminum films prepared from rod targets in the same investigation were visibly not smooth.)

The laser source can be adjusted to emit vapor or plasma, depending on the irradiation conditions. The degree of ionization of the emitted plasma is also under control, together with the energy of the emitted plasma ions. Since the energy of the ions is dependent on the plasma temperature, the uniformity of the laser irradiation can be important. The degree of ionization can be reduced by passing the ions through a low pressure gas, to enable charge exchange to take place. Each of these parameters is reasonably reproducible, and may be diagnosed with the appropriate instrumentation. Thus, the laser coating source can be well characterized and adjusted over many of the parameters of interest.

The coating rate is dependent upon both the laser and the target parameters, as well as the geometry of the coating setup. The carbon films previously mentioned were deposited at the rate of 0.1 Angstrom pulse, at a distance of about 5 cm. Thus, sub Angstrom control is offered by the laser coating technique, with thicknesses of 0.1 micron being obtained in about an hour and a half. Other workers have obtained rates of under 1 to 10^6 Angstrom sec for various materials⁵⁵ with peak laser powers ranging from 160 W to a GW.

These coating rates and degrees of control are within the range of possible application to the fabrication of such structures as superlattices,⁵⁶ quantum devices,⁵⁶ and multilayers.⁵⁷ The laser evaporative coating source does not require the gas handling hardware of metal organic vapor deposition systems, and is compatible with high vacuum techniques such as are found in molecular beam epitaxy systems. Other laser processes, including laser chemical vapor deposition and laser annealing, are being considered for fabricating some of these structures. It is not to be anticipated that the laser coating source will replace the various systems now in use for research fabrication. However, laser evaporative coating can reasonably be expected to find further research applications, perhaps eventually even commercial applications, but these await a more thorough compilation of the attributes of the laser evaporative source in relation to the fabrication of these novel microstructures.

ACKNOWLEDGEMENTS

The author wishes to indicate his appreciation of the collaborative efforts of D. E. Nagel, M. C. Peckerar, C. M. Dozier, D. B. Brown, and J. R. Greig in relation to x-ray lithography, and to express his regard for the many fine papers, direct reference to which was unfortunately precluded by length constraints.

REFERENCES

1. Bohn, W.L. (1984), "High Power Lasers and Their Application in Materials Processing," SPIE, 491, pp. 204-209.
2. Ready, J.F. (1978), *Industrial Applications of Lasers*, Academic Press, New York.
3. Bass, M., ed. (1983), *Laser Materials Processing*, Vol. 3, North-Holland Publishing Co., Amsterdam.
4. Metzbower, E.A., ed. (1983), *Lasers in Materials Processing*, Am. Soc. for Metals, Metals Park, Ohio.
5. Breinan, M.E. and D.B. Snow, in Metzbower, op. cit., p. 255.
6. Breinan, E.M. and B.H. Kear, in M. Bass, op. cit., p. 235.
7. Bauerle, D. (1984), *Laser Processing and Diagnostics*, Springer-Verlag, New York.
8. White, C.W. and P.S. Peerey, eds. (1980), *Laser and Electron Beam Processing of Materials*, Academic Press, New York.
9. Poate, J.M. and J.W. Mayer, eds. (1982), *Laser Annealing of Semiconductors*, Academic Press, New York.
10. Osgood, R.M., S.R.J. Brueck, and H.R. Schlossberg, eds. (1982), *Laser Diagnostics and Photochemical Processing for Semiconductor Devices*, Vol. 17, Elsevier, New York.
11. Tang, C.C. ed. (1983), *Laser Processing of Semiconductor Devices*, Vol. 385, SPIE, Bellingham, WA.
12. Eden, J.G., et al., in Osgood, et al., op. cit., p. 185.
13. Meyers, M.A. and L.E. Murr, eds. (1980), *Shock Waves and High-Strain-Rate Phenomena in Metals*, Plenum Press, New York.
14. Nellis, W.J., L. Seaman, and R.A. Graham, eds. (1981), *Shock Waves in Condensed Matter*, Am. Inst. of Phys., New York.
15. Asay, J.R., R.A. Graham, G.K. Straub, eds. (1983), *Shock Waves in Condensed Matter*, North-Holland, Amsterdam.
16. Harding, J., ed. (1984), *Mechanical Properties at High Rates of Strain, 1984*, Inst. of Phys., London.
17. Trainor, R.J., N.C. Holmes, and R.A. Anderson (1982), "Ultrahigh Pressure Laser-Driven Shock Wave Experiments," In Nellis, et al., op. cit., pp. 145-154.
18. Guirguis, R.H. and E.S. Oran, in Asay, et al., op. cit., p. 351.
19. Ariga, S. and R. Sigel (1977), "Picosecond Microphotography of Laser-Irradiated Solid Targets," SPIE, Bellingham, WA, 97, p. 421.
20. Meyers and Murr, op. cit., p. 488.

21. Goettle, K.A., H. Mao, and P.M. Bell (July 1985), "Generation of static pressures above 2.5 Mbar..." *Rev. Sci. Instrum.*, 56, p. 1420.
22. Skelton, E.F. (Sept. 1984), "High-pressure research with synchrotron radiation," *Physics Today*, pp. 44-52.
23. O'Keefe, J.D., C.H. Skeen, and C.M. York (Oct. 1973), "Laser-induced deformation modes in thin metal targets," *J. Appl. Phys.*, 44, p. 4622.
24. Grun, J., S.P. Obenshain, B.H. Ripin, R.R. Whitlock, E.A. McLean, J. Gardner, M.J. Herbst, and J. Stamper (Feb. 1983), "Ablative acceleration of planar targets to high velocities," *Phys. Fluids*, 26, pp. 588-597.
25. Clauer, A.H., J.H. Holbrook, and B.P. Fairand (1981), "Effects of Laser Induced Shock Waves on Metals," in Meyers and Murr, op. cit., Ch. 38.
26. Kimerling, L.C. and J.L. Benton, "Defects in Laser-Processed Semiconductors," in White and Percy, op. cit., p. 385.
27. Pearce and Zaleckas (Aug. 1979), "A new approach to lattice damage gettering," *J. Electrochem. Soc.*, 126, p. 1436.
28. Wright, R.N., D.E. Mikkola, and S. LaRouche, in Meyers and Murr, op. cit., p. 706.
29. Meyers, M.A. and R.N. Orava, in Meyers and Murr, op. cit., p. 820.
30. Bergmann, O.R., "Industrial Uses of Explosive Pressure—from Rock Blasting to Metal Bonding and Synthetic Diamond," in Asay, et al., op. cit., p. 429.
31. Lehmberg, R.H. and S.P. Obenshain (June 1983), "Use of Induced Spatial Incoherence for Uniform Illumination..." *Optics Comm.*, 46, pp. 27-31.
32. Bate, Robert T., Texas Instruments, private communication.
33. Nagel, D.J. (1981), *Ultraviolet and Vacuum Ultraviolet Systems*, Vol. 279, SPIE, Bellingham, WA, pp. 98-110.
34. Nagel, D.J. (1984), "Plasma Sources for X-ray Lithography," *VLSI Electronics Microstructure Science*, N.G. Einspruch, Vol. 8, Ch. 6.
35. Nagel, D.J. (1985), "Laser-Plasma Sources for X-ray Lithography," *Microelectronic Engineering*, K.D. van der Mast and S. Radelaar, Vol. 3, North Holland, Amsterdam, pp. 557-564.
36. Nagel, D.J., M.C. Peckerar, R.R. Whitlock, J.R. Greig, and R.E. Pechacek (Nov. 1978), "Submicrosecond X-ray Lithography," *Elec. Lett.*, 14(24), pp. 781-782.
37. Nagel, D.J., J.M. McMahon, R.R. Whitlock, J.R. Greig, R.E. Pechacek and M.C. Peckerar (1978), "Lithography and High Resolution Radiography with Pulsed X-rays," *Japanese J. Appl. Phys.*, 17, pp. 472-475.
38. Nagel, D.J., R.R. Whitlock, J.R. Greig, and R.E. Pechacek (1978), "Laser Plasma Source for Pulsed X-ray Lithography," *SPIE*, 135, pp. 46-53.
39. Peckerar, M.C., J.R. Greig, D.J. Nagel, R.E. Pechacek, and R.R. Whitlock (1978), *Proc. of the Symposium on Electron and Ion Beam Science and Tech., Eighth Int. Conf.*, Vol. 78-5, R. Bakish, Electrochem. Soc., Princeton, NJ, pp. 432-443.

40. Whitlock, R.R. (to be published), X-ray Lithography with Plasma Sources: A Compendium, NRL Memorandum Report 5731.
41. Peckerar, M., R. Fulton, P. Blaise, D. Brown, and R. Whitlock (Nov. 1979), Radiation effects in MOS devices caused by x-ray and e-beam lithography, *J. Vac. Sci. Tech.* 16(6), pp. 1658-1661.
42. Hughes, H.L. (Dec. 1979), "Radiation Hardness of LSI VLSI Fabrication Processes," *IEEE Transactions on Nuclear Sci.*, Vol. NS-26, No. 6, pp. 5053-5055.
43. Matsunawa, A., et al., Proceedings of the Fourth International Congress on Applications of Lasers and Electro Optics (CALEO 85), held 11-14 Nov 1985, San Francisco, CA.
44. Whitlock, R.R. and J.A. Sprague (Sept. 1984), "Thickness Variations in X-ray Filters and Laser Targets," *Appl. Phys. Lett.*, 45, pp. 504-506.
45. Yaakobi, B., J. Kim, J.M. Soures, H.W. Deckman, and J. Dunsmuir (Oct. 1983), "Submicron x-ray lithography using laser-produced plasma as a source," *Appl. Phys. Lett.*, 43, pp. 686-688.
46. Peckerar, M.C., C.M. Dozier, D.B. Brown, D. Patterson, D. McCarthy, and D. Ma (Dec. 1982), "Radiation effects introduced by x-ray lithography in MOS devices," *IEEE Trans. Nuc. Sci.*, NS-29, pp. 1697-1701.
47. Nagel, D.J., C.M. Brown, M.C. Peckerar, M.L. Ginter, J.A. Robinson, T.J. McIlrath, and P.K. Carroll (May 1984), "Repetitively Pulsed Plasma Soft X-ray Source," *Appl. Opt.*, 23, pp. 1428-1433.
48. Gohil, P., H. Kapoor, D. Ma, M.C. Peckerar, T.J. McIlrath, and M.L. Ginter (July 1985), "Soft X-ray Lithography Using Radiation from Laser-Produced Plasmas," *Appl. Opt.*, 24, pp. 2024-2027.
49. O'Neill, E., M.C. Gower, L.C.E. Turcu, and Y. Owadano, "X-ray Lithography Using a KrF Laser-Plasma Source," accepted for *Applied Optics*.
50. Rose, Don, Intel Corp., private communication.
51. Hayasaka, T., S. Ishihara, H. Kinoshita, and N. Takeuchi (Aug. 1985), "A step and repeat x-ray exposure system for 0.5 micron pattern replication," *J. Vac. Sci. Technol.*, B3(6), pp. 1581-1586.
52. *Lasers and Applications*, Oct. 1985, pp. 36-40.
53. Duley, W.W. (1983), *Laser Processing and Analysis of Materials*, Plenum Press, NY.
54. Marquardt, C.L., R.L. Williams, and D.J. Nagel (1985), "Deposition of amorphous carbon films from laser produced plasmas," *Mat. Res. Soc. Symp. Proc.*, Vol. 38, pp. 325-335.
55. *Superlattices and Microstructures*, Vol. 1, 1985.
56. Chemla, D.S. (May 1985), "Quantum wells for photonics," *Phys. Today*, 37, pp. 57-64.
57. Marshali, G.E., ed. (1985), *Applications of Thin Film Multilayered Structures to Focused X-ray Optics*, Vol. 563, SPIE, Bellingham, WA.
58. Figure used by permission

LITHOGRAPHIC TECHNIQUES: AN OVERVIEW

M. C. Peckerar
U.S. Naval Research Laboratory
Washington, DC 20375-5000

ABSTRACT

The major lithographic methods used in the production of integrated circuits are described. The limitations of each of these methods are outlined and contrasted. Emphasis is given to the optical aspects of pattern replication as well as to topics relating to illumination sources. Areas of advanced development, such as e-beam and x-ray lithography, are described.

I. Introduction

Lithography is the technique of reproducing pre-determined patterns on arbitrary surfaces. In semiconductor work, the patterns are those of the devices to be fabricated on silicon wafers: diffusion tubs, metallization lines, oxide cuts, etc. We can list the goals of lithography of microelectronics:

- o To provide high-resolution images over as large an area as possible while controlling the critical dimensions (CDs) over the types of image plane topography normally found in IC processing.

- o To align the image with underlying features on the wafer surface.

- o To do the above tasks without damage to the devices fabricated.

Basically, these goals boil down to the following: the success of a lithographic process is defined as our ability to place a material boundary wherever we would like on a silicon wafer. This boundary could be the edge of a diffusion tub, the center point of a contact window, or any of a number of material delimiters needed to make an IC. Currently, the IC industry demands a capability to resolve submicron minimum features. These submicron images must be placed over the surface of a 4 inch diameter silicon wafer with 0.1 micrometer accuracy.

Our ability to set boundary positions is a major factor for consideration in determining *design rules*. Design rules are IC construction guidelines which tell us: (a) the minimum feature sizes for a given material or process; (b) how close we can reproducibly bring two features together without intolerable interactions occurring; and, (c) with what degree of accuracy we can place a given feature with respect to features already present on the substrate. These rules are important for a number of reasons. First, they set the maximum device density of the IC. Obviously, if the minimum MOSFET gate dimensions are $10\text{ }\mu\text{m} \times 10\text{ }\mu\text{m}$, we would have trouble fitting two such FETs in an area of $100\text{ }\mu\text{m}^2$. In addition, if we make the design rules "tight" (near the maximum performance limits of our processing tools), yields may be reduced.

Minimum feature sizes are not set simply by the optimum resolving power of the lithographic tool used. We have to take into account the surface on which the image is to be defined. If the surface is not flat, the image may appear out of focus. If the underlying surface is reflective, standing-wave patterns can form, changing the image dimensions. Two distinct images placed close together may interfere with each other. This is one example of a proximity effect. So far, the concepts of resolution, focus and alignment accuracy are used rather loosely. In succeeding sections these concepts will be given some mathematical substance.

The discussion below begins with an overview of current lithographic practice. The purpose here to describe the ranges of applicability (in terms of minimum resolved feature size and placement accuracy) of various types of lithographic systems. The points at which emerging techniques (such as deep-UV, X-ray and e-beam systems) become useful, are labelled. Various types of UV and

X-ray lithographic systems are described. This is followed by criteria for evaluating lithographic systems. Special emphasis is given to system optics and to source development.

1. An Overview of Conventional Lithographic Methods

The process of optical lithography for microelectronics is similar to the somewhat more familiar process of photography. In lithography, silicon wafers are, essentially, turned into photo-plates by the application of photo-resist (a thin, light-sensitive plastic film). In some sense, the process of lithography is simpler than that of photography. In photography, light of many colors and intensities is used to create an image. In lithography, the range of exposing wavelengths is extremely narrow. Every attempt is made to assure uniform intensity over the exposure field. The image is a shadow image of the desired set of shapes. The shadow image is created by a photographic mask. Some regions of the mask are opaque, stopping the incident light. Other regions are transparent. Light passing through the transparent regions falls on the underlying photo-resist (PR) exposing it. This is illustrated in Fig. 1. In some cases, where very high resolution is desired, the PR is exposed by a tightly focused electron or ion beam. This beam "writes" the pattern directly on the work-piece, filling in the shapes to be exposed much like a child coloring in a coloring book.

There are a number of variations of the optical or beam process. These variations are summarized in Fig. 2. Entries along the top of the figure indicate three separate exposure techniques: focused beam, pattern projection and simple shadow mask. Entries along the left-hand column indicate three different types of exposure source. This leads to eight distinctly different types of microcircuit lithography, each of which has been tried with some degree of success. The ninth entry, e-beam flood of a stencil-mask held close to the work-piece (with no intervening electron optics) was attempted by Westinghouse Electric Corporation in their "Ellipse" system. However, as of this writing, technical difficulties associated with this approach have not been surmounted.

If we read the figure from left to right, we get an historical survey of the field. The first lithography tools employed shadow masks which were in contact with the work-piece. Each time the mask came in contact with the wafer, though, there was a possibility of mask damage occurring. To remedy this, proximity-printers were used. Here, the mask was removed from the wafer by about 25 μm . This helped to reduce mask damage, but it severely degraded resolution (for reasons discussed below).

The next development in the field occurred when Perkin-Elmer Corporation introduced the full-wafer projection system. Here, a high-quality image of the mask is projected, like a photo-slide, onto the wafer. Resolution was better than that obtained with a proximity printer (but not as good as that seen with contact printers!). The optical field of full wafer systems is relatively large. The industry, at this writing, is going to 5" diameter wafers. It is difficult to maintain resolution over fields this large for a number of reasons. Even though the optical exposure source is nearly monochromatic, a number of spectral lines are admitted to the system. Chromatic aberrations can become a problem, as does astigmatism. Front-surface mirror lenses have been developed

to minimize chromatic aberration. But the wafer deformation through processing may cause large portions of the wafer to be out of focus in a full-wafer projection system. To remedy these problems, the exposure field size may be reduced to fill only a part of the wafer. Such a system is called a wafer stepper, since the image of a single chip is "stepped" across the wafer, a chip at a time.

As a final development, beam-forming lithographies are currently available. The photon beam occupies a central position in most conventional lithography schemes. The shadow masks used by all of the optical lithographies mentioned above are frequently made with such devices, often called "flashers". A lens-formed beam is shot onto an unpatterned, resist covered photo-plate. The beam is flashed on and off, delivering a precise amount of energy to expose the resist. The table on which the plate sits is moved under computer control to move the mask beneath the central optic axis and sweep out the desired exposure pattern.

Electron and ion beams are frequently employed for extremely high resolution resulting from the very short effective wavelength of these particles. These beams, though, are usually moved off the center-line to expose a small field before the table is moved. Electron and ion beams are also used to expose wafers directly as well as to make mask plates.

2. Evaluation Criteria for Lithographic Systems

The three most important evaluation criteria of any lithographic system are: minimum resolved feature size, depth-of-focus and positioning accuracy. The first two of these criteria are related to the optics of the image forming system. In fact, they are determined by a single aspect of the system optics: numerical aperture. Positioning accuracy is determined by the alignment subsystem. In paragraphs below, useful formulae for characterizing minimum resolved feature sizes and depth-of-focus are presented. Some fundamentals of alignment systems are presented.

First, let us examine the concept of numerical aperture (NA). This is shown in Fig. 3. The NA is seen to be the sine of the half-angle α subtended by the final lens aperture at the image plane multiplied by the index of refraction of the medium between the lens and the image plane. (For a microscope, α is measured from the object plane.) We can view the aperture as a spatial frequency filter. To faithfully reconstruct an image, many light-wave spatial frequencies must be summed. The smaller the NA, the fewer the number of these spatial frequencies that can be summed. This degrades image quality. Typically, we use the Rayleigh formula to relate minimum resolved feature size ΔX , to NA:

$$(1) \quad \Delta X = \lambda / 2(NA) = \lambda / 2n \sin \alpha$$

where:

- n - index of refraction of the medium surrounding the lens.
- α - half-angle subtended by the aperture at the image plane.
- λ - wavelength of the illuminating radiation

The relationship of NA to depth-of-focus (DF) is a bit less obvious. But inspection of Fig. 3 reveals the salient points. High numerical aperture systems have large cross over angles, α . This means that the light beams diverge rapidly on passing through their plane of optimum focus. The larger the value of α , the more rapidly the focused beams diverge for a unit displacement of the image plane. The DF can be taken as the image plane displacement which causes a point to spread into a disc whose diameter is that of the minimum resolved feature size. It can be shown that (under this assumption) the DF is given by:

$$(2) \quad DF = \lambda / 2(NA)^2$$

Fig. 4 is a plot of both depth-of-focus and minimum resolved feature size as a function of numerical aperture for conventional UV sources (436 nm) and for deep-UV sources (200 nm). Currently available UV and deep UV systems have NAs as high as 0.4. Thus submicron resolving power is well within the capability of such machines. However, if we flip to other axis of this figure, we see a less tractable problem. The DF is also submicron. Typically, it is possible to maintain the focal plane position to within a micron-per-centimeter over a silicon wafer radius. Stepper field sizes are usually 1cm^2 . Very high resolution optical systems defocus over the image field. This is a major drawback in high yield processing. This is a prime source of motivation for the development of x-ray and e-beam systems with greater depth of focus.

3. E-beam and X-Ray Lithography

The first submicron systems to become commercially available were e-beam systems. As mentioned above, these systems write with submicron diameter pencil beams of electrons. Electrons are brought to a focus and there is a cross-over angle which creates a finite depth of focus. But this angle is as small as 0.1 milliradian. Depth-of focus is rarely a problem here. Still, in commercially available systems (which write with 20 keV beams), the beam diameter is not the resolution limit. The interaction of the beam with the work piece does create the resolution limit. The beam splays out as it strikes the resist, depositing energy at a distance from the initial point of impact. Electrons can be re-directed (or "backscattered") from the bulk back into the resist. This creates what is called a proximity effect: unintentional exposure of resist a distance from desired exposure points. When a group of tightly spaced features appear, the problem is worse. Exposure contributions in a single ideally unexposed region can appear from each of the intentionally exposed features.

To model these effects, Monte Carlo techniques have been developed. Here, a single electron is followed about in its path through the solid. Various types of electron-matter interaction are given statistical weights based on likelihood of occurrence. Random number generators are used to select what (if any) interaction occurs over a given path length. Single electron histories are developed for a large number of electrons. Statistical distributions giving probabilities of position and energy deposition are thus derived. The results of such modeling are shown in Fig. 5. These results can be used to develop schemes to minimize proximity effect. However, the calculations are time consuming and expensive. Thus, for dense patterns, it is currently not commercially feasible to do such "first principles" corrections. Some heuristically

developed algorithms are helpful. It appears that such corrections are good to the half-micron level.

Resolution, though, is not the main problem associated with e-beam lithography for present integrated circuits. The whole e-beam process is inherently slow. The beam moves from exposure "pixel" to exposure "pixel" in a serial fashion. In a full raster-scan machine even unexposed pixels are addressed while the beam is blanked to prevent exposure. In the vector-scan mode, the beam is moved to an exposure field and rastered within the exposure field. Current machines write pixel exposure rates of 20-40 MHz (20-40 million pixels exposed in a second). This can mean exposure lasting hours for densely populated circuits on 4 inch silicon wafers. New machines, like the Aeble 150 (developed by Perkin-Elmer, under government contract) have "variable aperture" options, which can adjust pixel sizes from 2 μm diameters down to submicron diameters during the writing process. This can reduce exposure times by over an order of magnitude.

Machine reliability is also an important issue. A single e-beam machine may cost over two million dollars. Even large corporations may have only a single such machine. If the machine is damaged, major production hold-ups can occur. The high speed circuitry necessary to drive the machine and the associated computers are very complicated and it frequently takes days (if not weeks) to de-bug a problem. Thus, a "parallel" pixel exposure tool (which exposes a large number of pixels at once), without the complicated electronics, would be highly desirable for densely integrated circuits.

X-ray lithography can, potentially, provide such a tool. Here, short wavelength x-rays are used to create shadow images. Since lenses are not used, there is no depth-of-focus problem. Resolution is set by penumbral blur of the relatively broad x-ray source. This effect, as well as several other geometric distortion effects, are shown in Fig. 6. Conventional x-ray sources are electron-impact sources. As the source is separated from the work-piece, the penumbral problem is alleviated. But the x-ray intensity drops as the square of the separation.

This last statement underlines one of the major barriers to the implementation of x-ray technology for lithography. The sources are not bright enough. PMMA, a popular high resolution resist for submicron work, requires about a joule of energy incident per-square centimeter. Typical exposure times, even for the highest brightness electron impact sources, may be as long as minutes per square centimeter exposure field. This certainly does not allow the 20 wafer an hour through-put offered by commercial optical wafer-steppers.

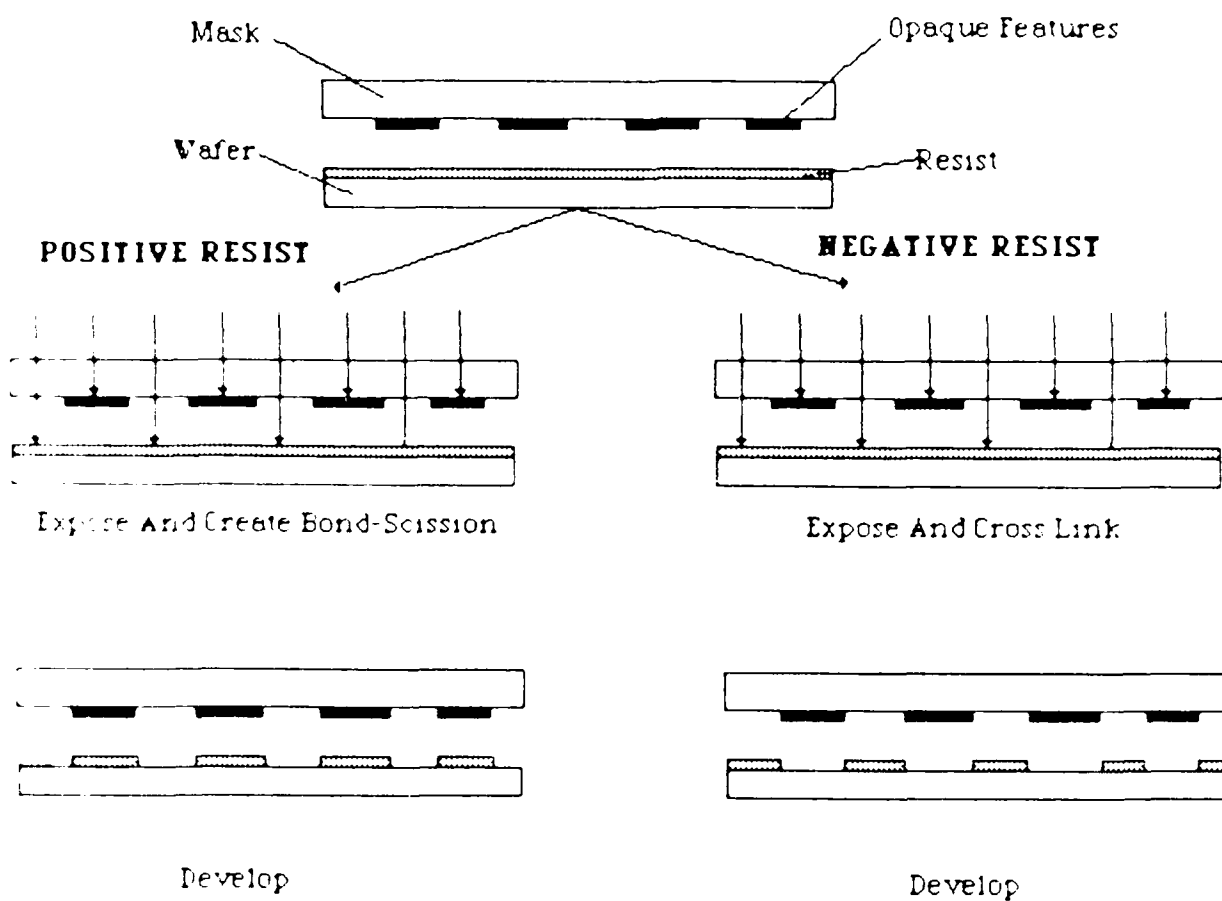
A second major difficulty with x-ray technology is the difficulty of obtaining good x-ray masks. To pass soft x-rays, thin membranes are required for the clear portions of the mask. A heavy metal absorber is used for the opaque region. A typical mask structure (using a boron nitride membrane and a gold absorber) is shown in Fig. 7. The metal absorber must not stress the underlying membrane and create pattern shifting. The membrane must be stiff enough to keep patterns fixed over time. The membrane, must, of course, be free of pinholes or other types of defects. There is no hard data on reliability or manufacturability of x-ray masks.

4. Summary and Conclusions

The major types of lithographic systems currently in use or in development have been reviewed. The various types of UV-optical systems (contact, proximity, full-wafer, wafer-stepper and deep-UV) were discussed. Newer types of systems keyed for the submicron integrated market were also summarized. UV-optical systems are capable of submicron resolution on flat surfaces. However, depth-of-focus problems inhibit their usefulness in a real production environment. E-beam systems do not suffer from resolution or depth-of-focus problems. But those presently available are too slow and lack the reliability to be used in direct-write submicron production. X-ray lithography has the potential to overcome all these problems. But source-brightness and mask making problems must be solved.





ACKNOWLEDGEMENT

The author would like to express his gratitude to Mr. C. J. Taylor for conversations relating to this paper and for many years of instruction in the lithographic art.



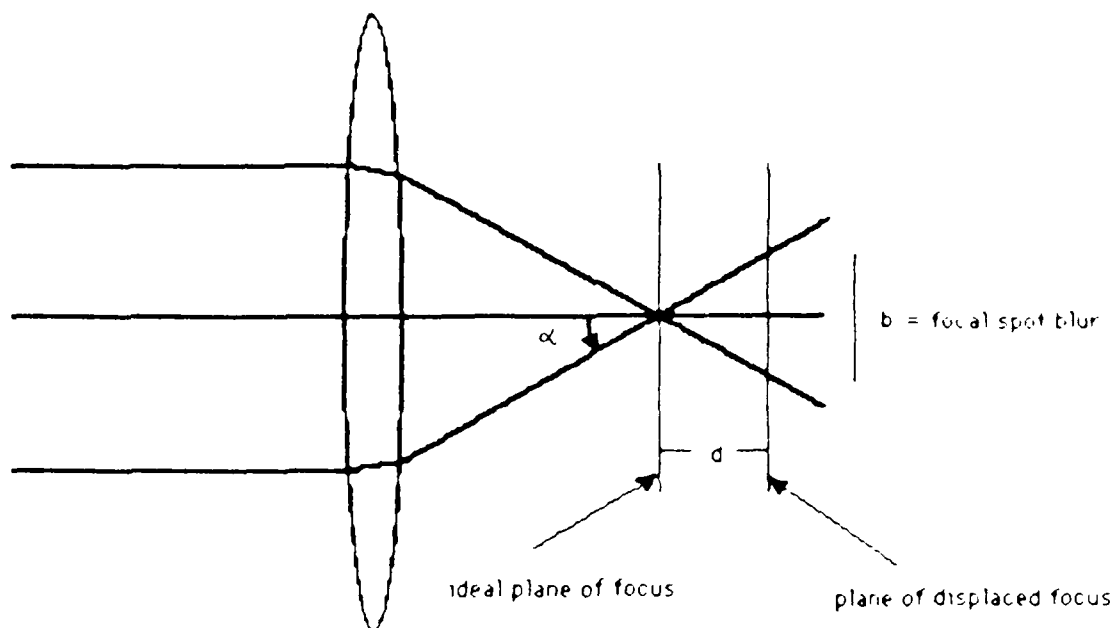
THE RESIST MASKING PROCESS

Figure 1. Photo-resist exposure in IC lithography.

	FOCUSED BEAM (DIRECT-WRITE)	PATTERN PROJECTION	MASK (PROXIMITY or CONTACT)
			
PHOTONS	Laser Chemistry	UV Scanning or Step & Repeat	UV & X-Ray
ELECTRONS	Raster or Vector Scan	Pattern on Cathode	
IONS	Field-Ion Sources	Open Mask	Channeling in Mask

Types of fine-line lithography, as distinguished by the method of pattern replication (horizontally) and the quanta employed to expose resists (vertically).

Figure 2. A comparison of various lithographic techniques (courtesy of D.J. Nagel).



$$NA = n \sin (\alpha)$$

b gets larger as α increases
 Thus, as NA increases, b increases
 for a given d .

RELATIONSHIP OF NA TO DEPTH-OF-FOCUS

Figure 3. An illustration of how numerical aperture influences depth-of-focus.

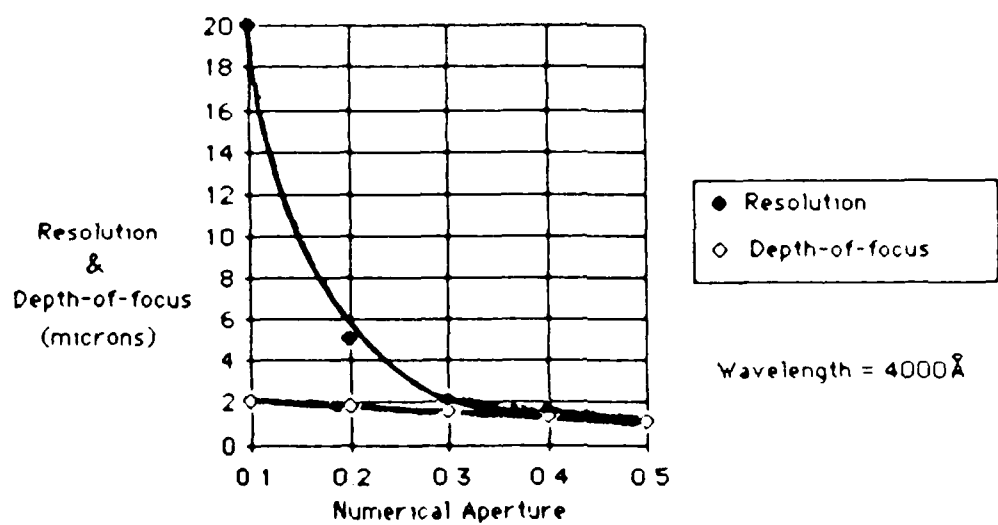


Figure 4. Resolution and depth-of-focus as a function of numerical aperture.

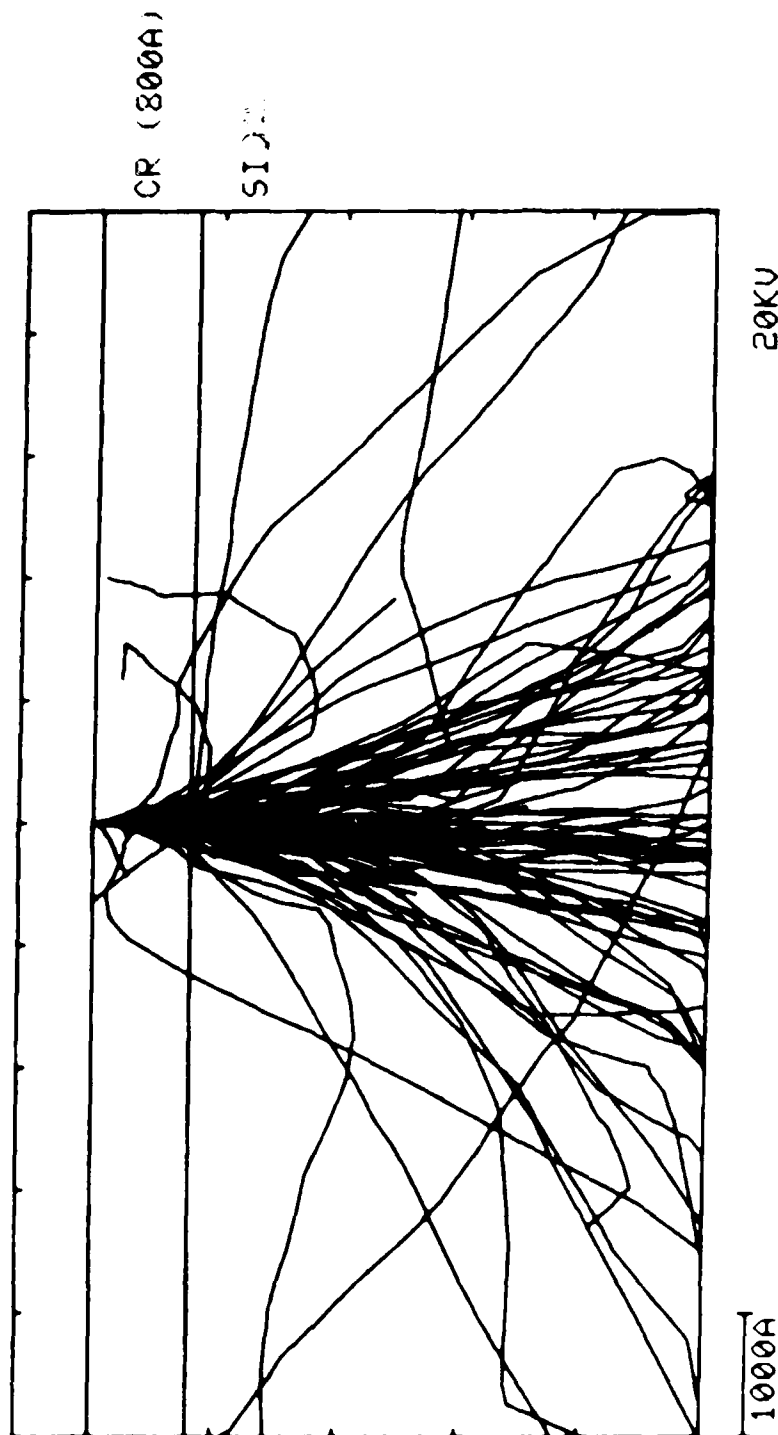
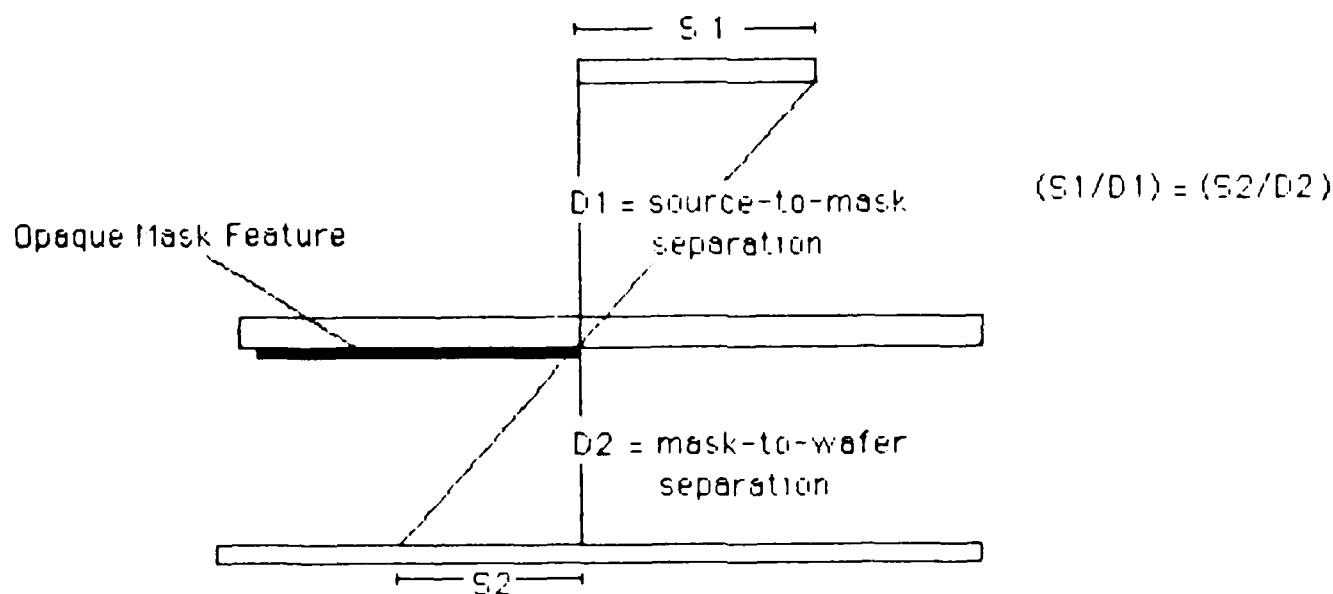
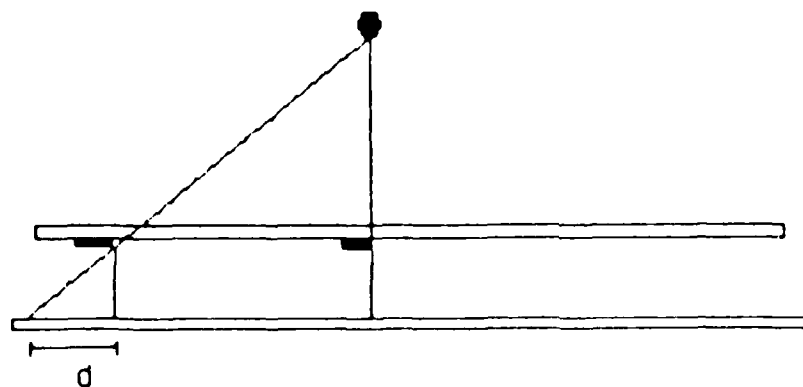


Figure 5. Monte Carlo simulations of electron trajectories through an IC mask plate. The plate consists of a chrome thin film over glass. The incident beam had an energy of 20 keV. The individual electron tracks are evident. Energy is deposited far from the point of initial impact.

RESOLUTION LOSS AND REGISTRATION ERROR IN X-RAY LITHOGRAPHY

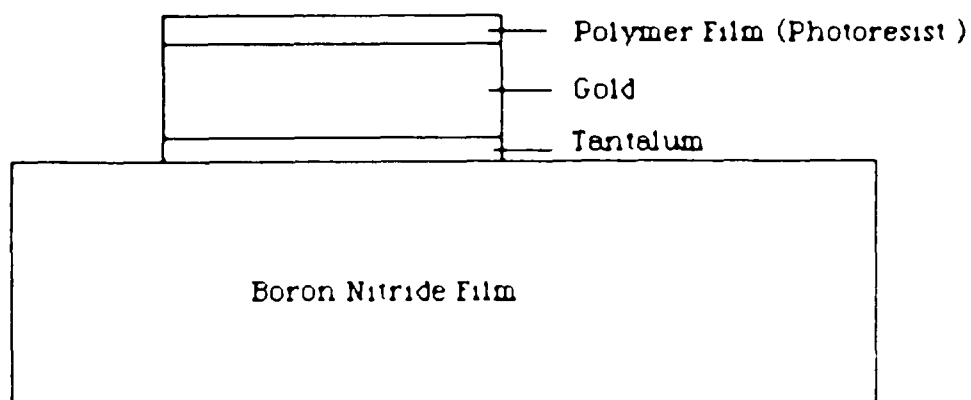


A) Penumbral Blur The mask image does not cast a clean shadow. A region of extent S_2 is partially illuminated by a source of extent S_1



B) Registration error Features at the edge of the mask are displaced an amount d due to projection effects from a point source. If the mask-to-wafer separation is uncertain, this effect is difficult to correct for

Figure 6. Illustrations of the origin of penumbral blur, and other geometric distortion effects obtained in x-ray lithography.



The thin film of tantalum is used as a base layer to initiate the plating of the gold absorber layer

The photoresist is used to absorb photoelectrons kicked out of the gold, and to absorb gold M-line emission

Figure 7. A typical x-ray mask.

II. High Peak Power and Average Power Lasers

Critical components of laser systems include the power of the pump and transfer mechanism, pumping mechanisms and the laser. The efficiency and, especially, the reliability of these components are primary concerns in repetitively-pulsed laser systems, and these are to find widespread use. Capacitive energy storage systems are generally available, with switches being a major concern in the power system. Solid state systems, which do not have the erodable gaps present in gas phase switches, may be used in the high peak and average power electrical systems which provide energy to repetitively-pulsed lasers.

The means of pumping the inverted population varies widely, with discharge tubes being used for gas systems and flash lamps employed for solid state lasers. In either case, the pump must be renewed periodically in excimer systems. The cost of excimer lamps, which may be less per shot operated at 1 kHz or slower repetition rates, is the critical factor for typically 10^6 shots. Some excimer systems report that pump afterglow is negligible, while others are rated as high as 100×10^6 shots. Nd:YAG lasers, which are rated for millions of shots if operated below damage threshold and kept clean. However, the lamps require replacement after about 10^6 shots, depending on how hard they are driven.

The characteristics of commercially-available repetitively-pulsed laser systems are tabulated in Figure 1. Figures 2 and 3 are plots of peak and average power for excimer and Nd:YAG systems. The rates are indicated for excimer systems, which generally have rates between 10 and 100 Hz. Nd:YAG systems in the 1-50 Hz range have pulse lengths of 10 nsec if Q-switched and near 30 psec if mode-locked.

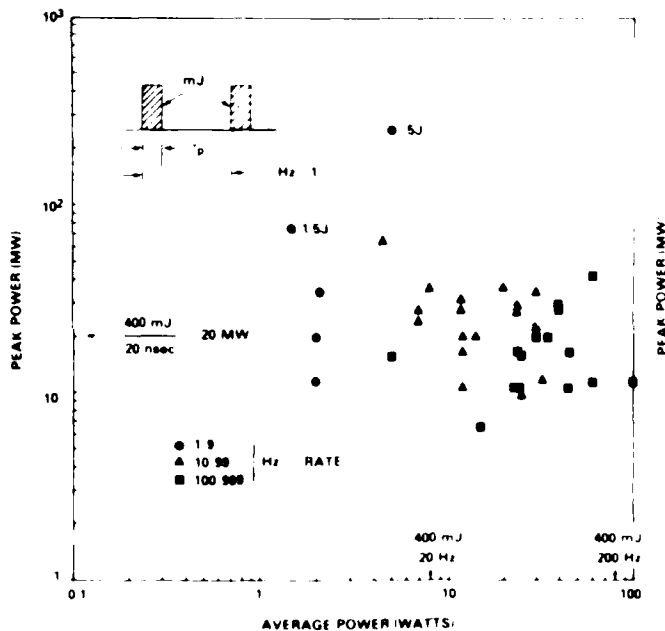


Figure 2. Peak vs. average power for commercially available KrF excimer lasers of the indicated repetition rates. 40-200 psec, 20 nsec wide with rate between 20 and 200 Hz are typical. As shown in the inset for pulse energies of 400 mJ, the peak power is approximately 10 times the average power is 4 times the repetition rate.

KrF excimer lasers now available commercially are generally capable of 100-200 MW peak and 100 W average power. Systems now under development are capable of the same peak and one kilowatt average power. The stability and cost of the pump and transfer mechanism heavily influence their utility for X-ray operation.

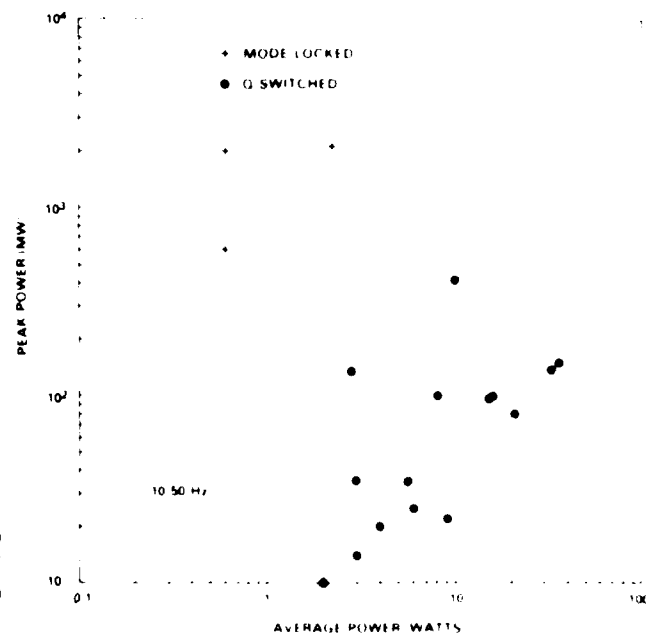


Figure 3. Peak vs. average power for Nd:YAG lasers. Commercially available systems are capable of 100-200 MW peak and 100 W average power. Systems now under development are capable of the same peak and one kilowatt average power. The stability and cost of the pump and transfer mechanism heavily influence their utility for X-ray operation.

1. *Pharmaceuticals* (1997) 10, 115-120.
 2. *Pharmaceuticals* (1997) 10, 121-126.
 3. *Pharmaceuticals* (1997) 10, 127-132.
 4. *Pharmaceuticals* (1997) 10, 133-138.
 5. *Pharmaceuticals* (1997) 10, 139-144.
 6. *Pharmaceuticals* (1997) 10, 145-150.
 7. *Pharmaceuticals* (1997) 10, 151-156.
 8. *Pharmaceuticals* (1997) 10, 157-162.
 9. *Pharmaceuticals* (1997) 10, 163-168.
 10. *Pharmaceuticals* (1997) 10, 169-174.
 11. *Pharmaceuticals* (1997) 10, 175-180.
 12. *Pharmaceuticals* (1997) 10, 181-186.
 13. *Pharmaceuticals* (1997) 10, 187-192.
 14. *Pharmaceuticals* (1997) 10, 193-198.
 15. *Pharmaceuticals* (1997) 10, 199-204.
 16. *Pharmaceuticals* (1997) 10, 205-210.
 17. *Pharmaceuticals* (1997) 10, 211-216.
 18. *Pharmaceuticals* (1997) 10, 217-222.
 19. *Pharmaceuticals* (1997) 10, 223-228.
 20. *Pharmaceuticals* (1997) 10, 229-234.
 21. *Pharmaceuticals* (1997) 10, 235-240.
 22. *Pharmaceuticals* (1997) 10, 241-246.
 23. *Pharmaceuticals* (1997) 10, 247-252.
 24. *Pharmaceuticals* (1997) 10, 253-258.
 25. *Pharmaceuticals* (1997) 10, 259-264.
 26. *Pharmaceuticals* (1997) 10, 265-270.
 27. *Pharmaceuticals* (1997) 10, 271-276.
 28. *Pharmaceuticals* (1997) 10, 277-282.
 29. *Pharmaceuticals* (1997) 10, 283-288.
 30. *Pharmaceuticals* (1997) 10, 289-294.
 31. *Pharmaceuticals* (1997) 10, 295-300.
 32. *Pharmaceuticals* (1997) 10, 301-306.
 33. *Pharmaceuticals* (1997) 10, 307-312.
 34. *Pharmaceuticals* (1997) 10, 313-318.
 35. *Pharmaceuticals* (1997) 10, 319-324.
 36. *Pharmaceuticals* (1997) 10, 325-330.
 37. *Pharmaceuticals* (1997) 10, 331-336.
 38. *Pharmaceuticals* (1997) 10, 337-342.
 39. *Pharmaceuticals* (1997) 10, 343-348.
 40. *Pharmaceuticals* (1997) 10, 349-354.
 41. *Pharmaceuticals* (1997) 10, 355-360.
 42. *Pharmaceuticals* (1997) 10, 361-366.
 43. *Pharmaceuticals* (1997) 10, 367-372.
 44. *Pharmaceuticals* (1997) 10, 373-378.
 45. *Pharmaceuticals* (1997) 10, 379-384.
 46. *Pharmaceuticals* (1997) 10, 385-390.
 47. *Pharmaceuticals* (1997) 10, 391-396.
 48. *Pharmaceuticals* (1997) 10, 397-402.
 49. *Pharmaceuticals* (1997) 10, 403-408.
 50. *Pharmaceuticals* (1997) 10, 409-414.
 51. *Pharmaceuticals* (1997) 10, 415-420.
 52. *Pharmaceuticals* (1997) 10, 421-426.
 53. *Pharmaceuticals* (1997) 10, 427-432.
 54. *Pharmaceuticals* (1997) 10, 433-438.
 55. *Pharmaceuticals* (1997) 10, 439-444.
 56. *Pharmaceuticals* (1997) 10, 445-450.
 57. *Pharmaceuticals* (1997) 10, 451-456.
 58. *Pharmaceuticals* (1997) 10, 457-462.
 59. *Pharmaceuticals* (1997) 10, 463-468.
 60. *Pharmaceuticals* (1997) 10, 469-474.
 61. *Pharmaceuticals* (1997) 10, 475-480.
 62. *Pharmaceuticals* (1997) 10, 481-486.
 63. *Pharmaceuticals* (1997) 10, 487-492.
 64. *Pharmaceuticals* (1997) 10, 493-498.
 65. *Pharmaceuticals* (1997) 10, 499-504.
 66. *Pharmaceuticals* (1997) 10, 505-510.
 67. *Pharmaceuticals* (1997) 10, 511-516.
 68. *Pharmaceuticals* (1997) 10, 517-522.
 69. *Pharmaceuticals* (1997) 10, 523-528.
 70. *Pharmaceuticals* (1997) 10, 529-534.
 71. *Pharmaceuticals* (1997) 10, 535-540.
 72. *Pharmaceuticals* (1997) 10, 541-546.
 73. *Pharmaceuticals* (1997) 10, 547-552.
 74. *Pharmaceuticals* (1997) 10, 553-558.
 75. *Pharmaceuticals* (1997) 10, 559-564.
 76. *Pharmaceuticals* (1997) 10, 565-570.
 77. *Pharmaceuticals* (1997) 10, 571-576.
 78. *Pharmaceuticals* (1997) 10, 577-582.
 79. *Pharmaceuticals* (1997) 10, 583-588.
 80. *Pharmaceuticals* (1997) 10, 589-594.
 81. *Pharmaceuticals* (1997) 10, 595-600.
 82. *Pharmaceuticals* (1997) 10, 601-606.
 83. *Pharmaceuticals* (1997) 10, 607-612.
 84. *Pharmaceuticals* (1997) 10, 613-618.
 85. *Pharmaceuticals* (1997) 10, 619-624.
 86. *Pharmaceuticals* (1997) 10, 625-630.
 87. *Pharmaceuticals* (1997) 10, 631-636.
 88. *Pharmaceuticals* (1997) 10, 637-642.
 89. *Pharmaceuticals* (1997) 10, 643-648.
 90. *Pharmaceuticals* (1997) 10, 649-654.
 91. *Pharmaceuticals* (1997) 10, 655-660.
 92. *Pharmaceuticals* (1997) 10, 661-666.
 93. *Pharmaceuticals* (1997) 10, 667-672.
 94. *Pharmaceuticals* (1997) 10, 673-678.
 95. *Pharmaceuticals* (1997) 10, 679-684.
 96. *Pharmaceuticals* (1997) 10, 685-690.
 97. *Pharmaceuticals* (1997) 10, 691-696.
 98. *Pharmaceuticals* (1997) 10, 697-702.
 99. *Pharmaceuticals* (1997) 10, 703-708.
 100. *Pharmaceuticals* (1997) 10, 709-714.
 101. *Pharmaceuticals* (1997) 10, 715-720.
 102. *Pharmaceuticals* (1997) 10, 721-726.
 103. *Pharmaceuticals* (1997) 10, 727-732.
 104. *Pharmaceuticals* (1997) 10, 733-738.
 105. *Pharmaceuticals* (1997) 10, 739-744.
 106. *Pharmaceuticals* (1997) 10, 745-750.
 107. *Pharmaceuticals* (1997) 10, 751-756.
 108. *Pharmaceuticals* (1997) 10, 757-762.
 109. *Pharmaceuticals* (1997) 10, 763-768.
 110. *Pharmaceuticals* (1997) 10, 769-774.
 111. *Pharmaceuticals* (1997

11/11/1964

• • • • •

Until recently, little attention has been paid to integrated design of the laser focusing and target systems. Target debris has been observed to coat nearby optical elements, notably the focusing lens. Repetitively-pulsed lasers which are run for long periods vaporize significant amounts of target material. It may be necessary to employ thin roll-to-roll plastic shields between the target and near-by the lens.

IV. Laser-Plasma Transients

The laser pulse and the target provide the energy and matter within the plasma. As indicated in Figure 5, many effects accompany photon emission from hot, dense plasma: electron, ion, plasma, vapor, and debris droplet emissions are of interest and possible use. For example, the recombinant plasma vapor can be used to prepare thin films of refractory materials⁴.

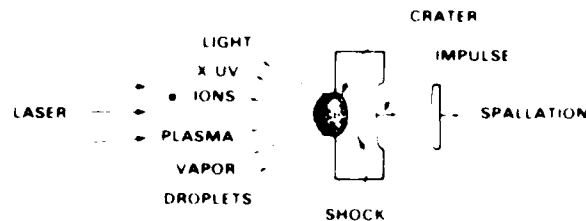


Figure 5. Schematic of the effects produced by the interaction of a high-power laser pulse with solid targets, namely front-surface ablation, electron, ion, plasma, vapor, and droplet emission, and cratering. Internal shock waves and spallation are produced near-surface spallation. The spall-like emission of high-speed matter from the target imparts an acceleration and impulse to the entire target.

The multiplicity of effects from the laser of interest is a general problem. For example, droplet ejection complicates the generation of uniform thin films⁴ indicated by the post-position vapor coating of both sides and surface roughness. A computer is expected to employ the x-ray emission.

Defense against vapor and debris include thin film target, which is a thin film of a low-pressure material, gas, rotating patterns and thin targets, and a target of a low density. It is a problem to protect optics from the target. The target is a thin film of a low density, which will pass through relatively thin protective materials. The target is a thin film of a low density, which will pass through relatively thin protective materials. The target is a thin film of a low density, which will pass through relatively thin protective materials.

V. X-Ray Emission

Earlier reviews of the spectral, spatial and temporal characteristics of laser-induced x-ray emission are available^{1,2,5,6}. Selected examples of recent progress are given in the next subsections. Needed measurements are then outlined.

A. Recent Plasma X-ray Line and Continuum

Recent progress in the field of laser-induced x-ray emission from laser-produced plasmas is the subject of this section. The independent spectra from targets heated by pulsed laser with lengths of 100 ns to 100 ps, experimental measurements for many targets, covering a wide range of laser intensities, and the ability of the model. The laboratory work has been done in the past few years, laser pulse, shorter laser wavelengths, and higher repetition rates.

Sakuma and his group reported that the x-ray emission from laser-produced plasmas is a function of laser intensity^{7,8}. The independence of their results is a significant step towards the development of a theory of laser-induced x-ray emission. The results are in good agreement with the results of the model. The results are in good agreement with the results of the model. The results are in good agreement with the results of the model.

Morizaki and his group reported that the x-ray emission from laser-produced plasmas is a function of laser intensity^{9,10}. The results are in good agreement with the results of the model. The results are in good agreement with the results of the model. The results are in good agreement with the results of the model. The results are in good agreement with the results of the model. The results are in good agreement with the results of the model.

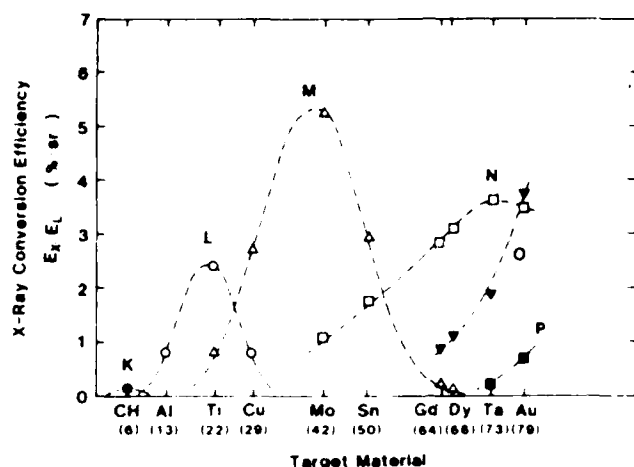


Figure 6. Measured x-ray conversion efficiency for 1-ns pulses of 0.51 μm (2nd harmonic of 1.02 μm) laser light focused to $10^{14} \text{ W cm}^{-2}$ on the indicated targets, with contributions from the various atomic shells (K, L, M...).⁸

Recently, Lepin and collaborators employed 145-ps, 8-fs pulses of the fourth harmonic of Nd:YAG laser (266 nm) focused to $10^{14} \text{ W cm}^{-2}$ to measure absolute x-ray spectral conversion efficiencies for several elements.⁹ A model developed by Alatorre, et al.,¹⁰ gave very good agreement with the data, as indicated in Figure 7. The excellent agreement around the periodic table between experiment and the calculation that their model may be directly related to the experimental plasma temperature.

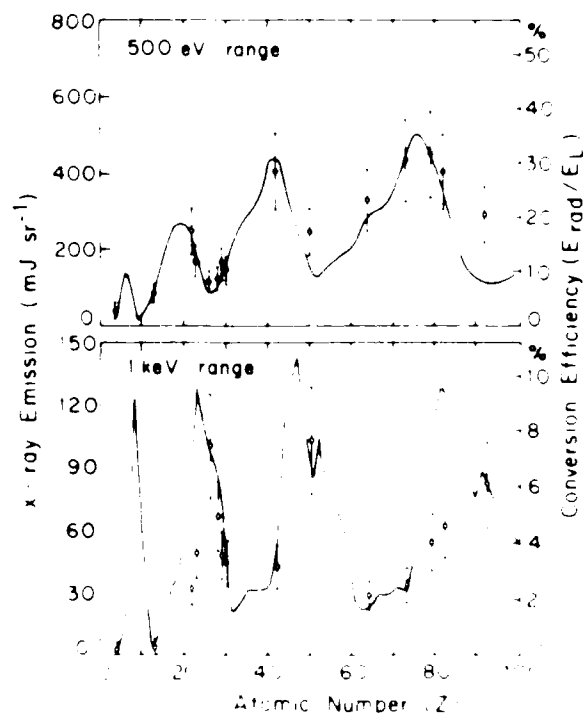
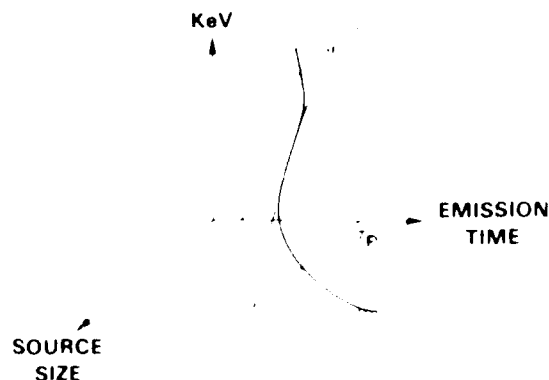


Figure 7. Spectral conversion efficiency for 145-ps, 8-fs pulses of the fourth harmonic of Nd:YAG laser (266 nm) focused to $10^{14} \text{ W cm}^{-2}$ on the indicated targets, with 0.51 μm (4th harmonic of 2.02 μm) laser light focused to $10^{14} \text{ W cm}^{-2}$ on the indicated targets. Theoretical model of Alatorre, et al.,¹⁰ is shown for comparison.

Figure 8 shows the x-ray emission spectrum for a 145-ps, 8-fs pulse of the fourth harmonic of Nd:YAG laser (266 nm) focused to $10^{14} \text{ W cm}^{-2}$ on a 100- μm diameter target. The x-ray emission spectrum is shown for the 100- μm diameter target. The x-ray emission spectrum is shown for the 100- μm diameter target. The x-ray emission spectrum is shown for the 100- μm diameter target.

b. Needed Laser-Plasma X-Ray Measurements

Despite the major recent progress just cited, great gaps in our knowledge of x-ray emission from laser-plasmas remain. Ideally, we would know how to calculate in detail the time-varying emission from each plasma volume element into each direction for the full X-ray spectrum for chosen laser, focusing and target conditions. This represents a huge amount of information, even for one set of conditions. More realistically, it would be useful to know effective temporal, spatial and spectral characteristics, as illustrated in Figure 8. The spatially-integrated X-ray emission appears over time comparable to the laser pulse FWHM τ_p . The harder radiation tends to have a shorter FWHM, since it appears only at the highest irradiances. Softer radiation is emitted over a longer time, appearing earlier in the laser pulse and extinguishing later at the plasma edge. Similarly, the time-integrated apparent source size is smaller at higher energies, and larger at lower energies (which are produced in the wings of the focal spot and because of expansion at late times). The effective source parameters in Figure 8 depend on the viewing direction. Suffice it to say that full characterization of laser-driven x-ray sources is complex.



Experiments on the effects of the frequency of the stimulus on the response of the system have been carried out. The results show that the system is more sensitive to the frequency of the stimulus than to the amplitude of the stimulus. The system is also more sensitive to the frequency of the stimulus than to the duration of the stimulus.

Finally, mention should be made of requirements for diagnostics development. Spectral determination with, say, multiple filtered diodes at diverse emission directions requires many channels for data transmission and recording. Compact arrays of filters, scintillators and fiber optics are under development to address such a need. A compact, complete, transportable laser-target interaction chamber is being developed at this laboratory. It includes a fast pumping system, a rotating target, and prealigned diagnostics: temporal (silicon and vacuum diodes), spatial (pinhole and collimation cameras) and spectral (crystal and grating spectrographs).

VI. X-ray Transport

X-ray optics are commonly employed between sources and experiments. They can serve multiple purposes: collection of radiation over a solid angle larger than that intercepted by the sample, wavelength selection (monochromatization) and focusing x-radiation onto the region of interest. X-ray optics can also be designed to produce highly parallel radiation to test space instruments.

X-ray tubes emit uncollimated line and continuum spectra. They are usually employed with no optics, or with simple apertures. Sometimes, lens, totally-reflecting mirrors are used with tubes to concentrate radiation onto samples, as in some small-angle scattering work. Monochromators are used with x-ray tubes in absorption spectroscopy.

Synchrotron radiation sources commonly emit intense continuum spectra collimated with narrow divergence in one or two dimensions. Complex x-ray optics in vacuum or He-filled beam lines are commonly used to collect, monochromatize and focus synchrotron radiation. Grazing-incidence optics and large-angle crystal monochromators are most often used.

Plasma x-ray sources have, until recently, been used without optics between the source and sample. However, the same features which cause synchrotron radiation beam lines to be built and used also apply to plasma sources: improved collection efficiency, wavelength selection and flux concentration. Hence, beam lines to transport plasma x-radiation to samples are now being designed. The first beam line is being installed at Sandia National Laboratory in Livermore, CA. It consists of grazing-incidence mirrors and a grazing-incidence grating to provide concentrated tunable soft x-rays from ErF laser-produced plasmas in an ultra-high vacuum chamber for surface science measurements, laser photoemitted desorption.

Grazing-incidence x-ray optics are attractive since they allow very large collection solid angles. Figure 4 shows schematically a configuration in which a concave grating can be used up to about 40 eV, a multilayer to about 400 eV and a crystal at higher photon energies. The multilayer can be deposited on a fixed, concave surface or on a flat, flexible substrate. Concave crystals can be produced by elastic or plastic deformation. In the latter case, the laser and sample positions at the expense of moving the laser plasma and sample is coherent. However, motions for laser foot have been well engineered, with complex articulated arms developed for laser medical and materials processing applications. Here, only simple translations of the second laser mirror and the legs are needed. Two orthogonal target motions are required to move the plasma in a complex but well-defined curved path. The dispersion element can be executed only one linear translation and deformation to maintain the Rowland circle geometry. The geometry in Figure 4 is the reverse of that in Bragg spectrometer employed on electron microprobes, where the x-ray source, sample and take-off angle are fixed. There the crystal translates in a line and rotates, and the detector describes a complex but straight-forward motion.



Figure 4. Schematic of optics to collect, monochromatize and focus x-rays from a laser-produced plasma on a sample. The curved surface is a fixed, concave grating, multilayer, or crystal, depending on the photon energy. The sample and detector elements can move in a plane perpendicular to the fixed laser mirror and target motion. A fixed incidence angle is maintained on sample.

It is anticipated that the design of efficient and versatile beam lines for laser-plasma x-radiation will prove a continuing challenge for x-ray opticians, just as design of synchrotron radiation beam lines has advanced the state-of-the-art of x-ray optics.

VII. Applications

Uses of X-UV radiation from laser-heated plasmas have been categorized 13:

Plasma Physics, including plasma temperature and density diagnostics, and flash radiography of dense plasmas.

Atomic and Molecular Physics, especially emission and absorption spectroscopy, and potentially, photoelectron spectroscopy.

Solid-State (Surface) Physics, notably time of flight photo-ion spectroscopy and possibly dynamic photo-electron spectroscopy.

Dynamic Structure Studies, including flash x-ray diffraction, small-angle scattering or EXAFS transmission or reflection measurements, to study rapid changes in structure, such as melting.

Energy Deposition, in order to drive chemical reactions: to induce ionization, heating, phase changes or plasma formation (the latter to ablatively accelerate material); or to pump lasers, especially in the X-UV region.

Instrument Calibration, especially the active (electronic) and passive (e.g., film) equipment used to diagnose plasmas and other short-pulse x-ray sources. Laser-plasma x-ray standard sources are also under development.

Replication of natural materials, as in biological x-ray microscopy, or man-made structures, such as x-ray masks which are replicated during microcircuit production.

Eason and his colleagues at the Rutherford Appleton Laboratory have been especially active in developing and refining applications of x-rays from laser-heated plasmas 14. They have done flash stroboscopic and time-resolved streaked transmission EXAFS, surface reflection EXAFS, pulsed x-ray diffraction and soft x-ray contact microscopy.

The replication techniques of microscopy and lithography may become quite important commercially. X-ray microscopy to resolve features of the live cells in the 200- to 2000 Å range could be used clinically in 5 to 10 years. If x-ray lithography does displace optical (UV) lithography for mass production of integrated circuits, and if laser-plasma sources are preferable to discharge-plasma or storage ring sources, then lasers will be engineered for highly-reliable x-ray production and integrated into alignment and exposure stations. The commercial time scale for this may also be about 5 to 10 years.

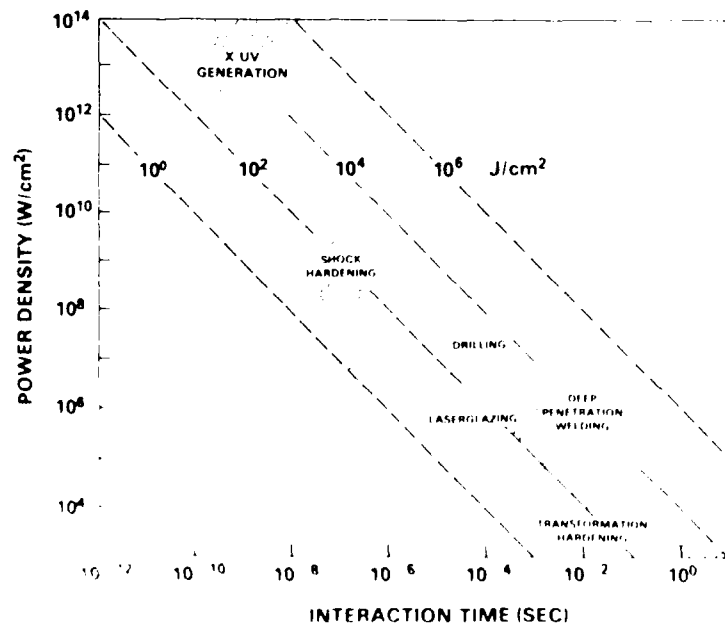


Figure 12. Regions of irradiation (W/cm²), interaction time (sec) and fluence (J/cm²) for commercial utilization of pulsed lasers.

Pulsed lasers are in use for diverse industrial processes, as indicated in Figure 10. That plot is an extension of an earlier diagram¹⁵ to include high-irradiance laser-plasma X-UV generation for the types of applications cited above. A recent, detailed review of such uses of short-pulse lasers is available.¹⁶

VIII. Conclusion

The next few years should witness design and construction of prototype and commercial laser systems dedicated to x-ray production, more detailed characterization of the parametric dependence of laser-plasma X-UV emission, design and use of integrated target chamber/beam line/experimental chamber systems and demonstration/refinement of additional applications. Laser-plasma X-UV sources may prove to be local alternatives to storage rings, with high peak x-ray powers and intermediate (~kHz) repetition rates well suited to signal averaging.

Acknowledgments

Collaborations with H. Pepin, P. Alaterre, M. Chaker, M. C. Peckerar and T. P. Toomen are most pleasant. Helpful conversations with R. L. Byers, R. W. Eason, L. Esterowitz, B. J. Feldman, Y. Kato, H. Kuroda, J. M. McMahon and T. Mochizuki are appreciated. R. R. Whitlock is thanked for comments on the manuscript.

References

1. T. R. Farre, Editor, 1986 Buying Guide Laser and Applications, Vol. IV, No. 13, Dec. 1985.
2. S. Basu and R. L. Byer, Optics Letters, 1986.
3. S. Basu, T. J. Kane and R. L. Byer, IEEE J. Quantum Electronics, August 1986.
4. C. L. Marquardt, R. T. Williams, D. J. Nagel, Mat. Res. Soc. Symp. Proc., 38, 325 (1985).
5. D. J. Nagel, SPIE Vol. 125, 46 (1978).
6. D. J. Nagel, VLSI Electronics: Microstructural Science, Academic Press, New York (1984) p. 137.
7. N. Nakano and H. Kuroda, Phys. Rev. A27, 2168 (1983).
8. Mochizuki, T. Yabe, K. Okada, H. Hamada, N. Ikeda, S. Kiyokawa and C. Yamanaka, Institute of Laser Engr. Report, Osaka University (1985).
9. H. Pepin, P. Alaterre, M. Chaker, R. Fabbro, B. Faral, D. J. Nagel and M. C. Peckerar, J. Vac. Sci. Tech. (1986).
10. P. Alaterre, H. Pepin, R. Fabbro and B. Faral, Phys. Rev. A (1986).
11. D. J. Nagel, C. M. Brown, M. C. Peckerar, M. L. Ginter, J. A. Robinson, T. J. McIlrath and P. K. Carroll, Appl. Optics, 23, 1428 (1984).
12. T. P. Toomen, private communication.
13. D. J. Nagel, SPIE Vol. 448, 17 (1984).
14. R. W. Eason, D. K. Bradley, J. D. Hares, A. J. Rankin, S. Djalil Tabatabaer, J. G. Lunney, P. C. Cheng, R. Feder, A. G. Michette, R. J. Rosser, F. O'Neill, Y. Owadano, P. Rumsby and A. Show, this volume.
15. E. M. Breinan and B. H. Kear in M. Bass (Ed.) Laser Materials Processing, North Holland (1983) p. 238.
16. R. R. Whitlock, Proc. of 1985 IC ALEO Laser Inst. Of America (1986).

END
DATE
FILMED
MARCH
1988
DTIC